

# 2DSOIL - A Modular Simulator of Soil and Root Processes

*Release 03 (March, 2001)*

Dennis Timlin, Yakov Pachepsky, and Martinus Th. van  
Genuchten, ed.

Alternate Crops and Systems Laboratory, Beltsville, MD and Soil Physics and Pesticide  
Research Laboratory, Riverside Ca.



## EXECUTIVE SUMMARY

Because of the complexity of the various linkages in agricultural systems, research questions are often best studied via simulation modeling. The goal of this project was to develop the framework for a generic, two-dimensional soil simulator that could easily be modified and incorporated into crop models. Most agricultural crops are grown in rows and operations are carried out parallel with rows. As a consequence, root growth, wheel traffic, tillage fertilizer banding, furrow and drip irrigation, among other operations, all produce variations in soil conditions in two dimensions, perpendicular to the rows. Soil modeling is now increasingly being focused at these two dimensions. Plant modelers, however, wishing to incorporate comprehensive soil models into their plant models require soil code that can be easily interfaced with a plant model and subsequently modified to incorporate different management practices. The development and upgrading of detailed models requires a large investment of time and resources. The tools developed as part of this project will simplify the process of building the model and incorporating modifications as research finds new information to include.

The 2DSOIL model is a modular, comprehensive two-dimensional soil simulator that is specifically designed to be combined with existing plant models. Modules of the present release, 2DSOIL.03, simulate water, solute, heat and gas movement, as well as root activity of plants, nitrogen dynamics, and chemical interactions in a two-dimensional soil profile. An uneven soil surface, mulching, and local applications of water and chemical can be easily modeled. The modules interact by means of soil state variables that are important for plants and the environment. The modules are highly independent because details of a particular module's activity are unknown to other modules. Several modules were adapted from existing models; others were developed specifically for 2DSOIL. 2DSOIL is written in FORTRAN and may be run on 486 or more advanced MS-DOS or MS-WINDOWS based computers.

The modular structure of 2DSOIL allows users to add their own modules of soil and plant processes, and soil management practices. The users can also easily replace modules of 2DSOIL.03 with more appropriate ones for their specific problems, or with more accurate modules as they become available.

Potential users are soil and plant modelers, environmental scientists, agronomists, crop scientists and others who are interested in investigating environmental quality and crop productivity as affected by management practices and possible climate changes.

<b>EXECUTIVE SUMMARY</b>	<a href="#">i</a>
<b>ABSTRACT</b>	<a href="#">vii</a>
<b>TECHNICAL REQUIREMENTS AND TECHNICAL SUPPORT</b>	<a href="#">viii</a>
<b>LIST OF SYMBOLS</b>	<a href="#">ix</a>
Chapter 1: Introduction and Background Dennis Timlin and Yakov Pachepsky	<a href="#">1</a>
Chapter 2: Definition of Objects and Time Stepping; the <i>Synchronizer</i> Module Yakov Pachepsky and Dennis Timlin	<a href="#">13</a>
Input file <i>Time.dat</i>	<a href="#">14</a>
Chapter 3: Grid and Boundary Settings: <i>Get_Grid_and_Boundary</i> Module Yakov Pachepsky and Dennis Timlin	<a href="#">17</a>
Grid setting	<a href="#">17</a>
Codes for boundary nodes	<a href="#">19</a>
Grid Data file <i>Grid_bnd.dat</i>	<a href="#">23</a>
Chapter 4: Time-dependent Boundary Settings: <i>Settdb</i> Module Yakov Pachepsky and Dennis Timlin	<a href="#">29</a>
Piece-wise boundary settings	<a href="#">29</a>
Data files <i>VarBW.dat</i> , <i>VarBS.dat</i> , <i>VarBH.dat</i> , and <i>VarBG.dat</i>	<a href="#">32</a>
Chapter 5: Soil-atmosphere Boundary Setting: <i>SetSurf</i> Modules Basil Acock, Yakov Pachepsky, and Dennis Timlin	<a href="#">37</a>
Using daily meteorological data: <i>SetSurf02</i> module	<a href="#">38</a>
Incident radiation submodel	<a href="#">38</a>
Temperature-vapor pressure submodel	<a href="#">43</a>
Radiation interception submodel	<a href="#">46</a>
Potential evapotranspiration submodel	<a href="#">50</a>
Precipitation-Irrigation Submodel	<a href="#">54</a>
Heat movement submodel	<a href="#">54</a>
Gas movement submodel	<a href="#">57</a>
Data files ' <i>Weather.dat</i> ' and ' <i>Furnod.dat</i> '	<a href="#">57</a>
Using customized agro-meteorological data: <i>SetSurf01</i> module	<a href="#">61</a>
Chapter 6: Water Flow: WaterMover Module Jirka Šimůnek, Yakov Pachepsky, and Martinus Th. van Genuchten	<a href="#">65</a>
The two-dimensional model of water flow and its finite element implementation	<a href="#">65</a>
Data files ' <i>Param_W.dat</i> ' and ' <i>Nodal_W.dat</i> '	<a href="#">71</a>

The unsaturated soil hydraulic properties: Using closed-form approximations in the submodule SetMat01 .....	<a href="#">73</a>
Data file ' <i>Closefrm.dat</i> ' .....	<a href="#">77</a>
The unsaturated soil hydraulic properties: Using piece-wise polynomial approximations in the submodule SetMat02 .....	<a href="#">77</a>
Data file ' <i>Hydprop.dat</i> ' .....	<a href="#">81</a>
Chapter 7: Solute Transport: SoluteMover module	
Jirka Šimůnek, Martinus Th. van Genuchten, and Yakov Pachepsky .....	<a href="#">83</a>
Parameters of the SoluteMover module .....	<a href="#">89</a>
Data files ' <i>Param_S.dat</i> ' and ' <i>Nodal_S.dat</i> ' .....	<a href="#">93</a>
Chapter 8: Heat Transport: HeatMover Module	
Dennis Timlin, Yakov Pachepsky, and Jirka Šimůnek .....	<a href="#">97</a>
The two-dimensional model of heat movement and its finite element implementation .....	<a href="#">97</a>
Parameters of the HeatMover module .....	<a href="#">101</a>
Data files ' <i>Param_T.dat</i> ' and ' <i>Nodal_T.dat</i> ' .....	<a href="#">102</a>
Chapter 9: Gas Transport: GasMover Module	
Yakov Pachepsky and Dennis Timlin .....	<a href="#">105</a>
The two-dimensional model of solute movement and its finite element implementation .....	<a href="#">105</a>
Parameters of the GasMover module .....	<a href="#">109</a>
Data files ' <i>Param_G.dat</i> ' and ' <i>Nodal_G.dat</i> ' .....	<a href="#">111</a>
Chapter 10: Root Water Uptake: Root_Water_Uptake Module	
Basil Acock, Yakov Pachepsky, and Dennis Timlin .....	<a href="#">115</a>
Plant status dependent model: Water_Uptake01 .....	<a href="#">115</a>
Data files ' <i>Param_R.dat</i> ' and ' <i>Nodal_R.dat</i> ' .....	<a href="#">129</a>
Plant status independent model: Water_Uptake02 .....	<a href="#">131</a>
Data files ' <i>Param_U.dat</i> ' and ' <i>Nodal_U.dat</i> ' .....	<a href="#">132</a>
A simple model of above ground plant growth, ShootImitator module .....	<a href="#">134</a>
The data file ‘ <i>Param_p.dat</i> ’ .....	<a href="#">138</a>
Interfacing 2DSOIL with a crop model .....	<a href="#">138</a>
Chapter 11: Intrasoil Chemical Reactions: <i>MacroChem</i> Module	
Yakov Pachepsky .....	<a href="#">141</a>
Model of chemical interactions .....	<a href="#">141</a>
Equilibrium relationships .....	<a href="#">142</a>
The computer code of the chemical equilibrium model. ....	<a href="#">147</a>
Input files ' <i>Param_E.dat</i> ' and ' <i>Nodal_E.dat</i> ' .....	<a href="#">148</a>

Chapter 12: Nitrogen Transformation in Soil: <i>Soilnitrogen</i> Module	
Yakov Pachepsky and Dennis Timlin . . . . .	<a href="#">151</a>
Model of nitrogen transformation . . . . .	<a href="#">151</a>
Input files 'Param_N.dat' and 'Nodal_N.dat' . . . . .	<a href="#">157</a>
Rate correction factors for temperature and soil water content . . . . .	<a href="#">159</a>
Chapter 13: Input and Output of Data	
Yakov Pachepsky and Dennis Timlin . . . . .	<a href="#">163</a>
Data input . . . . .	<a href="#">163</a>
<i>DataGen</i> , A Simple Grid Generator . . . . .	<a href="#">164</a>
Conversion of units for chemical application . . . . .	<a href="#">166</a>
Output of simulation results . . . . .	<a href="#">167</a>
Error messages . . . . .	<a href="#">170</a>
Chapter 14: Example Problems	
Dennis Timlin and Yakov Pachepsky . . . . .	<a href="#">181</a>
Example 14.1: Alternate and furrow irrigation: root development . . . . .	<a href="#">181</a>
Example 14.2: Soil temperature regime in ridge and interridge zones as affected by plant development . . . . .	<a href="#">187</a>
Example 14.3: Leaching of the saline soil column . . . . .	<a href="#">190</a>
Example 14.4: Nitrogen dynamics in the soil and plant uptake of nitrogen . . . . .	<a href="#">195</a>
Chapter 15: Addition or Replacement of Soil Process Modules.	
Dennis Timlin and Yakov Pachepsky . . . . .	<a href="#">199</a>
Rules for introducing a new module . . . . .	<a href="#">199</a>
Overview of the examples . . . . .	<a href="#">201</a>
Example 15.1: A management module for chemical application . . . . .	<a href="#">201</a>
Example 15.2: Simulation of root respiration . . . . .	<a href="#">203</a>
Solute uptake module . . . . .	<a href="#">205</a>
The examples: Specific applications and simulation results . . . . .	<a href="#">212</a>
Example 15.1. A chemical application module: influence of the root system on chemical transport . . . . .	<a href="#">212</a>
Example 15.2: Adding a module of root respiration: a two-dimensional pattern of CO <sub>2</sub> content in soil induced by root respiration . . . . .	<a href="#">217</a>
Chapter 16: Modules and Variables of 2DSOIL	
Dennis Timlin and Yakov Pachepsky . . . . .	<a href="#">221</a>
Structure of the code . . . . .	<a href="#">221</a>
Notes on compiling 2DSOIL with different arrangements of subroutines . . . . .	<a href="#">226</a>
Variables of 2DSOIL.03 . . . . .	<a href="#">228</a>
LIST OF REFERENCES . . . . .	<a href="#">251</a>



## **ABSTRACT**

2DSOIL - A New Modular Simulator of Soil And Root Processes. Release 03 (March, 2001)

Dennis Timlin, Yakov Pachepsky, and Martinus Th. van Genuchten, Eds.

The various linkages in agricultural systems are so complex that research questions are often studied most effectively with the help of simulation modeling. The development and upgrading of detailed models requires a large investment of time and resources. Therefore, it is necessary to simplify the process of building the model and incorporating modifications as research finds new information to include. The goal of this study was to develop the framework for a generic soil simulator that could easily be modified and incorporated into crop models. Soil and root processes in the simulator are represented by modules that interact on the spatial-temporal grid covering the soil profile and the simulated time interval. Data were divided into public and private components to minimize information passing between modules. This modular structure and information hiding simplifies replacement or addition of modules and promotes code reuse. The classes of modules include: (a) control modules that oversee interactions between processes, (b) water, solute, heat, and gas transport modules, (c) interphase chemical transformation modules, (d) biochemical transformation modules, and (e) root growth and uptake modules. A representative simulator, 2DSOIL, was assembled according to the proposed design. Examples include the incorporation of 2DSOIL into a simple crop model and the expansion of 2DSOIL with a management module to simulate chemical application. The documentation includes instructions for adding customized modules.

## **TECHNICAL REQUIREMENTS AND TECHNICAL SUPPORT**

A 486 MS-DOS based personal computer is recommended. A DOS extender will be necessary if the program code size exceeds the conventional memory available (generally about 600K).

The authors of 2DSOIL used a FORTRAN77 compiler developed by the Salford Software Systems<sup>1</sup>. This software uses DBOS as a DOS extender. There are several calls to non-standard routines that are supported only by University of Salford compilers; these are present in only one subroutine to control screen output. The program can be linked without including this subroutine. We have used VISUAL FORTRAN, for details please contact the authors.

Work on 2DSOIL is a continuous effort. We encourage users to contact us if they have comments or suggestions, or if they find any problems. Two of the developers (Yakov Pachebsky and Dennis Timlin) are located at:

USDA-ARS Alternate Crops and Systems Laboratory Bldg. 007, Rm. 116, BARC-W	Timlin: 301-504-6255 <a href="mailto:DTIMLIN@ASRR.ARSUSDA.GOV">DTIMLIN@ASRR.ARSUSDA.GOV</a>
Hydrology and Remote Sensing Laboratory Bldg 007, Rm 104 10300 Baltimore Ave Beltsville, MD 20705	Pachebsky: 301-504-7468 <a href="mailto:YPACHEPSKY@ASRR.ARSUSDA.GOV">YPACHEPSKY@ASRR.ARSUSDA.GOV</a>

The best means of contact is through E-MAIL. Users should send us their E-MAIL addresses so that we can send them information and updates. Copies and updates can be obtained by using FTP to SOILPHYS.ARSUSDA.GOV. Use the username anonymous with your e-mail address as a password.

---

<sup>1</sup>Mention of a trade name or product does not constitute a recommendation or endorsement for use by the USDA

## LIST OF SYMBOLS

$\alpha$	parameter in soil water retention model, $\text{cm}^{-1}$
$\alpha_M$	characteristic time of mature root mass growth, $\text{day}^{-1}$
$\alpha_Y$	characteristic time of root maturity, $\text{day}^{-1}$
$\alpha_\diamond$	solar altitude, rad
$\alpha'_\diamond$	apparent solar elevation, rad
$\beta$	angle between row orientation and solar azimuth, rad
$\gamma$	psychrometric constant, $\text{kPa}\cdot(\text{°C})^{-1}$
$\gamma_I$	activity coefficient of univalent non-associated ion
$\Gamma_e$	boundary of element $e$
$\delta$	solar declination
$\Delta\epsilon$	water vapor pressure deficit, kPa
$\Delta l_y$	length of young roots that appear in a soil cell during a time step, cm
$\Delta m_R$	initial mass of roots in a soil cell when roots grow from another cell, g
$\Delta P_{M,D}$	turgor pressure available to expand a root after overcoming soil mechanical resistance, bar
$\Delta t$	time interval, day
$\Delta u$	threshold water uptake by new roots, g day $^{-1}$
$\epsilon$	canopy extinction coefficient
$\epsilon_t$	time weighing factor
$\varepsilon$	actual water vapor pressure for day, kPa
$\varepsilon_w$	saturated water vapor pressure at wet bulb temperature, kPa
$\zeta$	solar azimuth, rad
$\eta$	cloud cover factor
$\theta$	volumetric soil moisture content, $\text{cm}^3 \text{cm}^{-3}$ of soil
$\theta_l$	volumetric soil moisture content minus the exclusion volume of univalent anions, $\text{cm}^3 \text{cm}^{-3}$
$\theta_a$	parameter in soil water retention model, $\text{cm}^3 \text{cm}^{-3}$ of soil
$\theta_k$	parameter in soil water retention model, $\text{cm}^3 \text{cm}^{-3}$ of soil
$\theta_m$	parameter in soil water retention model, $\text{cm}^3 \text{cm}^{-3}$ of soil
$\theta_r$	residual water content, $\text{cm}^3 \text{cm}^{-3}$
$\theta_s$	soil moisture content at saturation, $\text{cm}^3 \text{cm}^{-3}$
$\vartheta_a$	air-filled porosity, $\text{cm}^3 \text{cm}^{-3}$ of soil
$\vartheta_{a,Tr}$	threshold value of air-filled porosity below which gas diffusion does not occur, $\text{cm}^3 \text{cm}^{-3}$
$\kappa_i$	weight coefficients showing proportion of actual root growth to potential growth in soil cell $i$
$\varkappa_i$	weight coefficients showing proportion of actual root water uptake to potential water uptake
$\Lambda$	thermal conductivity of the soil, $\text{J cm}^{-1} \text{C}^{-1} \text{day}^{-1}$
$\Lambda_a$	thermal conductivity of air, $\text{J cm}^{-1} \text{C}^{-1} \text{day}^{-1}$
$\Lambda_{cl}$	thermal conductivity of clay, $\text{J cm}^{-1} \text{C}^{-1} \text{day}^{-1}$

$\Lambda_{om}$	thermal conductivity of soil organic matter, $J \text{ cm}^{-1} \text{ C}^{-1} \text{ day}^{-1}$
$\Lambda_{da}$	thermal conductivity of dry air, $J \text{ cm}^{-1} \text{ C}^{-1} \text{ day}^{-1}$
$\Lambda_{ss}$	thermal conductivity of sand and silt, $J \text{ cm}^{-1} \text{ C}^{-1} \text{ day}^{-1}$
$\Lambda_v$	thermal conductivity of water vapor, $J \text{ cm}^{-1} \text{ C}^{-1} \text{ day}^{-1}$
$\lambda_L$	longitudinal dispersivity, cm
$\lambda_T$	transversal dispersivity, cm
$\mu$	relative change in soil hydraulic conductivity per unit pressure head, $\text{cm}^{-1}$
$v_c$	albedo of crop
$v_s$	albedo of soil
$\xi$	carbon supply ratio (proportion of carbon that was initially directed to the shoot but sent to roots due to water stress)
$\Pi$	precipitation (or irrigation), cm
$\pi_{R,D}$	root osmotic potential at dawn, bar
$\rho_R$	root mass per unit of soil volume, $\text{g cm}^{-3}$
$\rho_{R,T}$	threshold root mass per unit of soil volume, $\text{g cm}^{-3}$
$\rho_s$	soil bulk density, $\text{g cm}^{-3}$
$\sigma$	soil specific water capacity, $\text{cm}^{-1}$
$\tau_c$	tortuosity factor of solute diffusion
$\tau_g$	tortuosity factor of gas diffusion
$\nu$	row orientation measured eastward from north, degrees
$\varphi$	local latitude, degrees
$\phi_n$	finite element basis functions for node $n$ , $\text{cm}^2$
$\psi_L$	leaf water potential, bar
$\psi_R$	root water potential during the day, bar
$\psi_{R,D}$	root water potential at dawn, bar
$\psi_s$	soil water potential, bar
$\psi^{sa}$	average soil water potential in cells where new roots appear, bar
$\psi_{s,D}$	soil water potential at dawn, bar
$\Omega_e$	area of element $e$
$a$	atmospheric transmission coefficient
$\hat{a}$	coefficient of the basis function of triangular element, cm
$A$	area of the soil cell, $\text{cm}^2$
$A_C$	leaf area per unit soil surface area covered by crop canopy (leaf area index)
$A_{C,e}$	effective leaf area index allowing for the fact that light at low angles traverses more leaves to reach the soil
$A_L$	total plant leaf area, $\text{cm}^2$
$b$	coefficient of the basis function of triangular element, cm
$b_e$	saturation water vapor pressure change per one degree of temperature change, $\text{kPa}^{\circ\text{C}}{}^{-1}$
$b_g$	surface gas flux change per unit of gas content in soil air at the soil surface (gas transfer coefficient), $\text{cm day}^{-1}$
$b_R$	amount of carbon needed to produce one unit of root dry mass, $\text{g g}^{-1}$

$b_T$	surface heat flux change per degree of soil surface temperature (surface conductance of heat exchange), $\text{J} \cdot \text{cm}^{-2} \text{ day}^{-1} \text{ C}^{-1}$
$b_{tort}$	tortuosity change per unit of the air-filled porosity
$B_{R,max}$	rate at which carbon would be supplied to growing roots if all translocated carbon went to roots, $\text{g day}^{-1}$
$B_{R,min}$	rate at which carbon would be supplied to growing roots if all potential shoot growth had been satisfied, $\text{g day}^{-1}$
$B_V$	actual rate of carbon supply to vegetative parts of the shoot and root, $\text{g per plant per day}$
$B_{V,max}$	maximum rate of carbon supply to vegetative parts of the shoot and root, $\text{g per plant per day}$
$c$	solute concentration, $\text{g per cm}^3$ of the soil solution
$\hat{c}$	coefficient of the basis function of triangular element, $\text{cm}$
$\hat{C}$	total heat capacity of the soil solid material and water, $\text{J g}^{-1}$
$C_{om}$	heat capacity of soil organic matter, $\text{J g}^{-1}$
$C_{sm}$	heat capacity of soil solid mineral constituents, $\text{J g}^{-1}$
$C_w$	heat capacity of water, $\text{J g}^{-1}$
$CEC$	soil cation-exchange capacity, $\text{eq L}^{-1}$
$cs$	Michaelis-Menten constant of denitrification, $\text{g cm}^{-3}$
$d$	lateral distance from the row, $\text{cm}$
$d_{e,n}$	length of soil domain boundary segment which serves as border of element $e$ and ends at node $n$ , $\text{cm}$
$d_{rs}$	row spacing, $\text{cm}$
$d_{sc}$	radius of soil cylinder surrounding a root, $\text{cm}$
$d_{sh}$	width of shadow cast by row crop measured perpendicular to the row, $\text{cm}$
$d_{Tr}$	width of soil surface associated with transpiration, $\text{cm}$
$D_{0,st}$	gas molecular diffusion coefficient at standard conditions, $\text{cm}^2 \text{ day}^{-1}$
$D_g$	gas molecular diffusion coefficient in soil air, $\text{cm}^2 \text{ day}^{-1}$
$D_m$	ion or molecule diffusion coefficient in free water, $\text{cm}^2 \text{ day}^{-1}$
$D_{xx}$	solute dispersion coefficient reflecting dispersion in the 'x' direction caused by a concentration gradient in the 'x' direction, $\text{cm}^2 \text{ day}^{-1}$
$D_{xz}$	solute dispersion coefficient reflecting dispersion in the 'x' direction caused by a concentration gradient in the 'z' direction, or in the 'z' direction caused by a concentration gradient in the 'x' direction, $\text{cm}^2 \text{ day}^{-1}$
$D_{zz}$	solute dispersion coefficient reflecting dispersion in the 'z' direction that is caused by a concentration gradient in the 'z' direction, $\text{cm}^2 \text{ day}^{-1} E_c$
$E_{c,high}$	potential transpiration rate from the crop, $\text{cm day}^{-1}$
$E_{c,low}$	limiting value of transpiration rate above which transpiration does not influence plant resistance to water stress, $\text{cm day}^{-1}$
$E_s$	limiting value of transpiration rate below which transpiration does not influence plant resistance to water stress, $\text{cm day}^{-1}$
$E^a$	potential evaporation rate from soil surface, $\text{cm day}^{-1}$
fa	actual evaporation rate from soil surface, $\text{cm day}^{-1}$
	Fraction of the mineral nitrogen available for immobilization

$f_\pi$	factor describing ability of plant to osmoregulate when water stressed (= change in osmotic potential/change in water potential)
$f_{\text{Beer}}$	Beer's law correction for radiation interception
$f_c$	fraction of the solar radiation intercepted by the crop
$f_{\text{cl}}$	proportion of sky covered with cloud (1 - full cover)
$f_D$	proportion of total radiation that is diffuse
$f_D^0$	proportion of the diffuse radiation on cloudless days
$f_{Di}$	proportion of diffuse radiation intercepted by "solid" rows of plants assuming they are opaque cylinders
$f_{di}$	proportion of direct radiation intercepted by rows of plants
$f_e$	Microbial synthesis efficiency
$f_h$	Humification fraction
$f_{ET}$	correction factor to convert pan evaporation to potential evapotranspiration
$f_{CPR}$	proportion of carbon supply partitioned to root
$f_{rg}$	root growth reduction factor
$f_{str}$	water stress response function = proportion of potential transpiration rate that is actually used by plant
$f_R$	proportion of radiation not adsorbed by ozone or water vapor
$f_V^c$	correction factor for convection on hot, still days
$F_L$	latent heat of evaporation, $\text{J g}^{-1}$
$g$	gas content, g per $\text{cm}^3$ of the soil air
$g_{surf}$	gas content at the soil surface, $\text{g cm}^{-3}$ of the soil air
$g_{ox}$	soil oxygen content, g per $\text{cm}^3$ of soil air
$G_g$	surface gas flux component that does not depend on soil surface gas content, $\text{g cm}^{-2} \text{ day}^{-1}$
$G_T$	surface heat flux component that does not depend on soil surface temperature, $\text{J} \cdot \text{m}^{-2} \text{ day}^{-1}$
$h$	soil water pressure head, cm
$h_s$	air-entry capillary head, cm
$h_{2,high}$	the lowest soil water pressure head at which plant can maintain the potential transpiration rate, cm
$h_{2,low}$	the highest soil water pressure head at which plant can maintain the potential transpiration rate, cm
$H$	soil suction, cm
$H_c$	height of top leaves above soil, cm
$I$	ionic strength of the soil solution, $\text{mol L}^{-1}$
$I_e$	effective ionic strength of the solution, $\text{mol L}^{-1}$
$I_R$	rain intensity, $\text{cm day}^{-1}$
$J$	day of the year (Julian date)
$K_1$	selectivity coefficient of Ca-Na cation exchange
$K_2$	selectivity coefficient of Mg-Na cation exchange
$k$	soil hydraulic conductivity, $\text{cm}^3$ of water per $\text{cm}^2$ of soil per day
$\bar{k}$	average soil hydraulic conductivity over element, $\text{cm day}^{-1}$
$K_k$	parameter of the soil hydraulic conductivity model, $\text{cm day}^{-1}$

$K_s$	saturated hydraulic conductivity of soil, cm day <sup>-1</sup>
$k_h$	Potential mineralization rate fro the stable humus pool, day <sup>-1</sup>
$kL$	Potential plant residue decomposition rate, day <sup>-1</sup>
$km$	Potential rate of the organic fertilizer decomposition, day <sup>-1</sup>
$km'$	Potential rate of the organic fertilizer decomposition, day <sup>-1</sup>
$kn$	Potential rate of nitrification, day <sup>-1</sup>
$L_M$	density of mature roots in the soil cell, cm cm <sup>-3</sup>
$l_Y$	length of existing mature roots in the soil cell, cm
$l_y$	length of existing young roots in the soil cell, cm
$m$	concentration of non-associated ion or ion pair in the soil solution, mol L <sup>-1</sup>
$m'$	total analytical concentrations of ions in soil solution, mol L <sup>-1</sup>
$m_R$	root mass in soil cell, g
$M$	total contents of ions in the soil solution, soil adsorbing complex and soil solid salts expressed in mol per L of soil
$M_{Calc}$	content of solid calcite expressed in mol CaCO <sub>3</sub> per L of soil
$M_{Gyps}$	content of solid gypsum expressed in mol CaCO <sub>3</sub> per L of soil
$n$	parameter of the soil water retention model
$nq$	Ratio of the mineral nitrate amount to the mineral ammonium amount characteristic to the particular soil material
$n_g$	parameter of gas diffusion coefficient dependence on temperature
$n_{\Gamma_x}$	transversal component of the vector that has a unit length and is normal to the border of element
$n_{\Gamma_z}$	vertical component of the vector that has a unit length and is normal to the border of element
$N$	total number of observations in a data set
$N_e$	total number of elements
$N_n$	total number of nodes
$N_P$	total number of plants per meter of a row
$N_{S/D}$	nitrogen supply/demand ratio of the plant
$P_L^0$	leaf turgor pressure at the beginning of the interval, bar
$P_{LT}^0$	threshold leaf turgor pressure at the beginning of the time step, bar
$P_{CO_2}$	partial pressure of CO <sub>2</sub> in the soil air, MPa
$P_L$	leaf turgor pressure, bar
$P_{LT}$	threshold leaf turgor pressure at the end of time step, bar
$P_M$	soil mechanical resistance pressure, bar
$P_{M,D}$	soil mechanical resistance pressure at dawn, bar
$P_{R,D}$	root turgor pressure at dawn, bar
$P_{R,T}$	threshold turgor pressure at which root growth starts to grow, bar
$q_{e,n}$	water flux through soil domain boundary to/from element, cm day <sup>-1</sup>
$q_x$	volumetric water fluxes in 'x' direction, cm <sup>3</sup> of water per cm <sup>2</sup> of surface per day
$q_z$	volumetric water fluxes in 'z' direction, cm <sup>3</sup> of water per cm <sup>2</sup> of surface per day
$Q_g$	boundary gas flux, g cm <sup>-2</sup> day <sup>-1</sup> at the surface and g day <sup>-1</sup> or g cm <sup>-1</sup> day <sup>-1</sup> for inner boundary nodes

$Q_T$	boundary heat flux, $\text{J cm}^{-2} \text{ day}^{-1}$ at the surface and $\text{J day}^{-1}$ or $\text{J cm}^{-1} \text{ day}$ for inner boundary nodes
$r_0$	C/N ratio of the decomposer biomass and humification products
$r_L$	C/N ratio of plant residues
$r_m$	C/N ratio of the organic fertilizer
$r_c$	crop surface roughness parameter
$r_M$	total resistance of the water path from soil to leaf through mature roots, bar day $\text{g}^{-1} \text{ cm}^{-1}$
$r_{RM}$	radial resistance of mature roots, bar day $\text{g}^{-1} \text{ cm}^{-1}$
$r_{RY}$	radial resistance of young roots, bar day $\text{g}^{-1} \text{ cm}^{-1}$
$r_s$	resistance of soil to water flow to roots, bar day $\text{g}^{-1} \text{ cm}^{-1}$
$r_v$	root vascular resistance, bar day $\text{g}^{-1} \text{ cm}^{-1}$
$r_Y$	total resistance of the water path from soil to leaf through mature roots, bar day $\text{g}^{-1} \text{ cm}^{-1}$
$R$	actual radiation incident at earth's surface, $\text{W} \cdot \text{m}^{-2}$
$R_n$	actual radiation incident at earth's surface at noon, $\text{W} \cdot \text{m}^{-2}$
$R_{0,n}$	potential radiation incident at earth's surface at noon, $\text{W} \cdot \text{m}^{-2}$
$R_{00,n}$	radiation incident at the top of the atmosphere at noon, $\text{W} \cdot \text{m}^{-2}$
$R_d$	direct solar radiation flux at the earth's surface, $\text{W} \cdot \text{m}^{-2}$
$R_D$	diffuse solar radiation flux at the earth's surface, $\text{W} \cdot \text{m}^{-2}$
$R_i$	actual radiation incident at earth's surface, $\text{W} \cdot \text{m}^{-2}$
$R_I$	daily solar radiation integral, $\text{J} \cdot \text{m}^{-2}$
$R_{Nc}$	net radiation incident on the crop assuming complete cover, $\text{W} \cdot \text{m}^{-2}$
$R_{Ns}$	net radiation on the soil surface assuming bare soil, $\text{W m}^{-2}$
$R_s^e$	equivalent total radiation falling on the soil, $\text{W m}^{-2}$
$R_c^e$	equivalent total radiation intercepted by the crop, $\text{W m}^{-2}$
$R_u$	net upward long wave radiation, $\text{W} \cdot \text{m}^{-2}$
$S_{Ca}$	exchangeable calcium content expressed in mol per liter of soil
$S_{Mg}$	exchangeable magnesium content expressed in mol per liter of soil
$S_{Na}$	exchangeable sodium content expressed in mol per liter of soil
$S$	water extraction rate from the element (soil cell), $\text{day}^{-1}$
$\bar{S}$	average nodal water extraction rate from an element, $\text{day}^{-1}$
$\dot{S}$	nodal water extraction rate, $\text{day}^{-1}$
$S_c$	solute extraction rate, $\text{g cm}^{-3} \text{ day}^{-1}$
$\bar{S}_c$	average nodal solute extraction rate, $\text{g cm}^{-3} \text{ day}^{-1}$
$\dot{S}_c$	nodal solute extraction rate, $\text{g cm}^{-3} \text{ day}^{-1}$
$S_g$	gas extraction rate, $\text{g cm}^{-3} \text{ day}^{-1}$
$\bar{S}_g$	average nodal gas extraction rate, $\text{g cm}^{-3} \text{ day}^{-1}$
$\dot{S}_g$	nodal gas extraction rate, $\text{g cm}^{-3} \text{ day}^{-1}$
$t$	simulated time, days
$t_{dn}$	time of dawn, hours
$t_d$	daylength or photoperiod, hours
$t_{dk}$	time of dusk, hours
$T$	soil temperature, $^\circ\text{C}$

$t_{gr}$	time counted after emergence, day
$t_{maxhr}$	time of maximum air temperature measured from dawn, hr
$T_{min}$	minimum air temperature during the day, °C
$T_a$	air temperature, °C
$T_{dk}$	air temperature at sunset, °C
$T_{dry}$	dry bulb temperature, °C
$T_{max}$	maximum air temperature during the day, °C
$T_{mint}$	minimum air temperature during the next day, °C
$T_{surf}$	temperature at the soil surface, °C
$T_{wet}$	wet bulb temperature, °C
$T_y$	air temperature at sunset of the previous day, °C
$u$	actual value of water uptake by roots from soil cells, cm day <sup>-1</sup>
$u^0$	auxiliary value of water uptake by existing roots from soil cells, cm day <sup>-1</sup>
$U_1$	total water uptake by old and new roots for the leaf water potential equal to its threshold value and satisfied shoot growth, cm day <sup>-1</sup>
$U_2$	total water uptake by old and new roots when leaf turgor pressure equals to 2 bars and shoot does not grow, cm day <sup>-1</sup>
$U_B$	total water uptake by old roots for the leaf water potential equal to its value at the beginning of time step, cm day <sup>-1</sup>
$V$	wind speed at 2 m height, km hr <sup>-1</sup>
$W_R$	average root dry weight per unit length, g·cm <sup>-1</sup>
$x$	transversal coordinate (horizontal coordinate for planar flow and radial coordinate for the axisymmetrical flow), cm
$X_{om}$	volumetric fraction of an organic matter in soil, cm <sup>3</sup> per cm <sup>3</sup> of soil
$X_{sm}$	volume fraction of a mineral soil components
$z$	vertical coordinate directed upward, cm
$Z$	radius-vector of the Earth

# Chapter 1: Introduction and Background

Dennis Timlin and Yakov Pachepsky

## **1.1 The importance of two-dimensional soil modeling**

Farm management practices lead to dependencies of soil conditions on the distance from the plant row (Allmaras and Nelson, 1971; Logsdon et al., 1990; Logsdon and Allmaras, 1991). Management practices that affect the two-dimensional spatial distribution of soil and canopy conditions in row crops include the creation of soil ridges, furrow irrigation, placement of plant residues, banded fertilizer application, and mixed canopy geometry. Comprehensive soil models are needed to adequately represent the two-dimensional nature of management practices in row crops and their effects on the below-ground root environment.

Differences in soil conditions between row and interrow zones may have a large impact on the fate of applied agro-chemicals (Timlin et al., 1992). Agricultural chemicals that are not taken up by plants (or degraded into harmless by-products) may find their way into water supplies. A current research priority is to determine which agricultural management practices minimize the movement of chemicals to groundwater. Two-dimensional crop and soil simulation models have several advantages for research. One advantage is the ability to test the leaching potential of various hazardous compounds without actually applying them in the field. Another is to rapidly investigate the effects of different management actions on chemical movement in soils.

Comprehensive soil models, such as RZWQM and LEACHM, are one-dimensional. Existing two-dimensional soil models take into account very few soil processes (Šimůnek et al., 1992; Benjamin et al., 1990). Nevertheless, these models demonstrate the usefulness of a two-dimensional approach for quantifying the multi-dimensional nature of the soil environment under row crops. Plant growth models, which recently have become quite sophisticated, still rely on

simplified representations of soil processes. As a result, the predictive capabilities of these models are less than optimal.

A major drawback to the effective incorporation of sophisticated soil codes into plant models has been the complexity of the soil codes. Usually, the more processes a modeler attempts to incorporate, the more complex the model becomes.

The purpose of this project was to develop a comprehensive simulator for two dimensional soil problems with a modular structure that would simplify model development and maintenance. This goal is to simplify the integration of soil code with a crop model. This document describes a soil simulator, 2DSOIL, that provides for ready replacement of modules, simple addition of new modules, and consequently, an ability to select modules that correspond to the soil properties under consideration. The majority of soil-crop modelers use FORTRAN, and so this language has been chosen for this soil simulator. 2DSOIL is not offered as a finished product but as a vehicle for other scientists to test their own modules and to assemble plant-soil models that correspond to their own problem environments.

## **1.2 The design of 2DSOIL**

### **1.2.1 Modular Design**

The purpose of decomposing a system into modules is to be able to hide code and data from programmers modifying other modules in the system (Einbu, 1994). The goal is to separate the user of the module from the developer (Thomas, 1989). Modules should be designed in a manner that will enhance reuse, maintainability, and reliability of the code. This goes beyond previous philosophy where modularization was influenced by the 'everything is a hierarchy' view of programming (Kirk, 1990). Modules should have loose inter-unit coupling and high internal cohesion (Witt et al., 1994). Loose coupling is characterized by independence, a simple interface between modules, a limited number of interfaces, and a minimum of information passing. High cohesion is characterized by interdependent elements packaged together and information hiding (Blum, 1992; Witt et al., 1994).

The design requirements for modules as outlined above do not require a special programming language (Blum, 1992), although they are more easily implemented using an object oriented programming (OOP) language. In OOP, each object (module) contains specific information (data) and is coded to perform certain operations (functions). Our design, which is coded in FORTRAN, follows OOP precepts as far as possible, but within the constraints of FORTRAN. Loose coupling is implemented by having each module input and manage its own data. By doing this, the functions and data are kept together in the object (module). High cohesion is achieved by developing distinct, independent modules, each for a specific soil or root process.

Soil and root processes belong to one of the following classes:

- transport processes, e.g., water, heat, nitrate, and oxygen movement;
- root processes, e.g., water uptake,  $\text{NH}^{+4}$  uptake, root respiration;
- interphase exchange processes, e.g., reversible  $\text{Ca}^{2+}$  exchange;
- biotransformation processes, e.g., denitrification,  $\text{CO}_2$  respiration;
- management processes, e.g., tillage, ammonium phosphate application.

The soil and root process modules in 2DSOIL are based on this grouping (Fig. 1.1). Note that every class is on the same level, and hence that there is no hierarchy among the classes. Each class may include several process modules. The design assumes that only process modules needed in a particular application will be included in the simulator.

### **1.1.1 Data and the interaction of modules**

Modules interact by passing or sharing data. To share data among process modules, the data must be represented consistently in all modules. To provide for loose coupling of modules, the amount of data accessible to all modules must be minimized. The minimum data set available to all modules has to be independent of the model or algorithms used to represent the processes, and must also be sufficient to describe the state of the system at any particular time. The soil and root environment is partly characterized by the volumetric contents of substances (e.g., water content, bulk density, oxygen concentration, and root length density). Potentials of physical fields and related physical values are also used, e.g., matric potential, and temperature. These

values are state variables of the soil-root system. The state variables are subject to changes caused by fluxes of energy or matter into or out of the system. Calculations of changes in one soil state variable may require the values of several other soil state variables. For instance, temperature and soil water content are needed to calculate changes in ammonium concentration caused by nitrification. Similarly, several processes may contribute to changes in the concentration of a particular substance. For example, both root respiration and decomposition of organic materials contribute to carbon dioxide production and uptake. Therefore, soil state variables and fluxes have to be available to all modules.

Values of the soil and root state variables can be recorded and calculated for specific locations within a soil profile; these locations must be the same for all modules. The spatial reference system in the generic simulator is introduced by a spatial grid which is a polygonal geometric structure representing either a vertical profile of the soil for the one-dimensional mapping of soil variables, or a vertical plane cross-section for the two-dimensional case. The grid is discussed in greater detail in Section 3 of this manual.

Modules have to be synchronized to calculate state variables and fluxes for simulated times which are the same for all modules. To do this, we used a sequential iteration approach (Yeh and Tripathi, 1991) in which process modules are execute sequentially as shown in Fig. 1.2. It is assumed that the values of fluxes are available at the beginning of each time step, before the transport codes are called. Each process module may have its own requirements for a time increment at any point in the simulation. For example, the time interval between fertilizer applications can be two months, the atmospheric boundary can be modified hourly, and calculations of infiltration may require time increments on the order of seconds. Combining

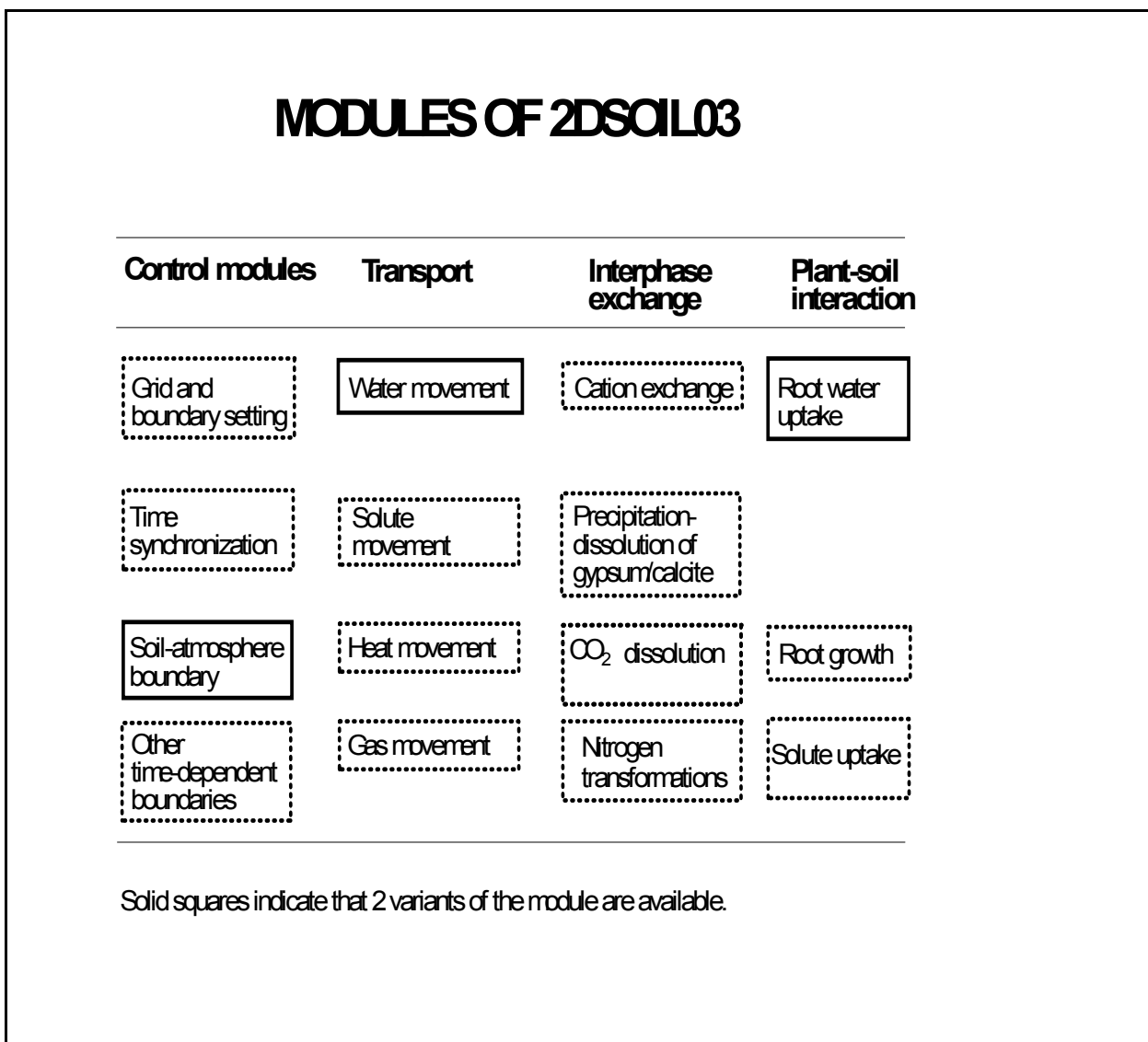


**Figure 1.1** Modules of 2DSOIL release 03

modules which work with different time steps into one simulator, is referred to as asynchronous coupling (ten Berge et al., 1992).

The general data structure that allows modules to be loosely coupled constitutes the framework of the generic simulator. This framework is supported by control modules. If a process module (such as a plant model) follows this framework, it can be included in the

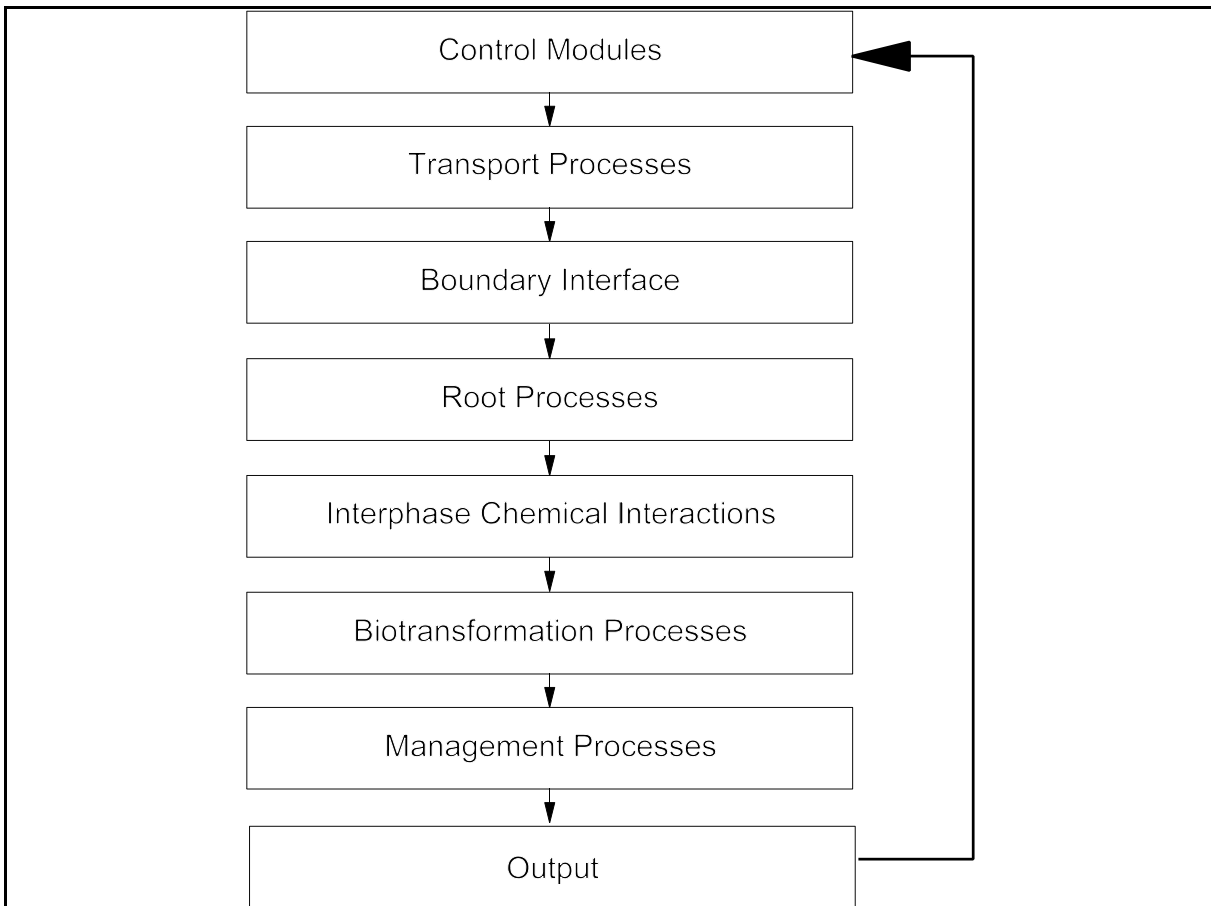


**Figure 1.2** Flow chart illustrating the sequence of operations in 2DSOIL

simulator. The control module '*Synchronizer*' chooses the actual time step that the whole simulator will use. It is invoked at the beginning of every time step and uses as input the requirements of all modules for the next time step and the numbers of iterations that have occurred during the previous time step as. *Synchronizer* calculates the optimum time increment that (a) allows for convergence of iterations within modules and, (b) enables the simulator to read or to deliver data at specified times. If there are no modules with time step requirements, the

time step will increase gradually until it reaches a prescribed maximum value. Current time step, simulated time, number of iterations, and time step limitations are also available to all process modules to use.

### 1.1.2 Data structure

We used the concept of encapsulation of information to facilitate the independence of the modules. Encapsulation, a characteristic of object oriented programming, is the grouping into a

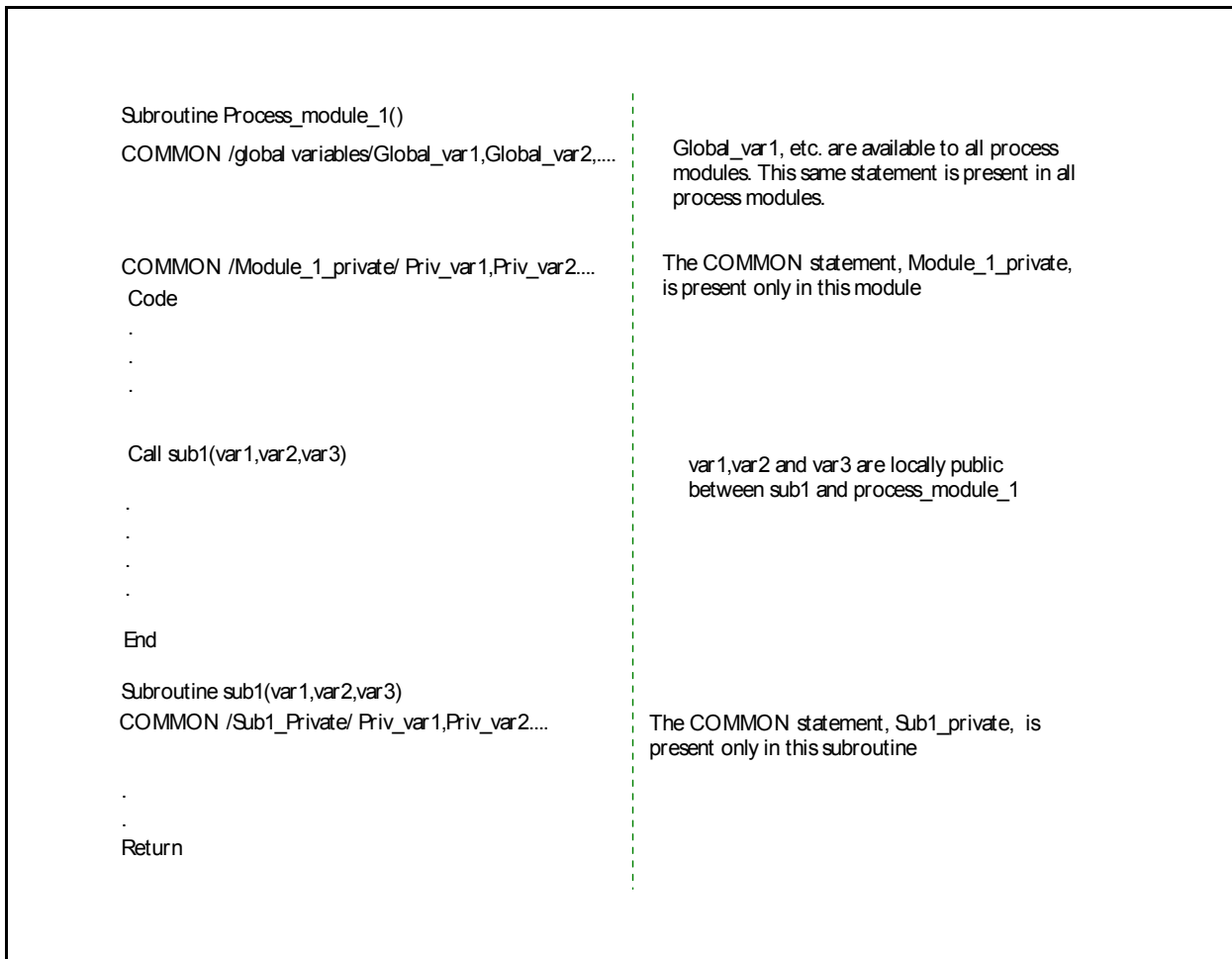


**Figure 1.3** Illustration of the implementation of global, locally public, and private variables in 2DSOIL

single module of both data and the operations that modify or use those data (Wirfs-Brooks et al.,

1990). The data and operations, encapsulated in a single module, can be hidden from the developers of other program units.

In order to implement data encapsulation in FORTRAN, public variables, i.e. variables available to all modules, were gathered into a separate public data field (Fig. 1.3). This global public field includes soil and root state variables, fluxes, nodal coordinates and temporal variables described in the previous section. Each process module also has its own private data field which is not available to other process modules (Fig. 1.3). Such a field may include control variables to read or print data, parameters of the numeric algorithms coded in the module, state variables and fluxes from the previous time step, and variables for communication between submodules that calculate coefficients in the model equations. If any module requires data from an external file to fill its private data field, the module opens and reads that file itself. A module can also produce output according its own schedule.

Submodules that calculate coefficients for specific equations are also encapsulated within modules. Neither data nor equations of submodules are needed for the functioning of other process modules. The recommended data structure includes a subdivision of the private information of each process module into information that is locally public within the module, i.e., available to all submodules, and information that is hidden within submodules (Fig. 1.3). The hidden information is read independently and therefore the submodule can be easily replaced or modified. A need to replace a submodule is as common as a need to replace a process module. Consider, for example, the water movement module that requires hydraulic conductivity values and water content as a function of water potential. It may be desirable to be able to replace the equations that calculate these values (Alessi, 1992). The replacement will not affect the process module which needs the value of the hydraulic conductivity. Therefore, the submodule can read its own parameters from its own data file and have them hidden from the process module and the whole simulator.

Global public variables are passed in COMMON blocks to modules and submodules; no arguments are used in CALL statements at the process level. Errors are minimized by the use of INCLUDE statements, so as to insert a file containing a list of named COMMON blocks into each process module. If it is desirable to transfer certain private variables into a public field, then only the insert file referenced in the INCLUDE statement has to be changed. Locally public

variables, i.e. variables shared between process modules and submodules, are passed by means of CALL statements.

COMMON blocks are also used to store private information within a module or submodule. This feature saves the value of any private variables between invocations of a subroutine. COMMON blocks containing private information are present in only one module. Because there is no reference to this block in other program units, the information remains hidden.

### **1.1.3 Structure of a process module**

The general sequence of operation in each process module (Fig. 1.3) consists of reading the time-independent data, calculating the auxiliary variables to determine the optimum time step, checking whether it is time to execute a block of code representing a process, and (if it is time to execute) reading the time-dependent data, changing the public variables, changing the private variables, calculating the requirements for time increments, and providing output data. Several of these steps may be absent in certain process modules.

<pre> Subroutine Mngm() Include 'public.ins'  Common /Mngmt/ tAppl, cAppl, NumAp, nAppl(NumBPD),       Mod_Num  If(LInput.eq.1) then   Open(40,file='Param_M.dat')   Read(40,*,Err=20) tAppl, cAppl, NumAp    Read(40,*,Err=20) (nAppl(i),i=1,NumAp)    Num_Mod=Num_Mod+1   Mod_Num=Num_Mod    tNext(Mod_Num)=tAppl   Close(40)  Endif If(Abs(Time-tNext(Num_Mod)).lt.0.1*Step) then   Do i=1,NumAp     Conc(nAppl(i))=cAppl/ThNew(nAppl(i))   Enddo   tNext(ModNum)=1.E+32 Endif Return 20 Stop 'Mngm data error' End </pre>	<p>Public variables are in "Public.ins"</p> <p>Private information is in a common block</p> <p>Input time independent information Time of application Total mass of chemical per node Number of nodes where applied</p> <p>Node numbers to which chemical is applied</p> <p>Update the number of modules and assign a number to this module Assign the execution time for this module</p> <p>If it is time to carry out any calculations change public variables generate the next proposed time step (only one application here so the next time step is assigned an unreachable value)</p>
---	--

**Figure 1.4** Basic structure and sequence of operations in a process module.

An example of a typical module is shown in Fig. 1.4. This module simulates a chemical application. At the start of the module, designated by the public variable *LInput*, the module reads time-independent private data that are listed in the private COMMON block. The number, *NumMod*, of the module in the invocation sequence is used as an index for arrays that hold time step requirements for each module. This number is stored as private information. The public variable *tNext* stores the time- to- execute code for this particular activity; therefore, one of the future time steps has to terminate exactly at this time. When the execution time comes, concentrations of the chemical (which are public) in prescribed nodes are changed by dividing mass of chemical applied (which is private) by soil water content (which is public). Finally, the public variable *tNext* is assigned an unreachable value which means that there are no further calls on this module.

## **1.2 Modules of 2DSOIL Release 03**

The second version of 2DSOIL contained a number of soil processes: water flow, simultaneous convective-dispersive transport of several solutes, heat transport, gas movement, root water uptake, root growth, cation exchange, and carbonate-hydrogen chemistry in the soil solution. In this third version we have added nitrogen transformations along with an additional example (see Chapter 12). 2DSOIL has also been interfaced with a potato model; details are available in a separate documentation. A soil grid manager, a time synchronizer, a soil-atmosphere boundary manager, and a time-dependent boundary definer are the required modules.

The management of time synchronization and ordering of modules has also been changed. The module *Synchronizer* is now called at the beginning of the program. There is no longer an Object\_Time module and Obj\_Time.Dat file. The latter has been replaced by the file Time.Dat. The modules are now given identifying numbers (ModNum) dynamically as the program executes.

Several modules of 2DSOIL were adopted from other simulators in the public domain. All adopted codes were transformed to fit the modular structure of 2DSOIL. A careful comparison and selection process was followed in order to find the most reliable and computationally efficient codes. References are given in the sections that describe each module.



# Chapter 2: Definition of Objects and Time Stepping; the Synchronizer Module

**Yakov Pachepsky and Dennis Timlin**

## 2.1 Function of the modules

The structure of 2DSOIL allows a modeler to use a subset of the modules that represent the soil-root processes of interest. There is no need to prepare data files for processes that are not needed in the simulations. As each process module is called, a variable, *NumMod*, is incremented. Use of this variable allows an identifying number to be associated with each module; this number is generally used as an array index.

Selection of the time step is an extremely important part of the total calculation procedure. Several rules were adopted from other studies (Shcherbakov et al., 1981; Vogel, 1987; Šimůnek et al., 1991) to regulate the time stepping in 2DSOIL:

- (1) Any transport module may have restrictions on the time step that are connected with the numerical stability of calculations. These possible time step values are supplied by the modules themselves and are stored in the public *DtMx* array. *DtMx(i)* corresponds to the *i*th module (identified by the variable *ModNum*) according to Table 2.1.
- (2) If a certain module has an iterative numerical procedure and convergence of this procedure depends on the time step, then the calculations will start with a very small time step, *Step*, to ensure convergence.
- (3) If the number of iterations during the previous time step was less than a particular threshold, the time step is increased by *dtMul1* times. If the number of iterations was larger than a threshold value during the previous time step, then the time step is reduced by *dtMul2* times. The public variable *Iter* contains the number of iterations.

- (4) If a scheduled change in the boundary conditions or in the spatial distribution of a variable is expected, then one of the time steps must be finished exactly at the time of such a change.
- (5) If some module has its own time stepping schedule, then the end of its last time step must coincide with the end of one of the time steps generated for the whole program.
- (6) If the results are to be printed to a file, then the time step must be chosen so that the time coincides with the time specified for output.
- (7) If there is a large difference between the time step values allowed by rules (1)-(3) and by (4)-(6), then the time step allowed by (1)-(3) is halved to prevent sharp changes in the time step value.
- (8) If during the calculations the time step becomes smaller than some threshold value, then the calculations are ended.

Applied together, these rules, in general, provide smooth time stepping. The **Synchronizer** module reads the step control constants from the '**Time.dat**' file and calculates time steps for the overall program according to the rules mentioned above. The model itself has only one time step at any particular point in the simulation. Although each process module may have its own requirement with respect to the time step, the purpose of the **Synchronizer** module is to evaluate all requirements and then choose a time step to satisfy the the process module with the most limiting requirement. The file **Time.dat** contains the parameters for controlling the time step control of overall program which are global in scope.

## **2.2 Input file *Time.dat***

The structure of this file is shown in Table 2.2. A reasonable value for the initial step may be  $(tFin-Time)/10^6$ . A reasonable value for the minimum time step may be  $(tFin-Time)/10^{12}$ . The value *DtMul1* is within the range (1.1;1.5) and the *DtMul2* value has the range.

Table 2.1. Format of the file **Time.dat**.

Record	Type	Variable	Description
<b><u>Time Stepping Control Parameters</u></b>			
1	-	-	Comment line.
2	<i>Time</i>		Initial time.
2	<i>Step</i>		Initial time increment $\Delta t$ [ T ].
2	<i>dtMin</i>		Minimal acceptable time step [ T ].
2	<i>dtMul1</i>		If the number of iterations required at a particular time step is less than or equal to 3, then $\Delta t$ for the next time step is multiplied by a dimensionless number $dtMul1 \geq 1.0$ .
2	<i>dtMul2</i>		If the number of required iterations is greater than or equal to 7, then $\Delta t$ for the next time step is multiplied by $dtMul2 < 1$ .
2	<i>tFin</i>		Time to stop calculations.

The following example of the file **Time.dat** illustrates the format for the data required by the module:

```
**** Example 2.1: INPUT FILE 'TIME.DAT'
Time Step dtMin dtMul1 dtMul2 tFin
0      1.E-05 1.E-11   1.33     0.7    10
```

A free-format is used in 2DSOIL. The position and format of numbers in a record are arbitrary, although the sequence of numbers cannot be changed. Note that the units of time can range from days to seconds. Any consistent set of units must be used. Hence the units for other parameters, such as the hydraulic conductivity ( $L T^{-1}$ ), must be consistent with the adopted time.



## **Chapter 3: Grid and Boundary Settings:**

### ***Get\_Grid\_and\_Boundary Module***

**Yakov Pachepsky and Dennis Timlin**

Values of the soil and root state variables are recorded and calculated for specific locations within a soil profile, and these locations have to be the same for all modules. The spatial reference system in 2DSOIL is represented by a spatial grid (Fig. 3.1) which has a polygonal geometric structure representing a vertical plane cross-section of the soil. The grid illustrated in Fig. 3.1 is for a soil system where the soil surface has the shape of a ridge and furrow. The spatial locations where values of the state variables and fluxes are known are called nodes. The nodes provide the necessary spatial reference for interactions among soil and root processes, and for the boundary interface with plant and atmosphere models. The nodal coordinates, therefore, have to be available to all modules. The nodal coordinate system is also needed for the numerical solution of transport equations that describe the movement of water, solutes, heat, and gases in the soil. The nodal grid is set by the control module **Get\_Grid\_and\_Boundary**.

#### **3.1 Grid setting**

The 2DSOIL code does not generate the grid, it simply reads data defining the grid from the input file '**Grid\_bnd.dat**'. Since the program is very much oriented to the use of the finite element method for numerical estimation of intrasoil transport, data for nodes (grid nodes) and elements (grid cells) are both required. If the user replaces a soil transport process module with another that uses the finite difference numerical technique, then the information on elements is not used.

The coordinate system of 2DSOIL uses a vertical coordinate that is zero at the base of the profile and increases upwards. Both radial and planar geometry can be considered. The grid may

consist of quadrilateral and triangular elements. The only definite requirement is the continuity and non-intersection of horizontal grid lines (Neuman, 1972; Šimůnek et al., 1992). For practical purposes this means that there is a layer of quadrilateral elements between any pair of horizontal lines. Triangular elements may exist at the boundaries. An example of a simple grid with triangular and quadrilateral elements is shown in Fig. 3.1.

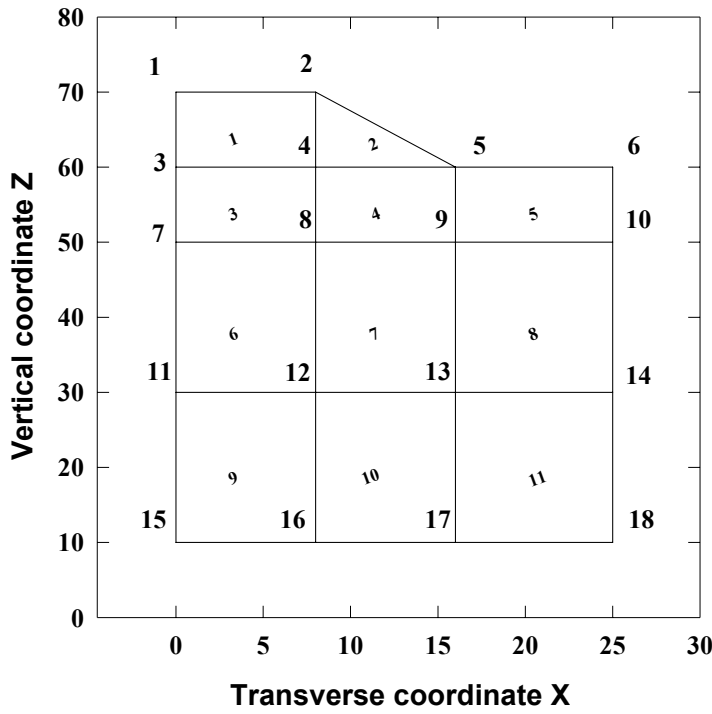


**Figure 3.1** An example of the grid for a soil domain with numbered nodes and elements (soil cells).

It is preferable from a computational point of view, but not essential, to number nodes along the direction (vertical or horizontal) in which the number of nodes is the least. If, for example, the grid has a maximum of 25 nodes horizontally and a maximum of 10 nodes vertically, then the numbering should be along the vertical lines. Node number 1 must be in the upper left corner of the grid. In general, element numbering is in the same direction as node

numbering as illustrated in Fig. 3.1. There are no definite recommendations for selecting sizes and total number of elements although it is desirable to have neighboring elements with dimensions that differ by no more than about 1.5 times. It is also important to have the smallest elements in the zones of high gradients (Šimůnek et al., 1992). In general, a 200-node grid should be able to give a reasonably good description of the transport processes in soil.

The two-dimensional soil domain may contain several subdomains containing soils with different properties. The subdomains typically represent soil genetic horizons, but may also represent soil plow layers and plow-pans, and different soil materials in row and interrow positions, among other features. Subdomains must be numbered and the number of each subdomain will be referenced for every node and element that lies in the subdomain. Coordinates and a soil subdomain number are given for every node. The subdomain is referred to by a material number that is stored in the public variables  $MatNumN(i)$ , with  $i$  varying from one to  $NumNP$ , the total number of nodes. Elements of the grid each have an identifying number, and four corner nodes  $KX(e,1)$ ,  $KX(e,2)$ ,  $KX(e,3)$ ,  $KX(e,4)$  associated with them. The corner nodes are numbered counter-clockwise. The third and fourth node number are the same for triangular elements. In addition to corner node numbers, the elements also have soil subdomain material numbers  $MatNumE(e)$ ,  $e=1,2,\dots, NumEl$ ; where  $NumEl$  is the total number of elements.

### **3.2 Codes for boundary nodes**

A code must be associated with every boundary node where matter or energy enters or leaves the system. The codes used in 2DSOIL are given in Table 3.1. The source numbering system is used in several older finite element models (Šimůnek et al., 1992).

In general, 2DSOIL uses three types of boundary conditions for water, solute, heat, and gas movement:

- (1) First-type boundary conditions, where the state variable is constant, i.e., the pressure head, solute concentration, temperature, or gas content is constant at the boundary node during the entire simulation time, or the state variable has constant values during several time intervals;

- (2) Second-type boundary conditions where the flux of water, solute, heat, or gas is prescribed during the simulation time, or where this flux has constant values during several time intervals;
- (3) Third-type boundary conditions at the soil-atmosphere boundary where the flux is dependent also on the soil surface condition.

Nodes that are coded with numbers -4 and +4 are at the external boundaries of the soil domain. Nodal codes +6 and -6 are applied to intrasoil sources and sinks of energy or matter (for example, a drainage tile or hot water line). Water, solute, heat, and gas transport codes are stored in the public variables  $CodeW(i)$ ,  $CodeS(i)$ ,  $CodeH(i)$ , and  $CodeG(i)$ , respectively, where index  $i$  varies from one to  $NumBP$ , the total number of boundary nodes. Codes of boundaries for different transport processes do not have to coincide. For example, if leaching of solute from the soil is considered and the pressure head on the column surface is constant but the concentration of solute in the leaching water is time-dependent, then the nodes of this upper boundary will have code 1 for water movement and code 3 for solute movement. If some boundary nodes for water flow correspond to an impermeable layer, then these nodes are coded by zeroes for solute (heat or gas) boundaries. Thus, the total number of boundary nodes for water, solute, heat, and gas are always the same.

Table 3.1. Codes for boundary nodes.

code	Type of boundary			
	Water movement	Solute movement	Heat movement	Gas Movement
0	Impermeable surface	Impermeable surface	Impermeable surface	Impermeable surface
1	Constant pressure Constant moisture content	Constant solute concentration	Constant temperature	Constant gas content in soil air
2	Saturated seepage face	-	-	-
-2	Unsaturated seepage face	-	-	-
3	Time-dependent pressure head	Time-dependent concentration	Time-dependent temperature	Time-dependent gas content
-3	Time-dependent water flux	Time-dependent solute flux	Time-dependent heat flux	Time-dependent gas flux
4	Soil-atmosphere boundary with prescribed pressure head	Soil-atmosphere boundary with prescribed concentration	Soil atmosphere boundary with temperature prescribed	Soil atmosphere boundary with gas content prescribed
-4	Soil-atmosphere boundary with prescribed water flux	Soil-atmosphere boundary with prescribed solute flux	Soil atmosphere boundary with heat flux prescribed	Soil atmosphere boundary with gas flux prescribed
6	Time dependent pressure within soil domain	Time dependent concentration within the soil domain	Time-dependent temperature within soil domain	Time-dependent gas content within soil domain
-6	Time dependent water flux within soil domain	Time-dependent solute flux within soil domain	Time-dependent heat flux within soil domain	Time-dependent gas flux within soil domain

At the soil-atmosphere boundary, one must initially set *CodeW*=-4. The **WaterMover** module will later distinguish between the case of -4 for a period of evaporation and +4 for a period of precipitation. Note that irrigation should be coded as +3 or -3, i.e., time dependent pressure or water flux. Sprinkler irrigation, however, can also be set in the weather file or **SetSurf.dat** as rainfall.

The soil boundary can include seepage faces, i.e., segments where water can flow out of a saturated soil under hydrostatic pressure. Seepage faces are coded 2 if they are initially saturated and -2 if they are initially unsaturated. Presumably seepage takes place along the whole seepage face. Therefore, additional information is required to show which nodes belong to a particular seepage face. The variable *NSeep* gives the number of seepage faces and is an input parameter. If *NSeep*=0, then no further information on seepage faces is necessary. If *NSeep* ≠ 0, then the number of nodes *NSP* and a list of nodes *NS* are to be given for every seepage face (Table 3.1).

Every boundary node must also have an associated width that is necessary for flux calculations. In the case of planar flow the variable *Width* has the unit of length, whereas for axisymmetric flow the unit in area. The strip associated with the boundary node is perpendicular to the direction of the prescribed flux. The method to determine a value for *Width* is illustrated in Fig. 3.2. In Fig. 3.2a boundary nodes  $N_1$ ,  $N_2$ , and  $N_3$  lay on the horizontal soil-atmosphere surface where fluxes are in the vertical plane. The length of segment AB is the width associated with node  $N_2$ , here  $AB = \frac{1}{2}(x_2-x_1) + \frac{1}{2}(x_3-x_2)$ . In Fig. 3.2b, boundary nodes  $N_4$ ,  $N_5$  and  $N_6$  are located at the vertical boundary of the soil domain where the fluxes are in the horizontal plane. The length of segment CD is the width associated with node  $N_5$ ,  $CD = \frac{1}{2}(y_4-y_5) + \frac{1}{2}(y_5-y_6)$ . In Fig. 3.2c, boundary nodes  $N_7$ ,  $N_8$ , and  $N_9$  are situated on the horizontal soil-atmosphere surface and flow is axisymmetrical. The area of the dashed annulus is the width associated with node  $N_8$ . The internal radius of this ring is equal to  $\frac{1}{2}(x_8-y_7)$  and the external radius is equal to  $\frac{1}{2}(x_9-x_8)$ . In Fig 3.2d the nodes  $N_{10}$ ,  $N_{11}$ , and  $N_{12}$  are positioned on the vertical boundary and flow is now axisymmetrical. The area of the dashed strip equals the width of the strip associated with node  $N_{11}$  and is equal to  $\frac{1}{2}(y_{10}-y_{11}) + \frac{1}{2}(y_{11}-y_{12})$ .

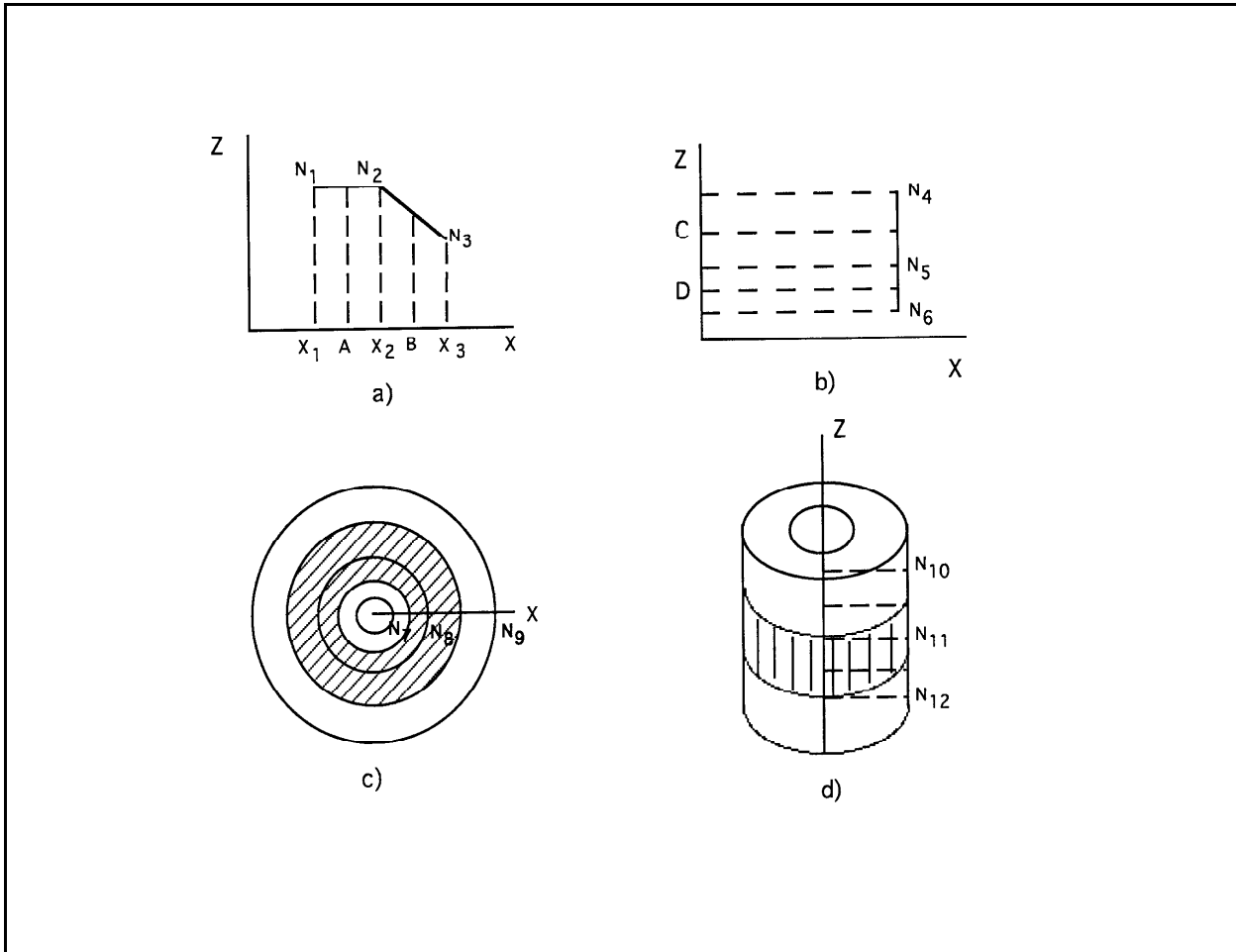


**Figure 3.2** Derivation of the *Width* value: (a) transversal boundary, planar flow, (b) vertical boundary, planar flow, (c) transversal boundary, axisymmetrical flow, and (d) vertical boundary, axisymmetrical flow. Additional comments are in the text.

### 3.3 Grid Data file *Grid\_bnd.dat*

A description of the file content is given in Table 3.2. This table is followed by Example 3.3, an illustration of a grid data file which has been constructed for the grid in Fig. 3.1 to show several features of the code. Other examples of grids can be found in Chapter 14 of this manual.

In the grid file given in Example 3, soil properties are considered to differ for the layers above and below the line  $z=50$  cm. The example file listing illustrates the use of the values of

*MatMumN* and *MatNumE*. Nodes 5 and 6 are at the bottom of a ditch. The level of water in the ditch is constant and therefore *CodeW* is 1 for these nodes. At the same time it is desired to change the concentration of the solute in the water over time, so that *CodeS* is 3 for these nodes. Heat transport is not considered; hence, the value of *CodeH* is set to zero. Since the bottom of the ditch is impermeable to gases, *CodeG* is zero there also. Nodes 1 and 2 are at the soil-atmosphere boundary; therefore, *CodeW* and *CodeS* have the value of -4. For purposes of this example, the gas fluxes will be determined as known time-dependent variables without any relation to atmospheric conditions. Thus, *CodeG* is equal to -3 and not to -4. Node 12 represents a tile drain where water is subject to positive hydrostatic pressure. The pressure head and concentration of the solute will be constant (*CodeW*=1 and *CodeS*=1). The pressure head is specified in the file used to initialize pressure heads (**Nodal\_w.dat**) and described in a later chapter (6). Nodes 15-18 represent an initially unsaturated seepage face and, hence, the gas content in soil air is assumed to be constant there since air are in contact with the atmosphere outside the soil boundary. The value of *Width* at node 2 is equal to 8.0 because the fluxes to/from the atmosphere are parallel to the *z* direction.

Table 3.2. Format of the file '**Grid\_bnd.dat**'.

Record	Variable	Description
1	- - -	Comment line. <u>Dimensions</u>
2	- - -	Comment line.
3	<i>KAT</i>	Type of flow system to be analyzed 1 for axisymmetrical flow 2 for vertical flow in a cross-section.
3	<i>NumNP</i>	Number of nodes.
3	<i>NumEl</i>	Number of elements (quadrilateral and/or triangular).
3	<i>NumBP</i>	Number of boundary nodes for which boundary conditions are prescribed.
3	<i>IJ</i>	Maximum number of nodes along a transverse grid line (this is number of nodes along the horizontal or vertical transverse line that has the largest number of nodal points).
3	<i>NMat</i>	Total number of soil subdomains in the soil domain.
		<u>Nodal Information</u>
4	- - -	Comment line.
5	<i>n</i>	Nodal number.
5	<i>x(n)</i>	<i>x</i> - coordinate of node <i>n</i> [units=L] (always a horizontal coordinate).
5	<i>z(n)</i>	<i>z</i> - coordinate of node <i>n</i> [units=L] (always a vertical coordinate).
5	<i>MatNumN(n)</i>	Index for soil subdomain associated with node <i>n</i> . Record 5 is required for each node <i>n</i> , starting with <i>n</i> =1 and continuing sequentially until <i>n</i> = <i>NumNP</i> .
		<u>Element Information</u>
6,7	- - -	Comment lines.
8	<i>e</i>	Element number.
8	<i>KX(e,1)</i>	number of corner node 1.
8	<i>KX(e,2)</i>	number of corner node 2.
8	<i>KX(e,3)</i>	number of corner node 3.
8	<i>KX(e,4)</i>	number of corner node 4. Indices 1,2,3, and 4 refer to corner nodes of an element <i>e</i> taken in a counter-clockwise direction. For triangular elements <i>KX(e,4)</i> must be equal to <i>KX(e,3)</i> .
8	<i>MatNumE(e)</i>	Index of soil subdomain that is associated with element <i>e</i> . Record 8 is required for each element <i>e</i> , starting with <i>e</i> =1 and continuing sequentially until <i>e</i> = <i>NumEl</i> .

Table 3.2 - continued.

Record	Variable	Description
<u>Boundary Information</u>		
9,10	- -	Comment lines.
11	$n$	Boundary node number.
11	$CodeW(i)$	Code specifying the type of <i>water</i> movement boundary condition applied to the node. Permissible values are 0, 1, $\pm 2$ , $\pm 3$ , $\pm 4$ , $\pm 6$ (see Section 3.2). Index $i$ denotes the sequential number on the boundary node $n$ in this file.
11	$CodeS(i)$	Code specifying the type of <i>solute</i> movement boundary condition applied to the node. Permissible values are 0, 1, $\pm 3$ (see Section 3.2). Index $i$ denotes the sequential number of the boundary node $n$ in this file.
11	$CodeH(i)$	Code specifying the type of <i>heat</i> movement boundary condition applied to the node. Permissible values are 0, 1, $\pm 3$ , $\pm 4$ , $\pm 6$ (see Section 3.2). Index $i$ denotes the sequential number of the boundary node $n$ in this file.
11	$CodeG(i)$	Code specifying the type of <i>gas</i> movement boundary condition applied to the node. Permissible values are 0, 1, $\pm 3$ , $\pm 4$ , $\pm 6$ (see Section 3.2). Index $i$ denotes the sequential number of the boundary node $n$ in this file.
11	$Width(i)$	Width [units=L] of the boundary associated with boundary node $n$ . In the case of planar geometry ( $KAT=2$ ) $Width(i)$ includes half of the boundary length of each element connected to the node $n$ along the boundary, cm. In the case of axisymmetric flow ( $KAT=1$ ) $Width(i)$ represents the area of the boundary strip, $\text{cm}^2$ , associated with node $n$ . Set this value to zero for internal nodes.

Record 11 is required for each boundary node.

### Seepage Face Information

12,13	- -	Comment lines.
14	$Nseep$	Number of seepage faces expected to develop. The file ends here if $NSeep=0$ .
15	- -	Comment line.
16	$NSP(1)$	Number of nodes on the first seepage face.
16	$NSP(2)$	Number of nodes on the second seepage face.
16	$NSP(Nseep)$	Number of nodes on the last seepage face.
17	- -	Comment line.
18	$NP(1,1)$	Sequential global number of the first node on the first seepage face.
18	$NP(1,2)$	Sequential global number of the second node on the first seepage face.
18	$NP(1,NSP(1))$	Sequential global number of the last node on the first seepage face.

Records 17 through 18 are needed for each seepage face.

```
**** Example 3.3: GRID & BOUNDARY INFORMATION: 'GRID_BND.DAT'
KAT  NumNP  NumEl  NumBP IJ
2      18      11      9      4
n      x(n)    z(n)   MatNumN(n)
1      0.0     70.0    1
2      8.0     70.0    1
3      0.0     60.0    1
4      8.0     60.0    1
5      16.0    60.0   1
6      25.0    60.0   1
7      0.0     50.0    1
8      8.0     50.0    1
9      16.0    50.0   1
10     25.0    50.0   1
11     0.0     30.0    2
12     8.0     30.0    2
13     16.0    30.0   2
14     25.0    30.0   2
15     0.0     10.0    2
16     8.0     10.0    2
17     16.0    10.0   2
18     25.0    10.0   2
Element information
e      KX(e,1)  KX(e,2)  KX(e,3)  KX(e,4)  MatNumE(e)
1      1          3          4          2          1
2      2          4          5          5          1
3      3          7          8          4          1
4      4          8          9          5          1
5      5          9          10         6          1
6      7          11         12         8          2
7      8          12         13         9          2
8      9          13         14         10         2
9      11         15         16         12         2
10     12         16         17         13         2
11     13         17         18         14         2
Boundary information
n      CodeW(I)  CodeS(I)  CodeH(I)  CodeG(I)  Width(I)
1      -4          -4          0          -3        4.0
2      -4          -4          0          -3        8.0
5      1            3          0          0        8.5
6      1            3          0          0        7.0
12     6            1          0          0        0.0
15     -2           0          0          1        4.0
16     -2           0          0          1        8.0
17     -2           0          0          1        8.5
18     -2           0          0          1        4.5
Seepage face information
NSEep
1
NSP(1) ..... NSP(NSeep)
4
NP(NSP,1)   NP(NSP,2)   NP(NSP,3)   NP(NSP,4)
15           16           17           18
```



# Chapter 4: Time-dependent Boundary Settings: *Settdb* Module

**Yakov Pachepsky and Dennis Timlin**

This section describes boundary settings that depend only on time, not on the status of the soil surface or atmospheric conditions only. Dependencies on time of the boundary conditions are considered in this section. The next chapter, 5, describes soil-atmosphere boundaries where surface fluxes depend on atmospheric conditions.

## 4.1 Piece-wise boundary settings

2DSOIL recognizes two types of boundary values: fluxes or state variables. Thus, pressure head or water flux may be the boundary value for water flow, solute concentration or solute flux for solute transport, temperature or heat flux for heat movement, and gas content or gas flux for gas movement.

For heat movement one may specify either a boundary temperature or the parameters  $b^T$  and  $G^T$  in the general boundary heat flux equation:

$$Q_T = -b_T T_{surf} + G_T \quad (4.1)$$

where  $b_T$  and  $G_T$  are parameters that depend on the module used and  $T_{surf}$  is the temperature at the soil surface. This equation may be used in two cases:

- (1) When the surface heat flux is prescribed ( $b_T=0$ ,  $G_T$  is the prescribed flux)
- (2) When conductive and/or radiative heat exchange occurs between the soil surface and the air above it. In this case  $Q_T = -b_T(T_{surf} - T_a)$ , where  $b_T$  is the heat transfer coefficient,  $T_{surf}$  is the temperature of the boundary node, and  $T_a$  is the air temperature. This case is equivalent to the assumption that  $G_T = b_T T_a$ .

Gas boundary conditions are similar to those for heat movement, and also involve two possible formulations:

$$g_{surf,j} = \text{const}$$

or

$$Q_{g,j} = -b_{g,j} g_{surf,j} + G_{g,j} \quad (4.2)$$

where  $b_{g,j}$  and  $G_{g,j}$  are parameters that depend on the module used,  $g_{surf,j}$  is the gas concentration at the soil surface, and the index,  $j$ , is the number of the gas under consideration.

The first formulation corresponds to a constant gas content at the boundary node. The second formulation corresponds to one of two cases:

- (1) When the potential surface gas flux is prescribed ( $b_j=0$ ,  $G_j$  is the prescribed gas flux)
- (2) When conductive gas exchange occurs between the soil surface and the air over it. Here  $Q_{g,j} = -b_{g,j}(g_{surf,j} - g_{a,j})$ , where  $b_g$  is the surface conductance of gas exchange,  $g_{surf,j}$  is the content of the  $j$ th gas at the boundary node, and  $g_{a,j}$  is the content of the  $j$ th gas in the atmospheric air. In this case  $G_{g,j} = b_g g_{a,j}$

The dependence of boundary values on time is assumed to be piece-wise. An example of such a dependence is shown in Fig. 4.1 for nodes 5 and 6 of the grid shown in Fig. 3.1. These nodes are at the bottom of a shallow furrow with constant water height but variable solute concentration and temperature. Boundary values change sharply several times, and boundary values are constant between those times. The program requires values of the boundary variable and times of boundary alterations for every boundary node that has code +3, +6, -3, or -6 (see section 3.2).

The time-dependent boundary information for every soil transport process under consideration is input from special data files. These data files contain the times  $tTDB(I)$  as the end of the current time interval for the transport process  $I$ . Thus file **VarBW.dat** contains  $tTDB(1)$  values for water transport, file **VarBS.dat** includes  $tTDB(2)$  values for solute transport, file **VarBH.dat** contains  $tTDB(3)$  values for heat transport, and file **VarBG.dat** has  $tTDB(4)$  for

gas transport. Every file provides nodal numbers and boundary values for every time interval. The first interval begins at the time calculations are initiated (*Time* in Table 2.2) and ends at the first of the  $tTDB$  times. The second interval begins at the first  $tTDB$  time and ends at the second  $tTDB$  time, and so on.

The  $tTDB$  values mark time intervals during which all time-dependent boundary values

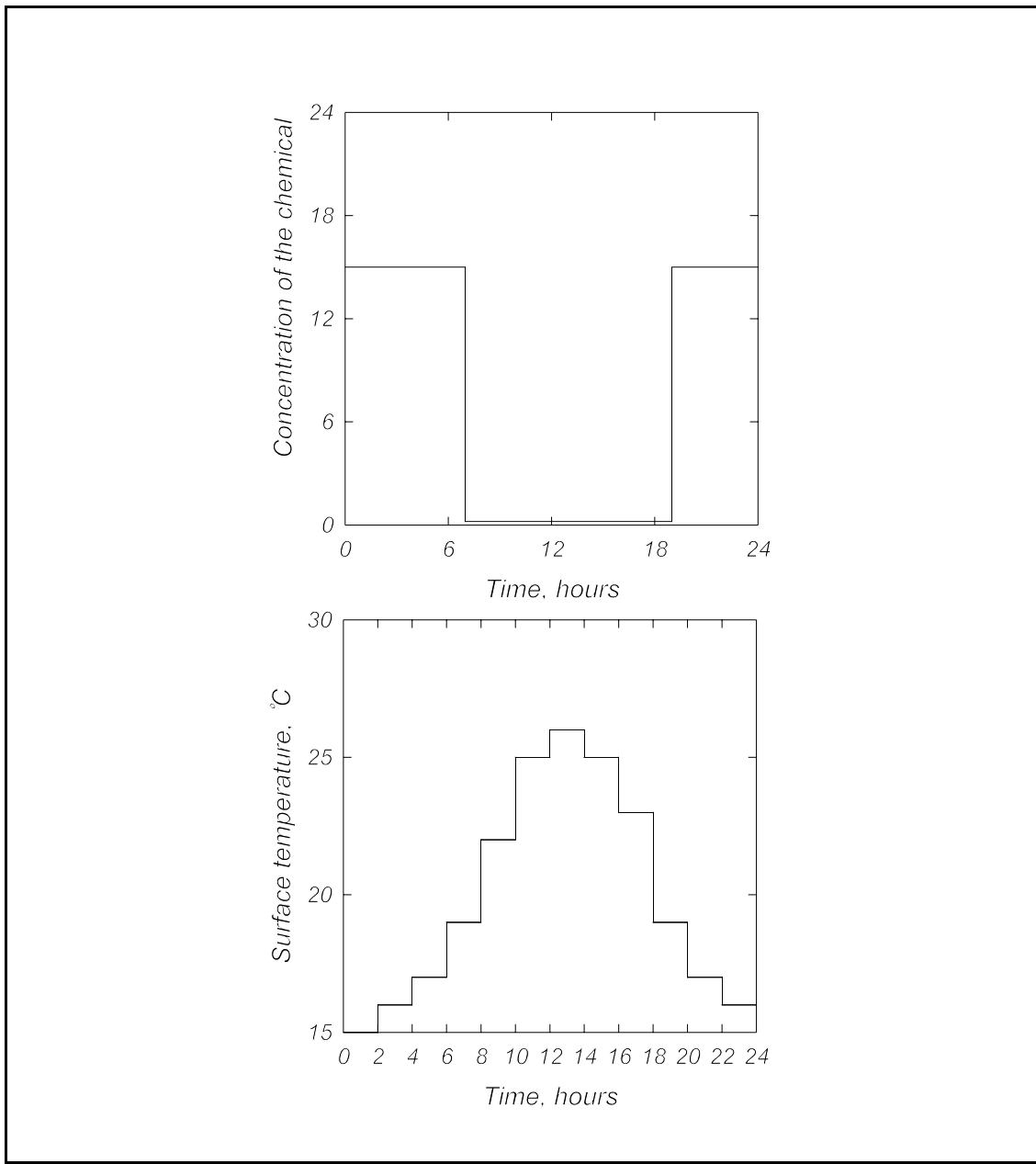


**Figure 4.1** An example of piecewise dependencies of soil boundary solute concentration and temperature on time.

are constant. If some nodes do not change their boundary values at some  $tTDB$ , then these nodes need not be listed for this  $tTDB$ . It is only for the first value of  $tTDB$  that all time-dependent boundary nodes and boundary values in these nodes must be specified. However, it is preferable to give boundary values for all time-dependent boundary nodes at all tTDB to avoid mistakes.

When fluxes are given on the boundaries, it is important to use the correct dimensions. If the code of a boundary point is -3, then the flux has a dimension  $\text{cm day}^{-1}$  for water flow and  $\text{J cm}^{-2} \text{ day}^{-1}$  for heat transport. In the latter case the flux per unit area is to be given. If the code of the boundary node is -6, then the nodal flux has dimension  $\text{cm}^2 \text{ day}^{-1}$  for planar water flow and  $\text{cm}^3 \text{ day}^{-1}$  for axisymmetrical water flow,  $\text{J cm}^{-1} \text{ day}^{-1}$  for a planar heat flow and  $\text{J day}^{-1}$  for axisymmetrical heat flow, and  $\text{g cm}^{-1} \text{ day}^{-1}$  for a planar gas flow and  $\text{g day}^{-1}$  for axisymmetrical gas flow. These examples assume that the units of time are given as days.

#### **4.2 Data files *VarBW.dat*, *VarBS.dat*, *VarBH.dat*, and *VarBG.dat***

The structures of these four files are shown in Tables 4.1-4.4. The tables are followed by examples of these files (Examples 4.1 and 4.2) that are given for time-dependent boundaries of Fig. 4.1. It is worth mentioning that the time intervals for heat and solute boundary conditions are different in the examples. Other examples can be found in Chapter 14 of this manual.

Table 4.1. Format of the file '**VarBW.dat**'.

---

Record	Variable	Description
1,2	- - -	Comment lines.
3	$tTDB(1)$	The <u>end</u> of the time interval for which the boundary information of record 4 is given.
4	$n$	Node number of the boundary point.
4	$VarBW(i)$	value of pressure head for nodes with $CodeW(n)=3$ and $CodeW(n)=6$ .
Water flux per unit of area, $\text{cm day}^{-1}$ (positive if into soil) for nodes with $CodeW(n)=-3$ . Volumetric water flux at nodes with $CodeW(n)=-6$ , $\text{cm}^3 \text{day}^{-1}$ for planar flow, and $\text{cm}^2 \text{day}^{-1}$ for axisymmetric flow. The value $i$ is equal to the sequential number of the node $n$ in the boundary node list of file ' <b>Grid_bnd.dat</b> '. Records 3,4 are both repeated for every time interval involving constant boundary variables. Record 4 is provided separately for each time-dependent boundary node.		

---

Table 4.2. Format of the file '**VarBS.dat**'.

---

Record	Variable	Description
1,2	- - -	Comment lines.
3	$tTDB(2)$	The <u>end</u> of the time interval for which the boundary information of record 4 is given.
4	$n$	Node number of the boundary point.
4	$VarBS(i,1)$	Concentration of the 1st solute at the node $n$ , $\text{g cm}^{-3}$ . The value $i$ is equal to the sequential number of the node $n$ in the boundary node list of the file ' <b>Grid_bnd.dat</b> '.
4	$VarBS(i,2)$	Same as above for the 2nd solute.
4	$VarBS(i,NumSol)$	Same as above for the last solute.
Both records 3 and 4 are repeated for every time interval of constant boundary variables. Record 4 is given separately for each time-dependent boundary node.		

---

Table 4.3. Format of the file '**VarBH.dat**'.

---

Record	Variable	Description
1,2	- - -	Comment lines.
3	$tTDB(3)$	The <u>end</u> of the time interval for which the boundary information of record 4 is given.

---

- 4         $n$               Nodal number of the boundary point.
- 4         $VarBH(i,1)$  Temperature value for nodes with  $CodeT(n)=3$  and  $CodeT(n)=6$ . If the boundary code is negative, then set this value to zero.
- 4         $VarBH(i,2)$  Coefficient  $b_T$  in Eq. (4.1),  $J \text{ cm}^{-2} \text{ day}^{-1} (\text{ }^\circ\text{C})^{-1}$  at nodes with  $CodeT(n)=-3$ ,  $J \text{ cm}^{-1} \text{ day}^{-1} (\text{ }^\circ\text{C})^{-1}$  at nodes with  $CodeT(n)=-6$  for planar flow, and  $J \text{ day}^{-1} (\text{ }^\circ\text{C})^{-1}$  at nodes with  $CodeT(n)=-6$  for axisymmetrical flow. If the boundary code is positive, then set this value to zero.
- 4         $VarBH(i,3)$  Coefficient  $G_T$  in Eq. (4.1),  $J \text{ cm}^{-2} \text{ day}^{-1}$  at node with  $CodeT(n)=-3$ ,  $J \text{ cm}^{-1} \text{ day}^{-1}$  at node with  $CodeT(n)=-6$  for planar flow, and  $J \text{ day}^{-1}$  at nodes with  $CodeT(n)=-6$  for axisymmetrical flow. If the boundary code is positive, then set this value to zero.

The value  $i$  is equal to the sequential number of node  $n$  in the boundary node list of the file **Grid\_bnd.dat**. Both records 3 and 4 are repeated for every time interval of constant boundary variables. Record 4 is given separately for each time-dependent boundary node.

---

—

Table 4.4. Format of the file '**VarBG.dat**'.

Record	Variable	Description
1,2	- -	Comment lines.
3	$tTDB(4)$	The <u>end</u> of the time interval for which the boundary information of record 4 is given.
4	$n$	Node number of the boundary point.
4	$VarBG(i, 1, 1)$	Constant boundary content of the first gas $g_{surf,1}$ in Eq. (4.2). If the boundary code is negative, then set this value to zero.
4	$VarBG(i, 1, 2)$	Coefficient $b_{g,1}$ in Eq.(4.3) for the first gas, $\text{cm day}^{-1}$ at nodes with $CodeG(n)=-3$ , $\text{cm}^2\text{day}^{-1}$ at nodes with $CodeG(n)=-6$ for planar flow, and $\text{cm}^3\text{ day}^{-1}$ at nodes with $CodeG(n)=-6$ for axisymmetrical flow. If the boundary code is positive, then set this value to zero.
4	$VarBG(i, 1, 3)$	Coefficient $G_{g,1}$ in Eq. (4.3)for the first gas, $\text{g cm}^{-2}\text{day}^{-1}$ at nodes with $CodeG(n)=-3$ , $\text{g cm}^{-1}\text{ day}^{-1}$ at nodes with $CodeG(n)=-6$ for planar flow, and $\text{g day}^{-1}$ at nodes with $CodeG(n)=-6$ for axisymmetrical flow. If the boundary code is positive, then set this value to zero.
.	.	.
4	$VarBG(i, NumG, 1)$	Constant boundary content of the last gas $g_{surf, NumG}$ in Eq. (4.2). If the boundary code is negative, then set this value to zero.
4	$VarBG(i, NumG, 2)$	Coefficient $b_{g, NumG}$ in Eq.(4.3) for the first gas, $\text{cm day}^{-1}$ at nodes with $CodeG(n)=-3$ , $\text{cm}^2\text{day}^{-1}$ at nodes with $CodeG(n)=-6$ for planar flow, and $\text{cm}^3\text{ day}^{-1}$ at nodes with $CodeG(n)=-6$ for axisymmetrical flow. If the boundary code is positive, then set this value to zero.
4	$VarBG(i, NumG, 3)$	Coefficient $G_{g, NumG}$ in Eq. 4.2 for the first gas, $\text{g cm}^{-2}\text{day}^{-1}$ at nodes with $CodeG(n)=-3$ , $\text{g cm}^{-1}\text{ day}^{-1}$ at nodes with $CodeG(n)=-6$ for planar flow, and $\text{g day}^{-1}$ at nodes with $CodeG(n)=-6$ for axisymmetrical flow. If the boundary code is positive, then set this value to zero.
		The value $i$ is equal to the sequential number of node $n$ in the boundary node list of the file ' <b>Grid_bnd.dat</b> '. Both records 3 and 4 are repeated for every time interval of constant boundary variables. Record 4 is given separately for each time-dependent boundary node.

\*\*\*\* Example 4.1: TIME-DEPENDENT SOLUTE BOUNDARY: FILE 'VARBS.DAT'  
 End of the interval (days) Node number Boundary value  
 0.29167  
     5               0.15  
     6               0.15  
 0.79167  
     5               0.002  
     6               0.002  
 1.00000  
     5               0.15  
     6               0.15  
 END OF FILE 'VARBS.DAT'\*\*\*\*

\*\*\*\* Example 4.2: TIME-DEPENDENT HEAT BOUNDARY: FILE 'VARBH.DAT'  
 End of the interval (days) Node number VarBH(1) VarBH(2) VarBH(3)  
 0.08333  
     5               15           0           0  
     6               15           0           0  
 0.16667  
     5               16           0           0  
     6               16           0           0  
 0.25  
     5               17           0           0  
     6               17           0           0  
 0.33333  
 .  
 .  
 0.91667  
     5               17           0           0  
     6               17           0           0  
 1.0  
     5               16           0           0  
     6               16           0           0  
 END OF FILE 'VARBH.DAT'\*\*\*\*

# Chapter 5: Soil-atmosphere Boundary Setting: *SetSurf*

## Modules

**Basil Acock, Yakov Pachepsky, and Dennis Timlin**

Unlike the time-dependent boundaries discussed in the previous section, the soil-atmosphere boundary does not have set values of fluxes or concentrations. Potential values of fluxes or concentrations are generated for the soil-atmosphere boundary by the **SetSurf** module. Other modules may modify these potential values to provide physically possible - actual - fluxes or concentrations.

Existing soil models and submodels use two different methods to set the soil-atmosphere boundary. Some, e.g., LEACHM (Wagenet and Hudson, 1987), SESP (Timlin et al., 1989), and GRASP (Tillotson and Fontaine, 1991), rely on daily meteorological data. Others , e.g., an alfalfa growth model (Thompson and Fick, 1980), RZWQM (Ahuja et al., 1991), and SHAW (Flerchinger and Saxton, 1989), require more detailed information, including precise durations and intensities of the precipitation/infiltration events. The two approaches each have their own advantages and disadvantages. Data for the former approach are easier to obtain, and long-term changes in the soil environment during plant growth and development are easier calculated. Use of the latter approach can provide a much more realistic description of transport in soils during short time intervals but the data are more difficult to obtain. Combining the two approaches presents an important future task. Both are available separately in 2DSOIL at the present stage of development. The module **SetSurf01** reads detailed boundary information but does not generate other information; the values are simply used in the form they are read in. The module **SetSurf02** reads daily data but can generate evapotranspiration on an hourly basis.

## **5.1 Using daily meteorological data: SetSurf02 module**

This module uses daily meteorological information. It transforms these data to hourly updated soil surface boundary conditions for water, solute, heat, and gas within the soil domain. Several parameters of the crop canopy are used to distinguish bare soil from soil covered by the canopy.

The module reads in the following standard meteorological data:

$J$  - day of the year (Julian date),

$R_I$  - daily solar radiation integral,

$T_{max}$  - maximum air temperature during the day,

$T_{min}$  - minimum air temperature during the day,

$\Pi$  - precipitation (or irrigation),

$V$  - wind speed at 2 m height,

$T_{wet}$  - wet bulb temperature,

$T_{dry}$  - dry bulb temperature,

$c_1, c_2, \dots, c_{NumSol}$  - concentrations of solutes in the precipitation or irrigation water,

$g_1, g_2, \dots, g_{NumG}$  - contents of gases in the atmosphere.

The model of soil-atmosphere interaction uses relationships of celestial geometry, crop canopy geometry, and radiation balance theory. This model is described below as a sequence of submodels. Before any calculations are performed, the model changes the units of the input data:  $R_I$  to  $\text{J}\cdot\text{m}^{-2}$ ;  $T_{max}$ ,  $T_{min}$ ,  $T_{wet}$  and  $T_{dry}$  to  $^{\circ}\text{C}$ ;  $\Pi$  to cm;  $V$  to  $\text{km}\cdot\text{h}^{-1}$ ;  $c_1, c_2, \dots, c_{NumSol}$  and  $g_1, g_2, \dots, g_{NumG}$  to  $\text{g cm}^{-3}$ .

### **5.1.1 Incident radiation submodel.**

This submodel produces values of

$\delta$  - solar declination,

$t_d$  - daylength, hours,

$R_{00,n}$  - radiation incident at the top of the atmosphere at noon,  $\text{W}\cdot\text{m}^{-2}$ ,

*a* - atmospheric transmission coefficient,

$R_{0,n}$  - potential radiation incident at earth's surface at noon,  $\text{W}\cdot\text{m}^{-2}$ ,

$R_n$  - actual radiation incident at earth's surface at noon,  $\text{W}\cdot\text{m}^{-2}$ ,

$\eta$  - cloud cover factor,

$f_{cl}$  - proportion of sky covered with cloud (1=full cover),

$t_{dn}$  - time of dawn, hours,

$t_{dk}$  - time of dusk, hours,

$R$  - actual radiation incident at earth's surface,  $\text{W}\cdot\text{m}^{-2}$ .

Index  $I$  indicates that the value is found at time  $t_I = (I - 0.5)$  hours. Input values are  $J$ , Julian day number;  $\varphi$ , local latitude; and  $R_I$ , daily solar radiation integral.

Table 5.1 shows dependencies among the variables and the corresponding equation numbers in this chapter.

Table 5.1. Dependencies among variables of the incident radiation submodel and the corresponding equation numbers in the submodel.

Solar declination is calculated using the algorithm of Robertson and Russelo (1968)

$$\delta = \beta_1 + \sum_{i=2}^{i=5} [\beta_i \sin(0.01721(i-1)J) + \beta_{i+4} \cos(0.01721(i-1)J)] \quad (5.1)$$

where the coefficients  $\beta_i$  are equal to

$$\beta_1 = 0.3964; \beta_2 = 3.631; \beta_3 = 0.03838; \beta_4 = 0.07659; \beta_5 = 0.0; \beta_6 = -22.97;$$

$$\beta_7 = -0.3885; \beta_8 = -0.1587; \beta_9 = -0.01021.$$

The equation relating solar altitude and declination to latitude and hour angle is commonly found in books on celestial mechanics, and is also given in the Smithsonian Meteorological Tables (1966, p. 495). Daylength is defined (p. 506) as the interval between sunrise and sunset; at both of these times the center of the sun's disk is 50° below the horizon. Setting solar altitude equal to -50°, we solve for the hour angle and then convert this to hours from solar noon. Doubling the answer gives daylength:

$$t_d = \frac{\pi}{24} \arccos\left(-\frac{0.014544 + \sin\varphi \sin\delta}{\cos\varphi \cos\delta}\right) \quad (5.2)$$

The equations for solar radiation incident on top of the earth's atmosphere are given in the Smithsonian Meteorological Tables (1966, p. 417). The conditional solar constant, i. e., the

$$R_{00,n} = 1325.4 \frac{\cos(\varphi - \delta)}{Z^2} \quad (5.3)$$

radiation flux on the top of the troposphere is assumed to be 1325.4 W·m<sup>-2</sup> (Budyko, 1974):

where  $Z = 1 + 0.01674 \sin[0.01721(J-93.5)]$  is the radius-vector of the earth.

The atmospheric transmission coefficient is estimated for different latitudes and times of year from the data of Budyko (1974):

$$\begin{aligned} \alpha &= 0.68 + (1.57\xi - 0.1) \frac{145-J}{1000}, & J \leq 145 \\ \alpha &= 0.68 + [\xi(2.04 - 0.37\xi) - 0.19] \frac{J-237}{1000}, & J \geq 237 \\ \alpha &= 0.68 & 145 < J < 237 \end{aligned} \quad (5.4)$$

where  $\xi = \varphi/30$ , with  $\varphi$  in degrees.

Potential radiation incident on the earth's surface at noon is found as

$$R_{0,n} = \frac{1}{2} R_{00,n} \left[ (0.93 - \frac{0.02}{\cos(\varphi-\delta)} + \alpha^{1/\cos(\varphi-\delta)}) \right] \quad (5.5)$$

This equation essentially reconstitutes the data given in Budyko (1974, Table 3) and was derived from an equation given in the Smithsonian Meteorological Tables (1966, p. 420). Instead of assuming that a constant 9% of extra-terrestrial radiation is adsorbed by water vapor and ozone, the percent adsorption was allowed to vary with atmospheric path length, i.e., solar altitude, according to the data given by Miller (1981).

Actual radiation incident at the earth's surface at noon ( $R_n$ ) under a cloudless sky is calculated from the given daily integral, and the assumption that the radiation flux density varies as a half sine wave over the photoperiod:

$$R_n = \frac{\pi}{3600 t_d} \frac{R_I}{2} \quad (5.6)$$

Cloud cover is accounted for by a factor  $\eta$  taken from Budyko (1974, Table 4). The following equation gives good estimates within the range of latitude from 10 to 55° N:

$$\eta = \begin{cases} 0.45 - 0.004\varphi, & \varphi \leq 25 \\ 0.30 + 0.002\varphi, & \varphi > 25 \end{cases} \quad (5.7)$$

The proportion of sky covered with cloud,  $f_{cl}$ , is calculated from the ratio of actual to potential radiation at noon using the cloud cover factor  $\eta$ :

$$f_{cl} = \frac{\sqrt{(\eta^2 + 1.52(1 - \frac{R_n}{R_{0,n}}) - \eta)}}{0.76} \quad (5.8)$$

Berliand's equation (Budyko, 1974) for actual incident radiation,  $R_n = R_{0,n} [1 - (\eta + 0.38f_{cl})f_{cl}]$  has been solved for  $f_{cl}$  to obtain eq 5.8. This equation gives a good fit of radiation data for the north central region of the U.S. (Baker, 1975).

Both time of dawn,  $t_{dn}$ , and time of dusk,  $t_{dk}$ , are derived from daylength,  $t_d$ :

$$t_{dn} = 12 - t_d/2 \quad (5.9)$$

$$t_{dk} = 12 + t_d/2 \quad (5.10)$$

Actual radiation incident at the earth's surface at time  $t_i$  is found according to the half sine wave pattern:

$$R_i = R_n \sin\left(\frac{\pi(i-0.5)}{t_d}\right) \quad (5.11)$$

Corrections are made for incomplete hours after dawn and before dusk.

### 5.1.2 Temperature-vapor pressure submodel

The temperature-vapor submodel produces values of:

$t_{maxhr}$  - time of maximum air temperature measured from dawn, hr,

$T_{dk}$  - air temperature at dusk, °C,

$\varepsilon$  - actual water vapor pressure for day (assumed constant), kPa

$\gamma$  - psychrometric constant, kPa·(°C)<sup>-1</sup>,

$T_a$  - air temperature, °C,

$b_\varepsilon$  - slope of saturation water pressure curve, kPa·(°C)<sup>-1</sup>,

$\Delta\varepsilon$  - vapor pressure deficit, kPa.

Index  $i$  indicates that the value is found for time  $t_i=(i-0.5)$  hours.

Input values are maximum air temperature for the day,  $T_{max}$ ; minimum air temperature for the day,  $T_{min}$ ; wet bulb temperature,  $T_{wet}$ ; dry bulb temperature,  $T_{dry}$ ; minimum air temperature for the following day,  $T_{mint}$ ; air temperature at sunset on the previous day,  $T_y$ , °C; time of dawn,  $t_{dn}$  (hours); time of dusk,  $t_{dk}$  (hours); actual radiation incident at earth's surface at noon,  $R_n$  (W·m<sup>-2</sup>); and daylength, hours,  $t_d$ .

Variables and the corresponding equation numbers that describe their dependencies are given in Table 5.2.

Table 5.2. Variables of the temperature-vapor pressure submodel and corresponding equation numbers included in the submodel.

Input values	Output values						
	$t_{maxhr}$	$T_{dk}$	$T_a$	$\varepsilon$	$\gamma$	$b_\varepsilon$	$\Delta\varepsilon$
$T_{max}$	12	13	14	.	.	.	.
$T_{min}$	.	13	14	15	.	.	.
$T_{dry}$	.	.	.	16	.	.	.
$T_{wet}$	.	.	.	16	16	.	.
$t_{dn}$	.	.	14	.	.	.	.
$t_{dk}$	.	.	14	.	.	.	.
$R_n$	12	.	.	.	.	.	.
$t_d$	12	13	14	.	.	.	.
$t_{mint}$	.	.	14	.	.	.	.
$t_y$	.	.	14	.	.	.	.
$t_{maxhr}$	.	13	14	.	.	.	.
$t_{dk}$	.	.	14	.	.	.	.
$T_a$	.	.	.	.	17	17	
$\varepsilon$	.	.	.	.	.	.	17
$\gamma$	.	.	.	.	.	.	.
$b_\varepsilon$	.	.	.	.	.	.	.
$\Delta\varepsilon$	.	.	.	.	.	.	.

The time of maximum air temperature measured from dawn was found by empirically fitting local data. For Mississippi conditions, for example, the equation is:

$$t_{maxhr} = \frac{t_d}{\pi} \left| \pi - \arcsin \left( \frac{T_{max}}{R_n(0.0945 - 8.06 \cdot 10^{-5} R_n + 6.77 \cdot 10^{-4} T_{max})} \right) \right| \quad (5.12)$$

where the expression after 'arcsin' is less than one. The air temperature at sunset is:

$$T_{dk} = \frac{T_{max} - T_{min}}{2} \left[ 1 + \sin \left( \frac{\pi t_d}{t_{maxhr}} + \frac{3\pi}{2} \right) \right] + T_{min} \quad (5.13)$$

Diurnal temperature variation approximated by a half sine wave during the day and by a logarithmic or linear dependency at night. At time  $t=t_i$  we have:

$$\begin{aligned}
T_{a,i} &= T_{\min} + \frac{T_{\max} - T_{\min}}{2} [1 + \sin(\frac{\pi t_d}{t_{\max hr}} + \frac{3\pi}{2})], \quad t_{dn} \leq t_i \leq t_{dk}, \\
T_{a,i} &= T_{\min} + T_* [(1 + \frac{T_y - T_{\min}}{T_*})^{\frac{t_{dn} - t_i}{2t_{dn}}} - 1], \quad t_i < t_{dn}, \quad T_y > T_{\min}, \\
T_{a,i} &= T_{\min} + (T_y - T_{\min}) \frac{t_{dn} - t_i}{2t_{dn}}, \quad t_i < t_{dn}, \quad T_y \leq T_{\min}, \\
T_{a,i} &= T_{dk} + T_* (1 + \frac{T_{dk} - T_{\min}}{T_*}) [(1 + \frac{T_{dk} - T_{\min}}{T_*})^{-\frac{t_i - t_{dk}}{2(24 - t_{dk})}} - 1], \quad t_i > t_{dk}, \quad T_{\min} < T_{dk}, \\
T_{a,i} &= T_{dk} + (T_{\min} - T_{dk}) \frac{t_i - t_{dk}}{2(24 - t_{dk})}, \quad t_i > t_{dk}, \quad T_{\min} \geq T_{dk}
\end{aligned} \tag{5.14}$$

These equations have given a good fit to data sets from Arizona and Mississippi, when the parameter  $T_*$  was set at 5°C.

Calculations of actual water vapor pressure for the day depend on the availability of wet and dry bulb temperature values. If those are not available, dew point temperature is assumed to be the minimum temperature and the algorithm of Weiss (1977) is used. The psychrometric constant depends on  $T_{\min}$ :

$$\varepsilon = 0.61 \frac{\exp(17.27T_{\min})}{(T_{\min} + 237.3)}; \quad \gamma = 0.0645 \tag{5.15}$$

If wet and dry bulb temperatures are known, then calculations include the value of the saturated water vapor pressure at wet bulb temperature  $\varepsilon_w$ , humidity ratio  $v$ , and latent heat of evaporation  $F_L$ :

$$\begin{aligned}
\varepsilon_w &= 0.61 \frac{\exp(17.27T_{wet})}{T_{wet} + 237.3}; \quad v = \frac{0.622\varepsilon_w}{101.3 - \varepsilon_w}; \\
F_L &= 2500.8 - 2.37T_{wet}; \quad \gamma = 62.81 \frac{1.006 + 1.846v}{L(0.622 + v)^2}; \\
\varepsilon &= \varepsilon_w - \gamma(T_{dry} - T_{wet})
\end{aligned} \tag{5.16}$$

The slope,  $b_\varepsilon$ , of the saturation water vapor pressure curve is estimated using the dry bulb temperature  $\varepsilon_d$ . The vapor pressure deficit,  $\Delta\varepsilon$ , is then calculated from:

$$\begin{aligned}\varepsilon_d &= 0.61 \frac{\exp(17.27/T_a)}{(T_a + 237.3)} \\ b_\varepsilon &= 0.61 \frac{\exp[17.27(T_a+1)]}{[(T_a+1)+237.3]} - \varepsilon_d \\ \Delta\varepsilon &= \varepsilon_d - \varepsilon\end{aligned}\tag{5.17}$$

### 5.1.3 Radiation interception submodel

This submodel works only if there is a crop cover. The submodel produces hourly values of

$\alpha_\diamond$  - solar altitude,

$\zeta$  - solar azimuth,

$f_D$  - proportion of total radiation that is diffuse

$\beta$  - angle between row orientation and solar azimuth

$d_{sh}$  - width of shadow cast by row crop measured at right angles to the row, cm,

$f_{di}$  - proportion of direct radiation intercepted by rows of plants assuming they are opaque cylinders,

$f_{Di}$  - proportion of diffuse radiation intercepted by "solid" rows,

$f_c$  - fraction of the solar radiation intercepted by the crop.

Index  $i$  indicates that the value is for time  $t_i = (i-0.5)$  hours.

Input values are local latitude,  $\varphi$  (degrees), row spacing,  $d_{rs}$  (cm), row orientation measured eastward from north,  $v$  (degrees), canopy extinction coefficient,  $\epsilon$ , height of top leaves above soil,  $H_c$  (cm), leaf area per unit soil area covered by crop canopy,  $A_c$ , solar declination,  $\delta$ , daylength,  $t_d$  (hours), atmospheric transmission coefficient,  $a$ , cloud cover factor,  $\eta$ , and proportion of sky covered with cloud,  $f_{cl}$ , (1=full cover).

Table 5.3 shows dependencies between variables and the corresponding equation numbers.

Table 5.3. Dependencies between variables of the radiation interception submodel and corresponding equation numbers in the submodel.

Input values	Output values							
	$\alpha_\diamond$	$\zeta$	$f_D$	$\beta$	$d_{sh}$	$f_{di}$	$f_{Di}$	$f_c$
$\phi$	18		.	.	.	.	23	24
$d_{rs}$	.	.	.	.	.	23	24	26-27
$u$	.	.	.	22	.	.	.	.
$\epsilon$	.	.	.	.	.	.	.	26-27
$H_c$	.	.	.	.	23	.	24	26-27
$A_c$	.	.	.	.	.	.	.	26-27
$\delta$	18	19	.	.	.	.	.	.
$t_d$	.	.	.	.	.	.	.	.
$a$	.	.	21	.	.	.	.	.
$\eta$	.	.	21	.	.	.	.	.
$f_{cl}$	.	.	21	.	.	.	.	.
$\alpha_\diamond$	.	19	21	22	23	.	.	.
$\zeta$	.	.	.	.	.	.	.	26-27
$f_D$	.	.	.	.	.	.	.	26-27
$u$	.	.	.	.	23	.	.	.
$d_{sh}$	.	.	.	.	.	23	.	26-27
$f_{di}$	.	.	.	.	.	.	.	26-27
$f_{Di}$	.	.	.	.	.	.	.	26-27
$f_c$	.	.	.	.	.	.	.	.

The equation relating solar altitude to solar declination, latitude, and hour angle is commonly found in books on celestial mechanics, and is also given in the Smithsonian Meteorological Tables (1966, p. 495). For hour angles at  $t=t_i$ , it gives

$$(\alpha_\diamond)_i = \arcsin \left| \sin \phi \sin \delta + \cos \phi \cos \delta \cos \left| \frac{\pi}{12} (i - 12 - \frac{1}{2}) \right| \right| \quad (5.18)$$

The equation for solar azimuth may be found in the Smithsonian Meteorological Tables (1966, p. 497). For hour angles at  $t=t_i$

$$\zeta_i = \pi + \arcsin \left\{ \frac{\cos \delta \sin \left| \frac{\pi}{12} (12 - i + \frac{1}{2}) \right|}{\cos (\alpha_\diamond)_i} \right\}, \quad i = 1, 2, \dots, 12, \quad (5.19)$$

$$\zeta_i = 2\pi - \zeta_{i+12}, \quad i = 13, 14, \dots, 24$$

According to equations and procedures given in the Smithsonian Meteorological Tables (1966, p. 420), direct solar radiation flux at the earth's surface is calculated as:

$$R_d = R_{00,n} a^{\frac{1}{\sin \alpha_\phi}} \quad (5.20)$$

Diffuse radiation at the earth's surface  $R_D = (f_R R_{00,n} - R_d)/2$ , where  $f_R$  is the proportion of radiation not adsorbed by ozone or water vapor,  $R_{00,n}$  is the radiation incident at the top of the atmosphere at noon, and  $a$  is the atmospheric transmission coefficient. Instead of assuming that  $a$  is a constant 9% of extra-terrestrial radiation adsorbed by water vapor and ozone, the percent adsorption is allowed to vary with atmospheric path length (i.e., solar altitude) according to data given by Miller (1981). As a result, we have for the proportion of diffuse radiation:

$$f'_D = 1 - \frac{1}{1 + (0.93 - \frac{0.02}{\sin \alpha_\phi}) a^{\frac{1}{\sin \alpha_\phi}}} \quad (5.21)$$

$$f_D = 1 - \frac{(1 - f_{cl})(1 - f'_D)}{1 - f_{cl}(n + f)}$$

where  $f'_D$  is the proportion of diffuse radiation on cloudless days, and where direct radiation is assumed to be inversely proportional to the percentage of the sky covered by clouds.

Canopy radiation interception is calculated for rowcrops that are approximated as opaque cylinders. The interception of diffuse and direct radiation by these cylinders is calculated for every hour of the day by a method proposed by Acock and Trent (1991). First, solar position and row orientation are used to calculate an apparent solar elevation,  $\alpha'_\phi$ , at right angles to the row that would give the same shadow length:

$$\alpha' = \arctan \left( \frac{\tan \alpha_\phi}{\sin |\beta|} \right) \quad (5.22)$$

The angle  $\beta$  is calculated as the difference between the solar azimuth and the row orientation (see Chapter 10). Next, the proportion of direct radiation intercepted is shadow width ( $d_{sh}$ ) divided by row width ( $d_{rs}$ ) :

$$d_{sh} = \frac{H_c}{\sin \alpha'_\phi}; \quad f_{di} = \frac{d_{sh}}{d_{rs}} \quad (5.23)$$

The proportion of sky,  $f_{D_i,d}$ , obscured by "opaque" rows at the distance  $d$  from the row is (Acock and Trent, 1991):

$$\begin{aligned} f_{D_i,d} &= \frac{2}{\pi} [\arctan\left(\frac{H_c}{2(d_{rs}-d)}\right) + \arctan\left(\frac{H_c}{2d}\right)], \\ f_{D_i} &= \min\left(1, \frac{1}{d_{rs}} \int_0^{d_{rs}} f_{D_i,x} dx\right) = \min\left[1, \frac{1}{\pi} \left(4 \arctan\frac{H_c}{2d_{rs}} - \frac{H_c}{d_{rs}} \ln \frac{1}{1 + (\frac{2d_{rs}}{H_c})^2}\right)\right] \end{aligned} \quad (5.24)$$

The values of  $f_{D_i,d}$  averaged from row to mid-row give  $f_{D_i}$ .

The proportion of total radiation intercepted by the crop is made dependent on sun altitude. If  $\alpha_\phi > 0$ , effective leaf canopy area index  $A_{c,e}$  replaces the original leaf area canopy index,  $A_c$ , allowing for the fact that light at low angles traverses more leaves to reach the soil:

$$A_{c,e} = \frac{A_c \max\left(1, \frac{d_{sh}}{d_{rs}}\right)}{\sin[\arccos(\cos \beta \cos \alpha_\phi)]} \quad (5.25)$$

The value of  $A_{c,e}$  is used to calculate Beer's law correction for radiation interception:  $f_{Beer} = 1 - \exp(-A_{c,e} \epsilon)$ . Further,  $f_c$  is the fraction of solar radiation intercepted by the crop:

$$f_c = [f_{D_i} f_D + f_{di} (1 - f_D)] f_{Beer} \quad (5.26)$$

If  $\alpha_\phi \leq 0$ ,  $A_{c,e}$  coincides with  $A_c$  and

$$f_c = \min\left(\frac{H_c}{d_{rs}}, 1\right) f_{Beer} \quad (5.27)$$

### 5.1.4 Potential evapotranspiration submodel

The evapotranspiration submodel produces hourly values of

$R_u$  - net upward long wave radiation,  $\text{W}\cdot\text{m}^{-2}$ ,

$v_s$  - albedo of soil,

$R_{Ns}$  - net radiation on a bare soil surface,  $\text{W}\cdot\text{m}^{-2}$ ,

$E_s$  - potential evaporation rate from soil surface,  $\text{cm}\cdot\text{day}^{-1}$ ,

$r_c$  - a crop surface roughness parameter,

$R_{Nc}$  - net radiation on the crop assuming complete cover,  $\text{W}\cdot\text{m}^{-2}$ ,

$E_c$  - potential transpiration rate from the crop,  $\text{cm}\cdot\text{day}^{-1}$ .

Input values are, wind speed at 2 m height,  $V$  ( $\text{km h}^{-1}$ ); row spacing,  $d_{Rs}$  (cm); height of the topmost leaves above the soil,  $H_c$  (cm); potential radiation incident at the earth's surface at noon,  $R_{\theta,n}$  ( $\text{W}\cdot\text{m}^{-2}$ ); actual radiation incident at the earth's surface at noon,  $R_n$  ( $\text{W}\cdot\text{m}^{-2}$ ); actual radiation incident at the earth's surface at time  $t$ ,  $R$ , ( $\text{W}\cdot\text{m}^{-2}$ ); soil moisture content for the grid nodes at the soil surface,  $\theta$ ; psychrometric constant,  $\gamma$  ( $\text{kPa}\cdot(\text{°C})^{-1}$ ); air temperature,  $T_a$  ( $\text{°C}$ ); slope of the saturation water vapor pressure curve,  $b_e$  ( $\text{kPa}\cdot(\text{°C})^{-1}$ ); vapor pressure deficit,  $\Delta e$  (kPa); and fraction of the solar radiation intercepted by the crop,  $f_c$ . The index,  $i$ , indicates that the value is found at time  $t_i=(i-0.5)$  hours.

Table 5.4 shows dependencies among the variables and the corresponding equation numbers.

Table 5.4. Dependencies among variables of the evapotranspiration submodel and corresponding numbers of equations included in the potential evapotranspiration submodel.

Input values	Output values						
	$R_u$	$v_s$	$R_{Ns}$	$E_s$	$r_c$	$R_{Nc}$	$E_c$
$f_{ET}$	.	.	.	32	.	.	36
$V$	.	.	.	32	.	.	36
$d_{rs}$	.	.	30	32	32	34	36
$H_c$	.	.	30	32	32	34	36
$R_{0,n}$	28	.	.	.	.	.	.
$R_n$	28	.	.	.	.	.	.
$R$	.	.	30	.	.	.	.
$\theta$	.	29	.	.	.	.	.
$\gamma$	.	.	.	32	.	.	36
$T_a$	28	.	.	32	.	.	36
$b_e$	.	.	.	32	.	.	36
$\Delta\epsilon$	.	.	.	32	.	.	36
$f_c$	.	.	30	.	.	34	.
$R_u$	.	.	31	.	.	35	.
$v_s$	.	.	31	.	.	.	.
$R_{Ns}$	.	.	.	32	.	.	.
$E_s$	.	.	.	.	.	.	.
$r_c$	.	.	.	.	.	.	.
$R_{Nc}$	.	.	.	.	.	.	36
$E_c$	.	.	.	.	.	.	.

Most equations for calculation of evapotranspiration are largely empirical, but the Penman (1963) equation is at least semi-mechanistic and has been widely tested. Penman's equation is used here to calculate potential water loss from both soil and plant. Penman's equation is assumed that after the crop canopy closes, water evaporation from soil will be negligible.

Net upward long-wave radiation is calculated using an approximation derived by Linacre (1968) multiplied by the ratio of potential and actual radiation at noon:

$$R_u = 11.2 * (100 - T_a) \frac{R_n}{R_{0,n}} \quad (5.28)$$

The albedo of exposed soil cells is estimated from the data of Bower (1971) as a function of soil water content ( $\theta$ ):

$$v_s = 0.3 - 0.5\theta \quad (5.29)$$

The sum of total radiation falling on the soil is assumed to be concentrated on the bare soil, and the equivalent total radiation  $R_s^e$  is calculated as:

$$R_s^e = R \left[ \frac{1-f_c}{1-\frac{H_c}{d_{rs}}} \right], \quad H_c < d_{rs} \quad (5.30)$$

$$R_s^e = 0, \quad H_c \geq d_{rs}$$

Radiation impinging on the soil is assumed to be spread uniformly over the bare soil between crop rows. The net radiation on the exposed soil cells is derived as:

$$R_{Ns} = (1-v_s)R_s^e - R_u \quad (5.31)$$

Penman's equation gives the potential evaporation rate from the soil:

$$E_s = f_{ET} \frac{\frac{b_e}{\gamma} \frac{3600}{2500.8 - 2.37T_a} R_{Ns} + 109.375(1 + 0.149Vf_v^s)\Delta\varepsilon}{\frac{b_e}{\gamma} + 1},$$

$$f_v^s = \min[1, 2(1 - \frac{\min(d_{rs}, H_c)}{d_{rs}})] \quad (5.32)$$

The correction factor  $f_v^s$  is used to gradually alter windspeed at the soil surface as the crop grows and the canopy closes. As the crop grows, turbulence increases at the soil surface and wind is gradually excluded.

Potential transpiration is calculated if a crop is growing. The crop surface roughness parameter,  $r_c$ , is assumed to gradually increase from 1 to 2 as the crop grows until half the soil surface is covered, after which it decreases to 1 as the canopy closes:

$$r_c = \max\left(1, \frac{1}{\left|\frac{H_c}{d_{rs}} - \frac{1}{2}\right| + \frac{1}{2}}\right) \quad (5.33)$$

Crop albedo  $v_c$  is chosen to be constant and equal to 0.23. This value has been used in many other studies, e.g., (Fritsch, 1967; Linacre, 1968; Ritchie, 1971).

Total radiation intercepted by the crop is assumed to be spread uniformly over the area covered by the crop, and an equivalent total radiation  $R_c^e$  is calculated as:

$$R_c^e = R \frac{f_c}{\min\left(1, \frac{H_c}{d_{rs}}\right)} \quad (5.34)$$

Net radiation on the crop is given by:

$$R_{Nc} = (1 - v_c) R_c^e - R_u \quad (5.35)$$

Potential transpiration rate is found from Penman's equation as follows:

$$E_c = f_{ET} \frac{24}{10000} \min\left(1, \frac{H_c}{d_{rs}}\right) \frac{\frac{b_e}{\gamma} \frac{3600}{2500.8 - 2.37T} R_{Nc} + 109.375(1 + 0.149Vf_v^c)\Delta\varepsilon}{\frac{b_e}{\gamma} + 1},$$

$$f_v^c = \begin{cases} \max(0.36/V, 1), & T_a > 25^\circ \\ 1, & T_a \leq 25^\circ \end{cases} \quad (5.36)$$

Here, the correction factor  $f_v^c$  is derived from the idea of a minimum effective wind speed caused by convection on hot, still days (Gates, 1968).

### 5.1.5 Precipitation-Irrigation Submodel.

This submodel calculates the rain intensity using a locally established relationship between the amount of rain/irrigation water and the duration of a precipitation/irrigation event. 2DSOIL uses a constant daily value of the mean intensity,  $I_R$ , which is an input parameter. Chemical concentrations of the irrigation or rain water can be given here also. Concentrations of chemicals in the precipitation/irrigation water are assumed to be constant during each event but may vary from one event to another.

For simulation of flood and/or furrow irrigation, a prescribed small negative pressure of head -1 cm is maintained at certain surface nodes until the prescribed amount of water has infiltrated.

### 5.1.6 Heat movement submodel

This submodel produces hourly values of the parameters  $b_T$  and  $G_T$  in the boundary condition equation:

$$Q_T = -b_T T_{surf} + G_T \quad (5.37)$$

Here  $Q_T$  is the total heat flux into the soil,  $\text{J}\cdot\text{cm}^{-2} \text{ day}^{-1}$ , and  $T_{surf}$  is soil surface temperature,  $^{\circ}\text{C}$ . The module **HeatMover** may further modify values of  $G_T$  as described in Chapter 8. These coefficients are also described in Chapter 3.

The input values are potential evaporation, ( $E_s, \text{cm}\cdot\text{d}^{-1}$ ) from exposed soil cells, as calculated in Eq. (5.32); air temperature,  $T_a$ ; windspeed at 2 m height,  $V (\text{km hr}^{-1})$ ; height of the crop,  $H_c$  (cm); and row spacing,  $d_{rs}$  (cm). Parameters  $b_T$  and  $G_T$  are obtained as combinations of parameters of submodels for components of the surface heat balance equation:

$$Q_T = \begin{cases} F_L E_s - F_L E_a - R_{conv} + R_{rain}, & \text{bare soil} \\ -R_{cond} + R_{rain}, & \text{under canopy} \end{cases} \quad (5.38)$$

where  $F_L E_s$  is energy for potentially available for evaporation of water,  $F_L E_a$  is energy actually used for evaporation of water,  $R_{conv}$  is the heat flux between soil and air due to a temperature difference and air movement,  $R_{rain}$  is the heat flux caused by rainfall,  $R_{cond}$  is the conductive heat flux; all fluxes are given in  $\text{J} \cdot \text{cm}^{-2} \text{ day}^{-1}$ . Equation 5.38 expresses the dependence of the heat flux into or out of the soil, on soil and air temperature, net radiation incident on the exposed soil surface, water evaporation rate, and rainfall. Under a plant, only the conductive heat flux and heat influx with rain water are considered.

Submodels for components of the heat balance are described next where we will show how  $b_T$  and  $G_T$  may be derived. For bare soil, convective heat transfer,  $R_{conv}$ , between the soil and atmosphere occurs when the soil surface is warmer than the air:

$$R_{conv} = b_{conv}(T_a - T_{surf}) \quad (5.39)$$

where  $b_{conv}$  is the coefficient of heat conduction between the soil and the atmosphere. This coefficient is calculated as (Linacre, 1968, Appendix 2):

$$b_{conv} = (0.0040 + 0.00139 V f_V^c) \cdot 6027.26 \quad (5.40)$$

where  $V$  is windspeed at 2 m ( $\text{km hr}^{-1}$ ), and  $f_V^c$  is a correction factor for windspeed given by Eq. (5.36). The numerical factor 6027.26 changes units from  $\text{cal cm}^{-2}$  as used in the formulation of Linacre. Heat influx  $R_{rain}$  due to rainfall is calculated based on the intensity and temperature of the rainwater (the latter assumed to be equal to the air temperature):

$$R_{rain} = I_R C_W T_a \quad (5.41)$$

where  $I_R$  is rain intensity,  $\text{cm day}^{-1}$ , and  $C_W$  is the specific heat capacity of water,  $\text{J g}^{-1} (\text{°C})^{-1}$ .

Beneath the crop canopy, conduction and rain heat transfer are assumed to be the only modes of heat transfer. Conduction is driven by the difference between air and soil surface temperature, and is limited by the conductance of the air boundary layer above the soil. This air

layer is assumed to be 1 cm thick and saturated with water vapor. The component  $R_{cond}$  of heat flux due to conduction is calculated as:

$$R_{cond} = \Lambda_a (T_{surf} - T_a) \quad (5.42)$$

where  $\Lambda_a$  is the thermal conductivity of air saturated with water vapor. The thermal conductivity of saturated air is calculated from a regression equation fitted to a graph of conductivity vs. temperature as prepared by De Vries (1966):

$$\Lambda_a = \left( \frac{0.058 + 0.00017T_a + 0.052e^{0.058T_a}}{1000} \right) 6027.26 \quad (5.43)$$

The numeric factor changes from units  $\text{cal cm}^{-2} \text{ min}^{-1} {}^\circ\text{C}^{-1}$  in the original formulation of Acock and Trent (1991) to  $\text{J cm}^{-1} \text{ k}^{-1} \text{ day}^{-1}$ . Substituting the heat balance components given by (5.39), (5.41), (5.42) into (5.37) and gathering coefficients of  $T_{surf}$ , we have for a base soil

$$\begin{aligned} b_T &= b_{conv} \\ G_T &= b_{conv} T_{surf} + I_R C_W T_a + F_L E_S - F_L E_a \end{aligned} \quad (5.44)$$

For soil beneath the plant, substituting components of the heat balance from (5.41) and (5.42) into (5.37), we have:

$$\begin{aligned} b_T &= \Lambda_a \\ G_T &= \Lambda_a T_a + I_R C_W T_a \end{aligned} \quad (5.45)$$

The *SetSurf02* module does not include the term  $F_L E_a$  in  $G_T$  for a bare soil. The value is subtracted from  $G_T$  by the **HeatMover** module since this parameter depends on the soil water status.

### 5.1.7 Gas movement submodel.

We assume that gas flux through the soil surface may be found as

$$Q_j = -b_j(g_{surf,j} - g_{a,j}) = -b_j g_{surf,j} + G_j \quad (5.46)$$

Where  $Q_j$  is the flux of gas  $j$  to atmosphere, ( $\text{g cm}^{-2} \text{ day}^{-1}$ ),  $g_{a,j}$  is content of this gas in the atmosphere,  $b_j$  is the conductance of the surface air layer for gas  $j$ , and  $G_j$  is the component of the surface gas flux that depends on gas sources other than concentration in the soil air at the surface. This approach has been successfully applied by Kirk and Nye (1991).

### 5.2 Data files 'Weather.dat' and 'Furnod.dat'

The '**Weather.dat**' file, used by the **SetSurf02** module, is described in Table 5.5. Units are converted immediately after the data are read, if necessary by using specific conversion factors. The *BSOLAR* factor is equal to radiation in  $\text{J}\cdot\text{m}^{-2}$  divided by radiation in units used in the '**Weather.dat**' file. The *BTEMP* factor is equal to the change in temperature (in the units used in the '**Weather.dat**' file) equivalent to a  $1^\circ\text{C}$  change. The *ATEMP* factor is equal to the temperature used in the '**Weather.dat**' file that is equivalent to  $0^\circ\text{C}$ . The *ERAIN* factor equals rainfall in  $\text{cm}\cdot\text{day}^{-1}$  divided by rainfall in the units used in the '**Weather.dat**' file. The *BWIND* factor is equal to windspeed in  $\text{km}\cdot\text{hr}^{-1}$  divided by windspeed in units used in the '**Weather.dat**' file.

An illustration of the use of these factors is shown in Example 5.1 following Table 5.5. Radiation data are expressed in langleys so that *BSOLAR*=41680, whereas *BTEMP* and *ATEMP* convert temperatures from  $^\circ\text{F}$  to  $^\circ\text{C}$ . *ERAIN* is set to change inches of rainfall to cm and *BWIND* values convert windspeed values from miles- $\text{hr}^{-1}$  to  $\text{km}\cdot\text{d}^{-1}$ . The parameter *IRAV*, which converts rainfall intensity values from  $\text{in d}^{-1}$  to  $\text{cm d}^{-1}$ , is given in the file but not used because of the switch, *MSW3*, being equal to 1 and since daily rain intensities are available.

The '**Furnod.dat**' data file is read only if furrow and/or flood irrigation is to be simulated. The description of the file in Table 5.6 is self-explanatory.

Table 5.5. Format of the file '**Weather.dat**'.

Record	Variable	Description
1,2	-	Comment lines.
3	<i>LATUDE</i>	Latitude of the site, degrees N.
4	-	Comment line.
5	<i>MSW1</i>	Switch to indicate if daily wet bulb temperatures are available (= 1 if yes).
5	<i>MSW2</i>	Switch to indicate if daily wind is available (= 1 if yes).
5	<i>MSW3</i>	Switch to indicate if daily rain intensities are available (= 1 if yes).
5	<i>MSW4</i>	Switch to indicate if daily concentrations of the chemicals in the rain water are available (= 1 if yes).
5	<i>MSW5</i>	Switch to indicate if flood irrigation will be applied (=1 if yes).
5	<i>MSW6</i>	Switch to indicate if daily values of relative humidity are available (=1 if yes)
6,7	-	Comment lines.
8	<i>BSOLAR</i>	Factor for changing solar radiation units.
8	<i>BTEMP</i>	Factor for changing temperature units.
8	<i>ATEMP</i>	Factor for changing temperature units.
8	<i>ERAIN</i>	Factor for changing rainfall units.
8	<i>BWIND</i>	Factor for changing windspeed units.
8	<i>BIR</i>	Factor for changing rainfall intensity units.
9,10	- -	Comment lines.
11	<i>WINDA</i>	The average windspeed for the site. Not used if <i>MSW2</i> =0.
11	<i>IRAV</i>	The average rain intensity for the site. Not used if <i>MSW3</i> =0.
11	<i>C(1)</i>	Concentration of the first solute in the rain water. Not used if <i>MSW4</i> =0.
11	<i>C(2)</i>	Same as above for the second solute.
11	<i>C(NumSol)</i>	Same as above for the last solute.
11	<i>PG</i>	Conductance of surface air layer to gas flow. Leave this record blank if gas movement will not be simulated and go to record 12.
11	<i>GAIR(1)</i>	Content of the first gas in the atmosphere. Leave this record blank if gas movement will not be simulated.
11	<i>GAIR(2)</i>	Same as above for the second gas
11	<i>GAIR(NumG)</i>	Same as above for the last gas.
12,13	- -	Comment line.
14	<i>JDAY</i>	Julian day number.
14	<i>RI</i>	Daily solar radiation integral.
14	<i>TMAX</i>	Maximum air temperature of the day.
14	<i>TMIN</i>	Minimum air temperature of the day.
14	<i>RAIN</i>	Rainfall/irrigation during the day (use a negative value if flood irrigation is used)
14	<i>WIND</i>	Windspeed at 2 meters if <i>MSW2</i> =1.
14	<i>TWET</i>	Wet bulb temperature if <i>MSW1</i> =1.
14	<i>TDRY</i>	Dry bulb temperature if <i>MSW1</i> =1.
14	<i>IR</i>	Rainfall intensity if <i>MSW3</i> =10.
14	<i>C(1)</i>	Concentration of the first solute in the rain water if <i>MSW4</i> =1.
14	<i>C(2)</i>	Same as above for the second solute.
14	<i>C(NumSol)</i>	Same as above for the last solute.
Record 14 is provided for every day of the period modeled.		

```
**** Example 5.1: WEATHER DATA FOR SETSURF02: FILE 'WEATHER.DAT'
Latitude, deg
40
MSW1      MSW2      MSW3      MSW4      MSW5      MSW6
0          1          0          0          0          0
--Factors for changing units-----
BSOLAR   BTEMP   ATEMP   ERAIN   BWIND   IRAV
41680      0.5556      32      0.394      0.625      0.394
--Average values for site-----
WINDA IRAV    C(1)      C(2).     PG      GAIR(1)
7.5       0.011      0.001      0.17      0.21
--Daily weather parameters -----
JDAY   RI      TMAX   TMIN   RAIN   WIND   TWET   TDRY   IR   C(1)  C(2)...
177    600.6   78.6   62.0   0.5           6.0
178    553.1   81.3   59.1   0.0           0.0
......
287    451.2   62.6   45.2   0.1           3.0
END OF FILE 'WEATHER.DAT'****
```

Table 5.6. File '**Furnod.dat**'.

Record	Variable	Description
1,2	-	Comment lines.
3	<i>NumFP</i>	Total umber of nodes under flood water during irrigation.
4	-	Comment line.
5	<i>NumF(1)</i>	Number of the first node under flood irrigation.
5	<i>NumF(2)</i>	Same as above for the second node.
5	<i>NumF(NumFP)</i>	Same as above for the last node.
6	-	Comment line.
7	<i>hNod(1)</i>	Pressure head at the first flooded node during irrigation.
7	<i>hNod(2)</i>	Same as above for the second node.
7	<i>hNod(NumFP)</i>	Same as above for the last node.

```
**** Example 5.2: FURROW DATA FOR SETSURF2: FILE 'FURNOD.DAT'
NumFP
3
NumF(1)  NumF(2)  NumF(3)
15        16        17
hNod(1)  hNod(2)  hNod(3)
-0.1     -0.1     -0.1
```

### **5.3 Using customized agro-meteorological data: SetSurf01 module**

The frequency of meteorological data collection may be more detailed than daily. This may occur in field experiments as well as in simulation runs with diurnal weather generators. The *Setsurf01* module will read such weather information but will not change units.

The data file, '**Setsurf.dat**', for the module **SetSurf01** is described in Table 5.7. The data file contains values of precipitation, evaporation from bare soil, and solute concentrations in rainfall and/or irrigation water. '**Setsurf.dat**' also contains boundary parameters for heat and gas movement.

Boundary condition parameter for heat movement reflect two possible formulations of the surface boundary conditions:

$$T_{surf} = \text{const} \quad (5.47)$$

or

$$Q_T = -b_T T_{surf} + G_T \quad (5.48)$$

Where  $T_{surf}$  is the surface temperature,  $Q_T$  is the heat flux,  $\text{J cm}^{-2} \text{ d}^{-1}$ , and  $b_T$  and  $G_T$  are coefficients described below. The first formulation corresponds to a constant temperature at the boundary node. The second formulation may be used in the following two cases:

- (1) Surface heat flux is prescribed ( $b_T=0$ ,  $G_T$  is prescribed flux)
- (2) Conductive heat exchange occurs between soil and air,  $Q_T = -b_T (T_{surf} - T_a)$ , where  $b_T$  is the conductance for heat exchange,  $T_{surf}$  is the temperature in the boundary node, and  $T_a$  is the air temperature. This case is equivalent to the assumption  $G_T=b_T T_a$ .

Gas movement boundary parameters are introduced very much like those for heat movement parameters. As for heat there are two formulations of the surface boundary conditions:

$$g_{surf,j} = \text{const} \quad (5.49)$$

or

$$Q_{g,j} = -b_{g,j} g_{surf,j} + G_j \quad (5.50)$$

where index  $j$  is the number of the gas under consideration,  $Q_{g,j}$  is gas flux,  $\text{cm}^{-2} \text{d}^{-1}$ , and the parameters,  $b_{g,j}$  and  $G_j$  are described below. The first formulation corresponds to a constant gas content at the boundary node. The second formulation may correspond to the following two cases:

- (1) The potential surface gas flux is prescribed ( $b_{g,j}=0$ ,  $G_j$  is prescribed flux)
- (2) Convective gas exchange occurs between soil and air, in which case  $Q_{g,j}=-b_{g,j}(g_{surf,j}-g_j)$ , where  $b_{g,j}$  is the gas transfer coefficient,  $g_{surf,j}$  is the content of the  $j$ th gas at the boundary node, and  $g_j$  is the content of the  $j$ th gas in the atmospheric. This case is equivalent to the assumption,  $G_j=b_{g,j}g_j$ .

If some of the above processes are not included in the simulation, the corresponding data must be omitted from the data file. Units of solute concentration and gas content are the same as in the corresponding **SoluteMover** and **GasMover** modules.

The surface data may be set at each node separately or at all nodes simultaneously, as shown in Example 5.3. For the first time interval,  $nCode=0$  and all nodes get the same values of boundary concentrations and fluxes. For the second time interval  $nCode\neq0$ , indicating that the boundary data for the two boundary nodes are set separately. Heat movement is not simulated in this example; hence, so surface parameters for heat movement are absent in this example.

Table 5.7. File '**Setsurf.dat**'.

Record	Variable	Description
1,2	-	Comment lines.
3	<i>tAtm</i>	Time <b>at the end</b> of the time interval.
3	<i>nCode</i>	Code indicating the surface nodes: <i>nCode</i> =0 means that data are valid for all nodes of the surface. <i>nCode</i> ≠ 0 means that data are given separately for every surface node.
4	<i>n</i>	Nodal number of the surface node. Set it arbitrary if <i>nCode</i> =0.
4	<i>VarBW(*,1)</i>	Precipitation rate during the time interval, cm day <sup>-1</sup> . The asterisk means that this value is valid for node <i>n</i> if <i>nCode</i> ≠ 0 and for all surface nodes if <i>nCode</i> =0.
4	<i>VarBW(*,2)</i>	Potential evaporation rate, cm·day <sup>-1</sup> . The asterisk means that this value is valid for node <i>n</i> if <i>nCode</i> ≠ 0 and for all surface nodes if <i>nCode</i> =0.
4	<i>VarBS(1)</i>	Concentration of the first solute in the rain/irrigation water. The asterisk means that the value is valid for node <i>n</i> if <i>nCode</i> ≠ 0 and for all surface nodes if <i>nCode</i> =0.
4	<i>VarBS(2)</i>	Same as above for the second solute.
4	...	...
4	<i>VarBS(NumSol)</i>	Same as above for the last solute.
4	<i>VarBT(*,1)</i>	Constant boundary temperature $T_{surf}$ . If the boundary code is -4, then set this value to zero. Asterisk means that the <i>VarBT(*,1)</i> value must be given for node <i>n</i> if <i>nCode</i> ≠ 0 and for all surface nodes if <i>nCode</i> =0.
4	<i>VarBT(*,2)</i>	Coefficient $b_T$ in Eq. (5.48), J cm <sup>-2</sup> day <sup>-1</sup> (°C) <sup>-1</sup> . If the boundary code is 4, then set this value to 0. Asterisk means that the <i>VarBT(*,2)</i> value must be given for node <i>n</i> if <i>nCode</i> ≠ 0 and for all surface nodes if <i>nCode</i> =0.
4	<i>VarBT(*,3)</i>	Coefficient $G_T$ in Eq. (5.48). If the boundary code is 4, then set this value to zero. Asterisk means that the <i>VarBT(*,2)</i> value must be given for node <i>n</i> if <i>nCode</i> ≠ 0 and for all surface nodes if <i>nCode</i> =0.4 <i>VarBG(*,1,1)</i> Constant boundary content of the first gas $g_{1,surf}$ in Eq.(5.49), g cm <sup>-2</sup> . If the boundary code is -4, then set this value to zero. Asterisk means that the <i>VarBG(*,1,1)</i> value must be given for node <i>n</i> if <i>nCode</i> ≠ 0 and for all surface nodes if <i>nCode</i> =0.
4	<i>VarBG(*,1,2)</i>	Coefficient $b_{gj}$ in Eq.(5.50) for the first gas, cm day <sup>-1</sup> . If the boundary code is 4, then set this value to zero. Asterisk means that the <i>VarBG(*,1,2)</i> value must be given for node <i>n</i> if <i>nCode</i> ≠ 0 and for all surface nodes if <i>nCode</i> =0.
4	<i>VarBG(*,1,3)</i>	Coefficient $G_{gj}$ in Eq.(5.50) for the first gas, g cm <sup>-2</sup> day <sup>-1</sup> . If the boundary code is 4, then set this value to zero. Asterisk means that the <i>VarBG(*,1,3)</i> value must be given for node <i>n</i> if <i>nCode</i> ≠ 0 and for all surface nodes if <i>nCode</i> =0.
4	<i>VarBG(*,2,1)</i>	Same as <i>VarBG(*,1,1)</i> for the second gas.
4	<i>VarBG(*,2,2)</i>	Same as <i>VarBG(*,1,2)</i> for the second gas.
4	<i>VarBG(*,2,3)</i>	Same as <i>VarBG(*,1,3)</i> for the second gas.
4	...	...
4	<i>VarBG(*,NumG,1)</i>	Same as <i>VarBG(*,1,1)</i> for the last gas.
4	<i>VarBG(*,NumG,2)</i>	Same as <i>VarBG(*,1,2)</i> for the last gas.
4	<i>VarBG(*,NumG,3)</i>	Same as <i>VarBG(*,1,3)</i> for the last gas.
The asterisk means that the record 4 is provided for all boundary nodes if <i>nCode</i> ≠ 0. Records 3 and 4 are provided for sequential time intervals that cover the simulation interval altogether.		

```
*** Example 5.3: DATA FOR SETSURF1: FILE 'SETSURF.DAT'
tAtm   nCode   n   Prec   rSoil    c(1)  Ts     bT GT    g1   bg1 Gg1 g2   bg2 Gg2
0.29      0          0   0.00   0.001      600  0.003 0.   0.   0.21   0.   0.
0.75      1          1   0.00   0.008      100  0.005 0.   0.   0.205  0.   0.
                  2   0.50   0.002      600  0.003 0.   0.   0.210  0.   0.
```

# Chapter 6: Water Flow: WaterMover Module

**Jirka Šimůnek, Yakov Pachepsky, and Martinus Th. van Genuchten**

The WaterMover module was extracted from the SWMS\_2D model (Šimůnek et al., 1992). This water flow simulation code has several important computational advantages. Among these are: 1) the ability to adjust the iteration domain to only that region where convergence criteria are not met, 2) having a table look-up of soil water and hydraulic conductivity values as a function of soil water potential, 3) the possibility to use both triangular and rectangular grid cells to describe complex shapes of the soil surface.

The original code was slightly modified to handle abrupt changes in the water flux at the soil surface, root activity in a strongly non-equilibrium moisture regime, and root water uptake as determined for individual soil elements. The original algorithm could deal with scaled stochastic and/or anisotropic hydraulic soil properties. This option was excluded from 2DSoil to improve structure simplicity.

## **6.1 The two-dimensional model of water flow and its finite element implementation**

The model considers two-dimensional Darcian water flow in a variably saturated soil. The code neglects deformations of a soil due to shrinking-swelling, assumes vapor transport to be negligibly small as compared to water flow in the liquid phase, treats soil as a locally isotropic medium, and allows temperature and solute concentrations to influence hydraulic parameters but not water potential gradients. The governing flow equation is given by the following appropriate form of the Richards' equation:

$$\frac{\partial \theta}{\partial t} - \frac{\partial}{\partial x} \left( k \frac{\partial h}{\partial x} \right) - \frac{\partial}{\partial z} \left[ k \left( \frac{\partial h}{\partial z} + 1 \right) \right] + S = 0 \quad (6.1)$$

for water flow in a vertical soil cross-section, and by

$$\frac{\partial \theta}{\partial t} - \frac{1}{x} \frac{\partial}{\partial x} \left( kx \frac{\partial h}{\partial x} \right) - \frac{\partial}{\partial z} \left[ k \left( \frac{\partial h}{\partial z} + 1 \right) \right] + S = 0 \quad (6.2)$$

for axisymmetrical water flow. Here,  $\theta$  is the volumetric water content ( $\text{cm}^3$  of water per  $\text{cm}^3$  of soil),  $h$  is the pressure head (cm),  $S$  is an extraction term that describes the joint action of all factors contributing to removal of the water from the soil ( $\text{cm}^3$  per  $\text{cm}^3$  of soil per day),  $x$  either is the horizontal coordinate in case of water flow in a vertical soil cross-section, or the radial coordinate in case of axisymmetrical flow, cm;  $z$  is the vertical coordinate measured upward from a reference horizontal plane, (cm);  $t$  is time,(days); and  $k$  is soil hydraulic conductivity, ( $\text{cm}^3$  of water per  $\text{cm}^2$  of soil per day). The reference plane may be placed at any arbitrary depth.

The water content  $\theta$  and hydraulic conductivity  $k$  depend on the pressure head  $h$ , and may also depend on the spatial coordinates  $x$  and  $z$ , time, the concentration of solutes, temperature, and other soil state variables. Two models describing the dependencies of  $\theta$  and  $k$  on  $h$  are given in Sections 6.3 and 6.5 of this manual. The extraction term  $S$  is determined mainly by root water uptake. Chapter 10 of this manual describes submodels for root water uptake.

The governing equations (6.1) and (6.2) for water flow are solved numerically (Šimůnek et al., 1992) to obtain spatial and temporal distributions of the pressure head  $h$  within the soil domain. Numerical solution was accomplished using the Galerkin finite element method with linear basis functions and triangular elements (soil cells). The soil domain for this purpose is divided into a network of triangular elements. Nodal points are located at the corners of the different elements. For the example of the grid in Fig. 3.1, one possible subdivision is shown in Fig. 6.1. The pressure head at any point is expressed as a linear combination of nodal pressure head values:

$$\hat{h}(x,z,t) = \sum_{n=1}^{N_n} \phi_n(x,z) h_n(t) \quad (6.3)$$

where  $N_n$  is the total number of nodes,  $\phi_n(x,z)$  are basis functions for node  $n$ , and  $h_n$  is the pressure head at node  $n$ . Basis functions are interpolation functions for the element.

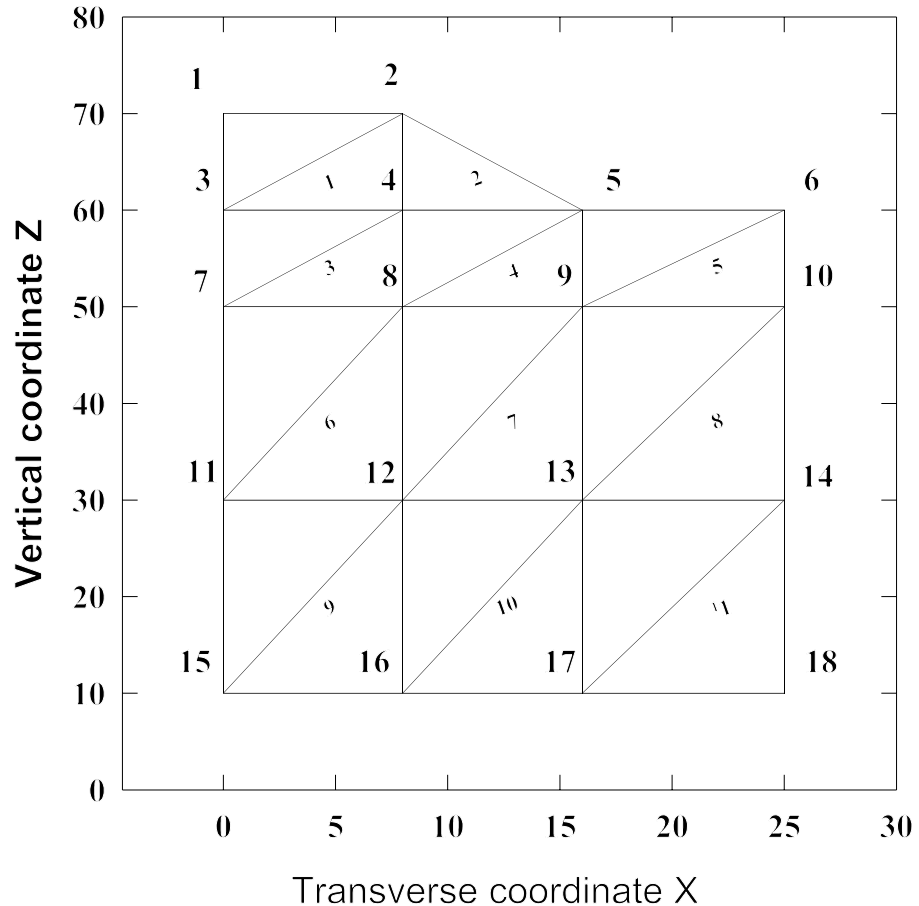


**Figure 6.1** Subdivision of rectangular elements to triangular elements.

The triangular element, as shown in Fig. 6.2, has the following interpolation functions (Istok, 1989):

$$\begin{aligned}
\Phi(x, z) &= \frac{1}{2A}(\hat{a}_s + \hat{b}_s x + \hat{c}_s z), \quad s = i, j, k \\
\hat{a}_i &= x_j z_k - x_k z_j, \quad \hat{b}_i = z_j - z_k, \quad \hat{c}_i = x_k - x_j \\
\hat{a}_j &= x_k z_i - x_i z_k, \quad \hat{b}_j = z_k - z_i, \quad \hat{c}_j = x_i - x_k \\
\hat{a}_k &= x_i z_j - x_j z_i, \quad \hat{b}_k = z_i - z_j, \quad \hat{c}_k = x_j - x_i \\
A &= \frac{1}{2}(\hat{a}_i + \hat{a}_j + \hat{a}_k) = \frac{1}{2}(\hat{c}_k \hat{b}_j - \hat{c}_j \hat{b}_k)
\end{aligned} \tag{6.4}$$

where  $A$  is the area of the element.

The Galerkin method is used to obtain equations for the nodal values of  $h$ . Area-averaged weighted residuals of Eq. (6.1) have to be equal to zero and must be true for every  $\phi_n$  taken as a weight. Consequently, for the whole soil domain we obtain:

$$\sum_{e=1}^{N_e} \int_{\Omega_e} \left[ \frac{\partial \theta}{\partial t} - \frac{\partial}{\partial x} \left( k \frac{\partial h}{\partial x} \right) - \frac{\partial}{\partial z} \left[ k \left( \frac{\partial h}{\partial z} + 1 \right) \right] + S \right] \phi_n d\omega = 0 \tag{6.5}$$

where  $\Omega_e$  designates the area of element  $e$ , and  $N_e$  is the total number of elements. After replacing  $h$  by  $\hat{h}$  and using Green's first identity, one has:

$$\begin{aligned}
&\sum_{e=1}^{N_e} \int_{\Omega_e} \left[ \frac{\partial \theta}{\partial t} \phi_n + k \left( \frac{\partial \hat{h}}{\partial x} \frac{\partial \phi_n}{\partial x} + \frac{\partial \hat{h}}{\partial z} \frac{\partial \phi_n}{\partial z} \right) \right] d\omega = \\
&\sum_{e=1}^{N_e} \int_{\Gamma_e} k \left[ \frac{\partial \hat{h}}{\partial x} n_{\Gamma,x} + \left( \frac{\partial \hat{h}}{\partial z} + 1 \right) n_{\Gamma,z} \right] \phi_n d\Gamma \\
&- \sum_{e=1}^{N_e} \int_{\Omega_e} k \frac{\partial \phi_n}{\partial z} d\omega - \sum_{e=1}^{N_e} \int_{\Omega_e} S \phi_n d\omega = 0
\end{aligned} \tag{6.6}$$

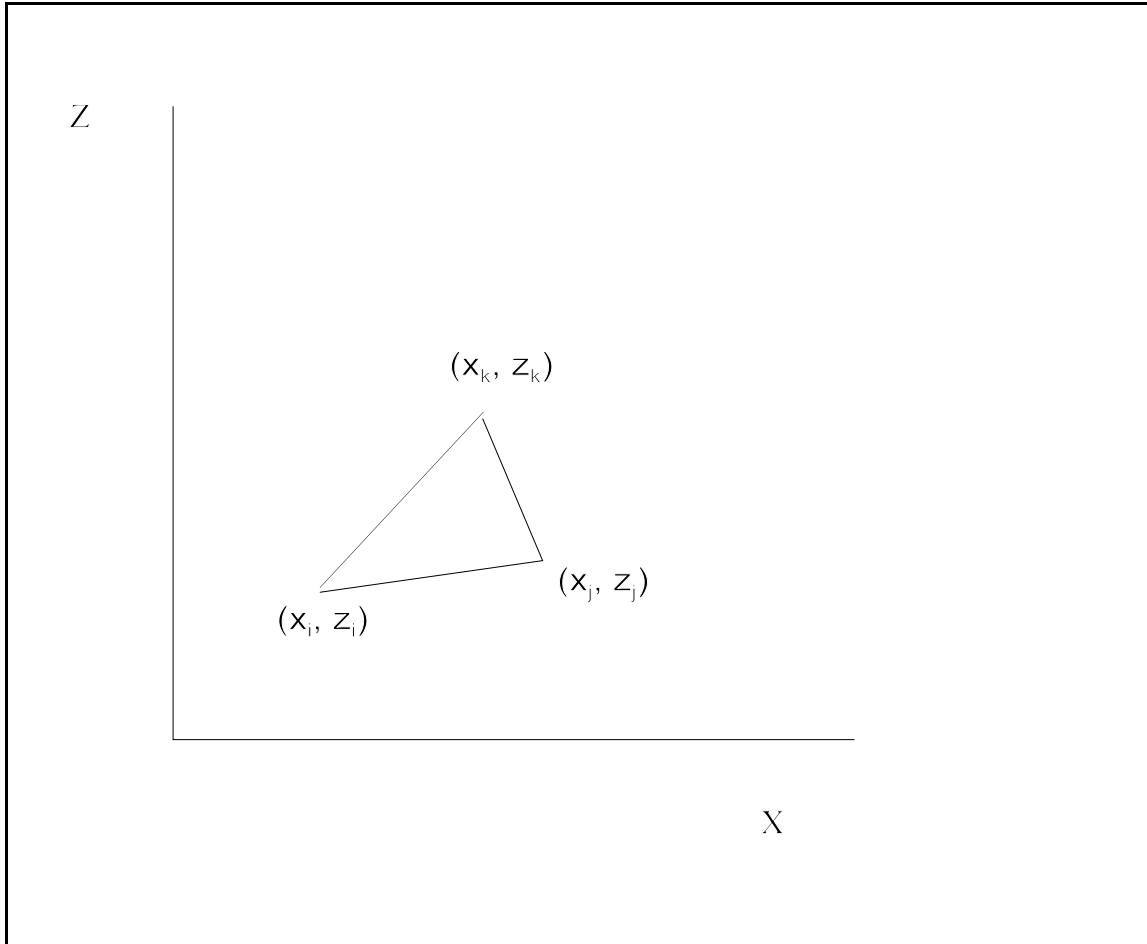


**Figure 6.2** Triangular element as used for the finite element discretization of the flow equations in 2DSOIL.

where  $\Gamma_e$  is the boundary of element  $e$ , and  $n_{\Gamma,x}$ ,  $n_{\Gamma,z}$  designate components of the unit normal vector to the boundary.

Further simplifications are based on two important assumptions. First, moisture content  $\theta$ , the soil hydraulic conductivity, the specific water capacity of the soil, and the water extraction rate  $S$  are assumed to vary linearly over each element. Second, nodal moisture content changes may be found as weighted averages of moisture content changes over an element according to the mass-lumping technique (Istok, 1989). Accepting these assumptions leads to a system of first-order ordinary differential equations for the nodal pressure head values:

$$[F] \frac{d\vec{\theta}}{dt} + [A] \vec{h} = \vec{Q} - \vec{B} - \vec{D} \quad (6.7)$$

where the vectors  $\bar{h}$ , and  $\theta$  include all nodal values of  $h$ , and  $\theta$ . The matrices  $[A]$  and  $[F]$  have as elements

$$A_{m,n} = \sum_e \frac{1}{4A_e} \bar{k}_e (\hat{b}_m \hat{b}_n + \hat{c}_m \hat{c}_n), \quad F_{m,n} = \delta_{mn} \sum_e \frac{A_e}{3} \quad (6.8)$$

where the summation involves all elements that have the nodes  $m$  and  $n$  among their corner nodes. The vectors  $\bar{B}$ ,  $\bar{Q}$ , and  $\bar{D}$  are given by

$$B_n = \sum_e \frac{\bar{k}_e}{2} \hat{c}_n, \quad Q_n = -\sum_e q_{e,n} \frac{d_{e,n}}{2}, \quad D_n = \sum_e \frac{1}{12} A_e (3\bar{S}_e + S_n) \quad (6.9)$$

where the summation involves all elements adjacent to node  $n$ . The parameters  $\hat{b}_n$ ,  $\hat{c}_n$ ,  $A_e$  have the same meaning as in Eq. (6.4);  $\bar{k}_e$  is the average hydraulic conductivity over the element;  $d_{e,n}$  is the length of the soil domain boundary segment that serves as the boundary of the element  $e$  and ends at the node  $n$ ; and  $q_{e,n}$  is the water flux through the soil domain boundary to/from element  $e$  near node  $n$ , such that  $q_{e,n}$  is positive when water flows out of the soil domain (cm per day).

Nodal water extraction rates are calculated as  $S_n = \sum_e A_e S_e / \sum_e A_e$  where the summation includes all elements that have node  $n$  at one of their corners. The average nodal water extraction rate,  $\bar{S}$ , of an element is found as the mean of 5 at its nodal values. A method of solution of system (6.7) is described in detail by Šimůnek et al. (1992). After every time step water flow velocities are calculated in accordance with Darcy's law, and derivatives of the pressure head are obtained directly from Eq. (6.3).

Slight modifications of the coefficients in Eqs. (6.8) and (6.9) allow axisymmetrical cases as described by Eq. (6.2) to be solved (Šimůnek et al., 1992). Boundary and initial conditions must be set to solve Eq. (6.7). Methods of time-dependent boundary settings are presented in Chapters 4 and 5 of this manual. Time-independent boundary pressure heads must be included in the initial distribution data as described in the next section.

## **6.2 Data files '**Param\_W.dat**' and '**Nodal\_W.dat**'**

Computations within the WaterMover module may be affected by several iteration and time-stepping parameters that are read from the file '**Param\_W.dat**'. It is difficult to recommend specific values for these parameters as they are dependent on the water redistribution pattern and especially on the values of boundary fluxes for the problem under consideration. Therefore, only ranges and/or limits are presented below.

The parameter *MaxIt* determines the maximum allowable number of iterations. Our experience suggests that this parameter is best set between 10 and 20. The rate of convergence (number of iterations) and the precision of computations is affected by the tolerance limits *TolAbs* and *TolRel*. Iterations may be stopped when the difference between the pressure heads of the previous iteration,  $h^{temp}$ , and the current iteration,  $h^{new}$ , obeys the inequality

$$|h^{new} - h^{temp}| \leq TolAbs + TolRel * |h^{new}| \quad (6.10)$$

everywhere in the soil domain. Recently Huang et al., (1996) proposed the use of a convergence criterion based on water content rather than matric potential. The advantage of this criterion is that convergence is much more rapid in dry soils. The convergence criterion is:

$$TolTh = \frac{d\theta}{dh} \frac{(hNew - hTemp)}{\theta_{sat} - \theta_r} \quad (6.11)$$

The value of *TolAbs* influences the precision and rate of convergence mainly for nodes where the soil is close to saturation. The value of *TolRel* does the same for nodes where the soil has a low moisture content. Values of *TolAbs* between 0.005 and 0.05 cm and values of *TolRel* between 0.005 and 0.0005 seem to be reasonable for the majority of problems. For *TolTh*, the value 0.001 usually works well.

The model does not allow evaporation to create arbitrarily low negative pressure heads on the soil-atmosphere boundary. When the pressure head decreases to the *hCritA* value, a further decrease in pressure head will be prevented, and the pressure head is forced to remain at *hCritA* (the pressure head potential that corresponds to the air-dry soil water content). At the

next time step the program will inspect potential fluxes across the surface. If the soil continues to dry (positive flux), then the pressure head is maintained at the  $hCritA$  level. Real fluxes will then be less than potential. If potential fluxes tend to rewet the soil, then they are allowed to act as real fluxes, and the pressure head becomes greater than  $hCritA$ . A range from -30,000 to -100,000 cm seems to be reasonable for  $hCritA$ .

The model can handle positive pressure heads along the soil-atmosphere boundary only in cases where the water flux on the surface is directed into the soil (or equal to zero). Therefore, it is advisable to avoid positive surface pressure heads if ponding due to rainfall may be changed to evaporation during a time step. The variable  $hCritS$  may be used for this purpose. This variable may be arbitrarily made positive if no 'rainfall ponding-evaporation' alterations will occur, but must be set to zero if such alterations will occur.

Time steps are regulated mainly by the *Synchronizer* module. The WaterMover module itself may decrease the time step if convergence is not reached within  $MaxIt$  iterations. The WaterMover cannot make the time step larger than *Synchronizer* does. However, it is advisable to set a reasonable upper limit for the time step in the WaterMover so as to prevent drastic changes in time steps during the calculations. This upper limit is assigned to a variable  $DtMx(1)$ , which may have values between 0.001 and 0.01 of the total simulated time.

Variables  $hTab1$  and  $hTabN$  mark the range of pressure head values that are most likely during the calculations. Dependencies of the moisture content and the hydraulic conductivity on the pressure head in this range will be tabulated at the very beginning of the calculations. Thereafter, interpolation between tabular values will avoid the time-consuming calculations of hydraulic properties from approximation formulas. Appropriate values for the hydraulic properties will be computed directly from the approximation formulas only if the absolute value of the pressure head during program execution lies outside the interval  $[-hTabN, -hTab1]$ .

The structure of data for the computational parameters is presented in Table 6.1. An example is given immediately after the table. Besides the computational parameters, *WaterMover* reads data on the initial pressure head distribution from the file '**Nodal\_W.dat**'. If there are constant head boundaries, then the values of the boundary heads must be given in the file. Table 6.2 shows the structure of data in the '**Nodal\_W.dat**' file, with our example following

the table. The example corresponds to the grid of Fig. 3.1 and to the file '**Grid\_bnd.dat**' of Example 3.3. The reference plane of the vertical coordinate is placed at the 270-cm depth.

### **6.3 The unsaturated soil hydraulic properties: Using closed-form approximations in the submodule SetMat01**

A widespread approach for describing the unsaturated soil hydraulic properties is to use closed-form equations. The approach used here was introduced by van Genuchten (1980) who used the statistical pore-size distribution model of Mualem (1976) to obtain a predictive equation for the unsaturated hydraulic conductivity function. Later, the original van Genuchten

Table 6.1. WaterMover module information on computational parameters - file '**Param\_w.dat**'.

Record	Variable	Description
1,2	-	Comment line.
3	<i>MaxIt</i>	Maximum number of iterations allowed during any time step.
3	<i>TolAbs</i>	Absolute pressure head tolerance.
3	<i>TolRel</i>	Relative pressure head tolerance.
3	<i>hCritA</i>	Value of the minimum allowed pressure head at the soil-atmosphere boundary (usually a value of matric potential for air-dry water content).
3	<i>hCritS</i>	Maximum allowed pressure head at the soil-atmosphere boundary (to allow runoff, a value of -1 will cause less numerical problems than a value of 0 or greater).
3	<i>dtMx(1)</i>	Maximum allowed time step in water transport calculations.
3	<i>hTab1</i>	Absolute value of lower limit of the pressure head interval for which a table of hydraulic properties will be generated internally for each material (must be greater than the 0.0, e.g., 0.001 cm).
3	<i>hTabN</i>	Absolute value of the upper limit of the pressure head interval for which a table of hydraulic properties will be generated internally for each material (e.g., 1000 cm).

\*\*\* Example 6.1: WATERMOVER COMPUTATIONAL PARAMETERS: file 'Param\_W.dat'

MaxIt TolAbs TolRel hCritA hCritS DtMx(1) hTab1 hTabN  
 20 .50 0.001 -1.E+05 1.E+06 1.0 0.001 100

Table 6.2. Format of file '**Nodal\_W.dat**'.

Record	Variable	Description
1,2	-	Comment lines.
3	$n$	Nodal number.
3	$hOld(n)$	Initial value of the pressure head at node $n$ .

Record 3 is provided for every node of the grid.  
If a 'constant head' boundary condition is to be imposed in some nodes, then the corresponding boundary values of the pressure head must be present in this table.

```
**** Example 6.2: INITIAL PRESSURE HEAD DISTRIBUTION - file 'Nodal_w.dat'
n hOld
1 -270
2 -270
3 -260
4 -260
5 2.5
6 2.5
7 -250
8 -250
9 -250
10 -250
11 -230
12 -230
13 -230
14 -230
15 -210
16 -210
17 -210
18 -210
```

equations were modified to add extra flexibility to the description of the hydraulic properties near saturation (Vogel and Cislerova, 1988). The most recent formulation may be found in the report of Šimunek et al. (1992) in which the soil water retention,  $\theta(h)$ , and hydraulic conductivity,  $k(h)$ , functions are given by

$$\theta(h) = \begin{cases} \theta_a + \frac{\theta_m - \theta_a}{(1 + \alpha h)^m}, & h < h_s \\ \theta_s & h \geq h_s \end{cases} \quad (6.12)$$

and

$$k(h) = \begin{cases} K_s [K_r(h)], & h \leq h_k \\ K_k + \frac{(h-h_k)(K_s - K_k)}{h_s - h_k}, & h_k < h < h_s \\ K_s & h \geq h_s \end{cases} \quad (6.13)$$

respectively, where

$$\begin{aligned} K_r &= \frac{K_k}{K_s} \left( \frac{S_\theta}{S_{\theta k}} \right)^{1/2} \left[ \frac{F(\theta_r) - F(\theta)}{F(\theta_r) - F(\theta_k)} \right]^2, & F(\theta) &= \left[ 1 - \left( \frac{\theta - \theta_a}{\theta_m - \theta_a} \right)^{1/m} \right]^m \\ S_\theta &= \frac{\theta - \theta_r}{\theta_s - \theta_r}, & S_{\theta k} &= \frac{\theta_k - \theta_r}{\theta_s - \theta_r}, & m &= 1 - \frac{1}{n}, & n > 1 \end{aligned} \quad (6.14)$$

Here,  $\theta_r$  and  $\theta_s$  denote the residual and saturated water contents, respectively, and  $K_s$  is the saturated hydraulic conductivity. To allow for a non-zero air-entry value,  $h_s$ , Vogel and Cislerova (1988) replaced the parameters  $\theta_r$  and  $\theta_s$  in the retention function by the fictitious (extrapolated) parameters  $\theta_a \leq \theta_r$  and  $\theta_m \geq \theta_s$  as shown in Fig. 6.3. The value,  $\theta_m$ , can be considered a measure of soil macroporosity. The approach maintains the physical meaning of  $\theta_r$  and  $\theta_s$  as measurable quantities. Equation (6.12) assumes that the predicted hydraulic conductivity function is matched to a measured value of the hydraulic conductivity at some water content  $\theta_k$  less than the saturated water content,  $\theta_s$ . The above set of soil hydraulic functions contains nine unknown parameters:  $\theta_r$ ,  $\theta_s$ ,  $\theta_w$ ,  $\theta_m$ ,  $\alpha$ ,  $n$ ,  $K_s$ ,  $K_k$ ,  $\theta_k$ . When  $\theta_a = \theta_r$ ,  $\theta_m = \theta_k = \theta_s$ , and  $K_k = K_s$ , the soil hydraulic functions reduce to the original expressions of van Genuchten (1980). To find the parameters from experimental data, one can use the program **GENPAR**, which is not included in this release of 2DSOIL but is available upon request from the authors.

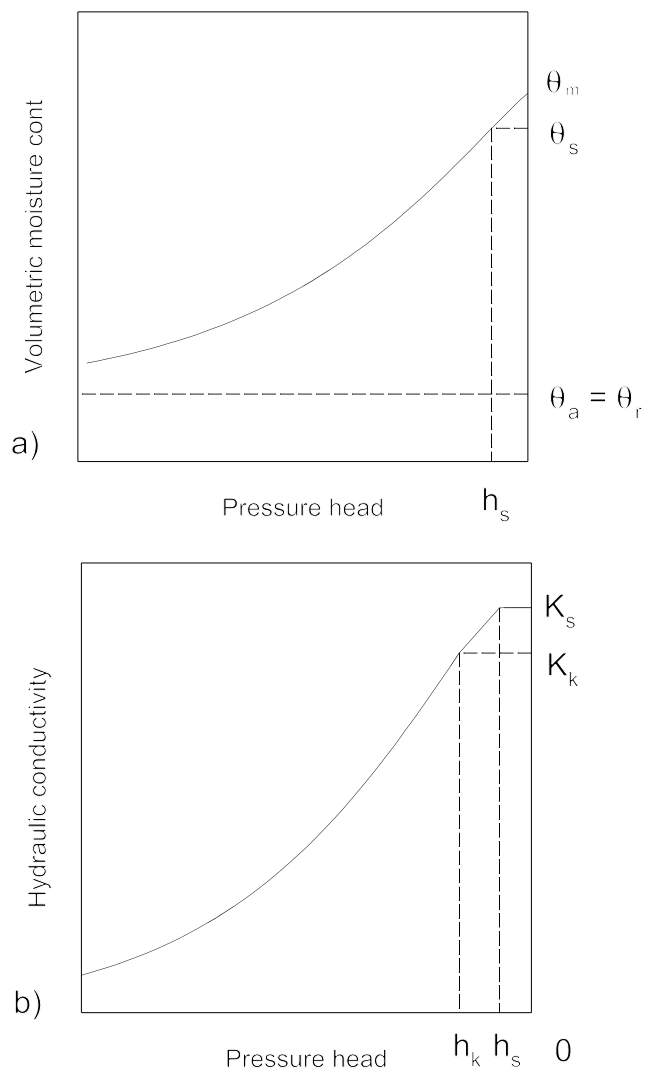


**Figure 6.3** Schematic of the relationship between pressure head and water content and pressure head and hydraulic conductivity as expressed in equations 6.11 and 6.12

#### **6.4 Data file '*Closefrm.dat*'**

This file contains parameters that appear in the closed-form soil hydraulic equations for all soil materials that differ in their properties. The structure of data file '**Closefrm.dat**' is given in Table 6.3. This table is followed by an example data file for a soil profile with three layers.

#### **6.5 The unsaturated soil hydraulic properties: Using piece-wise polynomial approximations in the submodule SetMat02**

Continuous and smooth relationships between the hydraulic conductivity and pressure head, and between moisture content and matric pressure head, may be constructed from a limited number of data points by using some method of interpolation or approximation that smooths the data. This process may result in a significant loss of information since the derivatives of the moisture content and hydraulic conductivity with respect to pressure head are very important for the water flow simulation. This loss of information can be illustrated by recasting Eq. (6.1) into the following form:

$$\frac{d\theta}{dH} \frac{\partial H}{\partial t} + k \left\{ \frac{d\ln(k)}{dH} \left[ \left( \frac{\partial H}{\partial z} + 1 \right) \frac{\partial H}{\partial z} + \left( \frac{\partial H}{\partial x} \right)^2 \right] + \frac{\partial^2 H}{\partial z^2} + \frac{\partial^2 H}{\partial x^2} \right\} + S = 0 \quad (6.15)$$

Table 6.3. WaterMover module information for parameters in close-form equations of the soil hydraulic properties- file '**Closefrm.dat**'.

Record	Variable	Description
1,2	-	Comment lines.
3	<i>Par(1,M)</i>	Parameter $\theta_r$ for material $M$ .
3	<i>Par(2,M)</i>	Parameter $\theta_s$ for material $M$ .
3	<i>Par(3,M)</i>	Parameter $\theta_a$ for material $M$ .
3	<i>Par(4,M)</i>	Parameter $\theta_m$ for material $M$ .
3	<i>Par(5,M)</i>	Parameter $\sigma$ for material $M$ .
3	<i>Par(6,M)</i>	Parameter $n$ for material $M$ .
3	<i>Par(7,M)</i>	Parameter $K_s$ for material $M$ .
3	<i>Par(8,M)</i>	Parameter $K_k$ for material $M$ .
3	<i>Par(9,M)</i>	Parameter $\theta_k$ for material $M$ .
Record 3 information is provided for each material $M$ (from 1 to $NMat$ ).		

```
*** Example 6.3: SOIL HYDRAULIC PARAMETERS - file 'Closefrm.dat'
    thr      ths      tha      thm      Alfa      n       Ks       Kk       thk
.0001    .399    .0001    .399    .0174   1.3757   10       10     .399
.02      .450     .01     .551    .0093   1.567    1.2      0.7     .420
.01      .411    .005     .490    .0120   1.440    3.5      2.4     .391
```

where the matric suction  $H$  is used instead of the pressure head  $h$ , i.e.,  $H=-h$  in unsaturated soil. This form of the Richards' equation clearly shows the coefficients that govern changes in the matric suction and hence the water content. These coefficients are the derivatives of the moisture content and hydraulic conductivity with respect to matric suction, i.e., the specific soil water capacity  $\sigma=d\theta/dH$ , and  $\mu=d\ln k/dH$ , respectively. We require that values of  $\sigma$ ,  $\mu$ , and  $k$ , as well as the values of the moisture content and  $H$ , be as close to the experimental data as possible, and still are situated on a continuous curve.

Although the use of analytical formulas to approximate hydraulic parameters can, to a certain extent, guarantee a reasonable closeness between calculated and measured  $\theta$  and  $H$ , or  $k$  and  $H$  values, analytical approximations do not guarantee that calculated and actual values of the derivatives,  $\sigma$  and  $\mu$ , are always close. This in turn can have an impact on the results of models that use these smoothed data in water flow simulations. We describe now a method for utilizing a piecewise continuous polynomial to interpolate water contents from soil matric potentials at the midpoints between pairs of measured data. The interpolating curve consists of a sequence of

cubic polynomials. Because splines are shape preserving, the shape of the piecewise polynomial function is close to the shape of measured water retention curves. Since cubic splines preserves first-order continuity, the derivatives are better preserved.

The method is illustrated in Fig. 6.4 for the water retention curve. Interpolation is done between midpoints of segments that connect neighboring pairs of the measurement points. If  $A_1, A_2, A_3$  are sequentially measured points and  $\hat{A}_2, \hat{A}_3$  are midpoints of the segments  $[A_1 A_2]$  and  $[A_2 A_3]$ , then the interpolating curve will join points the  $\hat{A}_2$  and  $\hat{A}_3$ . The interpolating curve is tangent to  $f[A_1 A_2]$  at the point  $\hat{A}_2$ , and tangent to  $[A_2 A_3]$  at the point  $\hat{A}_3$ .

In the region close to saturation the interpolating curve goes through saturation at  $H=0$  and the first measured data point after saturation. This first piece has a zero derivative at saturation and is tangent to the segment connecting the first and second measured unsaturated data points. The calculations are carried out according to the following equations. Let the water content be measured for  $N$  values of the suction, i.e., at  $H_{i,i+1,\dots,N} := 0, H_1, H_2, \dots, H_N$ .

1. An auxiliary set of intermediate values of  $H$  is introduced:

$$\bar{H}_0 = H_0; \bar{H}_1 = H_1; \bar{H}_i = [H_{i-1} H_i]^{\frac{1}{2}}, \quad i = 2, 3, \dots, N; \bar{H}_{N+1} = H_N \quad (6.16)$$

2. Approximate values of  $\theta$  and  $\sigma$  are calculated for values of  $\hat{H}$  from Eq. (6.16):

$$\begin{aligned} \bar{\theta}_0 &= \theta_0; \bar{\theta}_1 = \theta_1; \quad \bar{\theta}_i = \frac{1}{2}(\theta_{i-1} + \theta_i), \quad i = 2, 3, \dots, N; \bar{\theta}_{N+1} = \\ \bar{\sigma}_0 &= 0; \bar{\sigma}_1 = \left( \frac{\theta_2 - \theta_1}{\ln H_2 - \ln H_1} \right) \frac{1}{H_1}; \bar{\sigma}_i = \left( \frac{\theta_i - \theta_{i-1}}{\ln H_i - \ln H_{i-1}} \right) \frac{1}{H_i}, \quad i = 2, 3, \dots, N; \\ \bar{\sigma}_{N+1} &= \left( \frac{\theta_N - \theta_{N-1}}{\ln H_N - \ln H_{N-1}} \right) \frac{1}{H_N} \end{aligned} \quad (6.17)$$

where  $\bar{\sigma} (I = 2, 3, \dots, N)$  are values of the specific water capacity at midpoints  $\bar{\theta}_I$  between measured data.

3. On intervals between  $H_I$  and  $H_{I+1}$  ( $I = 1, 2, \dots, N$ ) the dependency of moisture content on suction is represented by cubic polynomials with cubics on these intervals being dependent on

$\ln H$ ; i.e.,  $\theta = f_{\theta,i}(\ln H)$ . The interval  $[H_0, H_1]$  has also a cubic polynomial, but this curve is dependent on  $H$  as:  $\theta = f_{\theta,0}(H)$ . Cubic polynomials provide for the following equalities at points  $H_i$  and  $H_{i+1}$ :

$$f_{\theta,i}|_{\bar{H}_i} = \bar{\theta}_i, \quad \frac{df_{\theta,i}}{dH}|_{\bar{H}_i} = \bar{\sigma}_i, \quad f_{\theta,i}|_{\bar{H}_{i+1}} = \bar{\theta}_{i+1}, \quad \frac{df_{\theta,i}}{dH}|_{\bar{H}_{i+1}} = \bar{\sigma}_{i+1} \quad (6.18)$$

In principle, the above cubic spline method is not to be used for extrapolation, i.e., for

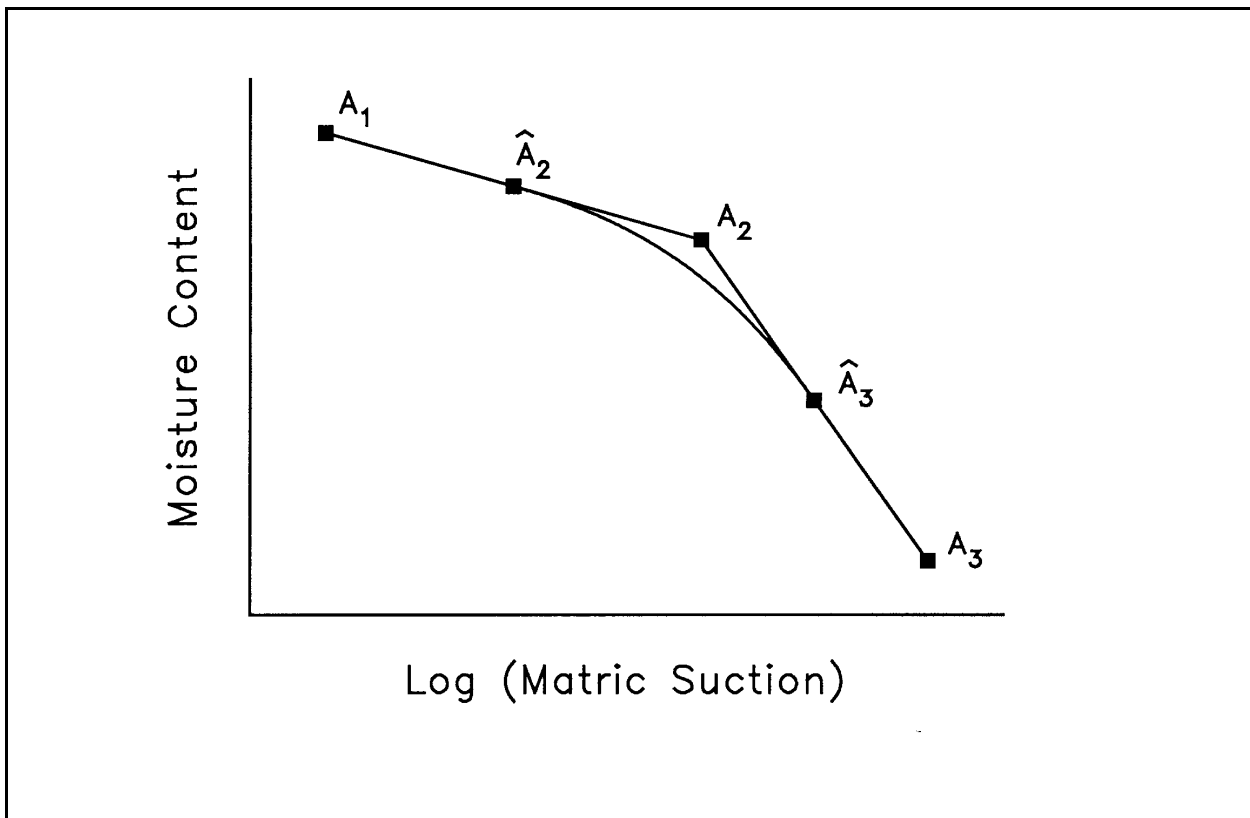


**Figure 6.4** Schematic of the piecewise polynomial method for approximation of water retention and hydraulic conductivity data.

calculation of water content or conductivity values outside the measurement range  $[H_0, H_N]$ . One cannot exclude, however, the possibility of crossing these limits during iterative water flow calculations. For such cases we have:

$$\theta = \theta_0, \text{ if } H < 0; \quad \theta = \theta_N (H_N/H)^{-\bar{\sigma}_{N+1} H_N / \theta_N}, \quad \text{if } H > H_N \quad (6.19)$$

Starting from the second point (the first measured point below saturation), the interpolating curve using this method is that of a cubic spline. Unlike the regular use of splines, here the interpolating curve goes through the estimated midpoints ( $H, \theta$ ), but not through the measured points ( $H, \theta$ ).

If  $\theta$  is replaced by  $\ln k$  and  $\sigma$  by  $B$ , then the above formulas can be used also for calculating hydraulic conductivity values. They are coded in the FORTRAN subroutine HYDSUB, which uses measured  $\theta$ ,  $H$ , and  $k$  values to find the polynomial coefficients to calculate  $\theta$ ,  $\sigma$ , and  $k$  for given  $H$  values, and also to calculate  $H$  for given  $\theta$ .

## **6.6 Data file '*Hydprop.dat*'**

This file contains measured dependencies of the moisture content and hydraulic conductivity on matric suction for all soil layers that differ in there properties. The dependencies are presented in tabular form. The first pairs of values for both 'moisture content-matric suction' and 'hydraulic conductivity - matric suction' are for a water-saturated soil, i.e., the matric suction must be equal to zero in the first pair. The structure of the data file '**Hydprop.dat**' is given in Table 6.4. The table is followed by an example for a soil profile having two layers. Intermediate lines are replaced by periods for the sake of brevity.

Table 6.4. Format of the file '**Hydprop.dat**'.

Record	Variable	Description
1	-	Comment line.
2,3	-	Comment lines.
4	<i>NOBR</i>	Number of measured pairs of moisture content and pressure head values.
5	$\psi(I)$	Measured value of the pressure head.
5	$\theta(I)$	Corresponding measured volumetric soil moisture content. Record 5 is provided for all measured pairs of soil material, $I=1,2,\dots,NOBR$ .
6,7	-	Comment lines.
8	<i>NOBC</i>	Number of measured pairs of hydraulic conductivity and pressure head values.
9	$\psi(I)$	Measured value of the pressure head.
9	$K(I)$	Corresponding measured value of the soil hydraulic conductivity. Record 9 is provided for all measured pairs of the soil material, $I=1,2,\dots,NOBC$ .
Records 2-9 must be provided for every soil material $M$ , $M=1,2,\dots,NMat$ , where $NMat$ is the total number of soil materials.		

\*\*\*\*Example 6.4: MEASURED SOIL HYDRAULIC PROPERTIES - FILE 'Hydprop.dat'

Water retention of soil material # 1

NOBR H Theta

8

0.000 0.419

..... .....

500.000 0.098

Hydraulic conductivity of the material # 1

NOBC H k

17

0.000 12.220

2.266 6.295

..... .....

80.243 0.045

Water retention of the material # 2

NOB H theta

8

0.000 0.311

..... .....

500.000 0.079

Hydraulic conductivity of the material # 2

NOB H k

17

0.000 6.200

0.698 1.860

..... .....

71.337 0.051

# Chapter 7: Solute Transport: SoluteMover module

Jirka Šimůnek, Martinus Th. van Genuchten, and Yakov Pachepsky

The **SoluteMover** module was extracted from the SWMS\_2D model (Šimůnek et al., 1992) and modified to provide better mass conservation for large surface fluxes. The solute is considered to be a dissolved substance that obeys the law of mass conservation. The original code was expanded to handle several solutes. However, the interdependence of mobilities of solute is not described, and interaction of solutes may occur only due to interactions between liquid and non-liquid soil phases.

The original SWMS\_2D code considers linear adsorption, and first and zero-order biological transformation and/or decay. These processes are described by other modules in 2DSOIL. Therefore, the relevant adsorption and decay options have been removed, and **SoluteMover** describes solute transport as affected only by solute extraction. Extraction combines the effects of transformations, decay, interactions with solid phases, and production/uptake. Where it may be numerically more efficient to include the transformations terms directly in the solute transport equations, this approach is not appealing from the standpoint of modularity. Hence, the transformation terms are included in 2DSOIL as separate modules.

## 7.1 Two-dimensional model for solute transport and its finite element implementation

The model considers two-dimensional solute transport in variably saturated soil. 2DSOIL neglects deformations of a soil due to shrinking-swelling, and allows temperature and solute concentrations to influence hydraulic parameters but not solute concentration gradients. Molecular diffusion, hydrodynamic dispersion, and advection are the main processes causing solute transport in this model.

The governing solute transport equation is

$$\frac{\partial(\theta c)}{\partial t} - \frac{\partial}{\partial x} \left[ \theta (D_{xx} \frac{\partial c}{\partial x} + D_{xz} \frac{\partial c}{\partial z}) \right] - \frac{\partial}{\partial z} \left[ \theta (D_{xz} \frac{\partial c}{\partial x} + D_{zz} \frac{\partial c}{\partial z}) \right] + \frac{\partial(q_x c)}{\partial x} + \frac{\partial(q_z c)}{\partial z} + S_c = 0 \quad (6.20)$$

for planar solute transport in a vertical soil cross-section, and

$$\frac{\partial(\theta c)}{\partial t} - \frac{1}{x} \frac{\partial}{\partial x} \left[ x \theta (D_{xx} \frac{\partial c}{\partial x} + D_{xz} \frac{\partial c}{\partial z}) \right] - \frac{\partial}{\partial z} \left[ \theta (D_{xz} \frac{\partial c}{\partial x} + D_{zz} \frac{\partial c}{\partial z}) \right] + \frac{1}{x} \frac{\partial(x q_x c)}{\partial x} + \frac{\partial(q_z c)}{\partial z} + S_c = 0 \quad (6.21)$$

for axisymmetrical solute transport. Here, as before,  $\theta$  is the volumetric water content ( $\text{cm}^3$  of water per  $\text{cm}^3$  of soil),  $c$  is the solute concentration (g per  $\text{cm}^3$  of soil solution),  $S_c$  is an extraction term that describes the joint action of all factors contributing to removal of solute from the soil solution, g per  $\text{cm}^3$  of soil per day;  $x$  is either the horizontal coordinate in case of transport in a vertical soil cross-section, or the radial coordinate in case of axisymmetrical transport, cm;  $z$  is the vertical coordinate measured upward from a reference plane, cm;  $t$  is time, days;  $D_{xx}$ ,  $D_{xz}$  and  $D_{zz}$  are dispersion coefficients,  $\text{cm}^2$  per day; and  $q_x$  and  $q_z$  are volumetric flux densities,  $\text{cm}^3$  of water per  $\text{cm}^2$  of soil per day.

The dispersion coefficients  $D_{xx}$ ,  $D_{xz}$  and  $D_{zz}$  depend on the values of the fluxes  $q_x$  and  $q_z$ , the molecular diffusion coefficient  $D_\theta$ , the moisture content, the longitudinal and transverse dispersivities  $\lambda_L$  and  $\lambda_T$ , the coordinates  $x$  and  $z$ , time, concentrations of solutes, temperature, and other soil state variables. We assume that

$$\begin{aligned}
q_x &= -k \frac{\partial h}{\partial x}, & q_z &= -k \left( \frac{\partial h}{\partial z} + 1 \right), \\
\theta D_{xx} &= \theta \tau_c D_{mol} + \lambda_L \frac{q_x^2}{|q|} + \lambda_T \frac{q_z^2}{|q|}, \\
\theta D_{xz} &= (\lambda_L - \lambda_T) \frac{q_x q_z}{|q|}, \\
\theta D_{zz} &= \theta \tau_c D_{mol} + \lambda_L \frac{q_z^2}{|q|} + \lambda_T \frac{q_x^2}{|q|}, \\
|q| &= \sqrt{q_x^2 + q_z^2}
\end{aligned} \tag{6.22}$$

where  $h$  is the pressure head,  $k$  is hydraulic conductivity,  $D_{mol}$  is the molecular diffusion coefficient in a free solution,  $\tau_c$  is tortuosity factor,  $\lambda_L$  is the longitudinal dispersivity, and  $\lambda_T$  is transverse dispersivity.

The governing solute transport equations, Eqs. (7.1) and (7.2), are solved numerically to obtain spatial and temporal distributions of the concentration  $c$  within the soil domain following Šimunek et al. (1992). We used the Galerkin finite element method with linear basis functions and triangular elements. The pressure head  $h$ , the hydraulic conductivity  $k$ , the molecular diffusion coefficient, and the concentration  $c$  are assumed to vary linearly over each element (Fig 3.1) as follows

$$\begin{aligned}
\tilde{h}(x, z, t) &= \sum_{n=1}^{N_n} \phi_n(x, z) h_n(t), \\
\tilde{c}(x, z, t) &= \sum_{n=1}^{N_n} \phi_n(x, z) c_n(t), \\
\tilde{k}(x, y, t) &= \sum_{n=1}^{N_n} \phi_n(x, y) k_n(t)
\end{aligned} \tag{6.23}$$

where  $N_n$  is the total number of nodes,  $\phi_n(x, z)$  are the basis functions for node  $n$ ; and  $h_n$ ,  $k_n$ , and  $c_n$  are the pressure head, hydraulic conductivity, and concentration at node  $n$ , respectively.

The Galerkin method leads to equations for the nodal values of  $c$ . Area-averaged weighted residuals of Eq. (7.1) have to be equal to zero for every  $\phi_n$  taken as a weight. Consequently, for the whole soil domain we obtain

$$\sum_{e=1}^{N_e} \int_{\Omega_e} \left[ -\frac{\partial(\theta c)}{\partial t} + \frac{\partial}{\partial x} (\theta D_{xx} \frac{\partial c}{\partial x} + \theta D_{xz} \frac{\partial c}{\partial z} - q_x c) + \frac{\partial}{\partial z} (\theta D_{xz} \frac{\partial c}{\partial x} + \theta D_{zz} \frac{\partial c}{\partial z} - q_z c) + S_c \right] \phi_n d\omega = 0 \quad (6.24)$$

where  $\Omega_e$  designates the area of the element  $e$ , and  $N_e$  is the total number of elements. After replacing  $c$  by  $\tilde{c}$  and using Green's first identity, Eq (7.5) becomes

$$\begin{aligned} & \sum_{e=1}^{N_e} \int_{\Omega_e} \left( -\frac{\partial(\theta c)}{\partial t} \right) \phi_n d\omega \\ & + \sum_{e=1}^{N_e} \int_{\Omega_e} \left[ -(-q_x \tilde{c} + \theta D_{xx} \frac{\partial \tilde{c}}{\partial x} + \theta D_{xz} \frac{\partial \tilde{c}}{\partial z}) \frac{\partial \Phi_n}{\partial x} - (-q_z \tilde{c} + \theta D_{xz} \frac{\partial \tilde{c}}{\partial x} + \theta D_{zz} \frac{\partial \tilde{c}}{\partial z}) \frac{\partial \Phi_n}{\partial z} \right] d\omega \\ & + \sum_{e=1}^{N_e} \int_{\Gamma_e} \left[ (-q_x \tilde{c} + \theta D_{xx} \frac{\partial \tilde{c}}{\partial x} + \theta D_{xz} \frac{\partial \tilde{c}}{\partial z}) n_{\Gamma,x} + (-q_z \tilde{c} + \theta D_{xz} \frac{\partial \tilde{c}}{\partial x} + \theta D_{zz} \frac{\partial \tilde{c}}{\partial z}) n_{\Gamma,z} \right] \phi_n d\Gamma \\ & - \sum_{e=1}^{N_e} \int_{\Omega_e} S_c \phi_n d\omega = 0 \end{aligned} \quad (6.25)$$

where  $\Gamma_e$  is the boundary of element  $e$ , and  $n_{\Gamma,x}$ , and  $n_{\Gamma,z}$  designate components of the unit vector is normal to the boundary.

Further simplifications are based on the assumptions that nodal mass changes may be found as weighted averages of mass changes over the element according to mass-lumping techniques:

$$\frac{d(\theta_n c_n)}{dt} = \frac{\sum_{e=1}^{N_e} \int_{\Omega_e} \frac{\partial(\theta c)}{\partial t} \phi_n d\omega}{\sum_{e=1}^{N_e} \int_{\Omega_e} \phi_n d\omega} \quad (6.26)$$

Accepting these assumptions leads to a system of first-order ordinary differential equations for the concentration values:

$$[Q] \frac{d\{\theta_c\}}{dt} + [G]\{\theta_c\} + \{f\} = -\{Q_S^B\} \quad (6.27)$$

where the vector  $\{\theta_c\}$  includes all nodal values of  $\theta_c$ . The matrices  $[Q]$  and  $[G]$  have as elements:

$$\begin{aligned} Q_{m,n} &= -\delta_{mn} \sum_e \int_{\Omega_e} \phi_n d\omega = -\sum_{e=1}^3 \frac{\gamma_e}{3} \delta_{mn} \\ G_{m,n} &= -\sum_e \left\{ \int_{\Omega_e} \left[ \tilde{k} \frac{\partial \tilde{h}}{\partial x} \phi_m + D_{xx} \frac{\hat{b}_m}{2A_e} + D_{xz} \frac{\hat{c}_m}{2A_e} \right] \hat{b}_n \right. \\ &\quad \left. + \left[ (\tilde{k} \frac{\partial \tilde{h}}{\partial z} + 1) \phi_m + D_{xz} \frac{\hat{b}_m}{2A_e} + D_{zz} \frac{\hat{c}_m}{2A_e} \right] \hat{c}_n \right\} d\omega = \\ &- \sum_e \frac{1}{4A_e} \left\{ \frac{\bar{k}_e + k_m/3}{4} [\hat{b}_n \Upsilon_b + \hat{c}_n \Upsilon_c] + D_{mol} (\hat{b}_m \hat{b}_n + \hat{c}_m \hat{c}_n) \overline{(\theta\tau)} \right. \\ &\quad \left. + \frac{-b_m b_n (\lambda_L \Upsilon_b^2 + \lambda_T \Upsilon_c^2) + (b_m c_n + b_n c_m) (\lambda_L - \lambda_T) \Upsilon_b \Upsilon_c + c_m c_n (\lambda_L \Upsilon_c^2 + \lambda_T \Upsilon_b^2)}{\sqrt{\gamma^2 + \gamma'^2}} \right\} \end{aligned} \quad (6.28)$$

where

$$\Upsilon_b = \sum_{p=1}^3 h_p b_p, \quad \Upsilon_c = \sum_{p=1}^3 h_p c_p + 2A \quad (6.29)$$

for an element, overlined symbols denote average values over an element, and where summation occurs over elements which have the nodes  $m$  and  $n$  among their corner nodes.

Because the solute extraction rate,  $S_c$ , in 2DSOIL is constant over an element, the vector  $\{f\}$  has components

$$f_n = \sum_e \frac{1}{3} A_e (S_c)_e \quad (6.30)$$

where summation involves elements that have the node  $n$  among its corner nodes.

Vector  $\{Q_S^B\}$  has non-zero components only for boundary nodes. This vector represents total solute fluxes. If the concentration is constant at a boundary, then  $dc_n/dt=0$  and, in accordance with (7.8),

$$(Q_S^B)_n = - \sum_{m=1}^{N_n} G_{m,n} c_m - f_n \quad (6.31)$$

If the solute flux is known at the boundary, then  $\{Q_S^B\}$  is included in vector  $\{f\}$ . If the dispersive flux is assumed to be zero at the boundary, then  $(Q_S^B)_n = Q_n c_n$  and the value of  $Q_n$  must be added to  $G_{nn}$ .

Methods used for solving (7.8) are similar to those described in detail by Šimůnek et al. (1992). A first-order finite difference approximation of the time derivatives leads to the following set of algebraic equations:

$$[Q] \frac{\{\theta c\}_{j+1} - \{\theta c\}_j}{\Delta t} + \epsilon_t [G]_{j+1} \{c\}_{j+1} (1 - \epsilon_t) [G]_j c_j + \epsilon_t \{f\}_{j+1} + (1 - \epsilon_t) \{f\}_j = 0 \quad (6.32)$$

where  $j$  and  $j+1$  denote the previous and current time levels, respectively;  $\Delta t$  is the time increment and  $\epsilon_t$  is a time weighing factor. Equation (7.13) can be rewritten in the form

$$[A] \{c\}_{j+1} = \{b\} \quad (6.33)$$

where

$$\begin{aligned} [A] &= \frac{1}{\Delta t} [Q] [\theta]_{j+1} + \epsilon_t [G]_{j+1} \\ \{b\} &= \frac{1}{\Delta t} [Q] \{\theta c\}_j - (1 - \epsilon_t) [G]_j \{c\}_j - \epsilon_t \{f\}_{j+1} - (1 - \epsilon_t) \{f\}_j \end{aligned} \quad (6.34)$$

Slight modifications of the coefficients in Eqs. (7.9), (7.10) and (7.11) allows the axisymmetrical case described by Eq. (7.2) to be solved (Šimůnek et al., 1992). Boundary and initial conditions must be defined to solve Eq. (7.8). Methods of setting the time-dependent boundary are

presented in Chapters 4 and 5 of this manual. Time-independent boundary concentrations must be included as part of the initial distribution data as described in section 7.3.

## **7.2 Parameters of the SoluteMover module**

Equation (7.3) shows that dispersion, as manifested by solute spreading during transport in the subsurface, is a result of the joint action of ionic or molecular diffusion and hydrodynamic dispersion [Bear, 1972; Simunek et al., 1992]. A good rule of thumb for groundwater is that the transverse and longitudinal dispersivities in (7.3) are related by  $\lambda_T = 0.1 \lambda_L$ . The ratio may be higher in soils.

For practical problems we make use of the fact that, in general,  $\lambda_T$  is significantly less than  $\lambda_L$  (Bear, 1972). Having  $\lambda_T=0$ , one must know the value of  $\lambda_L$ , which strongly depends on soil structure at high velocities and on soil texture at low velocities. The value of  $\lambda_L$  is also known to have high spatial variability. As a first approximation the following power dependence may be used:

$$\lambda_L = 0.012(\text{clay percentage})^2 \quad (6.35)$$

which appears reasonable for clay percentages between 20 and 60 percent(Pachepsky, 1992).

The tortuosity factor,  $\tau_c$ , in (7.3) strongly depends on soil structure and texture as well as on soil moisture content. Its value may be estimated as (Pachepsky, 1990)

$$\tau_c = \begin{cases} 0.59 - 0.12\log_{10}|h|, & h < -0.2\text{cm} \\ 0.67, & h \geq -0.2\text{cm} \end{cases} \quad (6.36)$$

This equation has proved to be a reasonable approximation for soils of different textures, and has been incorporated into the 2D SOIL code. Molecular diffusion coefficients in solution are tabulated in many sources. A summary of these as derived from a table in Beven et al. (1993), is given in Table 7.1. The concise review of Nye and Tinker (1977) also provides information necessary for estimating the value of  $D_{mol}$ .

Table 7.1 Representative values of dispersion parameters from published undisturbed core experiments (from Beven et al., 1993)

Study	Dispersion coefficient $\text{cm}^2 \text{ h}^{-1}$	Dispersivity (m)	Mean pore water velocity $(\text{cm h}^{-1})$	$\theta_m/\theta$
Elrick and French (1966)				
undisturbed	1.404	-	1.52	
Anderson and Bouma (1977)				
medium sand/sub-angular	4.17	-	0.0417	
blocky				
clay loam/prismatic	0.417	-	0.0417	
Cassel et al. (1974)				
Aberdeen undisturbed	0.197	-	0.0151	
Boetia undisturbed	0.161	-	0.0151	
Smettem (1984)	24.0 (102.8/1.2)	0.077 (0.218/0.013)	2.3 (5.8/0.6)	
Seyfried and Rao (1987)	4.04 (6.44/ 1.65)	150.6 (r84.4/95.3)	2.709 (4.1/1.7)	
Jury and Sposito (1985)				
Core—highest value	5.642	0.251	0.225	
Core—lowest value	3.367	0.197	0.171	
Dyson and White (1987)	23.075 (75.5/2.55)	0.066 (0.139/0.029)	2.941 (6.34/0.74)	
Abdulkabir (1989)				
Grass soil	0.230 (0.57/0.06)	-	1.409 (1.76/0.77)	0.41 (0.58/0.32)
Forest soil	5.55 (7.58/2.79)	-	52.4 (57.6/46.7)	0.38 (0.59)/0.27
Lancaster core	160.4	0.526	3.04	0.68

Table 7.1 Representative values of dispersion parameters from published undisturbed core experiments (from Beven et al., 1993)

Study	Dispersion coefficient $\text{cm}^2 \text{ h}^{-1}$	Mean pore water velocity		
		Dispersivity (m)	( $\text{cm h}^{-1}$ )	$\theta_m/\theta$
	54.2	0.357	1.52	0.95
	18.6	0.243	0.76	1.0
Slapton Wood core				
Upward flux	370.0	1.217	3.04	0.61
	31.5	0.706	1.53	0.44
	15.5	0.203	0.76	0.33
Downward flux	13.5	0.177	0.76	0.42
	8.4	0.220	0.38	0.47
Wierenga and van Genuchten (1989)				
Small cores	20.9	0.0087	1.01	
	(46.2/3.9)	(0.0094/0.0077)	(2.22/0.18)	
Large core	2.71	34.0	0.08	

Figures in parentheses are highest and lowest quoted values for each parameter

Table 7.2 Representative values of dispersion parameters from published field plot experiments (from Beven et al., 1993).

Study	Dispersion coefficient	Dispersivity (m)	Mean pore water velocity ( $\text{cm}^2 \text{ h}^{-1}$ )
Biggar and Nielsen (1976)	8.776 (66.5/0.35)	0.0547 (0.257/0.017)	1.826 (15.28/0.008)
Van de Pol et al. (1977)	1.531 (3.54/0.925)	0.0942 (2.72/0.04)	0.1625 (0.218/0.130)
Bowman and Rice (1986)			
Water applied semi-weekly	16.14 (47.9/6.5)	0.524 (1.41/0.208)	0.290 (0.367/0.197)
Water applied bi-weekly	21.759 (107.9/1.558)	0.445 (0.952/0.094)	0.293 (0.533/0.162)
Schulin et al. (1987)			
Br <sup>-</sup> as tracer	0.0604	0.0393	0.0163
Cl <sup>-</sup> as tracer	0.0471	0.0214	0.0220
Rice et al. (1986)	2.229 (6.67/1.13)	0.165 (0.21/0.14)	0.146 (0.46/0.071)
Jaynes et al. (1988)	88.90 (99.9/79.2)	0.178 (0.228/0.138)	5.00 (5.75/4.38)
Jaynes (1991)	149.6 (920.8/1.9)	0.288 (0.658/0.045)	4.75 (29.99/0.42)
Jury and Sposito (1985)	2.488 (3.00/1.313)	0.173 (0.257/0.197)	0.146 (0.179/0.117)
Butters and Jury (1989)			
Field Scale	-	0.102	-
Local scale	-	0.177	-

Figures in parenthesis are highest and lowest quoted for each parameter when available.

### **7.3 Data files '*Param\_S.dat*' and '*Nodal\_S.dat*'**

Parameters needed for computations by the **SoluteMover** module are read from the file '**Param\_S.dat**'. One of these parameters is the time-weighing factor  $\epsilon_{psi}$  ( $\epsilon$  in Eq 7.13). Values of  $\epsilon_{psi}$  between 0.5 and 0.8 usually give good results. When  $\epsilon_{psi} = 0$ , calculations for the next time step become faster, but the time step in general must be much smaller than for  $\epsilon_{psi} > 0.5$ . The second parameter,  $lUpW$ , is a switch that allows upstream weighing. Upstream weighing has been shown to diminish or eliminate numerical oscillations that often arise near steep concentration fronts and in areas with high flow velocities relative to dispersion (Yeh and Tripathi, 1990). It seems reasonable to always use this method in the algorithm when sharp concentration fronts are expected. A third parameter,  $CourMax$ , is the upper limit of the so-called Courant number, which is the ratio between the amount of water within an element and the amount of water brought to the element through boundaries during the current time step. Values of 0.3-0.5 have proved to be satisfactory.

Solute transport parameters are provided separately for each soil subdomain. For current calculations, materials are identified by the material number,  $MatNumN$ , specified for every node in the Grid\_and\_Boundary information file '**Grid\_Bnd.dat**'. Parameter values are discussed in the next section.

The structure of the data for the computational parameters is presented in Table 7.3. The example following the table holds for two soil materials and three solutes. In addition to the computational parameters, **SoluteMover** reads data about the initial concentration distribution from the file '**Nodal\_S.dat**'. If there are constant concentration boundaries, then the values of the boundary concentrations must be given in the file. Table 7.4 shows the structure of data in the '**Nodal\_S.dat**' file. The example following the table corresponds to the grid shown in Fig. 3.1 and to the file '**Grid\_Bnd.dat**' of Example 3.3.

Table 7.3. Format of the file '**Param\_S.dat**'.

Record	Variable	Description
1	-	Comment line. <u>Computational Information</u>
2	-	Comment line.
3	<i>NumSol</i>	Number of solutes under consideration.
4,5	-	Comment lines.
6	<i>epsi</i>	Temporal weighing coefficient.
6	<i>IUpW</i>	1 - upstream weighing formulation, 0 - original Galerkin formulation.
6	<i>CourMax</i>	Maximum allowed Courant number. <u>Material information</u>
7-9	-	Comment lines.
10	<i>Dmol(1)</i>	Ionic or molecular diffusion coefficient in free water for solute 1.
10	<i>Dmol(2)</i>	Same as above for solute 2.
10	<i>Dmol(NumSol)</i>	Same as above for the last solute.
11,12	-	Comment lines.
13	<i>Dlng(M,1)</i>	Longitudinal dispersivity of solute 1 of the material in subdomain <i>M</i> .
13	<i>Dlng(M,2)</i>	Same as above for solute 2.
13	<i>Dlng(M,NumSol)</i>	Same as above for the last solute. Record 13 is given for the soil material of each subdomain <i>M</i> (from 1 to <i>NMat</i> ).
14,15	-	Comment lines.
16	<i>Dtrn(M,1)</i>	Transverse dispersivity of solute <i>j</i> for the soil material in subdomain <i>M</i> .
16	<i>Dtrn(M,2)</i>	Same as above for solute 2.
16	<i>Dtrn(M,NumSol)</i>	Same as above for the last solute. Record 16 is given for the soil material in each subdomain <i>M</i> (from 1 to <i>NMat</i> ).

```
** Example 7.1: SOLUTEMOVER PARAMETERS: file 'Param_S.dat'
Number of solutes
      3
Computational parameters
epsi    1UpW    CourMax
0.55      1          0.5
Soil material and solute parameters
Diffusion coefficients
  Solute #1    Solute #2    Solute #3
  1.73        1.25        0.12
Longitudinal dispersivities of soil materials
  Sol # 1    Sol # 2    Sol # 3
      5          5          20          (material in subdomain # 1)
     10         10         40          (material in subdomain # 2)
Transverse dispersivities of soil layers
  Sol # 1    Sol # 2    Sol # 3
      2          2          20          (material in subdomain # 1)
      2          2          10          (material in subdomain # 2)
```

Table 7.4. Format of the file '**Nodal\_S.dat**'.

Record	Variable	Description
1,2	-	Comment lines.
3	<i>n</i>	Nodal number.
3	<i>Conc(n,1)</i>	Initial value of the concentration of the first solute at node <i>n</i> , mg L <sup>-1</sup>
3	<i>Conc(n,2)</i>	Same as above for the 2nd solute.
.		
3	<i>Conc(n,NumSol)</i>	Same as above for the last solute.
Record 3 is provided for every node of the grid. If some boundary nodes have constant concentrations, the concentration values must be present in this file.		

```
**** Example 7.2: INITIAL SOLUTE CONCENTRATION DISTRIBUTION - file
'Nodal_S.dat'
n  Conc(n,1)  Conc(n,2)  Conc(n,3)
1   0.17E-03   0.045E-03   1.3E-03
2   0.18E-03   0.047E-03   1.4E-03
3   0.41E-03   0.049E-03   0.0
4   0.45E-03   0.051E-03   0.0
5   0.23E-03   0.054E-03   0.0
6   0.27E-03   0.072E-03   0.0
7   0.29E-03   0.077E-03   0.0
8   0.33E-03   0.106E-03   0.0
9   0.35E-03   0.111E-03   0.0
10  0.37E-03   0.115E-03   0.0
11  0.29E-03   0.125E-03   0.0
12  0.44E-03   0.134E-03   0.0
13  0.44E-03   0.144E-03   0.0
14  0.56E-03   0.171E-03   0.0
15  0.57E-03   0.172E-03   0.0
16  0.59E-03   0.172E-03   0.0
17  0.60E-03   0.172E-03   0.0
18  0.63E-03   0.172E-03   0.0
```



# Chapter 8: Heat Transport: HeatMover Module

Dennis Timlin, Yakov Pachepsky, and Jirka Šimůnek

The **HeatMover** module calculates temperature changes in the soil due to diffusion of heat and movement of heat with water. This module has many features in common with the **SoluteMover** module described in Chapter 7.

## 8.1 The two-dimensional model of heat movement and its finite element implementation

The model considers two-dimensional transport of heat in a variably saturated soil. The governing heat transport equation is taken as

$$\frac{\partial(\hat{C}T)}{\partial t} - \frac{\partial}{\partial x}[\Lambda \frac{\partial T}{\partial x}] - \frac{\partial}{\partial z}[\Lambda \frac{\partial T}{\partial z}] + \frac{\partial(q_x C_w T)}{\partial x} + \frac{\partial(q_z C_w T)}{\partial z} = 0 \quad (8.1)$$

for heat transport in a vertical soil cross-section, and

$$\begin{aligned} \frac{\partial(\hat{C}T)}{\partial t} - \frac{1}{x} \frac{\partial}{\partial x}[x \Lambda \frac{\partial T}{\partial x}] - \frac{\partial}{\partial z}[\Lambda \frac{\partial T}{\partial z}] \\ + \frac{1}{x} \frac{\partial(x q_x C_w T)}{\partial x} + \frac{\partial(q_z C_w T)}{\partial z} + C_w S T = 0 \end{aligned} \quad (8.2)$$

for axisymmetrical heat transport. Sources or sinks of heat are not considered in these equations.  $T$  is the temperature ( $^{\circ}\text{C}$ ), and  $\hat{C}$  is the total heat capacity of the soil system (solid material and water) given by  $\hat{C} = C_{sm}X_m + C_{om}X_{om} + C_w\theta$ . The units of  $\hat{C}$  are Joules  $\text{cm}^{-3} \text{ }^{\circ}\text{C}^{-1}$ . Subscripted  $C$ 's are the heat capacities of the mineral matter (sm), organic matter (om), and water (w) in the soil pores per unit volume, subscripted  $X$ 's are the volume fractions, and  $\theta$  is the volumetric water

content.  $\hat{C}$  is not a constant because of its dependency on  $\theta$ . DeVries (1966) gives  $C_{sm}=1.93$  (0.46) and  $C_{om}=2.51$  (0.6) and  $C_w=4.18$  (1.0) as average values in Joules  $\text{cm}^{-3} \text{ }^{\circ}\text{C}^{-1}$  (cal  $\text{cm}^{-3} \text{ }^{\circ}\text{C}^{-1}$ ). Furthermore,  $x$  in Eq. 8.1 and 8.2 represents the horizontal coordinate in case of water flow in a vertical soil cross-section and the radial coordinate in case of axisymmetrical water flow,  $z$  is the vertical coordinate measured upward from the base of the soil profile; ( $z$  and  $x$  are both in cm), and  $t$  is time, days. The thermal conductivity,  $\Lambda$ , has units of Joules  $\text{cm}^{-1} \text{ day}^{-1} \text{ }^{\circ}\text{C}^{-1}$ , and depends on the moisture content. Modeling of these dependencies is discussed in the next section of this chapter.

Fluxes of heat are connected with rates of moisture content change ( $\partial\theta/\partial t$ ) and water extraction ( $S$ ) as follows

$$\begin{aligned} \frac{\partial\theta}{\partial t} + \frac{\partial q_x}{\partial x} + \frac{\partial q_z}{\partial z} + S &= 0, \quad \text{planar symmetry} \\ \frac{\partial\theta}{\partial t} + \frac{1}{x} \frac{\partial(xq_x)}{\partial x} + \frac{\partial q_z}{\partial z} + S &= 0, \quad \text{axial symmetry} \end{aligned} \quad (8.3)$$

Therefore, (8.1) may be recast as

$$\begin{aligned} \theta R \frac{\partial T}{\partial t} - \frac{1}{x} \frac{\partial}{\partial x} \left[ \frac{\Lambda}{C_w} \frac{\partial T}{\partial x} \right] - \frac{\partial}{\partial z} \left[ \frac{\Lambda}{C_w} \frac{\partial T}{\partial z} \right] + \\ + q_x \frac{\partial T}{\partial x} + q_z \frac{\partial T}{\partial z} &= 0 \end{aligned} \quad (8.4)$$

and (8.2) becomes

$$\begin{aligned} \theta R \frac{\partial T}{\partial t} - \frac{\partial}{\partial x} \left[ \frac{\Lambda}{C_w} \frac{\partial T}{\partial x} \right] - \frac{\partial}{\partial z} \left[ \frac{\Lambda}{C_w} \frac{\partial T}{\partial z} \right] \\ + q_x \frac{\partial T}{\partial x} + q_z \frac{\partial T}{\partial z} &= 0 \end{aligned} \quad (8.5)$$

In these equations  $R=1+\frac{C_{sm}X_{sm}+C_{om}X_{om}}{C_w\theta}$ . The governing equations for heat transport (8.4) and (8.5) are solved numerically to obtain spatial and temporal distributions of the heat content as

measured by the temperature ( $T$ ) within the soil profile. The Galerkin finite element method with linear basis functions and triangular elements is used.

As with water and solutes, the heat content is approximated by a linear combination of nodal concentration values:

$$\hat{T}(x,z,t) = \sum_{n=1}^{N_n} \phi_n(x,z) T_n(t) \quad (8.6)$$

where  $N_n$  is the total number of nodes,  $\phi_n(x,z)$  are basis functions for node  $n$  and  $T_n$  is the temperature in node  $n$ . Basis functions may be derived from interpolation functions for the elements. Interpolation functions for triangular elements are given in (6.4).

The Galerkin method gives equations for the nodal values of  $T$ . Area-averaged weighted residuals of (8.4) and (8.5) have to be equal to zero for every  $\phi_n$  taken as a weight. Consequently for the whole soil domain we have

$$\sum_{e=1}^{N_e} \int_{\Omega_e} \left[ \theta R \frac{\partial T}{\partial t} - \frac{\partial}{\partial x} \left( \frac{\Lambda}{C_W} \frac{\partial T}{\partial x} \right) - \frac{\partial}{\partial z} \left( \frac{\Lambda}{C_W} \frac{\partial T}{\partial z} \right) + q_x \frac{\partial T}{\partial x} + q_z \frac{\partial T}{\partial z} \right] \phi_n d\omega = 0 \quad (8.7)$$

where  $\Omega_e$  designates the area of element  $e$  and  $N_e$  is the total number of elements. After replacing  $T$  by  $\hat{T}$  and using Green's first identity, one has:

$$\begin{aligned} & \sum_{e=1}^{N_e} \int_{\Omega_e} \left( -\theta R \frac{\partial \hat{T}}{\partial t} \right) \phi_n d\omega \\ & + \sum_{e=1}^{N_e} \int_{\Omega_e} \left[ -\frac{\partial \hat{T}}{\partial x} \left( q_x \phi_n + \frac{\Lambda}{C_W} \frac{\partial \phi_n}{\partial x} \right) - \frac{\partial \hat{T}}{\partial z} \left( q_z \phi_n + \frac{\Lambda}{C_W} \frac{\partial \phi_n}{\partial z} \right) \right] d\omega + \\ & + \sum_{e=1}^{N_e} \int_{\Gamma_e} \left( \frac{\partial \hat{T}}{\partial x} n_{\Gamma,x} + \frac{\partial \hat{T}}{\partial z} n_{\Gamma,z} \right) \frac{\Lambda}{C_W} \phi_n d\Gamma \end{aligned} \quad (8.8)$$

where  $\Gamma_e$  is the boundary of element  $e$  and  $n_{\Gamma,x}$ ,  $n_{\Gamma,z}$  designate components of the unit vector normal to the boundary.

Further simplifications are based on two important assumptions. First, the moisture content,  $\theta$ , and soil water fluxes,  $q_x$ , and  $q_z$  vary linearly over each element. Second, nodal

temperature changes may be found as weighted averages of temperature changes over an element according to a mass-lumping technique (Istok, 1989).

Accepting these assumptions leads to a system of first-order ordinary differential equations for calculating temperature values:

$$[Q] \frac{d\vec{T}}{dt} + [G]\{\vec{T}\} = \{Q\}^D \quad (8.9)$$

where the vector  $\{\vec{T}\}$  includes all nodal values of  $T$ . Matrices  $Q$  and  $G$  have elements

$$\begin{aligned} Q_{m,n} &= \delta_{mn} \sum_e \frac{A_e}{12} (3\bar{\theta}\bar{R} + \theta_n R_n) \\ G_{m,n} &= \left[ -\frac{\hat{b}_m}{24} [3\bar{q}_x + (q_x)_n] - \frac{\hat{c}_m}{24} [3\bar{q}_z + (q_z)_n] \right. \\ &\quad \left. - \frac{1}{4A_e} \frac{\Lambda}{C_w} [\hat{b}_m \hat{b}_n + \hat{c}_m \hat{c}_n] \right] \end{aligned} \quad (8.10)$$

where the summation involves elements which have the nodes  $m$  and  $n$  among their corner nodes. Nodal water extraction rates are calculated as  $S_n = \Sigma A_e S_e / \Sigma A_e$  where the summation covers all elements that have node  $n$  at one of their corners. Values of the parameters  $\hat{b}_n$ ,  $\hat{c}_n$ , and  $A_e$  have the same meaning as in (6.4), while overlined values indicate average values over the element.

The vector  $\{Q^D\}$  has non-zero components only for boundary nodes. This variable represents the convective heat flux and is given by:

$$\{Q\}_n^D = - \sum_{m=1}^{M_n} S_{m,n} T_m \quad (8.11)$$

If the temperature is constant along a boundary, then  $dT_n/dt=0$  and, in accordance with (8.9), if the heat flux is constant at the boundary, then  $\{Q^D\}$  is replaced by the known total boundary flux divided by  $C_w$ .

The method for solving the system (8.9) is similar to those for systems (6.9) and (8.9). The axisymmetrical cases described by (8.5) can be calculated by making slight modifications to the coefficients in (8.10) and (8.11). Boundary and initial conditions must be set to solve (8.9). Methods of implementing time-dependent boundary settings are presented in Chapters 4 and 5 of this manual. Time-independent boundary temperature must be included in the initial distribution data as described in Section 8.3.

## **8.2 Parameters of the HeatMover module**

The thermal conductivity of a soil controls the diffusion of heat in soil. The overall thermal conductivity is an average of the thermal conductivities of the different soil components and depends on the relative proportions of these components. The method of calculating the average thermal conductivity is taken from DeVries (1966):

$$\Lambda = \frac{\sum_{i=1}^N \omega_i X_i \Lambda_i}{\sum_{i=1}^N \omega_i X_i} \quad (8.12)$$

where  $N$  is the number of components,  $\Lambda$  is the thermal conductivity of the soil,  $\omega_i$  is a weighing factor that depends on the ratios of the thermal conductivities of the component, the medium in which heat transport occurs (air or water) and the size and relative shapes of the granules,  $X_i$  is the volume fraction of the  $i$ 'th component, and  $\Lambda_i$  is the thermal conductivity of the  $i$ th component. Values of  $\omega_i$  are calculated as:

$$\omega_i = \frac{1}{3} \sum_{j=1}^3 \left[ 1 + \left( \frac{\Lambda_i}{\Lambda_o} - 1 \right) \Upsilon_j \right]^{-1} \quad (8.13)$$

where  $\Upsilon_j$  ( $j=1,2,3$ ) are shape factors that depend on the shapes of the particles. The sum of the three shape factors is unity so that for spherical particles  $\Upsilon_1 = \Upsilon_2 = \Upsilon_3 = 1/3$ . The parameter  $\Lambda_o$  represents the thermal conductivity of the reference medium (water for a moist soil, and air for a

dry soil). The components of the system that affect the thermal conductivities are the soil mineral particles, soil organic matter, soil air (containing water vapor), and soil water. The thermal conductivity of air containing water vapor is calculated as:

$$\Lambda_a = \Lambda_{da} + \Lambda_v \frac{\theta}{\theta_s} \quad (8.14)$$

Where,  $\Lambda_{da}$  is the thermal conductivity of dry air, and  $\Lambda_v$  is the thermal conductivity of water vapor. These two parameters are calculated as

$$\begin{aligned}\Lambda_{da} &= 0.058 + 1.74 \cdot 10^{-3} T_a \\ \Lambda_v &= 0.052 \cdot e^{(0.058 T_{surf})}\end{aligned} \quad (8.15)$$

The two equations were taken from figure 7.2, page 217 of De Vries (1966). The units for the conductivities in these equations are millicalories  $\text{cm}^{-1} \text{ day}^{-1} {}^\circ\text{C}^{-1}$ . In the program they are converted to Joules  $\text{cm}^{-1} \text{ day}^{-1} {}^\circ\text{C}^{-1}$ .

### **8.3 Data files '*Param\_T.dat*' and '*Nodal\_T.dat*'**

Parameters needed for calculations of heat transport are read from the file '**Param\_T.dat**'. One parameter is the time-weighting factor  $\epsilon_{psi}$  used in the final matrix equation for heat flow. See Section 7 (**SoluteMover**) for more information . Reasonable values of  $\epsilon_{psi}$  are between 0.5 and 0.8. Another parameter is  $HCritA$  which is described in more detail in Section 6 (**WaterMover**) and should be that same as the value used in the WaterMover module. Parameters needed to calculate heat capacities are also included in the data file '**Param\_T.dat**'. These are the mass percentages of sand, silt and clay particles. These parameters are provided separately for every soil layer. Materials are identified by the material number,  $MatNumN$ , specified for every node in the **Grid\_and\_Boundary** information file '**Grid\_Bnd.dat**'. The structure of the data file for the heat transport parameters is given Table 8.1. The example following the table holds for two soil materials. In addition to the

computational parameters, **HeatMover** reads data about the initial temperature distribution from file '**Nodal\_T.dat**'. If there are constant temperature boundaries, then the values of the boundary temperatures must be given in this file. Table 8.2 shows the structure of the '**Nodal\_T.dat**' file. The example following the table corresponds to the grid of Fig. 3.1 and to file '**Grid\_bnd.dat**' of Example 3.3.

Table 8.1 Format of the file '**Param\_T.dat**'

Record	Variable	Description
1,2	-	Comment line
		<u>Computational Information</u>
3	<i>epsi</i>	Temporal weighting coefficient.
3	<i>HcritA</i>	A threshold matric potential of soil. When the soil is drier than this, actual evaporation is less than potential evaporation. It should correspond to the value of hCritA used in the <b>Param_w.dat</b> file (Table 6.1).
		<u>Material information</u>
4,5	-	Comment lines.
6	<i>BulD(M)</i>	Bulk density of soil material in subdomain # M, g cm <sup>-3</sup>
6	<i>FracOm(M)</i>	Mass fraction of Organic matter in soil material in subdomain # M
6	<i>FracSind(M)</i>	Same as above for sand+silt
6	<i>FracClay(M)</i>	Same as above for clay
Record 6 is made for each soil material M, M=1,2,... Nmat and is given as a percentage.		

```
*** Example 8.1: HEAT MOVER PARAMETER INFORMATION ****
*** EPSI   HCritA
      0.5   1.E+06
Soil material information
(BulD)   (FracOm) (FracSind) (FracClay)
  1.59      0        95       05      (Soil material # 1)
  1.66      0        56       44      (Soil material # 2)
```

Table 8.2 Format of the file '**Nodal\_T.dat**'

Record	Variable	Description
1,2	-	Comment lines.
3	$n$	Nodal number
3	$T(n)$	Initial value of temperature at node $n$ , °C
Record 3 is provided for every node of the grid.		
Constant boundary temperature, if used, must be present in this file.		

```
*** Example 8.2: HEAT MOVER NODAL INFORMATION
      n      Tmpr
1       25
2       25
3       20
4       20
5       25
6       25
7       20
8       20
9       20
10      20
11      20
12      20
13      20
14      20
15      20
16      20
17      20
18      20
```

# Chapter 9: Gas Transport: GasMover Module

**Yakov Pachepsky and Dennis Timlin**

The **GasMover** module was written especially for 2DSOIL and has many features in common with the **SoluteMover** module described in Chapter 7. This module considers gas movement in the liquid-free pore space as caused by diffusion and gas production/extraction by biological activity in the soil.

## **9.1 The two-dimensional model of solute movement and its finite element implementation**

The model considers two-dimensional transport of several gases in variably saturated soil. The code neglects deformation of soil due to shrinking-swelling, and allows temperature and gas values to influence transport parameters. Molecular diffusion is the main process governing gas transport in this model; pneumatic effects are not considered. The governing gas transport equation is:

$$\frac{\partial(\vartheta g)}{\partial t} - \frac{\partial}{\partial x}[\vartheta D_g \frac{\partial g}{\partial x}] - \frac{\partial}{\partial z}[\vartheta D_g \frac{\partial g}{\partial z}] + S_g = 0 \quad (9.1)$$

for gas transport in a vertical soil cross-section and

$$\frac{\partial(\vartheta g)}{\partial t} - \frac{1}{x} \frac{\partial}{\partial x}[x \vartheta D_g \frac{\partial g}{\partial x}] - \frac{\partial}{\partial z}[\vartheta D_g \frac{\partial g}{\partial z}] + S_g = 0 \quad (9.2)$$

for axisymmetric gas transport. Here  $\vartheta$  is the air-filled porosity,  $\text{cm}^3$  per  $\text{cm}^3$  of soil;  $g$  is the gas content,  $\text{g}$  per  $\text{cm}^3$  of soil air;  $S_g$  is an extraction term that describes the joint action of all factors contributing to removal of the gas from the air-filled pore space,  $\text{g}$  per  $\text{cm}^3$  of soil per day;  $x$  is the horizontal coordinate in the case of planar water transport, and the radial coordinate for the case of axisymmetric water transport,  $\text{cm}$ ;  $z$  is the vertical coordinate measured upward from a reference plane,  $\text{cm}$ ;  $t$  is time, days; and  $D_g$  is the gas molecular diffusion coefficient in soil air,

$\text{cm}^2 \text{ day}^{-1}$ . The molecular diffusion coefficient  $D_g$  depends on moisture content, the spatial coordinates  $x$  and  $z$ , time, and concentrations of gases and temperature. The modeling of the molecular diffusion coefficient is discussed in a later section of this chapter. The extraction term,  $S_g$ , includes gas uptake and production by roots, chemical interactions, and microbiological activity. Chapter 15 of this manual describes an example of incorporating root respiration into 2DSOIL.

Air-filled porosity changes at a rate that is opposite to the rate of change of moisture content:

$$\frac{\partial \vartheta}{\partial t} = -\frac{\partial \theta}{\partial t} \quad (9.3)$$

where the sum of  $\theta$  and  $\vartheta$  is assumed constant and equal to  $\theta_s$ , i.e. saturated moisture content. Therefore, Eqs. (9.1) and (9.2) may be recast to

$$\vartheta \frac{\partial g}{\partial t} - \frac{\partial}{\partial x} (\vartheta D_g \frac{\partial g}{\partial x}) - \frac{\partial}{\partial z} (\vartheta D_g \frac{\partial g}{\partial z}) + S_g + \frac{\partial \theta}{\partial t} g = 0 \quad (9.4)$$

and

$$\vartheta \frac{\partial g}{\partial t} - \frac{1}{x} \frac{\partial}{\partial x} (\vartheta D_g x \frac{\partial g}{\partial x}) - \frac{\partial}{\partial z} (\vartheta D_g \frac{\partial g}{\partial z}) + S_g + \frac{\partial \theta}{\partial t} g = 0 \quad (9.5)$$

The governing equations of gas transport (9.4) and (9.5) are solved numerically to obtain spatial and temporal distributions of the gas content,  $g$ , within the soil domain. The soil domain for this purpose is divided into a network of triangular elements with nodal points representing corners of elements. One possible subdivision is shown in Fig. 6.1 which applies to the grid in Fig. 3.1. The gas content is approximated by a linear combination of nodal concentration values:

$$\hat{g}(x, z, t) = \sum_{n=1}^{N_e} \phi_n(x, z) g_n(t) \quad (9.6)$$

where  $N_n$  is the total number of nodes,  $\phi_n(x,z)$  are basis functions for node  $n$ , and  $g_n$  is the gas content at the node  $n$ . The basis functions are linear and are derived from interpolation functions which are given for triangular elements in Eq. (6.4). The Galerkin method is used to obtain equations for nodal values of  $g$ . Area-averaged weighted residuals of Eq. (9.4) must equal zero for every  $\phi_n$  taken as a weight. Consequently, for the whole soil domain we obtain:

$$\sum_{e=1}^{N_e} \int_{\Omega_e} \left[ \vartheta \frac{\partial g}{\partial t} - \frac{\partial}{\partial x} (\vartheta D_g \frac{\partial g}{\partial x}) - \frac{\partial}{\partial z} (\vartheta D_g \frac{\partial g}{\partial z}) + S_g + \frac{\partial \theta}{\partial t} g \right] \phi_n d\omega = 0 \quad (9.7)$$

where  $\Omega_e$  designates area of the element  $e$ , and  $N_e$  is the total number of elements. After replacing  $g$  by  $\hat{g}$  and using Green's first identity

$$\begin{aligned} & \sum_{e=1}^{N_e} \int_{\Omega_e} \left( -\vartheta \frac{\partial \hat{g}}{\partial t} \right) \phi_n d\omega - \sum_{e=1}^{N_e} \int_{\Omega_e} \frac{\partial \theta}{\partial t} \hat{g} \phi_n d\omega \\ & + \sum_{e=1}^{N_e} \int_{\Omega_e} \left[ -\frac{\partial \hat{g}}{\partial x} \frac{\partial \phi_n}{\partial x} - \frac{\partial \hat{g}}{\partial z} \frac{\partial \phi_n}{\partial z} \right] \vartheta D_g d\omega \\ & + \sum_{e=1}^{N_e} \int_{\Gamma_e} \left( \frac{\partial \hat{g}}{\partial x} n_{\Gamma,x} + \frac{\partial \hat{g}}{\partial z} n_{\Gamma,z} \right) \vartheta D_g \phi_n d\Gamma \\ & - \sum_{e=1}^{N_e} \int_{\Omega_e} S_g \phi_n d\omega = 0 \end{aligned} \quad (9.8)$$

where  $\Gamma_e$  is the boundary of the element  $e$ , and  $n_{\Gamma,x}, n_{\Gamma,z}$  designate components of the vector which has a unit length and is normal to the border.

Further simplifications are based on two important assumptions. First, the air-filled porosity,  $\vartheta$ , varies linearly over each element and  $S_g$ , the gas extraction rate, is constant over an element. Second, changes of nodal gas content are calculated as weighted averages of gas content changes over the element according to the mass-lumping technique (Istok, 1989). These assumptions lead to a system of first-order ordinary differential equations for the values of gas concentration:

$$[Q] \frac{d\{g\}}{dt} + [G]\{g\} + \{\mathbf{f}\} = \{Q\}^D \quad (9.9)$$

where vector  $\{g\}$  includes all nodal values of  $g$ . The matrices  $Q$  and  $G$  have elements

$$\begin{aligned} Q_{m,n} &= \delta_{mn} \sum_e \frac{A_e}{3} \hat{v}_n \\ G_{m,n} &= \sum_e \left[ -\frac{A_e}{3} \left( \frac{\partial \theta}{\partial t} \right)_n \delta_{mn} - \frac{\bar{v}_D}{4A_e} (\hat{b}_m \hat{b}_n + \hat{c}_m \hat{c}_n) \right] \end{aligned} \quad (9.10)$$

where summation is over elements having nodes  $m$  and  $n$ . Vector  $\{\mathbf{f}\}$  has components

$$f_n = \sum_e \frac{1}{12} A_e [(\bar{S}_g)_e + (S'_g)_n] \quad (9.11)$$

where summation is over elements having the node  $n$ . Gas extraction rates at the nodes are calculated as  $(S'_g)_n = \Sigma A_e (S_g)_e / \Sigma A_e$  where summation is over all elements that contain the node  $n$ . The average nodal gas extraction rate of element  $S_e$  is found as a mean of the nodal values for that element. The parameters  $\hat{b}_n$ ,  $\hat{c}_n$ ,  $A_e$  have the same meaning as in Eq. (6.4). Parameters with over lines are averaged over elements.

Vector  $\bar{Q}^D$  has non-zero components only for boundary nodes. It represents the total gas flux. If the concentration is constant at the boundary, then  $dg_n/dt=0$  and, in accordance with Eq. (9.9),

$$Q_n^D = - \sum_{m=1}^{N_n} G_{m,n} g_m - f_n \quad (9.12)$$

If the gas flux is constant at the boundary, then  $Q^D$  is replaced by the known total boundary flux. This flux is added to components of the vector  $\bar{f}$  in Eq. (9.9) and  $Q^D$  is zeroed.

Methods used for solving Eq. (9.9) are similar to those described in sections 7.9 and 8.9. Slight modifications of the coefficients in Eqs. (9.10) and (9.11) allows the solution of axisymmetric cases described by Eq. (9.5). Boundary and initial conditions must be defined to

solve Eq. (9.9). Information on time-dependent boundary settings are presented in Chapters 4 and 5 of this manual. Time-independent boundary concentrations are specified as initial data. The initialization file is described in section 9.3.

## **9.2 Parameters of the GasMover module.**

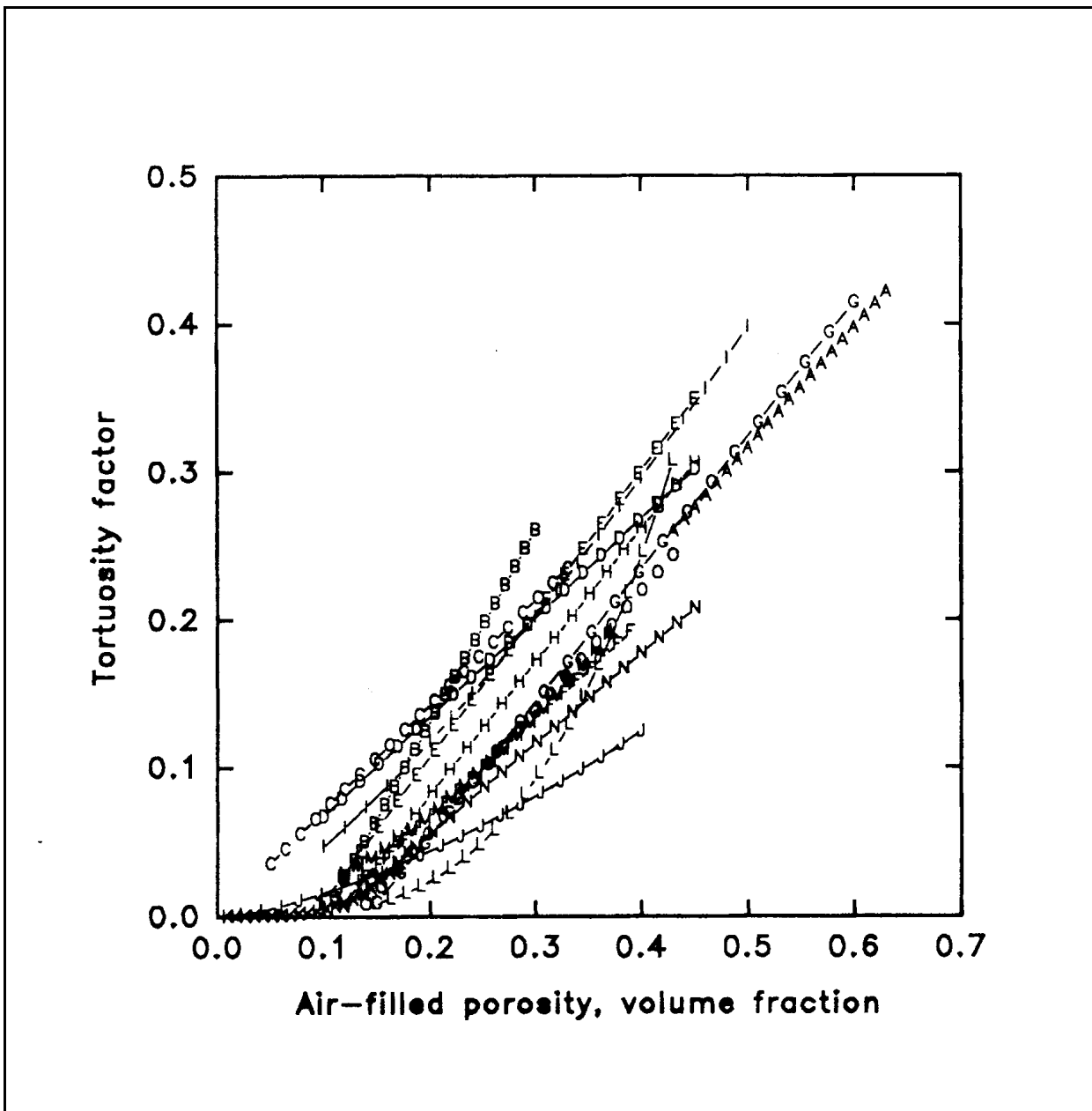
Molecular diffusion in soil air is the only mechanism that governs gas movement in the model. The gas diffusion coefficient in soils,  $D_g$ , depends on the diffusion coefficient in air  $D_0$  and on the soil conditions according to:

$$D_g = D_0 \tau_g = D_{0,st} \left( \frac{T}{273.15} + 1 \right)^{n_g} \tau_g \quad (9.13)$$

where  $D_{0,st}$  is the molecular diffusion coefficient at standard conditions (760 mm Hg and 273.15 K), and  $n_g$  is an exponent between 1.75 and 2.0 (American Institute of Physics Handbook, 1972). Here,  $n_g=2$  applies for all gases. The tortuosity factor  $\tau_g$  strongly depends on soil structure and texture as well as on soil moisture content. This relationship is illustrated in Fig. 9.1, where the averaged data for different gases have been compiled from various sources. The data indicate that there is a threshold level of air-filled porosity below which diffusion does not occur. The dependence of the tortuosity factor on air-filled porosity may be expressed as

$$\tau_g = \begin{cases} b_{Tort}(\vartheta - \vartheta_{Thr}), & \vartheta > \vartheta_{Thr} \\ 0, & \vartheta \leq \vartheta_{Thr} \end{cases} \quad (9.14)$$

where  $\vartheta_{Thr}$  is a threshold value of air-filled porosity, and  $b_{Tort}$  is a tortuosity change per unit of air-filled porosity. Reasonable values for the variables in Eq 9.14 are:  $\vartheta_{Thr}=0.12$  and  $b_{Tort}=0.65$ .



We suggest that some non-zero value of air-filled porosity exists near saturation. This value corresponds to entrapped air and is denoted as  $\vartheta_{min}$ . Consequently, air-filled porosity is calculated as

$$\vartheta = \begin{cases} \theta_s - \theta + \vartheta_{min}, & \theta < \theta_s \\ \vartheta_{min}, & \theta = \theta_s \end{cases} \quad (9.15)$$

### **9.3 Data files 'Param\_G.dat' and 'Nodal\_G.dat'**

Parameters for the **GasMover** module are read from the file '**Param\_G.dat**'. The first parameter is a time-weighing factor,  $epsi$ , used in the final matrix equation for gas transport. Values of  $epsi$  between 0.5 and 0.8 usually give good results. See Section 7 for a full description of this parameter. The other transport parameters are functions of soil conditions and are given separately for every soil material in the soil domain. The materials are identified by the material number,  $MatNumN$ , specified for every node in the **Grid\_and\_Boundary** information file '**Grid\_Bnd.dat**'. The parameters are fully described in Table 9.1 which also shows the structure of this file.

**GasMover** reads data on the initial gas contents from the file '**Nodal\_G.dat**'. If constant boundary value for gas content is used, then the values must be given in this file. Table 9.2 shows the format for the file '**Nodal\_G.dat**'. The example following the table corresponds to the grid in Fig. 3.1 and to the file '**Grid\_bnd.dat**' of Example 3.3.

Table 9.1. Format of the file '**Param\_G.dat**'.

Record	Variable	Description
1	-	Comment line. <u>Computational Information</u>
2	-	Comment line.
3	<i>NumG</i>	Number of gases under consideration.
4	-	Comment lines.
5	<i>epsi</i>	Temporal weighing coefficient. <u>Material information</u>
6-8	-	Comment lines.
9	<i>ThTot(1)</i>	Porosity of soil material in subdomain #1.
9	<i>ThTot(2)</i>	Same as above for soil material in subdomain #2.
9	<i>ThTot(NMat)</i>	Same as above for the soil material in the last subdomain.
10,11	-	Comment lines.
12	<i>ThATr(1)</i>	Threshold value of air-filled porosity for the soil material in subdomain #1.
12	<i>ThATr(2)</i>	Same as above for material in subdomain #2.
12	<i>ThATr(NMat)</i>	Same as above for the soil material in the last subdomain.
13,14	-	Comment lines.
15	<i>bTort(1)</i>	Tortuosity change per unit of the air-filled porosity for soil material in subdomain #1.
15	<i>bTort(2)</i>	Same as above for material in subdomain #2.
15	<i>bTort(NMat)</i>	Same as above for the soil material in the last subdomain.
16,17	-	Comment lines.
18	<i>ThAMin(1)</i>	Minimum value of the air-filled porosity for the soil material in subdomain #1.
18	<i>ThAMin(2)</i>	Same as above for material in subdomain #2.
18	<i>ThAMin(NMat)</i>	Same as above for the soil material in the last subdomain.
19,20	-	Comment lines.
21	<i>Dair(1)</i>	Diffusion coefficient in air for gas 1 in standard conditions, $\text{cm}^2$ per day
21	<i>Dair(2)</i>	Same as above for gas 2.
21	<i>Dair(NumG)</i>	Same as above for the last gas.

```
*** Example 9.1: GASMOVER PARAMETERS: file 'Param_G.dat'
Number of gases
      3
epsi
0.55
Soil material and gas parameters
Total porosities of soil materials (ThTot)
  Subdomain #1   Subdomain #2
  0.470       0.420
Threshold values of soil air-filled porosity (ThATr)
  Subdomain # 1   Subdomain # 2
  0.12        0.05
Reduced tortuosity changes (bTort)
  Subdomain # 1   Subdomain # 2
  0.60        0.80
Minimum air filled porosities
  Subdomain # 1   Subdomain # 2
  0.02        0.01
Gas diffusion coefficients in air at standard conditions, cm/day
  Gas # 1 (CO2)    Gas # 2 (Oxygen)    Gas # 3 (Methane)
  11920          15400            16900
```

Table 9.2. Format of the file '**Nodal\_G.dat**'.

Record	Variable	Description
1,2	-	Comment lines.
3	$n$	Nodal number.
3	$g(n,1)$	Initial value of the content for the first gas in soil air at node $n$ , g $\text{cm}^{-3}$ .
3	$g(n,2)$	Same as above for the second gas.
3	$g(n,\text{NumG})$	Same as above for the last gas.
Record 3 is provided for every node of the grid. Constant boundary gas content, if used, must be present in this file.		

\*\*\*\* Example 9.2: INITIAL GAS CONTENT DISTRIBUTION - file 'Nodal\_G.dat'

n	$g(n,1)$	$g(n,2)$	$g(n,3)$
1	1.3E-05	3.0E-04	0.0
2	1.3E-05	3.0E-04	0.0
3	1.3E-05	3.0E-04	0.0
4	1.3E-05	3.0E-04	0.0
5	1.3E-05	3.0E-04	0.0
6	1.3E-05	3.0E-04	0.0
7	1.3E-05	3.0E-04	0.0
8	1.3E-05	3.0E-04	0.0
9	1.3E-05	3.0E-04	0.0
10	1.3E-05	3.0E-04	0.0
11	1.3E-05	3.0E-04	0.0
12	1.3E-05	3.0E-04	0.0
13	1.3E-05	3.0E-04	0.0
14	1.3E-05	3.0E-04	0.0
15	1.3E-05	3.0E-04	0.0
16	1.3E-05	3.0E-04	0.0
17	1.3E-05	3.0E-04	0.0
18	1.3E-05	3.0E-04	0.0



# Chapter 10: Root Water Uptake: Root\_Water\_Uptake Module

**Basil Acock, Yakov Pachepsky, and Dennis Timlin**

There are two methods commonly used to describe water uptake by plant roots. Models like ROOTSIMU (Hoogenboom and Huck, 1986) require information on plant and root development because root activity and root water uptake depend not only on the soil and atmosphere environment but also on plant status, and the plant's ability to extract water and to grow roots. Other models like SWMS\_2D (Šimůnek et al., 1994) and CERES-Maize (Jones and Kiniry, 1986) do not require detailed information on the growth and development of the plant canopy and roots. Root distribution either does not change in time or changes independently of shoot status. Both of these approaches are available in 2DSOIL. The module **Water\_Uptake01** uses plant status information extensively and requires an additional module that will generate shoot-dependent variables that control water uptake and root growth. Module **Water\_Uptake02** does not simulate root development and so does not need the plant status information. Root densities must be supplied as input data, however.

## **10.1 Plant status dependent model: Water\_Uptake01**

This module is based on the root activity model developed by Acock and incorporated into the soybean crop simulator GLYCIM (Acock and Trent, 1991). In this model, root growth is driven by carbon supplied by the above ground plant. Carbon partitioning and water uptake are determined by leaf water and soil water potentials. If water in the root zone becomes limiting, the shoot can divert some carbon normally used for shoot and leaf growth to the roots to increase root growth into wetter areas of the soil. The model generates a relationship between the potential transpiration rate  $E_c$  and leaf water potential  $\psi_L$  for each time step. The shape of the relationship between  $\psi_L$  and  $E_c$  reported for a variety of plants (Stoker and Weatherly, 1971;

Hailey et al., 1973; Bunce, 1978) is shown in Fig. 10.1. The model assumes that characteristic points  $A, B, C, D$  separate intervals of different levels of carbon partitioning between the shoot and the root in the following way:

(1) At low transpiration demands, between points  $A$  and  $B$ , mature roots and new roots added using carbon "left over" after shoot growth is satisfied, can extract sufficient water. The slope of the relationship between leaf water potential and potential transpiration remains constant, at the level  $\Psi_{L,0}$ , and there is no diversion of additional carbon from the shoot to the root. In other words, until the leaf water potential reaches  $\Psi_{L,0}$  the plant can adjust leaf water potential to maintain water uptake as the potential transpiration rate changes.

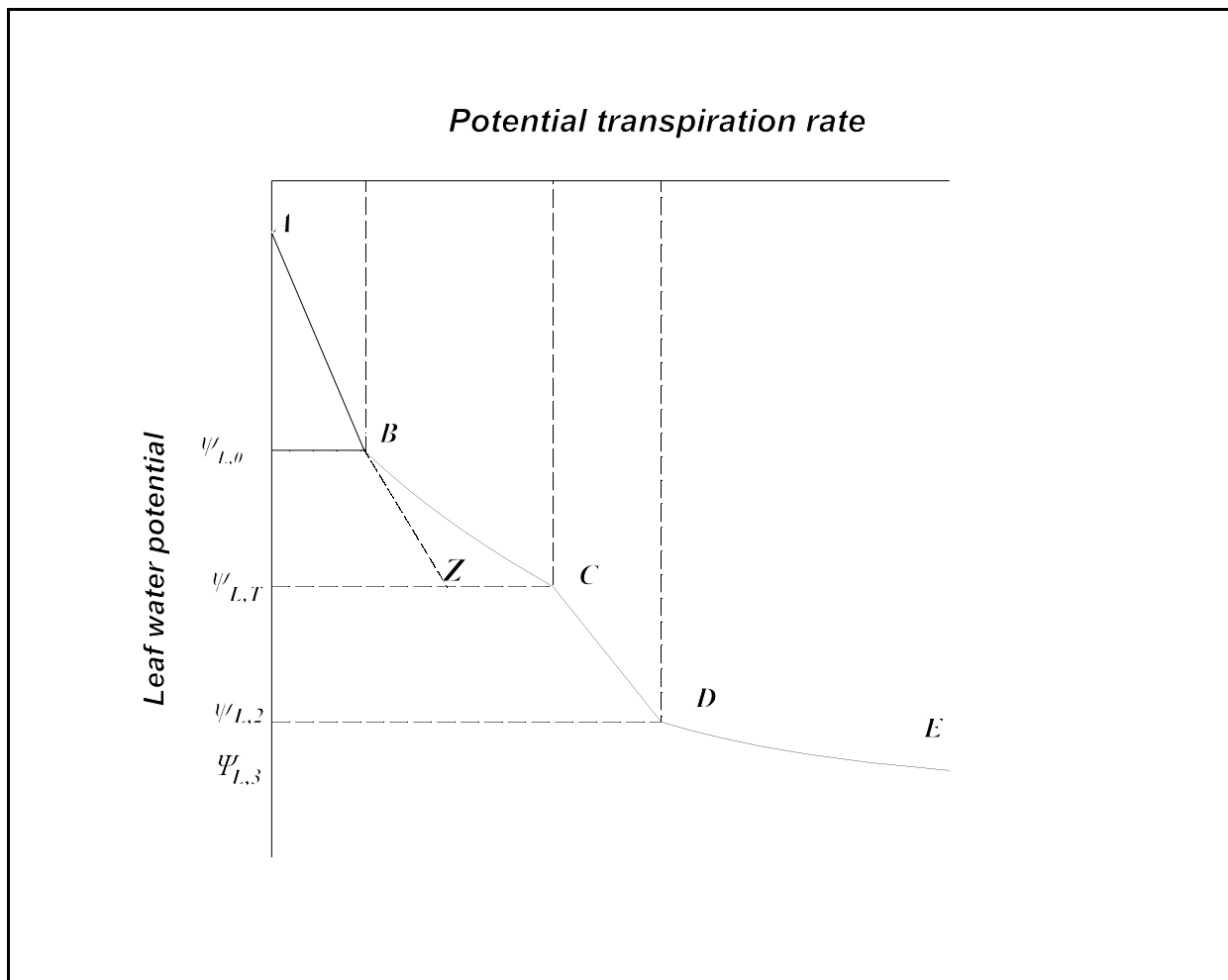


**Figure 10.1** Typical relationship between potential transpiration rate and water potentials in the soil-plant-atmosphere system. Here  $\Psi_{L,0}$  is the leaf water potential at low transpiration rates when there is no diversion of carbon to the roots, below this potential, the leaf water potential begins to decrease as the potential evaporation rate increases,  $\Psi_{L,T}$  is the leaf water potential when all available carbon goes to root growth (C),  $\Psi_{L,2}$  is the point at which the stomates begin to close (D), and  $\Psi_{L,3}$  is the point at which water uptake becomes negligible (E).

(2) At intermediate transpiration demands, between points  $B$  and  $C$ , the plant must decrease its leaf water potential in order to increase the leaf-soil water potential gradient. Simultaneously, additional carbon is diverted to the roots to increase the pool of young roots that have a lower resistance to water uptake. Beginning at point  $C$ , the plant uses all available carbon for root growth and the shoot no longer grows. The line segment  $Z-C$  represents additional water uptake that results when all available carbon is used to grow roots.

(3) At high transpiration demands, between points *C* and *D*, the roots are supplied with the maximum amount of carbon available and shoot growth stops. As transpiration demand increases, both leaf water potential  $\psi_L$  and leaf turgor pressure  $P_L$  decrease. At point *D*, the turgor pressure reaches the critical level and stomata begin to close.

(4) At very high transpiration demands, above point *D*, there is no shoot growth. Stomatal closure means that the plant can meet only a fraction of the transpiration demand and the actual transpiration rate falls below potential rate

The following relationships and hypotheses are incorporated into the model. All values below are defined for soil cells (elements) and are assumed to be constant within the cells. Physical units are g, cm, day, °C, and bars for pressures and potentials.

**1. Water uptake and root growth take place preferentially in the soil cells where soil conditions are most favorable for growth.** Root growth depends on the following soil state variables: soil water potential  $\psi_s$ , soil temperature  $T_s$ , and soil oxygen content  $g_{Ox}$ . A root growth reduction factor  $f_{rg}$  is calculated for every element as:  $f_{rg} = \min(f_{rg,1}(\psi_s), f_{rg,2}(T_s), f_{rg,3}(g_{Ox}))$ . The reduction factor components  $f_{rg,1}(\psi_s)$ ,  $f_{rg,2}(T_s)$ , and  $f_{rg,3}(g_{Ox})$  account for the effects of soil moisture, soil temperature, and soil redox status. A root growth reduction factor is calculated for each variable. The value with the smallest magnitude is considered to be most limiting and that minimum value is used to reduce potential root growth. The soil cells are then renumbered in the order highest to lowest based on their values of  $f_{rg}$ . The cells nearer the plant stem base have priority in the list when any two cells have the same value of  $f_{rg}$ .

The reduction of root growth due to changes in soil water potential is based on the concept of root osmoregulation. Greacen and Oh (1972) showed that roots osmoregulate with 90% efficiency against soil water potential changes and with 70% efficiency against changes in soil mechanical resistance. It seems unlikely, however, that roots can make these adjustments as rapidly as soil water potential can change during the day. Therefore, it is assumed that root osmoregulation is complete at dawn but operates at half the dawn efficiency during the day. It is also assumed that the expanding cells in the root tip, being in intimate contact with the soil, will have a water potential equal to that of the soil. The root osmotic potential at dawn  $\pi_{R,D}$  depends on soil water potential at dawn  $\psi_{s,D}$  and soil mechanical resistance pressure  $P_{M,D}$ :  $\pi_{R,D} = 0.9\psi_{s,D} - P_{M,D}$

$5.5 - 0.7P_{M,D}$ . The root turgor pressure at dawn  $P_{R,D}$ , is equal to the difference between root water potential at dawn  $\psi_{R,D}$  and root osmotic potential, i.e.,  $P_{R,D} = \psi_{R,D} - \pi_{R,D}$ . Since root and soil water potentials are assumed to be equal,  $P_{R,D} = 0.1\psi_{s,D} + 5.5 + 0.7P_{M,D}$ . Subtracting the threshold turgor pressure at which root growth starts,  $P_{R,T}$  ( $= 3.5$  bars), we obtain  $P_{R,D} = 0.1\psi_{s,D} + 2.0 + 0.7P_{M,D}$ . The turgor pressure available to expand the root after overcoming soil mechanical resistance at dawn is:  $\Delta P_{R,D} = P_{R,D} - P_{M,D}$ . At any other time of day a similar relationship is used with appropriate values of the variables:  $\Delta P_R = P_R - P_M$ . The threshold pressure for root growth to occur is 3.5 bars, and the maximum value that  $\Delta P_M$  can attain is 5.5 bars. Assuming root growth is proportional to  $\Delta P_M$  over this range, the proportion of maximum root growth possible at the given soil water potential and soil mechanical resistance pressure is:

$$r_{gl,1}(\psi_s) = (\Delta P_{M,D} - P_{R,D}) / (5.5 - P_{R,D}) = (P_R - \mu_R - 3.5) / 2$$

If the root osmoregulates with half efficiency during the day then , the change in root turgor pressure will equal half any change in root water potential. That is,  $P_R = P_{R,D} - (\psi_{R,D} - \psi_R)/2$ , where  $\psi_R$  is root water potential during the day. Recalling that  $\psi_R = \psi_s$  and substituting in the earlier equation, we have finally:

$$r_{gl,1}(\psi_s) = (P_{R,D} - P_M) / 2 - (\psi_{R,D} - \psi_{s,D}) / 4$$

The soil mechanical resistance,  $\mu_R$ , depends on the soil bulk density  $\rho_s$  and soil moisture content  $\theta$  as:

$$\mu_R = 0.5 + 100 * (0.14 - \theta) \exp[-8.08(1.66 - \rho_s)]$$

Root growth reduction due to changes of temperature is modeled using the data of White (1937), and root response to oxygen concentration is based on the data of Eavis et al. (1971):

$$f_{rg,2}(T) = (T/30)^b, \quad b = \begin{cases} 3.66, & T < 30^\circ \\ -15.4, & T \geq 30^\circ \end{cases} \quad (10.1)$$

$$f_{rg,3}(g_{Ox}) = \begin{cases} 0.15 + 4000g_{Ox}, & g_{Ox} \leq 2.13 \cdot 10^{-4} \\ 1.00, & g_{Ox} > 2.13 \cdot 10^{-4} \end{cases}$$

**2. The threshold turgor pressure required for shoot cell growth adjusts dynamically.** It has been shown that a decrease in turgor pressure is followed by a decrease in the threshold turgor pressure required for cell growth. Thus, growth over a period,  $\Delta t$ , is only decreased if the

turgor pressure falls more than the threshold turgor pressure can adjust in that time. The rate of threshold adjustment is higher at high turgor pressure. This relationship is expressed in the form:

$$\frac{P_{LT} - 2}{\max(P_L^0, P_{LT}^0) - 2} = \exp(-16.8\Delta t) \quad (10.2)$$

Here  $P_{LT}$  is the threshold leaf turgor pressure at the end of the  $\Delta t$  interval;  $P^0 LT$  is the threshold leaf turgor pressure at the beginning of the  $\Delta t$  interval; and  $P_L^0$  is leaf turgor pressure at the beginning of the  $\Delta t$  interval. This dependence is based on the data of Green et al. (1971).

**3. There is a dynamic relationship between leaf water potential and leaf turgor pressure that is controlled by osmoregulation.** Any change in leaf water potential during the day is partially balanced by a change in leaf osmotic potential. Measurements for soybean and cotton have shown changes in leaf osmotic potential to be equal to half the changes in leaf water potential. This appears to be one way plants become conditioned to water stress. In the model, temporal increments of leaf water potential and turgor pressure are proportional:

$$1 - f_\pi = \frac{\Psi_L - \Psi_L^0}{P_L - P_L^0} \quad (10.3)$$

Here, and subsequently,  $\psi_L$  is leaf water potential and  $P_L$  is leaf turgor pressure. The superscript 0 indicates the beginning of the time interval, and the absence of the superscript indicates the end of this interval. The parameter  $f_\pi$  is the factor in the model that simulates conditioning to water stress. The osmoregulation concept allows us to not only calculate changes in the leaf turgor pressure but also to calculate critical levels of the leaf water potential from known critical or threshold values of the turgor pressure. The threshold value of the leaf water potential  $\psi_{LT}$  that prevents all shoot expansion is:

$$\psi_{LT} = \max(\psi_L^0, \psi_{LT}^0) + \frac{P_{LT} - \max(P_L^0, P_{LT}^0)}{1 - f_\pi} \quad (10.4)$$

The leaf water potential at 2 bars of turgor pressure  $\psi_{L,2}$  is:

$$\Psi_{L,2} = \Psi_L^0 - \frac{2 - P_L^0}{1 - f_\pi} \quad (10.5)$$

The leaf water potential at zero turgor  $\psi_{L,0}$  is:

$$\Psi_{L,0} = \Psi_L^0 - \frac{P_L^0}{1 - f_\pi} \quad (10.6)$$

**4. Water uptake for existing and new roots is a function of root length and the difference between soil and leaf water potentials.** In each soil cell there are mature roots (older than two days), young roots, and new young roots. The new young roots appear during the current  $\Delta t$  interval. The model uses auxiliary water uptake variables to determine how the potential transpiration rate relates to various potential water uptake rates. These values correspond to points Z and C-Z on Fig. 10.1 and they are calculated as:

$$\begin{aligned} u_i^0 &= \left( \frac{L_M A_s}{r_M} + \frac{l_Y}{r_{Y_i}} \right) (\Psi_s - \Psi_{LT})_i \\ \Delta u_i &= \left( \frac{\Delta l_Y}{r_{Y_i}} \right) (\Psi_s - \Psi_{LT})_i \end{aligned} \quad (10.7)$$

where

$u_i^0$  - water uptake by existing roots from soil cell  $i$ , g·plant<sup>-1</sup>·day<sup>-1</sup>, when the leaf water potential equals the threshold value that prevents all shoot expansion. It corresponds to point Z in Fig. 10.1. This is the additional water uptake from roots grown with the extra carbon diverted from canopy growth.

$\Delta u_i$  - additional water uptake by new roots from soil cell  $i$ , g·plant<sup>-1</sup>·day<sup>-1</sup>, when all additional carbon is made available for root growth and the leaf water potential is less than the threshold value that prevents all shoot expansion, point C-Z in Fig. 10.1.

$I$  - order of favorability for root growth ( $i=1$  is the most favorable),

$L_M$  - density of mature roots in the soil cell, g cm<sup>-2</sup>,

- $A_s$  - area of the soil cell,  $\text{cm}^2$ ,  
 $l_Y$  - length of young roots in the soil cell from the previous time steps, cm,  
 $\Delta l_Y$  - length of young roots that appear in the soil cell during the current time interval, cm,  
 $r_M$  - total resistance of the water path from soil to leaf through mature roots,  $\text{bar}\cdot\text{day}\cdot\text{g}^{-1}\cdot(\text{cm of root})$ ,  
 $r_Y$  - same as above for the young roots,  $\text{bar}\cdot\text{day}\cdot\text{g}^{-1}\cdot(\text{cm of root})$ .  
 $r_V$  - root vascular resistance,  $\text{bar}\cdot\text{day}\cdot\text{g}^{-1}$  (cm root).  
RVRL Radial vascular root resistance per cm root  $\text{bar}\cdot\text{day}\cdot\text{g}^{-1}\cdot(\text{cm of root})$ .

Resistances to flow of water in the plant-soil system include soil resistances,  $r_s$ , root radial resistances,  $r_{RM}$  and  $r_{RY}$ , and root vascular resistance  $r_V$ . All are altered by water viscosity which is given as a function of temperature by Dalton and Gardner (1978) as:

$$\begin{aligned} r_V &= (\text{RVRL}) \frac{\sqrt{(x^2+y^2)}}{4} \\ r_Y &= (r_s + r_{RY} + r_V)/0.002275/(T+24.5) \\ r_M &= (r_s + r_{RM} + r_V)/0.002275/(T+24.5) \end{aligned} \tag{10.8}$$

Here  $x$  and  $y$  are the distances from the center of the cell to the stem of the plant. The radius of the soil cylinder through which water must travel to reach the root is normally considered to be a function of root density. However, it is actually a function of soil water content, soil hydraulic properties, and root water uptake rate. In this model, to avoid interactions, the radius of the soil cylinder is made a simple function of soil water potential:  $d_{sc} = 0.017 - 0.05 \psi_s$ . The equation is based on the data of Cowan (1965). Resistance to water flow in the soil,  $r_s$ , is calculated by assuming steady-state diffusion of water across the soil cylinder to the root surface (Gardner, 1960). The average root radius is assumed to be 0.017 cm (Taylor and Klepper, 1975), and  $r_s = \ln(d_{sc}^2/(3 \cdot 10^{-4}))/(4 \pi K \cdot 1019)$ , where  $K$  is an average soil hydraulic conductivity in the cell.

The values for vascular resistances were calculated from data of Bunce (1978). The overall plant resistance was partitioned between leaf, vascular, and root radial resistances in the proportions reported by Boyer (1971). Since the roots in both the Bunce and Boyer data were probably not growing very rapidly (transpiration demand was low), the root radial resistance obtained by this method was assumed to be the one for "old" roots. "Young" roots have a lower

resistance than "old" ones (Russel, 1977). The ratio of "old" to "young" resistances found by Brouwer (1965) was used to estimate a radial resistance for "young" soybean roots. In this model the roots remain "young" for two days after they are grown.

**5. The amount of new root growth and water uptake during the current time interval depend on the amount of carbon translocated from the shoot.** The rate of carbon translocation  $B_R$  to roots varies between  $B_{R,min}$  and  $B_{R,max}$ . The former occurs if roots get only the carbon left over after above ground growth is satisfied; the latter represents the case when roots get all the carbon translocated from the leaves. Therefore, the ratio  $\xi = (B_R - B_{R,min}) / (B_{R,max} - B_{R,min})$  may vary between 0 and 1.

If the ratio  $\xi$  is zero, i.e.  $B_R = B_{R,min}$ , then the total water uptake by old and new roots  $U_1$ , corresponding to point Z in Fig. 10.1 is equal to

$$U_1 = \sum_{i=1}^{i=N_e} u_i^0 + \sum_{i=1}^{i=i_1} \Delta u_i \kappa_i \quad (10.9)$$

Here water uptake by old roots is summed for all soil cells ( $N_e$ ) and water uptake by young roots is summed over those soil cells where new roots grow. These soil cells have numbers from 1 to  $i_1$ . Weighting factors  $\kappa_i$  are equal to 1 in all cells because roots grow at the potential rate except where cell # =  $i_1$ . In the last cell,  $i_1$ , the value of  $\kappa_i$  may be less than 1 because there may not be enough carbon to meet the potential growth rate. The weighting factors  $\kappa_i$  for this cell satisfy the following equations:

$$\begin{aligned}
& \sum_{i=1}^{i=i_1} (\Delta l_Y)_i \kappa_i = B_{R,\min} / (b_R W_R), \\
& \kappa_i = 1, \quad i = 1, 2, \dots, i_1 - 1, \\
& \kappa_{i_1} = \frac{B_{R,\min} / (b_R W_R) - \sum_{i=1}^{i=i_1-1} (\Delta l_Y)_i}{(\Delta l_Y)_{i_1}} \\
& \kappa_i = 0, \quad i > i_1
\end{aligned} \tag{10.10}$$

Here  $b_R$  is amount of carbon needed to make unit root dry mass, g·g<sup>-1</sup>, and  $W_R$  is the average root dry weight per unit length, g·cm<sup>-1</sup>.

If the ratio  $\xi$  is 1, the total water uptake by old and new roots  $U_2$  corresponding to point C in Fig 10.1 is equal to:

$$U_2 = \sum_{i=1}^{i=N_e} u_i^0 + \sum_{i=1}^{i=i_2} \Delta u_i / \kappa_i \tag{10.11}$$

Here  $u_i^0$  represents uptake by the roots grown with additional carbon. The difference between  $U_1$  and  $U_2$  lies in the number of cells with young roots. This number  $i_2$  for  $U_2$  and corresponding weighting factors,  $\kappa_i$ , satisfy the following equations:

$$\begin{aligned}
& \sum_{i=1}^{i=i_2} (\Delta l_Y)_i \kappa_i = B_{R,\max} / (b_R W_R), \\
& \kappa_i = 1, \quad i = 1, 2, \dots, i_2 - 1, \\
& \kappa_{i_2} = \frac{B_{R,\max} / (b_R W_R) - \sum_{i=1}^{i=i_2-1} (\Delta l_Y)_i}{(\Delta l_Y)_{i_2}} \\
& \kappa_i = 0, \quad i > i_2
\end{aligned} \tag{10.12}$$

**6. Low potential transpiration rates can be met from water uptake by old roots and new ones growing with the minimum carbon supply rate  $B_{min}$ .** In this case the leaf water potential at the beginning of the current time interval corresponds to point  $B$  in Fig. 10.1 and the water uptake rate  $U_B$  is equal to

$$U_B = U_1 \frac{\Psi_L^0 - \Psi_s^a}{\Psi_{LT} - \Psi_s^a} \tag{10.13}$$

Here  $\Psi_s^a$  is the average soil water potential in the cells where new roots extract water. If the transpiration demand,  $E$ , is less than  $U_B$ , then the leaf water potential at the end of the current time interval,  $\Psi_s$ , will be larger than at the beginning,  $\Psi_s^0$  and is calculated as:

$$\Psi_L = \Psi_s^a + \frac{E}{U_B} (\Psi_L^0 - \Psi_s^a) \tag{10.14}$$

The root carbon supply ratio  $\xi$  is equal to zero and the shoot has no growth limitation.

**7. Intermediate potential transpiration rates reduce shoot growth by some fraction.** At these transpiration rates the demand for water uptake cannot be met without shoot water potential falling to the point where the shoot loses turgor and stops growing for part of the time interval. When this happens, additional carbon is sent to the roots to increase root growth. The potential transpiration rate ranges between  $U_B$  and  $U_2$ . The carbon supply ratio  $\xi = (\psi^0 L - \psi_L)/(\psi^0 L - \psi_{LT})$ , and leaf water potential has a non-linear dependence on transpiration rate:

$$E_C = \frac{\psi_s^a - \psi_L}{\psi_s^a - \psi_{LT}} [U_1 + (U_2 - U_1) \frac{\psi_L^0 - \psi_L}{\psi_L^0 - \psi_{LT}}] \quad (10.15)$$

**8. High potential transpiration rates can be met from water uptake by mature roots and new roots growing with the maximum carbon supply  $B_{R,max}$ .** The potential transpiration rate at point C in Fig. 10.1 corresponds to the minimum transpiration demand that completely prevents shoot growth. If transpiration demand is higher than  $U_2$ , then leaf water potential exceeds its threshold value. Leaf water potential is calculated as:

$$\psi_L = \psi_s^a + \frac{E_C}{U_2} (\psi_{LT} - \psi_s^a) \quad (10.16)$$

The root carbon supply ratio  $\xi$  is equal to one and the shoot does not grow as all available carbon is translocated to the roots. Very high transpiration demands can result in leaf turgor pressures less than 2 bars and leaf water potentials less than  $\psi_{L,2}$ . In this case, stomatal closure occurs and the transpiration rate decreases. The leaf water potential is now calculated as:

$$\psi_L = \frac{\psi_s^a + \frac{E_C(\psi_s^a - \psi_{L,2})}{U_2(\psi_{L,2} - \psi_{L,0})} \psi_{L,0}}{1 + \frac{E_C(\psi_s^a - \psi_{L,2})}{U_2(\psi_{L,2} - \psi_{L,0})}} \quad (10.17)$$

The reduction of transpiration rate is found by multiplying the potential transpiration rate,  $E$ , by the ratio  $(\psi_L - \psi_{L,0})/(\psi_{L,2} - \psi_{L,0})$ .

**9. At the beginning of the day, leaf water potential is fixed at the dawn value.** At dawn, the leaf water potential is set to the soil water potential.

**10. The stomata close overnight and under water stress.** It is assumed that the fluxes of carbon dioxide and water are reduced to 10% of the maximum rate when the stomata close at night and the plants have not experienced water stress. The value of 10% is derived from the data of Boyer (1970). If the plants have experienced stress, the stomata are assumed to close to the point where fluxes are reduced to 1% of the maximum rate. If stomata close at any time during the day, leaf osmoregulation occurs.

**11. The turgor pressure itself may influence carbon partitioning between shoot and root.** If turgor pressure is less than 5 bars and decreasing, shoot growth potential is partially reduced by sending some additional carbon to the roots. The carbon supply ratio is altered and the value of  $1-(1-\xi)(P_L-2)/3$  is used instead of  $\xi$ .

**12. Water uptake from each soil cell depends on the leaf water potential, root carbon partitioning ratio, and the potential for new root growth.** Initially the approximate water uptake of mature and young roots corresponding to available carbon and leaf water potential is found for every cell:

$$\tilde{u}_i = (u_i^0 + \Delta u_i \kappa_i) \left( \frac{\Psi_s - \Psi_L}{\Psi_s - \Psi_{LT}} \right), \quad , i=1,2,\dots,N_e \quad (10.18)$$

Here, the weights  $\kappa_i$  correspond to the amount of carbon available for root growth as:

$$\begin{aligned}
& \sum_{i=1}^{i=i_\xi} (\Delta l_Y)_i \kappa_i = (B_{R,\min} + \xi B_{R,\max}) / (b_R W_R), \\
& \kappa_i = 1, \quad i = 1, 2, \dots, i_\xi - 1, \\
& \kappa_{i_\xi} = \frac{(B_{\min} + \xi B_{\max}) / (b_R W_R) - \sum_{i=1}^{i=i_\xi-1} (\Delta l_Y)_i}{(\Delta l_Y)_{i_\xi}}, \\
& \kappa_i = 0, \quad i = i_\xi + 1, i_\xi + 2, \dots, N_e.
\end{aligned} \tag{10.19}$$

The final values of water uptake from soil cells precisely correspond to the transpiration rate:

$$u_i = \tilde{u}_i \kappa_i \tag{10.20}$$

where the weight coefficients  $\kappa_i$  provide for the equality between the sum of  $\tilde{u}_i$  and  $E_C$ :

$$\begin{aligned}
E_C &= \sum_{i=1}^{i=i_E} \tilde{u}_i \kappa_i, \\
\kappa_i &= 1, \quad i = 1, 2, \dots, i_E - 1, \\
\kappa_{i_E} &= \frac{E_C - \sum_{i=1}^{i=i_E-1} \tilde{u}_i}{\tilde{u}_{i_E}}, \\
\kappa_i &= 0, \quad i = i_E + 1, i_E + 2, \dots, N_e.
\end{aligned} \tag{10.21}$$

**13. Roots can grow into adjacent soil cells after their density in any one cell exceeds a threshold value.** Root growth occurs in the most favorable cells, and the total increment of new root mass is equal to  $(B_{R,\min} + \xi B_{R,\max}) \Delta t / b_R$ . Any increase in root mass in a cell that has a root mass above the threshold value,  $\rho_{R,T} A_s$ , is distributed between that cell and its neighbors in proportion

to the favorability for root growth in the new cells. The cells below the cell in question and on the side furthest from the plant have weights that determine whether the majority of root mass is distributed laterally or vertically. Potential root growth is proportional to the mass of existing roots in the given cell  $I$ :  $(\Delta m_R)_I = \alpha_M(m_R)_i \Delta t$ . The length of young roots in each cell decreases as they mature, and new roots may be added at the same time as new growth. New (young) root length is calculated as:

$$(\Delta l_Y)_I = -\alpha_Y(l_Y)_i \Delta t + (\Delta m_R)_I / W_R.$$

The decrease in length of young roots is reflected in the increase in length of mature roots:

$$(\Delta l_M)_I = \alpha_Y(l_Y)_i \Delta t / (A_s)_I.$$

#### **10.1.1 Data files '*Param\_R.dat*' and '*Nodal\_R.dat*'**

The parameters for this water uptake and root growth module are in the data file '**Param\_R.Dat**' and the description of the variables and file structure are in Table 10.1. The example listing of a file is in Example 10.1 that contains parameters for a soybean plant. For every soil cell, the initial root mass distribution and the numbers of neighboring soil cells are given in the file '**Nodal\_R.dat**'. The example listing in Example 10.2 corresponds to the grid in Fig. 3.1.

Table 10.1. Format of the file '**Param\_R.dat**'.

Record	Variable	Description
1,2	-	Comment lines.
3	<i>RRRM</i>	Radial resistance of old roots $R_{RM}$ in soil cell, bar·day·(cm root) $\cdot g^{-1}$ .
3	<i>RRRY</i>	Radial resistance of young roots $R_{RY}$ in soil cell, bar·day·(cm root) $\cdot g^{-1}$ .
3	<i>RVRL</i>	Vascular resistance $R_V$ per g of root between base of stem and soil cell, bar·day·(cm root) $\cdot g^{-1}$ .
4	-	Comment line.
5	<i>ALPM</i>	Potential relative old root growth rate $\alpha_M$ , day $^{-1}$ .
5	<i>ALPY</i>	Potential relative young root elongation rate $\alpha_Y$ , day $^{-1}$ .
5	<i>RTWL</i>	Average root dry weight per unit length $W_R$ , g·cm $^{-1}$ .
5	<i>RtMinWtPerUnitArea</i>	Threshold dry root mass $\rho_{RT}$ that must be present in a unit volume of soil cell before roots can grow into adjacent cells, g·cm $^{-3}$ .
6	-	Comment line.
7	<i>WI</i>	Weighting factor for the <u>left</u> adjacent cell to find the proportion of new roots proliferating to <u>cell</u> from given one.
7	<i>Wa</i>	Same as above for the <u>upper</u> adjacent cell.
7	<i>Wr</i>	Same as above for the <u>right</u> adjacent cell.
7	<i>Wr</i>	Same as above for the <u>lower</u> adjacent cell.
8	-	Comment line.
9	<i>BlkDn(1)</i>	Bulk density in the first soil layer, g cm $^{-3}$ .
9	<i>BlkDn(2)</i>	Same as above in the second layer.
.	.	.
9	<i>BlkDn(NMat)</i>	Same as above in the last layer.
10		Comment line

```
**** Example 10.1: WATER_UPTAKE01 PARAMETERS: FILE 'PARAM_R.DAT'
RRRM      RRRY      RVRL
167          313        7.3
ALPM       ALPY       RTWL      RtMinWtPerUnitArea
0.5           0.5        9.0E-05    9.0E-06
Wl         Wa         Wr         Wb
1.0         1.0        1.5        5.0
BlkDn (1)   BlkDn (2)     .....   BlkDn (Nmat)
1.4         1.35
END OF FILE 'PARAM_R.DAT'
```

Table 10.2. Grid information for Water\_Uptake01 module (file '**Nodal\_R.dat**').

Record	Variable	Description
1,2	-	Comment lines.
3	<i>e</i>	Number of soil cell (element)
3	<i>RTWT(e)</i>	Initial dry weight of roots in the soil cell <i>e</i> , g.
3	<i>iLeft</i>	Number of the left adjacent soil cell
3	<i>iUpper</i>	Number of the upper adjacent soil cell
3	<i>iRight</i>	Number of the right adjacent soil cell
3	<i>iLower</i>	Number of the lower adjacent soil cell

```
**** Example 10.2: WATER_UPTAKE01 GRID DATA: FILE 'NODAL_R.DAT'
e    RTWT    iLeft   iUpper   iRight  iLower
1     0        1       1       2       3
2     0        1       2       2       4
3    0.004     3       1       4       6
4     0        3       2       5       7
5     0        4       5       5       8
6     0        6       3       7       9
7     0        6       4       8      10
8     0        7       5       8      11
9     0        9       6      10      9
10    0        9       7      11     10
11    0       10      8      11     11
END OF FILE 'NODAL_R.DAT'
```

## 10.2 Plant status independent model: Water\_Uptake02

This model of root activity is essentially the same as that introduced by Feddes et al. (1978) with amendments from others (Wesseling and Brandyk, 1985; Vogel, 1987; Van Genuchten et al., 1992). This model does not take into account dynamic plant development and root growth in response to water deficits. This and similar models have been successfully used for grass canopies (Pachepsky and Zborishchuk, 1984). For a given soil cell, (element), the water uptake rate  $S$ , day<sup>-1</sup>, is equal to

$$S(h,x,z) = f_{str}(h) \ b_R(x,z) \ \frac{d_{Tr} E_c}{A} \quad (10.22)$$

where  $E_c$  is potential transpiration, cm day<sup>-1</sup>;  $d_{Tr}$  is the width of soil surface associated with transpiration, cm;  $b_R(x,z)$  is proportion of root mass in the soil cell at the elevation coordinate  $z$ , and lateral coordinate  $x$ ;  $A$  is the area of the soil cell, cm<sup>2</sup>;  $h$  is pressure head in the soil cell; and  $f_{str}$  is the water stress response function shown in Fig. 10.2. The water stress response function,  $f_{str}$ , depends on four parameters:  $h_0$ ,  $h_1$ ,  $h_2$ , and  $h_3$ . The parameters  $h_0$  and  $h_3$  are assumed constant,  $h_1$  depends on soil properties, and  $h_2$  depends on transpiration rate as:

$$\begin{aligned}
 h_2 &= h_{2,high} + (h_{2,low} - h_{2,high}) \frac{E_{c,high} - E_c}{E_{c,high} - E_{c,low}}, \quad E_{c,low} < E_c < E_{c,high} \\
 h_2 &= h_{2,high}, \quad E_c \geq E_{c,high} \\
 h_2 &= h_{2,low}, \quad E_c \leq E_{c,low}
 \end{aligned} \tag{10.23}$$

where  $E_{c,low}$ ,  $E_{c,high}$ ,  $h_{2,low}$ ,  $h_{2,high}$  are plant dependent parameters.

To estimate the order of magnitude and range of parameters, one may consider  $h_3 = -8000$  cm,

$E_{c,low} = 0.1$  cm/day,  $E_{c,high} = 0.5$  cm/day,

$h_{2,low} = -800$  cm,  $h_{2,high} = -200$  cm,  $h_l =$

25 cm, and  $h_0 = -10$  cm.

### 10.2.1 Data files '*Param\_U.dat*' and '*Nodal\_U.dat*'

The structures of the data files

'*Param\_U.dat*' and '*Nodal\_U.dat*'

are shown in Tables 10.3 and 10.4.

Listings of example files are in

Examples 10.3 and 10.4.

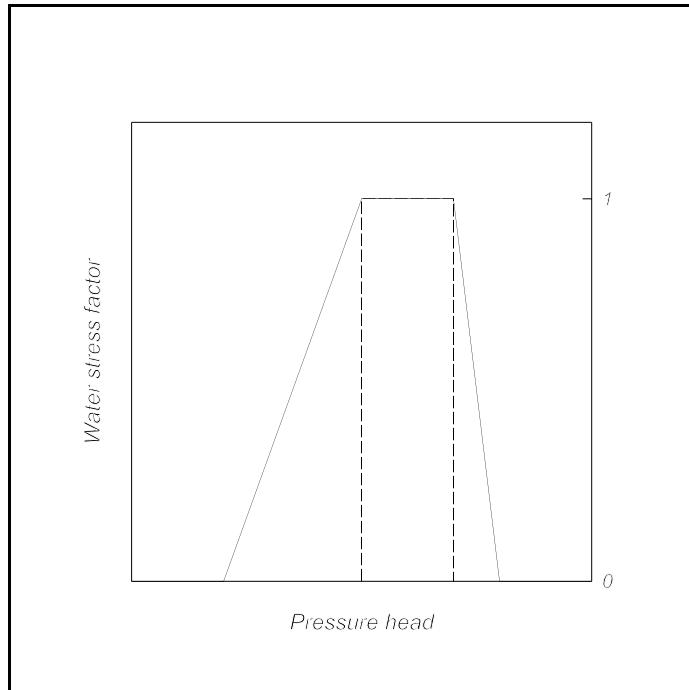


**Figure 10.2** Water stress response function as used by Feddes et al., 1978, and Šimůnek et al., 1992.

Table 10.3. Format of the file '**Param\_U.dat**'.

Record	Variable	Description
1,2	-	Comment lines.
3	$P_0$	Value of pressure head $h_0$ below which roots start to extract water from the soil, cm
3	$P_{2H}$	Value of the limiting pressure head $h_{2,high}$ , cm, below which the roots cannot extract water at the maximum rate (assuming a potential transpiration rate of $E_{c,high}$ ).
3	$P_{2L}$	Value of the limiting pressure head $h_{2,low}$ , cm, above which the roots can extract water only at the minimum rate (assuming a potential transpiration rate of $E_{c,low}$ ).
3	$P_3$	Value of the pressure head $h_3$ , cm, below which root water uptake ceases (usually wilting point).
3	$r_{2H}$	Critical potential transpiration rate $E_{c,high}$ , cm day <sup>-1</sup> .
3	$r_{2L}$	Critical potential transpiration rate $E_{c,low}$ , cm day <sup>-1</sup> .
4,5	-	Comment line.
6	$P_{optm}(1)$	Value of pressure head $h_1$ , cm, below which roots start to extract water at a maximum possible rate in soil material number 1.
6	$P_{optm}(2)$	As above for soil material # 2.
.	.	.
6	$P_{optm}(NMat)$	As above for soil material $NMat$

```
**** Example 10.3: WATER_UPTAKE_02 PARAMETERS : FILE 'PARAM_U.DAT'
P0=h0 * P2H=h2,high * P2L=h2,low * P3=h3 * r2H=Ec,high * r2L=Ec,low
-10.      -200.      -800.      -8000.      0.5      0.1
Soil material data
POptm(1)  POptm(2)  ....  POptm(NMat)
-25.      -40.0
END OF FILE 'PARAM_R.DAT'
```

Table 10.4. Format of the file '**Nodal\_R.dat**'.

Record	Variable	Description
1,2	-	Comment lines.
3	$n$	Element number.
3	$ROOTFR(n)$	Value of water uptake distribution $f_R(x,z)$ in soil root zone at element $n$ . $ROOTFR(n) = 0$ if element $n$ lies outside of the root zone. Record 3 is supplied for each elements where roots are present.

```
**** Example 10.4: WATER_UPTAKE_01 GRID DATA: FILE 'NODAL_R.DAT'
e    ROOTFR
2    0.27
3    0.73
END OF FILE 'NODAL_R.DAT'
```

### **10.3 A simple model of above ground plant growth, ShootImitator module**

**ShootImitator** is a very simple model of shoot and leaf development used in 2DSOIL for two purposes: (1) to supply necessary soil-atmosphere boundary information, and (2) to provide dynamic evapotranspiration for root water uptake modules. This particular module is provided as a place holder for a more comprehensive model of plant development when 2DSOIL is interfaced with a plant model. The module demonstrates what variables need to be shared, and allows 2DSOIL to be run before it is interfaced with a complete plant model.

The **ShootImitator** module uses a very simple model of CO<sub>2</sub> uptake as a function of light intensity. The model is taken from Acock et al. (1985) has the form of:

$$P_g = \frac{\alpha I \tau C}{\alpha I + \tau C}$$

Here P<sub>g</sub> is gross photosynthetic rate (mg CO<sub>2</sub> m<sup>-2</sup> s<sup>-1</sup>), C is carbon dioxide concentration (350 L L<sup>-1</sup>),  $\alpha$ , and  $\tau$  are constants ( $\alpha= 3.25 \mu\text{g CO}_2 \mu\text{mol}^{-1}$  photons, and  $\tau=5.69 \text{mm s}^{-1}$ ). It is assumed that 60% of the carbon actually becomes plant matter. A light partitioning coefficient is used to adjust for the amount of photosynthetically active light intercepted by the canopy. The time-dependent variables are calculated according as:

$$\begin{aligned}
\frac{dH_c}{dt} &= \begin{cases} 0.71 \frac{B_V}{B_{V,\max}} & t_{gr} < 75 \\ 0.1 \frac{B_V}{B_{V,\max}} & t_{gr} > 75 \end{cases} \\
\frac{dA_L}{dt} &= \begin{cases} 0.08H_c & t_{gr} < 75 \\ 0.01H_c & t_{gr} > 75 \end{cases} \\
\frac{B_V}{B_{V,\max}} &= \begin{cases} 1, & \Psi_s^a > -1 \\ \frac{8 + \Psi_s^a}{7}, & -8 < \Psi_s^a \leq -1 \\ 0, & \Psi_s^a \leq -8 \end{cases} \quad f_{CPR} = \begin{cases} 0.85 - 0.01t_{gr}, & t_{gr} \leq 60 \\ 0.2, & t_{gr} > 60 \end{cases} \\
B_{R,\max} &= 0.95B_V N_p, \quad B_{R,\min} = f_{CPR} B_V N_p, \quad b_R = 0.65N_{S/D} + 0.48(1 - N_{S/D}) \\
N_{fract} &= \begin{cases} 0.05 - 0.000533t_{gr} & t_{gr} \leq 75 \\ 0.01 & t_{gr} > 75 \end{cases} \\
N_{S/D} &= \frac{N_{upt}}{N_{fract} \times B_V \times 1.67}
\end{aligned}$$

(10.25)

Here,  $H_c$  is plant height (cm),  $A_L$  is total plant leaf area ( $\text{cm}^2$ ),  $B_{R,\min}$  is the rate of carbon supply to roots after satisfying shoot demand ( $\text{g plant}^{-1}$  per half soil slab),  $B_{R,\max}$  is the rate of carbon supply to roots when shoot growth ceases,  $b_R$  is mass of carbon per unit of root dry mass,  $t_{gr}$  is time counted after emergence,  $\Psi_s^a$  is average soil potential in root-inhabited soil cells, bars;  $f_{CPR}$  is the proportion of carbon supply partitioned to root;  $N_p$  is the number of plants per meter of row;  $N_{S/D}$  is the nitrogen supply/demand ratio of the plant (set equal to 1 if there is no nitrogen

module), and  $N_{\text{frac}}$  is the fraction of N in plant tissues. We assume that 60% of the total plant tissue is carbon. Carbon for root growth is partitioned as a function of time after emergence. Initially 85% of the carbon fixed goes to the roots. This amount decreases by 1% each 24 hour period until it reaches a minimum of 2%. The plant is also sensitive to nitrogen deficiency. The nitrogen demand is high early in the season and falls as the plant reaches maturity. The initial nitrogen demand assumes the plant must maintain a nitrogen concentration of 5%. This will decrease linearly to 1% as the plant reaches maturity ( $t_{\text{gr}}=75$ ). A weighting factor ( $N_{\text{S/D}}$ ) based on the ratio of actual N uptake to desired N uptake is calculated and used to adjust the shoot growth rate. The ratio is based on cumulative nitrogen uptake to allow the plant to store excess N.

Both soil-root surfaces and soil atmosphere surfaces are controlled by several plant status variables that are listed in Table 10.5. These are public variables in the plant block. These variables are defined by the **ShootImitator** and used by the **SetSurf** and **WaterUptake** modules. The public variables that are supplied by **ShootImitator** include the time-dependent values of  $H_c$ ,  $A_L$ ,  $B_{R,\text{min}}$ ,  $B_{R,\text{max}}$ , and  $b_R$ . **ShootImitator** also supplies some constant parameters such as geometrical parameters of the canopy that include: position of the stem base, row spacing, number of plants per 1 meter of a row, row orientation, and the canopy extinction coefficient.

Table 10.5. Public information that interfaces the ShootImitator (SI) module with the SetSurf02 (SS2), SetSurf01 (SS1), and WatUp01 (WU1) modules.

Variable	Meaning	Usage			
		SI	SS2	SS1	WU1
ITIME	Number of the current hour counting from midnight		P		U
IDAWN	Hour number when dawn occurs		P		U
IDUSK	Hour number of dusk occurs		P		U
xBSTEM	Horizontal coordinate of the stem base, cm	P	U	U	U
yBSTEM	Vertical coordinate of the stem base, cm	P			U
CONVR	Amount of carbon needed to make unit dry weight of root, g g <sup>-1</sup>	P			U

Variable	Meaning	Usage			
		SI	SS2	SS1	WU1
PCRL	rate at which carbon would be supplied to growing roots in a soil slab if all potential shoot growth had been satisfied, g per day per half soil slab	P			U
PCRQ	rate at which carbon would be supplied to growing roots in a soil slab if all translocated carbon went to roots, g per day per half soil slab	P			U
SGT	proportion of time for which shoot grows: limited by shoot turgor or carbon availability	U			P
PSIM	Average soil suction in soil cells with roots, bars	U			P
LAREAT	total leaf area per plant, cm <sup>2</sup>	P	U		
HEIGHT	Height of the plant, cm	P	U	U	
POPROW	plant population per meter of row	P			U
ROWSP	Row spacing, cm	P	U		
ROWANG	row orientation measured eastward from North, degrees	P	U		
VEGSRC	net mean carbon production per plant per day (g).	P			
CEC	Canopy extinction coefficient				
Nitrogen_t	Cumulative nitrogen uptake, g per plant	U			P

\* 'P' means that the value of a variable is produced by the module, 'U' means that the value of a variable is used by the module.

Table 10.6 Variables output by ShootImitator in the file 'Plant.out'

Variable	Description
Height	Plant Height, cm
Lareat	Total Leaf area per plant, cm <sup>3</sup>
Total_eor	Total water use per plant, g
Total_pcrs	Total amount of carbon actually used to grow roots, g
Cover	Leaf cover, %
Carbon_t	Cumulative net carbon use in the above ground part of the plant, g
PCarbon_t	Potential carbon production per plant, g
UCarbon_t	Cumulative carbon production in entire plant, g

Nitrogen_t	Cumulative nitrogen uptake, g per plant
NDef	Ratio of nitrogen requirement to nitrogen taken up
Psim	Average matric potential in the elements with roots, bars
Sgt_m	Daily mean of SGT

### 10.3.1 The data file 'Param\_p.dat'

The parameters needed by the **ShootImitator** are read from the data file '**Param\_p.dat**'.

The structure of the file is listed in Table 10.6 followed by a listing of a file as an example.

Table 10.6. Format of the file '**Param\_p.dat**'.

Record	Variable	Description
1,2	-	Comment lines.
3	POPROW	Plant population per meter of row.
3	ROWSP	Row spacing, cm.
3	ROWANG	Row orientation measured eastward from north, degrees.
3	xBSTEM	Horizontal coordinate of the stem base, cm.
3	yBSTEM	Vertical coordinate of the stem base, cm.
3	VEGSRC	net mean carbon production per plant per day (g). This variable is only used in Shootimitator3 which does not require values of radiation.
3	CEC	Canopy extinction coefficient.

\*\*\* Example 10.5: Shoot imitator data - file 'Param\_p.dat'.

```
POPROW  ROWSP  ROWANG  xBSTEM    yBSTEM    VEGSRC  CEC
14      50     140      25       60.      2.14     0.55
END OF FILE 'PARAM_P.DAT'
```

### 10.4 Interfacing 2DSOIL with a crop model

This section is included to demonstrate how 2DSOIL can be interfaced with plant shoot models. To interface 2DSOIL with a crop model, the crop modeler needs to concentrate only on the boundary interface. The modeler must (a) assign potential boundary fluxes of water, solutes, heat and gases from their atmosphere module to the nodal boundary fluxes, (b) receive actual

boundary flux values from the water transport module and use them as needed, (c) pass potential transpiration and carbon flux values from the plant module to the root module, (d) receive actual transpiration, water and nutrient fluxes from the root module and use them as needed, and (e) provide simulated times when the plant and atmosphere modules will be ready to exchange information. All variables needed for this exchange are global public variables, and no code has to be changed in the other modules of the soil simulator. If some other soil variables are needed by the plant and atmosphere components, they are accessible through the global COMMON block since all global public data for the boundary interface are available there. If some private root variables are needed by the shoot module, they can be made accessible by inserting a local public COMMON block of the root module into the boundary interface. Finally, if the crop modeler wants to use their own root module, the module must be rearranged to fit into the data structure of the design described here.



# Chapter 11: Intrasoil Chemical Reactions: *MacroChem*

## Module

**Yakov Pachepsky**

The soil chemistry of  $Ca^{2+}$ ,  $Mg^{2+}$ ,  $Na^+$ ,  $H^+$ ,  $Cl^-$ ,  $SO_4^{2-}$ , strongly influences the chemical and physical environment for nitrogen transformation, and degradation of xenobiotics in soils of some geographic areas . Furthermore, the long-term application of the same management practices shifts the potential equilibria among macro elements. Though chemical equilibrium is not generally attainable in field soils, soil chemical systems oscillate near equilibrium states and always tend to equilibrium. Therefore, shifts in potential equilibria lead to shifts in the environmental conditions for root activity and for chemical movement/transformation in soils. The macro element equilibria chemistry module in the 2DSOIL model describes a system of interphase chemical interactions that include dissolution-precipitation of gypsum and calcite, Ca-Mg-Na cation exchange, formation of ion pairs in solution, and dissolution of gaseous  $CO_2$ . The mathematical model was described elsewhere (Pachepsky and Platonova, 1988; Pachepsky. 1990).

### **11.1 Model of chemical interactions**

**Basic assumptions.** The chemistry of nine ions in the soil solution are simulated ( $Ca^{2+}$ ,  $Mg^{2+}$ ,  $Na^+$ ,  $H^+$ ,  $Cl^-$ ,  $SO_4^{2-}$ ,  $CO_3^{2-}$ ,  $HCO_3^-$ ,  $OH^-$ ), as well as the ion pairs formed by these ions ( $CaCO_3^0$ ,  $MgCO_3^0$ ,  $NaCO_3^-$ ,  $CaSO_4^0$ ,  $MgSO_4^0$ ,  $NaSO_4^-$ ,  $CaHCO_3^+$ ,  $MgHCO_3^+$ ,  $NaHCO_3^0$ ,  $CaOH^+$ , and  $MgOH^+$ ). The ion-exchange phase contains  $Ca^{2+}$ ,  $Mg^{2+}$ , and  $Na^+$ . The sum of these three ions is considered to be the cation exchange capacity (CEC), and this sum depends only on position in the soil profile, not on the chemical content. A solid salt phase, gypsum or calcite, may be also be present. The carbonate-hydrogen system is controlled by the partial pressure of  $CO_2$  in the soil air, which also depends on position in the soil profile. The following processes are taken into

consideration: 1) association of ions in the soil solutions; 2) transfers of  $CO_2$  to and from the soil air; 3) dissociation of carbonic acid and water; 4) ion exchanges between  $Na-Ca$  and  $Na-Mg$ ; 5) solution-precipitation of gypsum and calcite; and 6) electrostatic redistribution of ions, which leads to the formation of an exclusion volume free of anions.

The following symbols are used. The letter  $m$  indicates the concentration of an ion or an ion pair in the soil solution in mol L<sup>-1</sup>. Thus,  $m_{Ca}$  is the concentration of free (i.e., not bound in ion pairs)  $Ca^{2+}$ ;  $m_{CaHCO_3^+}$  is the concentration of the ion pair  $CaHCO_3^+$ , and so on. The total analytical concentrations of ions in solution, including their concentration in ion pairs, are symbolized with  $m'$ :  $m'_{Ca}$ ,  $m'_{Mg}$ , etc. The concentration (mol L<sup>-1</sup> of soil) of cations in the soil adsorption complex is symbolized by  $s_{Ca}$ ,  $s_{Mg}$ , and  $s_{Na}$ . The concentrations of gypsum and calcite,  $M_{Gyps}$  and  $M_{Calc}$ , are measured in mol L<sup>-1</sup> of soil for  $CaSO_4$  and  $CaCO_3$ , respectively. The total masses of ions in the liquid, solid, salt, and cation-exchange phases are symbolized by  $M_{Ca}$ ,  $M_{Mg}$ ,  $M_{SO_4}$ , and  $M_{Cl}$ , mol L<sup>-1</sup> of soil. The partial pressure of  $CO_2$  in the soil air is symbolized by  $P_{CO_2}$ , atm, the cation-exchange capacity by CEC, eq L<sup>-1</sup>, and the ionic strength of the soil solution by  $i$ . The soil moisture content is denoted by  $\theta$ , cm<sup>3</sup> of soil solution per cm<sup>3</sup> of soil;  $\theta_1$  is the volumetric moisture content minus the exclusion volume. Other symbols are given as used in the text.

### 11.1.1 Equilibrium relationships.

The major relationships and values for the various constants are given below. The model consists of several groups of equations that are responsible for different processes.

Mass conservation in the system:

$$\begin{aligned} M_{Ca} &= \theta_1 m_{Ca} + s_{Ca} + M_{Gyps} + M_{Calc}; \\ M_{Mg} &= \theta_1 m_{Mg} + s_{Mg}; \\ M_{Na} &= \theta_1 m_{Na} + s_{Na}; \\ M_{Cl} &= \theta_1 m_{Cl}; \\ M_{SO_4} &= \theta_1 m_{SO_4} + M_{Gyps}; \end{aligned} \tag{11.1}$$

Mass conservation in the solution:

$$\begin{aligned}
 m'_{Ca} &= m_{Ca} + m_{CaCO_3^0} + m_{CaHCO_3^+} + m_{CaSO_4^0} + m_{CaOH^-}; \\
 m'_{Mg} &= m_{Mg} + m_{MgCO_3^0} + m_{MgCO_3^+} + m_{MgSO_4^0} + m_{MgOH^+}; \\
 m'_{Na} &= m_{Na} + m_{NaCO_3^-} + m_{NaHCO_3^0} + m_{NaSO_4^-}; \\
 m'_{Cl} &= m_{Cl}; \quad m'_{H} = m_H; \quad m'_{OH} = m_{OH} + m_{CaOH^+} + m_{MgOH^+}; \\
 m'_{SO_4} &= m_{SO_4^0} + m_{CaSO_4^0} + m_{MgSO_4^0} + m_{NaSO_4^-}; \\
 m'_{CO_3} &= m_{CO_3^0} + m_{CaCO_3^0} + m_{MgCO_3^0} + m_{NaCO_3^-}; \\
 m'_{HCO_3} &= m_{HCO_3^-} + m_{CaHCO_3^-} + m_{MgHCO_3^-} + m_{NaHCO_3^0};
 \end{aligned} \tag{11.2}$$

Activity of ions in solution:

$$\begin{aligned}
 a_{Ca} &= \gamma_1^4 m_{Ca}; \quad a_{Mg} = \gamma_1^4 m_{Mg}; \quad a_{Na} = \gamma_1 m_{Na}; \\
 a_{Cl} &= \gamma_1 m_{Cl}; \quad a_{SO_4} = \gamma_1^4 m_{SO_4^0}; \quad a_H = \gamma_1 m_H; \\
 a_{OH} &= \gamma_1 m_{OH}; \quad a_{HCO_3} = \gamma_1 m_{HCO_3^-}; \quad a_{CO_3} = \gamma_1^4 m_{CO_3^0};
 \end{aligned} \tag{11.3}$$

Activity coefficient of a monovalent ion:

$$\gamma_1 = 10^{-\left(\frac{R_6\sqrt{I_e}}{1+R_7\sqrt{I_e}} - R_8 I_e\right)} \tag{11.4}$$

Effective ionic strength:

$$\begin{aligned}
 I_e &= \frac{1}{2} [(m_{Ca} + m_{Mg} + m_{CO_3^0} + m_{SO_4^0})^4 + m_{Na} + m_{Cl} \\
 &\quad + m_H + m_{OH} + m_{CaHCO_3^+} + m_{MgHCO_3^+} + m_{NaCO_3^-} + m_{NaSO_4^-}]
 \end{aligned} \tag{11.5}$$

Activity of ion pairs:

$$\begin{aligned}
 a_{CaCO_3^0} &= m_{CaCO_3^0}; \\
 a_{MgCO_3^0} &= m_{MgCO_3^0}; \\
 a_{CaHCO_3^+} &= m_{CaHCO_3^+} \gamma_1 \cdot 10^{-R_{11}I_e}; \\
 a_{MgHCO_3^+} &= m_{MgHCO_3^+} \gamma_1 \cdot 10^{-R_{12}I_e}; \\
 a_{CaSO_4^0} &= m_{CaSO_4^0} \gamma_1 \cdot 10^{-R_{13}I_e}; \\
 a_{MgSO_4^0} &= m_{MgSO_4^0}; \\
 a_{NaSO_4^-} &= m_{NaSO_4^-} \gamma_1 \cdot 10^{-R_{14}I_e}; \\
 a_{NaCO_3^-} &= m_{NaCO_3^-} \gamma_1 \cdot 10^{-R_{15}I_e}; \\
 a_{NaHCO_3^0} &= m_{NaHCO_3^0}; \\
 a_{CaOH^+} &= \gamma_1 m_{CaOH^+}; \\
 a_{MgOH^+} &= \gamma_1 m_{MgOH^+}; 
 \end{aligned} \tag{11.6}$$

Stability of ion pairs:

$$\begin{aligned}
 R_{21} a_{CaCO_3^0} &= a_{Ca} a_{CO_3}; R_{22} a_{MgCO_3^0} = a_{Mg} a_{CO_3}; \\
 R_{23} a_{NaCO_3^-} &= a_{Na} a_{CO_3}; R_{24} a_{CaSO_4^0} = a_{Ca} a_{SO_4}; \\
 R_{25} a_{MgSO_4^0} &= a_{Mg} a_{SO_4}; R_{26} a_{NaSO_4^-} = a_{Na} a_{SO_4}; \\
 R_{27} a_{CaHCO_3^+} &= a_{Ca} a_{HCO_3}; R_{30} a_{CaOH^+} = a_{Ca} a_{OH^+}; \\
 R_{28} a_{MgHCO_3^+} &= a_{Mg} a_{HCO_3}; R_{31} a_{MgOH^+} = a_{Mg} a_{OH^+}; \\
 R_{29} a_{NaHCO_3^0} &= a_{Na} a_{HCO_3}; 
 \end{aligned} \tag{11.7}$$

Components of the carbonate system:

$$\begin{aligned}
 R_0 P_{CO_2} &= m_{H_2CO_3}; R_1 m_{H_2CO_3} = a_H a_{HCO_3}; \\
 R_2 a_{HCO_3} &= a_H a_{CO_3}; R_3 = a_H a_{OH}
 \end{aligned} \tag{11.8}$$

Solubility:

$$\begin{aligned} a_{Ca} \quad a_{SO_4} &\leq R_4 \\ a_{Ca} \quad a_{CO_3} &\leq R_5 \end{aligned} \quad (11.9)$$

Electroneutrality:

$$\begin{aligned} 2(m'_{Ca} + m'_{Mg}) + m'_{Na} + m'_{H} = 2(m'_{SO_4} + m'_{CO_3}) \\ + m'_{OH} + m'_{Cl} + m'_{HCO_3}; \quad 2(s_{Ca} + s_{Mg}) + s_{Na} = EKO \end{aligned} \quad (11.10)$$

Exchangeable cations:

$$\frac{s_{Na}}{s_{Ca}} = \kappa_1 \frac{a_{Na}}{\sqrt{a_{Mg}}}; \quad \frac{s_{Na}}{s_{Mg}} = \kappa_2 \frac{a_{Na}}{\sqrt{a_{Mg}}} \quad (11.11)$$

Values of constants:

$PR_0 = 10^{2.47}$	$R_6 = 0.510$	$R_{14} = 0.42$	$PR_{25} = 2.36$
$PR_1 = 10^{6.35}$	$R_7 = 1.532$	$R_{15} = 0.21$	$PR_{26} = 0.42$
$PR_2 = 10^{10.32}$	$R_8 = 0.033$	$PR_{21} = 3.20$	$PR_{27} = 0.76$
$PR_3 = 10^{14.00}$	$R_{11} = 0.870$	$PR_{22} = 3.40$	$PR_{28} = 0.78$
$PR_4 = 10^{4.62}$	$R_{12} = 0.150$	$PR_{23} = 0.36$	$PR_{29} = -0.25$
$PR_5 = 10^{8.31}$	$R_{13} = 0.330$	$PR_{24} = 2.31$	$PR_{30} = -1.40$
$PR_{31} = 10^{-2.60}$			

The relationships in Eq. 11.1 to 11.11 allow one to use concentrations of  $Ca^{2+}$ ,  $Mg^{2+}$ ,  $Na^+$ ,  $Cl^+$ , and  $SO_4^{2-}$  in a volume of soil and the values for  $\theta_1$ ,  $P_{CO_2}$ , and CEC to find the distribution of ions among the soil solution, the ion-exchange phase, and the solid salt phases of the soil. All of the relationships in the model have been tested against measured data (Lindsay, 1979; Pachepsky, 1990).

The use of thermodynamic equations is advantageous as the majority of model parameters do not depend on the amounts of ions and salts in soils. Only selectivity coefficients of cation exchange are a function of soil composition (Bolt, 1982).

### **11.1.2 The computer code of the chemical equilibrium model.**

This code, LIBRA (Platonova and Pachepsky, 1988), calculates activities of ions in soil solutions and determines the concentration of ion pairs, estimates the degree of saturation with respect to gypsum and calcite of soil solutions and their solubility, calculates the relative abundance of carbonate- and bicarbonate-ions in soil solutions, evaluates the effect of applying gypsum to the soil on the compositions of the phases. LIBRA can be used to plan experiments to study cation-exchange equilibria in soils, evaluate the effect of soil moisture on the compositions of the phases, and find the composition of the soil solutions using data on the composition of water extracts. The model can also be used to predict changes in the composition of soil phases as a function of quality of input water.

The values of selectivity coefficients of cation exchange  $\kappa_1$  and  $\kappa_2$  are not, generally speaking, constant. The most important parameter that determines their values in soils of the arid zone is the effective ionic strength of the solution  $I_e$ , although at high organic-matter contents the proportion of  $Na^+$  in the sum of exchange cations is also highly significant.

The **MacroChem** module is based on the LIBRA code. This module is used to calculate redistribution of ions between soil phases at nodal points after every step of water and solute movement. This module, as implemented in 2DSOIL, operates at present with five solutes. These are ions of  $Ca^{2+}$ ,  $Mg^{2+}$ ,  $Na^+$ ,  $SO_4^{2-}$ ,  $Cl^-$ . Concentrations of these solutes are included in the list of public variables. The **MacroChem** module also calculates pH of the soil solution, contents of exchangeable cations, solid gypsum and calcite, ion pairs in solution, and concentrations of bicarbonate and carbonate ions. These values are currently included in the private information of the module. If these values will be required in calculations for plant development or soil processes, they can readily be transferred to the public domain.

## 11.2 Input files '**Param\_E.dat**' and '**Nodal\_E.dat**'

The number of parameters in the LIBRA model is not large because thermodynamic equations are used. The parameters are read from the '**Param\_E.dat**' data file (Table 11.1). The input data include factors for adjusting units. The factors *ExchUnitCa*, *ExchUnitMg*, and *ExchUnitNa* are equal to the amounts of exchangeable cations in mol·kg<sup>-1</sup> soil divided by those amounts in units used in the '**Param\_E.dat**' data file. The factors *SolidUnitGypsum* and *SolidUnitCalcite* are equal to the moles of *CaSO<sub>4</sub>* and *CaCO<sub>3</sub>* in solid salts per kg<sup>-1</sup> soil, divided by these amounts in units used in the '**Param\_E.dat**' data file. The factors *ConcUnitCa*, *ConcUnitMg*, *ConcUnitNa*, *ConcUnitSO4*, and *ConcUnitCl* are equal to the amounts of ions in mol·L<sup>-1</sup> divided by the amounts in units used in the '**Param\_E.dat**' data file. Example 11.1 following Table 11.1 contains the factors mentioned above for the case when the amounts of exchangeable cations have been measured in meq/kg of soil, the gypsum and calcite contents in g of solid salt per g of soil, and the concentrations in the solution in meq per L.

The initial distribution of exchangeable cations and solid salts is read from the file '**Param\_E.dat**'. Table 11.2 shows the contents of this file. In Example 11.2 following the table, exchangeable cations are in meq/kg of soil and solid salt contents are in g salt per g dry soil.

Table 11.1. Format for the file 'Param\_E.dat'.

Record	Variable	Description
1,3	-	Comment lines.
4	<i>ExchUnitCa</i>	Factor for changing exchangeable $\text{Ca}^{2+}$ units.
4	<i>ExchUnitMg</i>	Same as above for exchangeable $\text{Mg}^{2+}$ .
4	<i>ExchUnitNa</i>	Same as above for exchangeable $\text{Na}^+$ .
5	-	Comment line.
6	<i>SolidUnitGypsum</i>	Factor for changing gypsum content units.
6	<i>SolidUnitCalcite</i>	Same as above for calcite.
7	-	Comment line.
8	<i>ConcUnitCa</i>	Factor for changing units of $\text{Ca}^{2+}$ concentration.
8	<i>ConcUnitMg</i>	Same as above for $\text{Mg}^{2+}$ .
8	<i>ConcUnitNa</i>	Same as above for $\text{Na}^+$ .
8	<i>ConcUnitSO4</i>	Same as above for $\text{SO}_4^{2-}$ .
8	<i>ConcUnitCl</i>	Same as above for $\text{Cl}^-$ .
9,10	-	Comment lines.
11	<i>BulkDn(1)</i>	Bulk density of soil material in subdomain #1, g $\text{cm}^{-3}$ .
11	<i>BulkDn(2)</i>	Same as above for soil material in subdomain #2.
11	.....	.....
11	<i>BulkDn(NMat)</i>	Same as above for soil material in subdomain <i>NMat</i> .
12	-	Comment line.
13	<i>SelCoefCaNa(1)</i>	Selectivity coefficient of cation exchange Ca - Na on soil material 1 for the Gaines-Thomas isotherm equation, $(\text{mol/L})^{-\frac{1}{2}}$ .
13	<i>SelCoefCaNa(2)</i>	Same as above for soil material in subdomain #2.
13	.....	.....
13	<i>SelCoefCaNa(NMat)</i>	Same as above for soil material in subdomain <i>NMat</i> .
14	-	Comment line.
15	<i>SelCoefMgNa(1)</i>	Selectivity coefficient of cation exchange Mg-Na on soil material 1 for the Gaines-Thomas isotherm equation, $(\text{mol/L})^{-\frac{1}{2}}$ .
15	<i>SelCoefMgNa(2)</i>	Same as above for soil material in subdomain #2.
15	.....	.....
15	<i>SelCoefMgNa(NMat)</i>	Same as above for soil material in subdomain <i>NMat</i> .

```
*** Example 11.1: MACROCHEM PARAMETERS: file 'Param_E.in'
Conversion factors to recalculate original units into mol/kg soil
ExchUnitCa      ExchUnit Mg      ExchUnitNa (from eq/kg)
  0.5            0.5            1.0
SolidunitGypsum SolidUnitCalcite (from kg/kg soil)
  5.814          10.0
ConcUnitCa ConcUnitMg ConcUnitNa ConcUnitSO4 ConcUnitCl (from meq/l)
  5.0E-04        5.0E-04       1.0E-03     5.0E-04      1.0E-03
Soil material parameters in subdomains
BulkDn Mat # 1 (Bulk density, g/cc)
  1.4
SelCoefCaNa Mat # 1
  0.6
SelCoefMgNa Mat # 1
  0.7
END OF FILE 'PARAM_E.DAT'
```

Table 11.2. Format for the file '**Nodal\_E.dat**'.

Record	Variable	Description
1,2	-	Comment line.
3	<i>n</i>	Nodal number.
3	<i>ExchCa(n)</i>	Initial value of the exchangeable Ca content at node <i>n</i> .
3	<i>ExchMg(n)</i>	Same as above for Mg.
3	<i>ExchNa(n)</i>	Same as above for Na.
3	<i>GypsumNod(n)</i>	Initial value of solid gypsum content at node <i>n</i> .
3	<i>CalciteNod(n)</i>	Same as above for calcite.
3	<i>PCO2Nod(n)</i>	Carbon dioxide partial pressure in the soil air, atm. Leave blank if gas movement is included in current simulation.

Record 3 information is required for each node.

```
*** Example 11.2: MACROCHEM MODULE SOLID PHASE DATA: FILE NODAL_E
n    ExchCa  ExchMg  ExchNa GypsumNod CalciteNod PCO2Nod
1    0.07    0.05    0.02   0.05     0.05     0.06
.    ...     ...     ...    ..       .       ...
11   0.05    0.04    0.02   0.08     0.05     0.032
```



# Chapter 12: Nitrogen Transformation in Soil: *Soilnitrogen* Module

**Yakov Pachepsky and Dennis Timlin**

The area of nitrogen transformations in soils is important in agricultural modeling and many models have been developed. We have chosen to use the model SOILN that was developed by Johnsson et al. (1987). Recent comparisons of the performance of this model with others have shown that it simulates soil nitrogen transformation with similar accuracy or better than comparable models (de Willingen, 1991; Jabro et al., 1993).

## **12.1 Model of nitrogen transformation**

An illustration of the nitrogen pools and associated fluxes in the module **SOILNITROGEN** is shown in Fig. 12.1. Three organic pools are distinguished as:

- ▶ a fast cycling organic pool that includes plant residues and represents the organic residue-microbial biomass complex,
- ▶ a slow cycling organic pool that includes humus and represents stabilized decomposition products, and
- ▶ an organic fertilizer pool that is used for organic amendments if their chemical composition differs significantly from the composition of a plant residue pool.

State variables of the model are:

$N_h$  - elemental nitrogen (N) content in humus, mg L<sup>-3</sup>,

$C_h$  - elemental carbon (C) content in humus, mg L<sup>-3</sup>,

$N_L$  - elemental nitrogen content in the plant residues, mg L<sup>-3</sup>,

$C_L$  - elemental carbon content in the plant residues, mg L<sup>-3</sup>,

$N_m$  - elemental nitrogen content in the organic fertilizer, mg L<sup>-3</sup>,

$C_m$  - elemental carbon content in the organic fertilizer, mg L<sup>-3</sup>,

$N_{NH_4}$  - elemental mineral ammonium content in soil, mg L<sup>-3</sup>

$c_{NO_3}$  concentration of nitrate ions in the soil solution, mg L<sup>-3</sup>

All mineral ammonium is assumed to be immobile with respect to leaching whereas nitrate ions are present only in the soil solution. The following is a description of how the fluxes,  $Q_1$  -  $Q_{15}$  shown in Fig. 12.1, are calculated.

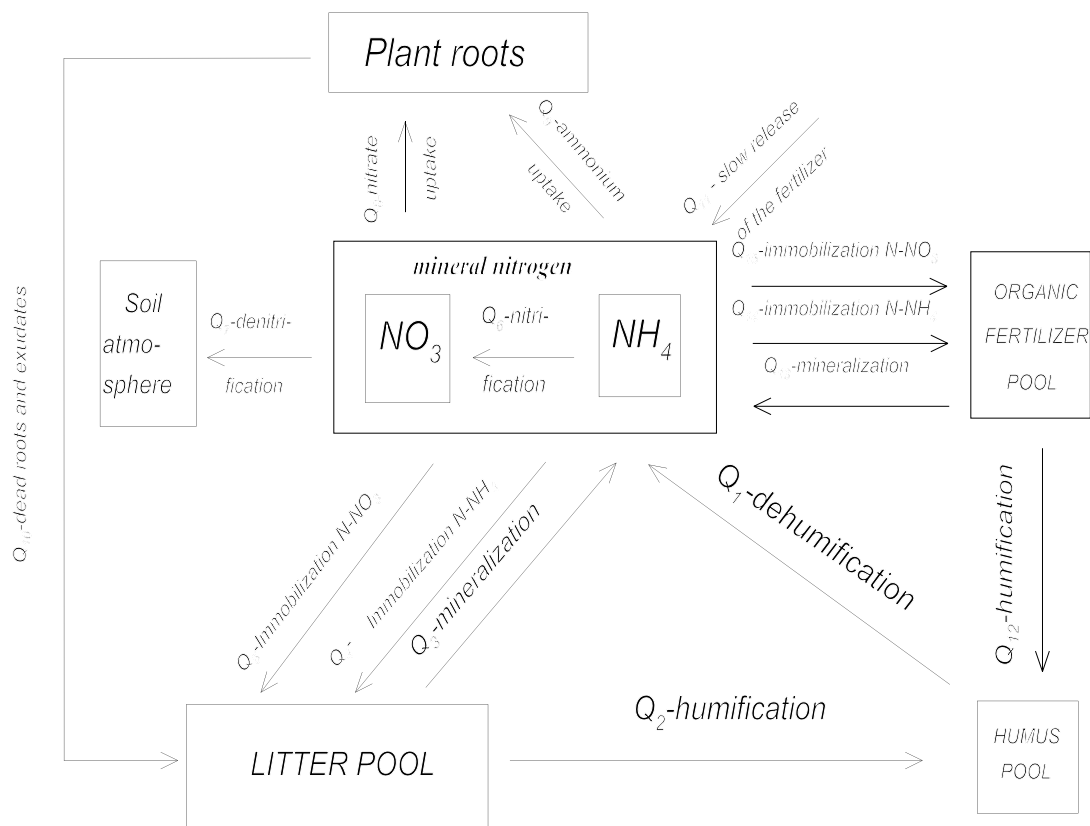


**Figure 12.1** Illustration of nitrogen pools and fluxes in the model **SOILN**

**1) The mineralization of N from stable soil organic matter ( $Q_1$ ).** The rate of nitrogen release from soil organic matter is proportional to amount of nitrogen in the organic matter:

$$Q_1 = k_h e_\theta e_T N_h \quad (12.1)$$

The rate constant is a product of the potential mineralization rate constant  $k_h$  and the rate correction factors  $e_\theta$  and  $e_T$ . The potential mineralization rate constant is valid at optimal water content and temperature. The correction factor for water,  $e_\theta$ , adjusts for deviations of soil water content from optimal; the temperature correction,  $e_T$ , adjusts for deviations of the soil temperature from optimal. The same rate constant in equation 12.1 is also used to calculate the rate,  $P_1$ , of carbon release from organic matter as:

$$P_1 = k_h e_\theta e_T C_h \quad (12.2)$$

**2) Immobilization in the stable humus pool of N and C from plant residues ( $Q_2$ ) and organic fertilizer ( $Q_{12}$ ).** The amount of nitrogen immobilized in the stable humus pool during the decomposition of plant residue is proportional to the amount of carbon transferred to the stable humus pool according to the C/N ratio of microorganisms,  $r_0$ :

$$Q_2 = \frac{P_2}{r_0} \quad (12.3)$$

Here  $P_2$  is the rate of carbon transfer from plant residues to humus. The rate,  $P_2$ , is proportional to the amount of carbon in plant residues and is calculated as:

$$P_2 = k_L e_\theta e_T f_e f_h C_L \quad (12.4)$$

The rate constant is a product of the rate constant for optimal conditions  $k_L$ , the correction factors for water and temperature,  $e_\theta$  and  $e_T$ , the proportion of carbon retained in soil after respiration  $f_e$  (microbial synthesis efficiency constant), and the proportion of carbon transferred to humus  $f_h$ .

The amounts of nitrogen and carbon from organic fertilizer immobilized in humus during the decomposition of organic fertilizer is calculated as:

$$Q_{12} = \frac{P_{12}}{r_0} \quad (12.5)$$

$$P_{12} = k_m e_\theta e_T f_e f_h C_m \quad (12.6)$$

Here  $P_{12}$  is the rate of carbon transfer from organic fertilizer to organic matter. The rate constant in (12.6) includes the potential rate constant for the decomposition of organic fertilizer,  $k_m$  and correction factors for soil water content and temperature.

**3) The mineralization of N and C from plant residues ( $Q_3$ ) and organic fertilizer ( $Q_{13}$ ).** The rate of nitrogen release from plant residues is proportional to the rate of the carbon release:

$$Q_3 = \frac{N_L}{C_L} P_3 \quad (12.7)$$

Here  $P_3$  is the rate of carbon release from plant residues. This rate is proportional to the carbon content in plant residues:

$$P_3 = k_L e_\theta e_T C_L \quad (12.8)$$

where the potential rate constant  $k_L$ , and correction factors  $e_\theta$  and  $e_T$  are the same as in (12.4). The decomposition of organic fertilizer is handled in the same manner as the decomposition of plant residues. The mineralization rate of N from organic fertilizer is calculated as:

$$Q_{13} = \frac{N_m}{C_m} P_{13} \quad (12.9)$$

Here  $P_{13}$ , the rate of carbon release from the organic fertilizer, is:

$$P_{13} = k_m e_\theta e_T C_m \quad (12.10)$$

where the potential rate constant,  $k_m$ , is the same as in (12.6).

**4) Immobilization of ammonium ( $Q_4$  and  $Q_{14}$ ) and nitrate ( $Q_5$  and  $Q_{15}$ ) in organic fertilizer and the litter pool.** During decomposition of organic fertilizer and litter, some nitrogen may be immobilized if the C:N ratio of the fertilizer or litter is very high. The potential rate of nitrogen transfer to the plant residues pool,  $Q_{4,5}^{pot}$ , is proportional to the rate of carbon transformation by microorganisms adjusted for their microbial synthesis efficiency  $f_e$  and the C/N ratio,  $r_0$ , of microorganisms:

$$Q_{4,5}^{pot} = \frac{f_e P_3}{r_0} \quad (12.11)$$

The potential rate of nitrogen transfer to the organic fertilizer pool is defined as:

$$Q_{14,15}^{pot} = \frac{f_e P_{13}}{r_0} \quad (12.12)$$

It is assumed that ammonium is preferentially immobilized over nitrate nitrogen.

When net immobilization occurs, there may not be enough mineral nitrogen to support rates  $Q_4^{pot}$ ,  $Q_5^{pot}$ ,  $Q_{14}^{pot}$ , and  $Q_{15}^{pot}$ . If there is sufficient mineral nitrogen, the actual immobilization fluxes are equal to the potential values. If the amount of mineral nitrogen is insufficient, the daily immobilization rate is assumed to be equal to a prescribed fraction,  $f_a$ , of the mineral nitrogen available for immobilization. The corresponding total immobilization flux is further distributed among fluxes  $Q_4$ ,  $Q_5$ ,  $Q_{14}$ , and  $Q_{15}$ . It is initially distributed among plant residues and the organic fertilizer pool in proportion to  $Q_{4,5}^{pot}$  and  $Q_{14,15}^{pot}$ , and later between ammonium and nitrates with preference to ammonium.

The fluxes of carbon,  $P_4$ ,  $P_5$ ,  $P_{14}$ , and  $P_{15}$ , are functions of fluxes of immobilized nitrogen as:

$$P_4 = Q_4 * r_0, \quad P_5 = Q_5 * r_0, \quad P_{14} = Q_{14} * r_0, \quad P_{15} = Q_{15} * r_0 \quad (12.13)$$

**5) Conversion of ammonium to nitrate (nitrification), Flux  $Q_6$ .** It is assumed that there is an equilibrium ratio,  $n_q$ , of mineral nitrate and ammonium which can not be exceeded during to nitrification.

$$Q_6 = \begin{cases} k_n e_\theta e_T (N_{NH_4} - \frac{\theta c_{NO_3}}{n_q}), & \text{if } \frac{\theta c_{NO_3}}{N_{NH_4}} < n_q \\ 0, & \text{if } \frac{\theta c_{NO_3}}{N_{NH_4}} \geq n_q \end{cases} \quad (12.14)$$

Here  $k_n$  is the potential nitrification rate in the absence of nitrate in the substrate.

**6) Denitrification ( $Q_7$ ).** This flux is controlled by water content, temperature and nitrate concentration:

$$Q_7 = k_d e_d e_T \frac{c_{NO_3}}{c_{NO_3} + c_s} \quad (12.15)$$

Here  $k_d$  is the potential denitrification rate,  $e_T$  is the correction factor reflecting temperature,  $c_s$  is the Michaelis-Menten constant, and  $e_d$  is water content correction factor. These correction factors are not those calculated for immobilization and mineralization.

**7) Plant uptake of nitrate ( $Q_8$ ) ammonium ( $Q_9$ ).** Nitrogen uptake is generally plant-specific and depends on how the plant develops. Therefore, these fluxes must be calculated in the root activity model or in a separate uptake module. The nitrate-nitrogen taken up by the plant must be accumulated in the variable  $cSink$  which is passed to the solute transport code.

**8) Nitrogen ( $Q_{10}$ ) and carbon ( $P_{10}$ ) from dead roots and plant exudates.** Carbon and nitrogen transfers from these sources are also calculated in an external module. At the present time 2DSOIL does not account for carbon and nitrogen from these sources. Neither  $Q_8$  and  $Q_9$  nor  $Q_{10}$  have any effect in the SoilNitrogen module.

**9) The gradual release of nitrogen from inorganic fertilizer into soil solution ( $Q_{11}$ ).** This flux is calculated in the management module that applies the fertilizer. Mass conservation equations complete the system of equations of the model:

$$\begin{aligned} \frac{dC_h}{dt} &= -P_1 + P_2 + P_{12}; & \frac{dN_h}{dt} &= -Q_1 + Q_2 + Q_{12}; \\ \frac{dC_L}{dt} &= -P_2 - P_3 + P_4 + P_5; & \frac{dN_L}{dt} &= -Q_2 - Q_3 + Q_4 + Q_5; \\ \frac{dC_m}{dt} &= -P_{12} - P_{13} + P_{14} + P_{15}; & \frac{dN_m}{dt} &= -Q_{12} - Q_{13} + Q_{14} + Q_{15}; \\ \frac{dN_{NH_4}}{dt} &= Q_1 + Q_3 + Q_{13} - Q_4 - Q_{14} - Q_6; \\ \frac{d(\theta c_{NO_3})}{dt} &= Q_6 - Q_7 - Q_5 - Q_{15} \end{aligned} \quad (12.16)$$

The correction factors,  $e_\theta$ ,  $e_T$ , and  $e_d$ , are calculated by a separate submodule which is discussed in Section 12.3. The initial values of the state variables  $N_h$ ,  $C_h$ ,  $N_L$ ,  $C_L$ ,  $N_m$ ,  $C_m$ ,  $N_{NH_4}$ , and  $c_{NO_3}$  have to be given for each node as described in the following section. They can be modified by management operations like harvest, plowing, fertilizer application, etc. We assume that management is simulated by separate modules. Any atmospheric deposition of N is handled by the **SetSurface** module.

## 12.2 Input files 'Param\_N.dat' and 'Nodal\_N.dat'

The parameters of the **SoilNitrogen** module are given in the file '**Param\_N.dat**'. The parameters must be provided for the soil material in each subdomain. The units are mg, L and day. A description of the file content is in the Table 12.1 and the following example, 12.1, contains a listing of a sample file. The initial values of the state variables of the model related to the soil solid phase are in the file '**Nodal\_N.dat**'. The initial values of nitrate concentrations are read in by the **SoluteMover** module along with the other solutes. The first solute must be nitrate.

A description of the file content is in the Table 12.2 and the following example is a listing of a sample file.

Table 12.1. Format of the file '**Param\_n.dat**'.

Record	Variable	Description
1-2	-	Comment lines
3	Integer <i>m</i>	Soil material number
3	<i>kh</i>	Potential mineralization rate fro the stable humus pool, day <sup>-1</sup>
3	<i>kL</i>	Potential plant residue decomposition rate, day <sup>-1</sup>
3	<i>km</i>	Potential rate of the organic fertilizer decomposition, day <sup>-1</sup>
3	<i>kn</i>	Potential rate of nitrification, day <sup>-1</sup>
3	<i>kd</i>	Potential rate of denitrification, mg L <sup>-1</sup> day <sup>-1</sup>
Record 3 must be repeated for the soil material in each subdomain <i>m</i> , <i>m</i> =1, <i>NMat</i>		
4,5	-	Comment lines
6	<i>m</i>	Soil material number
6	<i>fe</i>	Microbial synthesis efficiency
6	<i>fh</i>	Humification fraction
6	<i>r0</i>	C/N ratio of the decomposer biomass and humification products
6	<i>rL</i>	C/N ratio of plant residues
6	<i>rm</i>	C/N ratio of the organic fertilizer
6	<i>fa</i>	Fraction of the mineral nitrogen available for immobilization
6	<i>nq</i>	Ratio of the mineral nitrate amount to the mineral ammonium amount characteristic to the particular soil material
6	<i>cs</i>	Michaelis-Menten constant of denitrification, mg L <sup>-1</sup>
Record 6 must be repeated for each soil material in each subdomain <i>m</i> , <i>m</i> =1, <i>NMat</i>		

```
*** Example 12.1: SoilNit parameters: file 'Param_N.dat'
m Potential rate constants: kh      kL      km      kn      kd
1           7E-05   3.5E-02  7E-02  2E-01  5E-02
Ratios and fractions
m fe      fh      r0      rL      rm      fa      nq      cs
1 0.6    0.2    10     25     10    0.08    8    1.E-05
END OF FILE 'PARAM_N.DAT'
```

Table 12.2. Format of the file '**Nodal\_N.dat**'.

Record	Variable	Description					
1,2	-	Comment line.					
3	$n$	Nodal number.					
3	$Ch(n)$	Initial value of the carbon content in humus at node $n$ .					
3	$Nh(n)$	Same as above for the nitrogen.					
3	$CL(n)$	Initial value of the carbon content in plant residues at node $n$ .					
3	$NL(n)$	Same as above for the nitrogen.					
3	$Cm(n)$	Initial value of the carbon content in the organic fertilizer at node $n$ .					
3	$Nm(n)$	Same as above for the nitrogen.					
3	$NNH4(n)$	Initial value of the nitrogen content in the mineral ammonium at node $n$					
Record 3 information is required for each node.							
All values in mg L <sup>-1</sup>							
*** Example 12.2: SoilNit module initial solid phase data: FILE NODAL_N.DAT							
n	Nh	Ch	NL	CL	Nm	Cm	NNH4
1	1.5E-03	1.5E-02	5.0E-05	1.0E-03	0.0	0.0	5.0E-07
.	...	...	..	.	.	.	....
11	0.3E-03	0.3E-04	0.0	0.0			2.0E-09
End of file 'Nodal_N.DAT'							

### 12.3 Rate correction factors for temperature and soil water content

The factors,  $e_\theta$  and  $e_T$ , adjust the potential immobilization and mineralization rate constants for soil water content and temperature. The factor,  $e_d$ , adjusts the denitrification rate for soil water content. These factors are calculated in the module **SetAbio** as:

$$\begin{aligned}
 e_\theta &= \begin{cases} e_s + (1-e_s) \left( \frac{\theta_s - \theta}{\theta_s - \theta_h} \right)^m, & \theta_s \geq \theta > \theta_h \\ 1, & \theta_h \geq \theta > \theta_l \\ \left( \frac{\theta - \theta_w}{\theta_l - \theta_w} \right)^m & \theta_l \geq \theta > \theta_w \end{cases} \\
 \theta_h &= \theta_s - \Delta\theta_h, \quad \theta_l = \theta_w + \Delta\theta_l \\
 e_T &= Q^{\frac{T-t_b}{10}} \\
 e_d &= \begin{cases} \left( \frac{\theta - \theta_d}{\theta_s - \theta_d} \right)^d, & \theta > \theta_d \\ 0, & \theta \leq \theta_d \end{cases} \\
 \theta_d &= \theta_s - \Delta\theta_d
 \end{aligned} \tag{12.17}$$

Here

$\theta$  = volumetric water content,

$\theta_s$  = volumetric soil water content at saturation,

$\theta_w$  = minimum volumetric soil water content for process activity

$\theta_h$  = high volumetric water content for which the process is optimal

$\theta_l$  = low volumetric water content for which the process is optimal

$\Delta\theta_h$  = width of the water content interval where activity decreases  
as water content increases

$\Delta\theta_l$  = width of the water content interval where activity increases  
as water content increases

$e_s$  = relative effect of moisture when the soil is saturated

$T$  = soil temperature, °C

$t_b$  = base temperature at which  $e_T$  is 1

$Q$  = factor change in rate with a 10 degree C change in temperature

$\theta_d$  = threshold water content below which no denitrification occurs

$\Delta\theta_h$  = range of water contents where denitrification occurs

These data are given in the data file '**SetAbio.dat**' as shown in Table 12.3 and listing in Example 12.3.

Table 12.3. Format of the file '**SetAbio.dat**').

Record	Variable	Description
1-2	-	Comment lines
3	<i>m</i>	Number of the soil material
3	<i>ThSat(m)</i>	Volumetric soil water content at saturation for soil material <i>m</i>
3	<i>ThW(m)</i>	Minimum volumetric soil water content for process activity for soil material <i>m</i>
		Record 4 must be repeated for each soil material <i>m</i> , <i>m</i> =1,NMat
4-5	-	Comment lines
6	<i>dThH</i>	The highest volumetric water content for which the process is optimal
6	<i>dThL</i>	The lowest volumetric water content for which the process is optimal
6	<i>es</i>	Relative effect of moisture when the soil is saturated
6	<i>Th_m</i>	Exponent in dependencies of $e_s$ on $\theta$
7-8	-	Comment lines
9	<i>tb</i>	Base temperature at which $e_T = 1$
9	<i>QT</i>	Factor change in rate with a 10 degree change in temperature
10-11	-	Comment lines
12	<i>ThD</i>	Threshold water content below which no denitrification occurs
12	<i>Th_d</i>	Exponent in dependencies of $e_d$ on $\theta$

```
*** Example 12.3: Parameters of abiotic response: file 'SetAbio.dat'
Material Saturated water content ThSat    Wilting point ThW
1                      0.453                  0.157
2                      0.387                  0.137
Dehumification, mineralization, nitrification dependencies on moisture
dThH      dThL      es      Th_m
0.10     0.08     0.6     1.0
Dependencies of temperature
tb      QT
20      3
Denitrification dependencies on water content
dThD      Th_d
0.10     2.0
END OF FILE 'SetAbio.DAT'
```



# Chapter 13: Input and Output of Data

**Yakov Pachepsky and Dennis Timlin**

## 13.1 Data input

Each module of 2DSOIL reads data from files managed by that module. There is no input subroutine that reads all data and passes that data to the appropriate module. The structures of the files are described in the appropriate sections of this manual. Table 13.1 gives the module names and associated data files for this release of 2DSOIL. If the module is not used, then its input files need not be present. The program will produce an error message and give the location of the error if problems reading any input file is encountered (see Section 13.4).

Table 13.1. Data files of modules and submodules of 2DSOIL.02.

Module	Data files	Manual Section
Syncronizer	Time.dat	2
Get_Grid_and_Boundary	Grid_bnd.dat	3
ShootImitator	Param_P.dat	10
WaterMover	Param_W.dat, Nodal_W.dat	6
SetMat01	Closefrm.dat	6
SetMat02	Hydprop.dat	6
SoluteMover	Param_S.dat, Nodal_S.dat	7
HeatMover	Param_T.dat, Nodal_T.dat	8
GasMover	Param_G.dat, Nodal_G.dat	9
Water_Uptake01	Param_R.dat, Nodal_R.dat	10
Water_Uptake02	Param_U.dat, Nodal_U.dat	10
SoilNitrogen	Param_n.dat, Nodal_n.dat, SetAbio.dat	
MacroChem	Param_E.dat, Nodal_E.dat	11

Module	Data files	Manual Section
SetTDB	VarBW.dat, VarBS.dat, VarBT.dat, VarBG.dat	4
SetSurf01	SetSurf.dat	5
SetSurf02	Weather.dat, Furnod.dat <sup>2</sup>	5
Output	Output.dat	12

<sup>1</sup>The actual set of necessary files depends on the list of modules and on the presence of time-dependent boundaries.

<sup>2</sup>File 'Furnod.dat' is needed only if flooding irrigation is simulated.

### 13.2 DataGen, A Simple Grid Generator

A simple grid generator, **DATAGEN**, has been developed for 2DSOIL. The program will only generate rectangular grids, and the user has to manually draw the grid to determine some parameters. If a grid with a ridge and furrow structure is desired, the user must add the ridge part manually. The rectangular portion of the grid is referred to below as RC. The data file of **DATGEN** is called '**Datgen.dat**' and the structure is shown in Table 13.1. A listing of an example file is in Example 13.1 following Table 13.1.

An interactive mouse-based DOS program called 2DPREP and a MS-Windows based program for data input are also available from the authors. These simple programs are useful for creating grids and data files. They can be obtained from the FTP site listed at the beginning of this manual.

Table 13.1. Format of the file **Datagen.dat**.

Record	Variable	Description
1	-	Comment line.
2	IJ	Number of nodes in the horizontal (x) direction
2	e00	Number of the first element of the RC part of the grid.
2	n00	Nodal number of the first node of the RC of the grid.
2	NumNP	Total number on nodal points.
2	NumEl	Total number of elements.
3	-	Comment line.
4	x(1)	Horizontal coordinate of the first vertical grid line in the RC part.
4	x(2)	Same as above for the second vertical line.
4	x(IJ)	Same as above for the last vertical line.
5	-	Comment line.
6	y(1)	Vertical coordinate of the upper horizontal line in the RC part.
6	y(2)	Same as above for the second line.
7	y((NumNP-n00)/IJ+1)	Same as above for the bottom line of the RC part.
8	-	Comment line.
9	p(1)	Initial capillary pressure at nodes of upper grid line in the RC part.
9	p(2)	Same as above for the second line.
9	p((NumNP-n00+1)/NumVL)	Same as above for the bottom line of the RC part.

Example 13.1: Listing of the file 'Datagen.dat'

\*\*\*\* Example of the Datgen data files

```

IJ  E00  n00    NumNP  NumEl
22   67   61      357    320
x(j): 1    2    3    4    5    6    7    8    9    10   11   12   13   14   15
16   17   18   19   20   21   22
      0.0 10.0 15.0 20.0 24.0 30.0 35.0 40.0 45.0 50.0 55.0 60.0 65.0 70.0 75.0
80.0 85.0 90.0 92.0 95.0 98.0 100.0
y(i): 1->(NumNP-n00) / IJ+1
      130.0 125.0 120.0 115.0 110.0 105.0 102.0 100.0 97.0 95 90 85 75 60 45 30 0
hBottom
-30.

```

**DATAGEN** builds files called '**Grid\_bnd**', '**Output**', '**Nodal\_W**' and '**Nodal\_R**'. These files correspond to the same 2DSOIL files that have the extension '.dat'. The files will contain sequences of question marks that mark locations for data to be added manually. Portions of the grid that are outside of the rectangular boundary must be added manually. This outside portion may correspond to the ridge in Figure 3.1, for example. The program **DATAGEN.FOR** is supplied with 2DSOIL.

### 13.3 Conversion of units for chemical application

When fertilizer applications are carried out, it is necessary to convert the units from an areal basis of  $\text{kg ha}^{-1}$  to concentration on a volume basis,  $\text{mg L}^{-1}$ . The simulation domain, which is seen as a grid, has a polygonal structure with dimensions vertically into the soil and horizontally across the rows. It is also considered to be 1cm in width. The grid itself, therefore, can be considered to have volume. The first step in the conversion process is to scale the  $\text{kg ha}^{-1}$  chemical application rate to the surface area of the grid and find the total mass, in grams, of chemical to be applied to the grid. The total mass of chemical to be applied to the grid is obtained by multiplying the chemical application rate by the surface area of the grid. The surface area of the grid is simply the width (in meters) of the grid multiplied by 0.01 m.

The total number of grams of chemical to be applied must next be distributed among the nodes that will receive the chemical. Concentration at a node is obtained by using the area of the

elements that are associated with the nodes. This is illustrated in the following example and Figure 13.1. Assume you want to apply 150 kg/ha of nitrogen, and the grid is 30 cm wide (if the grid has a ridge and furrow, use the width below the ridge). The total application, in grams N, is:

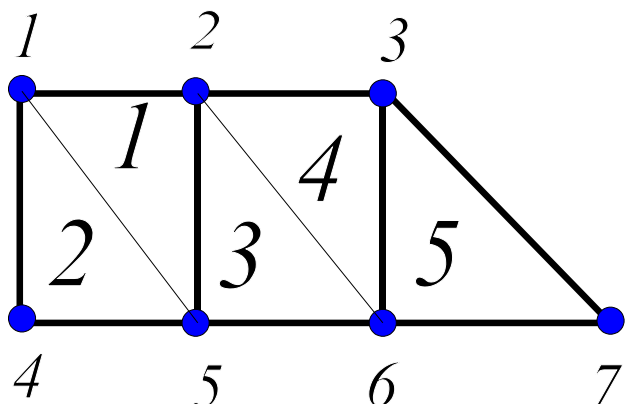


**Figure 13.1** Illustration of method to determine nodal concentrations from area applications

nodes at the surface of a ridge in Figure 13.1 (nodes 1, 2, and 3). Note that the grid is input as rectangular elements except at the edges of the ridges (element 5). The rectangular elements are shown as bold lines. The finite-element program actually subdivides each rectangular element

The factor, 10, scales  $\text{kg ha}^{-1}$  to g.

Suppose this will be applied to three

$$\frac{150 \times (0.01 \times 0.30)}{10} = 0.045$$

into two triangles. The nodal concentrations must be determined using the area of these triangles. The first element, 1, in Figure 13.1, has two nodes (1 and 2) that contribute to the chemical concentration out of the total of three nodes. Therefore, the contribution of the area of this triangle is 2/3 of its total area. Triangle 2 has one node (1) so it contributes only 1/3 of its area, triangle 3 contributes 1 node, triangle 4 contributes 2 nodes and triangle 5 contributes 1 node. The total area for application is calculated as:

$$\text{Total area} = \frac{2}{3}A_1 + \frac{1}{3}A_2 + \frac{1}{2}A_3 + \frac{2}{3}A_4 + \frac{1}{2}A_5.$$

Here 'A' refers to the area of the respective triangle. If the areas were all 6.25 cm<sup>2</sup>, for example, then the total area would be 14.58 cm<sup>2</sup>. The concentration for each node is calculated as:

$$\frac{0.043}{14.58} = 3.086 \times 10^{-3} \text{ g cm}^{-3} \text{ of soil}$$

Since nitrogen is in the form of nitrate in 2DSOIL, this number must be multiplied by 14/62 to obtain NO<sub>3</sub> concentration. Finally, if this number is used to initialize the solute concentrations in the file **Nodal\_S.dat**, it must be divided by water content to obtain g L<sup>-1</sup>. Water contents can be obtained by running the model through one time step and inspecting the file **Theta2D.out**.

### **13.4 Output of simulation results**

A single module, **Output**, is used to send output to disk files; only public soil state variables are output. There is an option to print with two formats. The first format outputs values of the variables together with the nodal coordinates for nodal variables or the coordinates of the center of the element in the case of elemental data in a three column format. This format is suitable for graphic packages to draw contour maps of two-dimensional distributions. The second format outputs nodal and element variable values in strings that correspond to sequences of nodes along the transverse lines of the grid. This format is more convenient for looking

through and quickly evaluating results, but it is not convenient for importing into graphic packages, and requires special data preparation (see below).

The first format produces files with the extension '.grp'; the second format output files with the extension '.out.' (Table 13.2). If a module is not used, then the corresponding public variable will not be printed.

Table 13.2. Output files of 2DSOIL.03.

Variable	Filename	Variable	Filename	Variable	Filename
hNew	h____2d.*	Q	Q____2d.*	Sink	Sink_2d.*
ThNew	Theta2d.*	Conc	Conc_2d.*	cSink	cSink2d.*
Vx	Vx____2d.*	Tmpr	Tmpr_2d.*	gSink	gSink2d.*
Vz	Vz____2d.*	g	g____2d.*	RTWT	RTWT_2d.*
RUTDN RUTDN2D.*					

The wildcard '\*' may be replaced with 'out' or 'grp'.

The module **Output** reads a data file called '**Output.dat**' that contains parameters to specify how and when the data are to be written to files. The structure of this file is given in Table 13.3 which is followed by Example 13.3, a listing of an example file. The parameters include the format switch and printout times. The initial distribution will be printed automatically after the first time step, so the first printout time must be greater than initial time. If the second format is used, the node numbers and elements must be given in the same sequence that they will print out (see Example 13.3 for an illustration). These data do not have to be supplied if the first format is used. The program currently allows a maximum of 80 print times. This value can be changed in the array dimension of the variable *tPrint*.

Table 13.3. Format of the file '**Output.dat**'.

Record	Variable	Description
1-2	-	Comment lines.
3	<i>NumPrint</i>	Number of specified print-times (maximum is 80).
3	<i>iForm</i>	Switch to select the printout format, =1 if first format is selected, =2 if second format is selected, =3 if both formats are to be used. The definition of formats is in Sect. 13.2.
4	-	Comment line.
5	<i>Tprint(1)</i>	First specified print-time
5	<i>Tprint(2)</i>	Second specified print-time.
.	.	.
5	<i>Tprint(NumPrint)</i>	Last specified print-time.
If <i>iForm</i> =1 then the file is ended here.		
6	-	Comment line.
7	<i>NumLinNod</i>	Total number of transverse grid lines.
7	<i>NumLinCell</i>	Total number of horizontal layers of elements (soil cells).
8	-	Comment line.
9	<i>NumPoint(i)</i>	Total number of values to be printed in the <i>i</i> -th printout line.
9	<i>NumNod(i,1)</i>	Number of the node that corresponds to the first value of the <i>i</i> -th printout line.
9	<i>NumNod(i,2)</i>	Number of the node that corresponds to the second value of the <i>i</i> -th printout line.
9	<i>NumNod(i,NumPoint(i))</i>	Number of the node that corresponds to the last value of the <i>i</i> -th printout line.
Record 9 is provided for all lines of printout $i=1, 2, \dots, NumLinNod$		
10	-	Comment line.
11	<i>NumCell(e)</i>	Total number of values to be printed in the <i>e</i> -th printout line.
11	<i>NumElem(e,1)</i>	Number of the element that corresponds to the first value of the <i>e</i> -th printout line.
11	<i>NumElem(e,2)</i>	Number of the element that corresponds to the second value of the <i>e</i> -th printout line.
11	<i>NumElem(e,NumPoint(e))</i>	Number of the element that corresponds to the last value of the <i>e</i> -th printout line.
Record 11 is provided for all lines of printout $e=1, 2, \dots, NumLinCell$		

```

*** Example 13.2: OUTPUT CONTROL INFORMATION - file 'Output.dat'
NumPrint    iForm
      3          3
TPrint(1),TPrint(2),...,TPrint(NumPrin
      1          10          30
NumLinNod   NumLinCell
      5          4
NumPoint     NodNum to print
      2          1          2
      4          3          4          5          6
      4          7          8          9          10
      4          11         12         13         14
      4          15         16         17         18
NumCell      NumElements to print
      2          1          2
      3          3          4          5
      3          6          7          8
      3          9          10         11

```

### **13.5 Error messages**

If a run time fatal error occurs during the data input, the number of the error message appears in the window and in the separate '**2DSOIL.log**' file. The latter contains also the number of the line with erroneous data. A list of errors is in the following Table 13.5.

Table 13.5. Error messages

Number	Meaning
1	No 'Time.dat' file found.
2	Error in record 1 of 'Time.dat' file.
3	Error in record 2 of 'Time.dat' file.
4	Error in record 3 of 'Time.dat' file.
5	Error in record 4 of 'Time.dat' file.
6	Error in record 5 of 'Time.dat' file.
7	Error in record 6 of 'Time.dat' file.
8	Error in record 7 of 'Time.dat' file.
20	No 'Grid_bnd.dat' file found.
21	Error in record 1 of 'Grid_bnd.dat' file.
22	Error in record 2 of 'Grid_bnd.dat' file.

Table 13.5. Error messages

Number	Meaning
23	Error in record 3 of 'Grid_bnd.dat' file.
24	Error in record 4 of 'Grid_bnd.dat' file.
25	Error in record 5 of 'Grid_bnd.dat' file.
26	Error in record 6 of 'Grid_bnd.dat' file.
27	Error in record 7 of 'Grid_bnd.dat' file.
28	Error in record 8 of 'Grid_bnd.dat' file.
29	Error in record 9 of 'Grid_bnd.dat' file.
30	Error in record 10 of 'Grid_bnd.dat' file.
31	Error in record 11 of 'Grid_bnd.dat' file.
32	Error in record 12 of 'Grid_bnd.dat' file.
33	Error in record 13 of 'Grid_bnd.dat' file.
34	Error in record 14 of 'Grid_bnd.dat' file.
35	Error in record 15 of 'Grid_bnd.dat' file.
36	Error in record 16 of 'Grid_bnd.dat' file.
37	Error in record 17 of 'Grid_bnd.dat' file.
38	Error in record 18 of 'Grid_bnd.dat' file.
40	No 'HydProp.dat' file found.
41	Error in the 'HydProp.dat' file.
42	Error in record 2 of 'HydProp.dat' file.
43	Error in record 3 of 'HydProp.dat' file.
44	Error in record 4 of 'HydProp.dat' file.
45	Error in record 5 of 'HydProp.dat' file.
46	Error in record 6 of 'HydProp.dat' file.
47	Error in record 7 of 'HydProp.dat' file.
48	Error in record 8 of 'HydProp.dat' file.
49	Error in record 9 of 'HydProp.dat' file.
50	No 'Param_W.dat' file found.
51	Error in record 1 of 'Param_W.dat' file.

Table 13.5. Error messages

Number	Meaning
52	Error in record 2 of 'Param_W.dat' file.
53	Error in record 3 of 'Param_W.dat' file.
55	No 'Nodal_W.dat' file found.
56	Error in record 1 of 'Nodal_W.dat' file.
57	Error in record 2 of 'Nodal_W.dat' file.
58	Error in record 3 of 'Nodal_W.dat' file.
60	No 'Closefrm.dat' file found.
61	Error in record 1 of 'Closefrm.dat' file.
62	Error in record 2 of 'Closefrm.dat' file.
63	Error in record 3 of 'Closefrm.dat' file.
70	No 'Param_S.dat' file found.
71	Error in record 1 of 'Param_S.dat' file.
72	Error in record 2 of 'Param_S.dat' file.
73	Error in record 3 of 'Param_S.dat' file.
74	Error in record 4 of 'Param_S.dat' file.
75	Error in record 5 of 'Param_S.dat' file.
76	Error in record 6 of 'Param_S.dat' file.
77	Error in record 7 of 'Param_S.dat' file.
78	Error in record 8 of 'Param_S.dat' file.
79	Error in record 9 of 'Param_S.dat' file.
80	Error in record 10 of 'Param_S.dat' file.
81	Error in record 11 of 'Param_S.dat' file.
82	Error in record 12 of 'Param_S.dat' file.
83	Error in record 13 of 'Param_S.dat' file.
84	Error in record 14 of 'Param_S.dat' file.
85	Error in record 15 of 'Param_S.dat' file.
86	Error in record 16 of 'Param_S.dat' file.
95	No 'Nodal_S.dat' file found.

Table 13.5. Error messages

Number	Meaning
96	Error in record 1 of 'Nodal_S.dat' file.
97	Error in record 2 of 'Nodal_S.dat' file.
98	Error in record 3 of 'Nodal_S.dat' file.
100	No 'Param_T.dat' file found.
101	Error in record 1 of 'Param_T.dat' file.
102	Error in record 2 of 'Param_T.dat' file.
103	Error in record 3 of 'Param_T.dat' file.
104	Error in record 4 of 'Param_T.dat' file.
105	Error in record 5 of 'Param_T.dat' file.
106	Error in record 6 of 'Param_T.dat' file.
125	No 'Nodal_T.dat' file found.
126	Error in record 1 of 'Nodal_T.dat' file.
127	Error in record 2 of 'Nodal_T.dat' file.
128	Error in record 3 of 'Nodal_T.dat' file.
130	No 'Param_G.dat' file found.
131	Error in record 1 of 'Param_G.dat' file.
132	Error in record 2 of 'Param_G.dat' file.
133	Error in record 3 of 'Param_G.dat' file.
134	Error in record 4 of 'Param_G.dat' file.
135	Error in record 5 of 'Param_G.dat' file.
136	Error in record 6 of 'Param_G.dat' file.
137	Error in record 7 of 'Param_G.dat' file.
138	Error in record 8 of 'Param_G.dat' file.
139	Error in record 9 of 'Param_G.dat' file.
140	Error in record 10 of 'Param_G.dat' file.
141	Error in record 11 of 'Param_G.dat' file.
142	Error in record 12 of 'Param_G.dat' file.
143	Error in record 13 of 'Param_G.dat' file.

Table 13.5. Error messages

Number	Meaning
144	Error in record 14 of 'Param_G.dat' file.
145	Error in record 15 of 'Param_G.dat' file.
146	Error in record 16 of 'Param_G.dat' file.
147	Error in record 17 of 'Param_G.dat' file.
148	Error in record 18 of 'Param_G.dat' file.
149	Error in record 19 of 'Param_G.dat' file.
150	Error in record 20 of 'Param_G.dat' file.
151	Error in record 21 of 'Param_G.dat' file.
155	No 'Nodal_G.dat' file found.
156	Error in record 1 of 'Nodal_G.dat' file.
157	Error in record 2 of 'Nodal_G.dat' file.
158	Error in record 3 of 'Nodal_G.dat' file.
160	No 'Weather.dat' file found.
161	Error in record 1 of 'Weather.dat' file.
162	Error in record 2 of 'Weather.dat' file.
163	Error in record 3 of 'Weather.dat' file.
164	Error in record 4 of 'Weather.dat' file.
165	Error in record 5 of 'Weather.dat' file.
166	Error in record 6 of 'Weather.dat' file.
167	Error in record 7 of 'Weather.dat' file.
168	Error in record 8 of 'Weather.dat' file.
169	Error in record 9 of 'Weather.dat' file.
170	Error in record 10 of 'Weather.dat' file.
171	Error in record 11 of 'Weather.dat' file.
172	Error in record 12 of 'Weather.dat' file.
173	Error in record 13 of 'Weather.dat' file.
174	Error in record 14 of 'Weather.dat' file.
180	No 'Furnod.dat' file found.

Table 13.5. Error messages

Number	Meaning
181	Error in record 1 of 'Furnod.dat' file.
182	Error in record 2 of 'Furnod.dat' file.
183	Error in record 3 of 'Furnod.dat' file.
184	Error in record 4 of 'Furnod.dat' file.
185	Error in record 5 of 'Furnod.dat' file.
186	Error in record 6 of 'Furnod.dat' file.
187	Error in record 7 of 'Furnod.dat' file.
190	No 'Setsurf.dat' file found.
191	Error in record 1 of 'Setsurf.dat' file.
192	Error in record 2 of 'Setsurf.dat' file.
193	Error in record 3 of 'Setsurf.dat' file.
194	Error in record 4 of 'Setsurf.dat' file.
220	No 'Param_R.dat' file found.
221	Error in record 1 of 'Param_R.dat' file.
222	Error in record 2 of 'Param_R.dat' file.
223	Error in record 3 of 'Param_R.dat' file.
224	Error in record 4 of 'Param_R.dat' file.
225	Error in record 5 of 'Param_R.dat' file.
226	Error in record 6 of 'Param_R.dat' file.
227	Error in record 7 of 'Param_R.dat' file.
228	Error in record 8 of 'Param_R.dat' file.
229	Error in record 9 of 'Param_R.dat' file.
235	No 'Nodal_R.dat' file found.
236	Error in record 1 of 'Nodal_R.dat' file.
237	Error in record 2 of 'Nodal_R.dat' file.
238	Error in record 3 of 'Nodal_R.dat' file.
240	No 'Param_U.dat' file found.
241	Error in record 1 of 'Param_U.dat' file.

Table 13.5. Error messages

Number	Meaning
242	Error in record 2 of 'Param_U.dat' file.
243	Error in record 3 of 'Param_U.dat' file.
244	Error in record 4 of 'Param_U.dat' file.
245	Error in record 5 of 'Param_U.dat' file.
246	Error in record 6 of 'Param_U.dat' file.
250	No 'Nodal_U.dat' file found.
251	Error in record 1 of 'Nodal_U.dat' file.
252	Error in record 2 of 'Nodal_U.dat' file.
253	Error in record 3 of 'Nodal_U.dat' file.
255	No 'Param_P.dat' file found.
256	Error in record 1 of 'Param_P.dat' file.
257	Error in record 2 of 'Param_P.dat' file.
258	Error in record 3 of 'Param_P.dat' file.
260	No 'Output.dat' file found.
261	Error in record 1 of 'Output.dat' file.
262	Error in record 2 of 'Output.dat' file.
263	Error in record 3 of 'Output.dat' file.
264	Error in record 4 of 'Output.dat' file.
265	Error in record 5 of 'Output.dat' file.
266	Error in record 6 of 'Output.dat' file.
267	Error in record 7 of 'Output.dat' file.
268	Error in record 8 of 'Output.dat' file.
269	Error in record 9 of 'Output.dat' file.
270	Error in record 10 of 'Output.dat' file.
271	Error in record 11 of 'Output.dat' file.
272	No 'Param_E.dat' file found.
273	Error in record 1 of 'Param_E.dat' file.
274	Error in record 2 of 'Param_E.dat' file.

Table 13.5. Error messages

Number	Meaning
275	Error in record 3 of 'Param_E.dat' file.
276	Error in record 4 of 'Param_E.dat' file.
277	Error in record 5 of 'Param_E.dat' file.
278	Error in record 6 of 'Param_E.dat' file.
279	Error in record 7 of 'Param_E.dat' file.
280	Error in record 8 of 'Param_E.dat' file.
281	Error in record 9 of 'Param_E.dat' file.
282	Error in record 10 of 'Param_E.dat' file.
283	Error in record 11 of 'Param_E.dat' file.
284	Error in record 12 of 'Param_E.dat' file.
285	Error in record 13 of 'Param_E.dat' file.
286	Error in record 14 of 'Param_E.dat' file.
287	Error in record 15 of 'Param_E.dat' file.
290	No 'Nodal_E.dat' file found.
291	Error in record 1 of 'Nodal_E.dat' file.
292	Error in record 2 of 'Nodal_E.dat' file.
293	Error in record 3 of 'Nodal_E.dat' file.
300	No 'VarBW.dat' file found.
301	Error in record 1 of 'VarBW.dat' file.
302	Error in record 2 of 'VarBW.dat' file.
303	Error in record 3 of 'VarBW.dat' file.
304	Error in record 4 of 'VarBW.dat' file.
325	No 'VarBS.dat' file found.
326	Error in record 1 of 'VarBS.dat' file.
327	Error in record 2 of 'VarBS.dat' file.
328	Error in record 3 of 'VarBS.dat' file.
329	Error in record 4 of 'VarBS.dat' file.
350	No 'VarBT.dat' file found.

Table 13.5. Error messages

Number	Meaning
351	Error in record 1 of 'VarBT.dat' file.
352	Error in record 2 of 'VarBT.dat' file.
353	Error in record 3 of 'VarBT.dat' file.
354	Error in record 4 of 'VarBT.dat' file.
375	No 'VarBG.dat' file found.
376	Error in record 1 of 'VarBG.dat' file.
377	Error in record 2 of 'VarBG.dat' file.
378	Error in record 3 of 'VarBG.dat' file.
379	Error in record 4 of 'VarBG.dat' file.
400	No 'Param_n.dat' file found
401	Error in record 1 of 'Param_n.dat' file.
402	Error in record 2 of 'Param_n.dat' file.
403	Error in record 3 of 'Param_n.dat' file.
404	Error in record 4 of 'Param_n.dat' file.
405	Error in record 5 of 'Param_n.dat' file.
406	Error in record 6 of 'Param_n.dat' file.
407	Error in record 7 of 'Param_n.dat' file.
408	Error in record 8 of 'Param_n.dat' file.
409	Error in record 9 of 'Param_n.dat' file.
410	Error in record 10 of 'Param_n.dat' file.
412	Error in record 11 of 'Param_n.dat' file.
413	Error in record 12 of 'Param_n.dat' file.
414	Error in record 13 of 'Param_n.dat' file.
415	Error in record 14 of 'Param_n.dat' file.
420	No 'SetAbio.dat' file found
421	Error in record 1 of 'SetAbio.dat' .
422	Error in record 2 of 'SetAbio.dat' .
423	Error in record 3 of 'SetAbio.dat' .

Table 13.5. Error messages

Number	Meaning
424	Error in record 4 of 'SetAbio.dat' .
425	Error in record 5 of 'SetAbio.dat' .
426	Error in record 6 of 'SetAbio.dat' .
427	Error in record 7 of 'SetAbio.dat' .
427	Error in record 8 of 'SetAbio.dat' .
429	Error in record 9 of 'SetAbio.dat' .
450	No 'Nodal_n.dat' file found
451	Error in record 1 of 'Nodal_n.dat' file.
452	Error in record 2 of 'Nodal_n.dat' file.
453	Error in record 3 of 'Nodal_n.dat' file.
454	Error in record 4 of 'Nodal_n.dat' file.
455	Error in record 5 of 'Nodal_n.dat' file.
456	Error in record 6 of 'Nodal_n.dat' file.
457	Error in record 7 of 'Nodal_n.dat' file.



# Chapter 14: Example Problems

Dennis Timlin and Yakov Pachepsky

Four examples are presented in this section. The purpose of the examples is (1) to illustrate the kinds of two-dimensional root and soil processes that can be simulated and (2) to give examples of data preparation for users of 2DSOIL.

## **14.1 Example 14.1: Alternate and furrow irrigation: root development**

Alternate furrow irrigation has been proposed as a water conserving irrigation management practice. In this example, the model output is used to compare water movement, root development, and root water uptake for alternate and regular furrow irrigation. The modules that are involved are **SetSur02**, **WatUptake01**, and **WaterMover**. Figure 14.1 gives a graphical representation of the finite element mesh utilized for the numerical simulations. Note that Figure 14.1 shows a gradual increase in spacing between vertical grid lines. A detail of the shape of the grid that represents the two furrows and one ridge of the soil surface is shown in Fig. 14.1b. The row spacing is 50 cm and the furrow depth is 10 cm. The soil hydraulic properties are characteristic for a loamy sand. For the sake of clarity, we assumed a uniform soil profile. The soil water retention and soil hydraulic conductivity relationships are shown in Fig. 14.2. The initial soil water potential was maintained at -300 cm at the 2-m depth and the initial soil moisture content was  $0.175 \text{ cm}^3 \text{ cm}^{-3}$ . The plant had an initial height of 3 cm and was placed in the middle of the ridge with the stem base at 10 cm in depth. The parameters for the root system corresponded to those for soybean. Soil temperature and soil oxygen concentration were constant over the soil profile. The simulation time began on May 10 (DOY 130) and ended on July 19 (DOY 200).

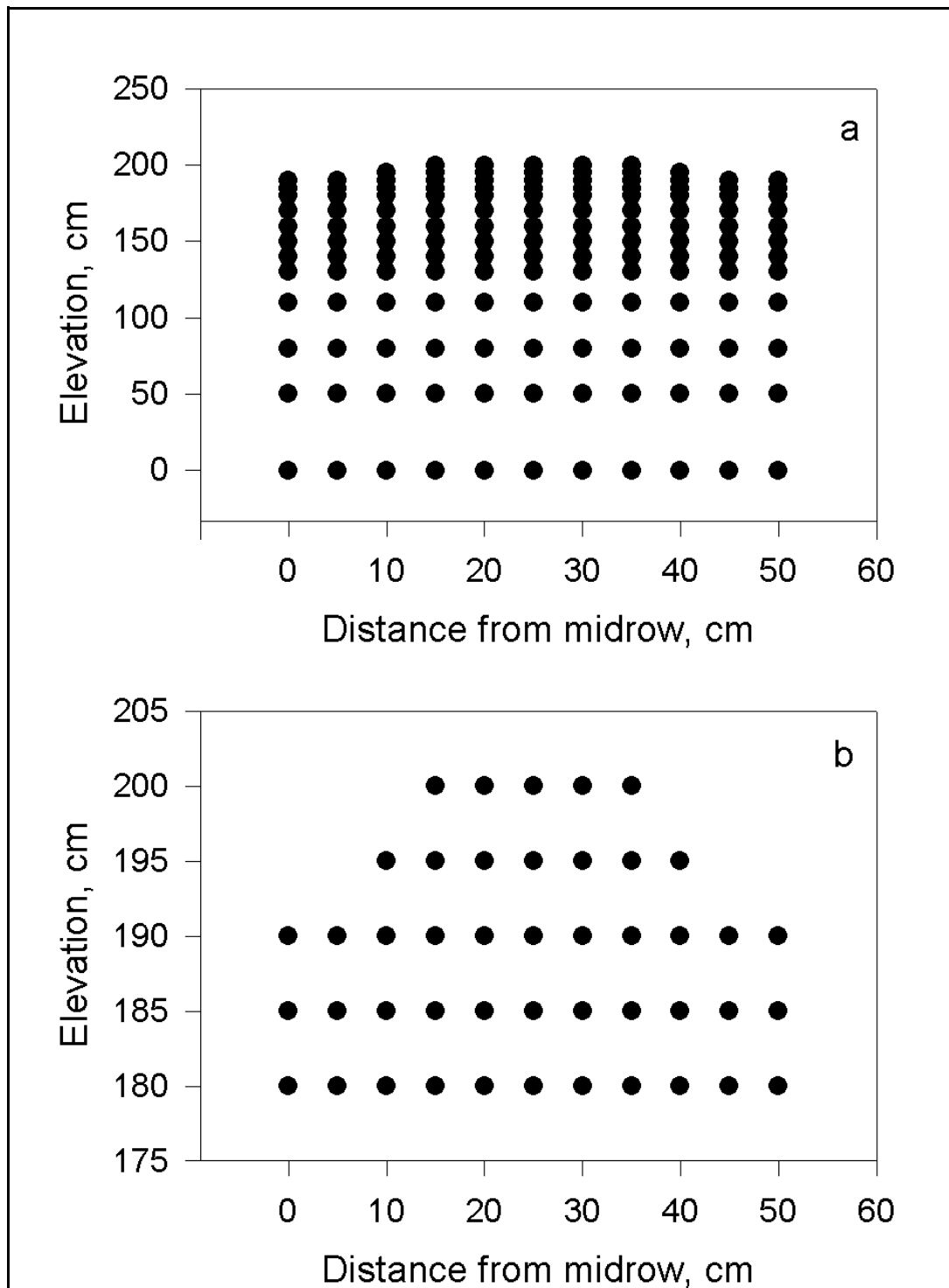


**Figure 14.1** Nodes of the grid that covers the soil domain for Example 14.1; a - general pattern, b - upper part. Elevation is measured from the reference plane at 200 cm depth.

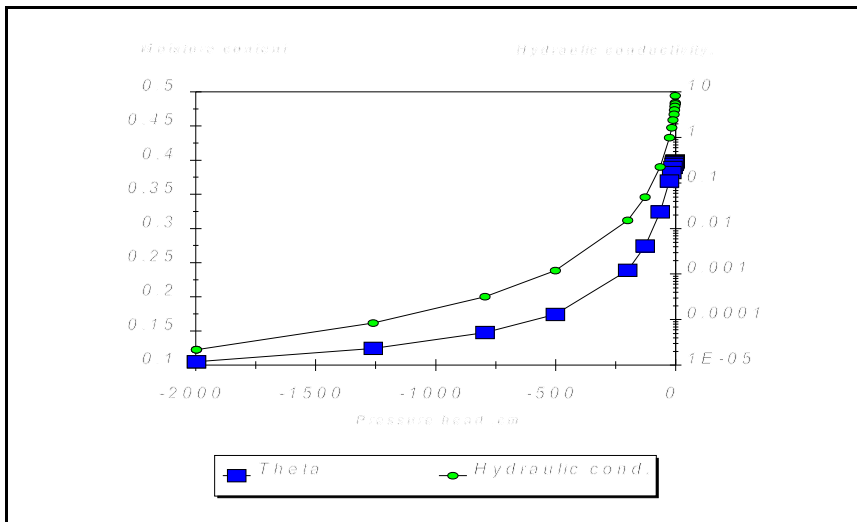


**Figure 14.2** Soil hydraulic parameters for Example 14.1.

The weather and irrigation data are summarized in Fig. 14.3. The total amount of rainfall was 3 cm and every two weeks 9.9 cm of irrigation water was applied as flood irrigation giving a total irrigation of 49.5 cm for the season.

The irrigation water for regular irrigation was applied in equal amounts to both furrows and only to the left furrow in alternate irrigation simulations. The same total amount of water was supplied for both scenarios.

The calculated root density distributions for July 10 (60 days after planting) are given in Fig. 14.4. The root pattern was nearly symmetrical for regular irrigation. The root pattern was significantly asymmetrical for alternate furrow irrigation because there was less root proliferation under the dry furrow. The depth of the root system was about 50 cm under the ridge. However total root mass was 10 % larger in regular irrigation than in alternate irrigation. The patterns of soil moisture distribution for July 10 are shown in Fig. 14.5. The soil is drier in the root zone under the stem in

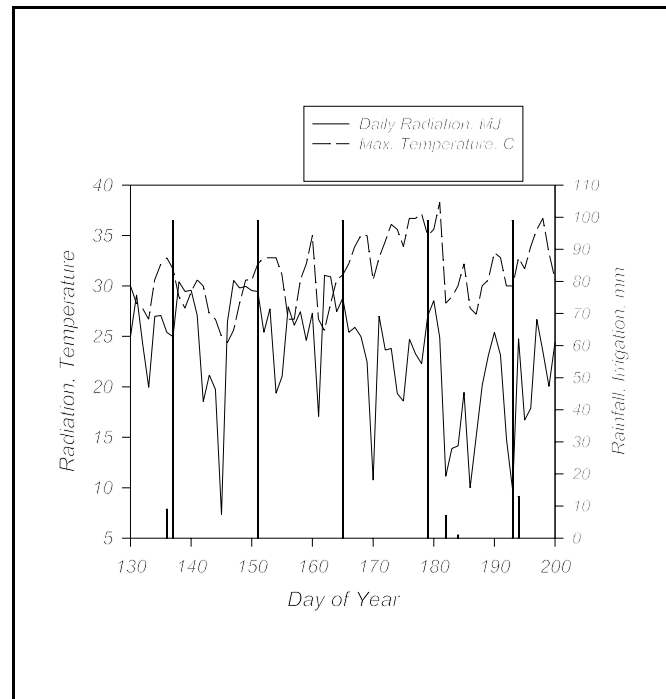


**Figure 14.3** Daily weather and irrigation data for Example 14.1.

the case of regular irrigation than in the case of alternate irrigation. This meant that more carbon was sent to grow roots in the case of regular irrigation because water availability was less. The soil moisture content is lower under the non-irrigated furrow than under the irrigated furrows. The difference is not large mainly because soil hydraulic conductivity is low and decreases very steeply as moisture content diminishes (Fig. 14.2). For regular irrigation, the simulated amount of soil water in the upper 55 cm at the end of the simulation is 13 % less than for alternate irrigation. The data shown here are not sufficient to compare the efficiency of two irrigation techniques for plant yield because a very simple plant model was used. If a more comprehensive plant model was used in place of the simple shoot imitator, the yield efficiency could be easily compared.

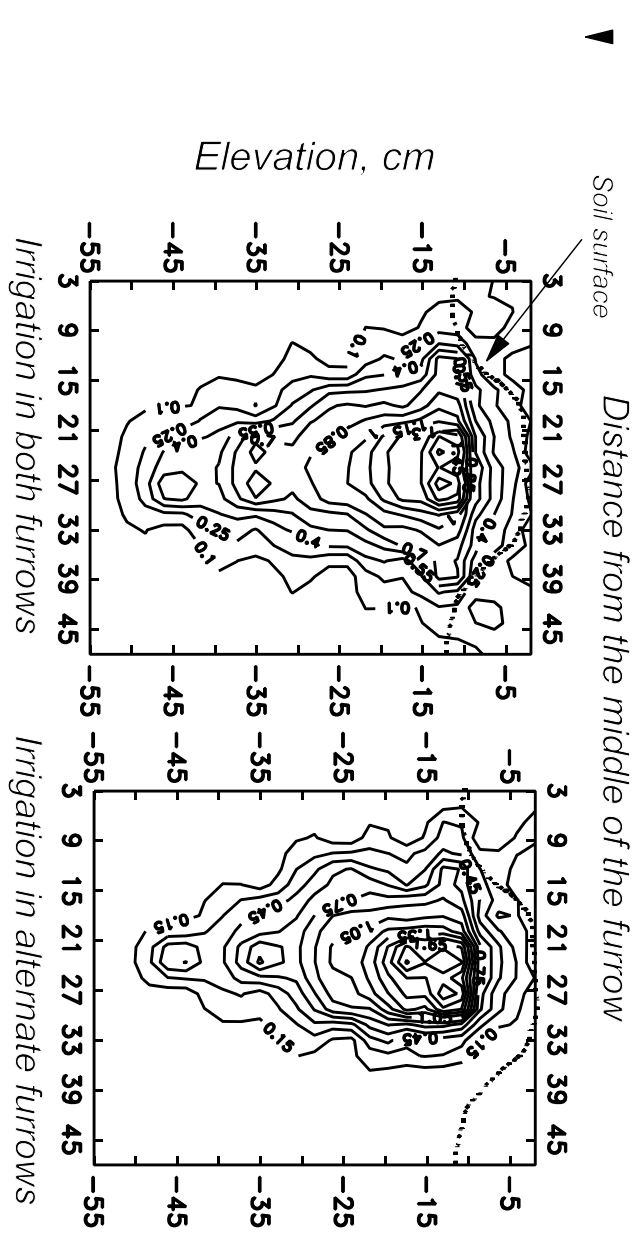


**Figure 14.4** Root Density ( $10^4 \text{ g cm}^{-3}$ ) distributions for regular (left) and alternate (right) irrigation after 60 days of plant development. Elevation is measured relative to the surface of the ridge and the horizontal coordinate is distance from the middle of the left furrow, cm. Water was applied to the left furrow in the case of alternate furrow irrigation.

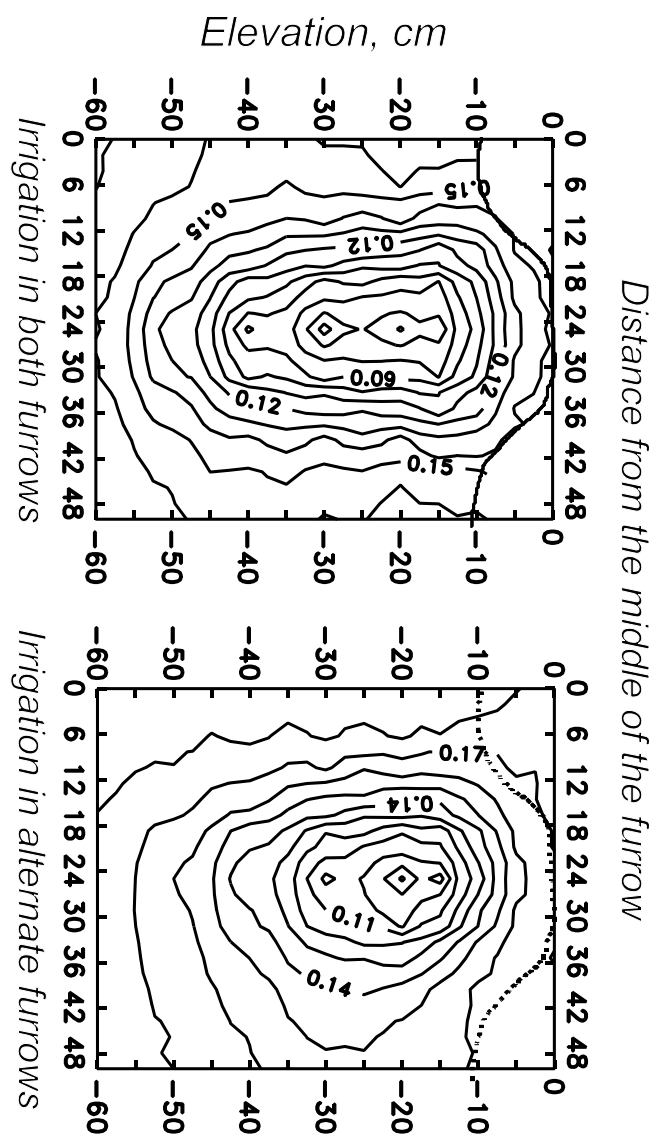


**Figure 14.5** Soil moisture content ( $\text{cm}^3 \text{ cm}^{-3}$ ) distributions for regular (left) and alternate (right) irrigation after 60 days of plant development. Elevation is measured relative to the ridge surface and the horizontal coordinate is distance from the middle of the left furrow, cm. Water was applied to the left furrow in the case of alternate furrow irrigation.

## **14.2 Example 14.2: Soil temperature regime in ridge and interridge zones as affected by plant development**

This example is a simulation of soil temperatures in a ridged soil for a three-month growing season. Ridge tillage is a common practice in areas where cool, wet soil conditions occur in the spring. Soil in ridges is generally drier and warms faster in the spring. In this example, however, the effect of ridges under conditions of low moisture availability will be described. The modules that are used are **SetSurf02**, **Heat Mover**, **WatUptake01**, and **WaterMover**.

Figure 14.6 is a graphical representation of the finite element grid at the surface. Below 190 cm the numbering of nodes and elements continues as in the row at 190 cm. The nodes within the ridge are more closely spaced than in the interridge zone. The soil consists of two layers, a sandy loam texture over a loam and the soil hydraulic functions are in Fig. 14.7. Temperature and soil matric potential were held constant at the bottom boundary. The value for temperature was 25 °C and matric potential was -300 cm. The atmospheric data are similar to those presented in Fig. 14.3; however, precipitation was less. The details are in the file **Weather.Dat**. The plant was placed at the center of the furrow five cm deep and soybean root parameters were used. Soil oxygen was constant over the profile and solute movement was not simulated. Simulated time began at DOY 130 and ended at DOY 168.

Soil temperatures for the first several days (134-136) of the simulation are shown in Fig. 14.8. Because the plant shades the soil on the ridge, there is no evaporation from the soil surface. As a result, soil temperatures remain near air temperature (30.6 and 32.2 °C) for days 134 and 135. In the interridge zone, however, the soil dries to air-dry and the actual evaporation rate becomes less than the potential rate. A portion of solar radiation now goes to heat the soil. As a result, the additional heat from solar radiation heats the soil in the interridge zones to a

temperature greater than the air temperature. At 10 cm from the center, the plant shade first covers this node

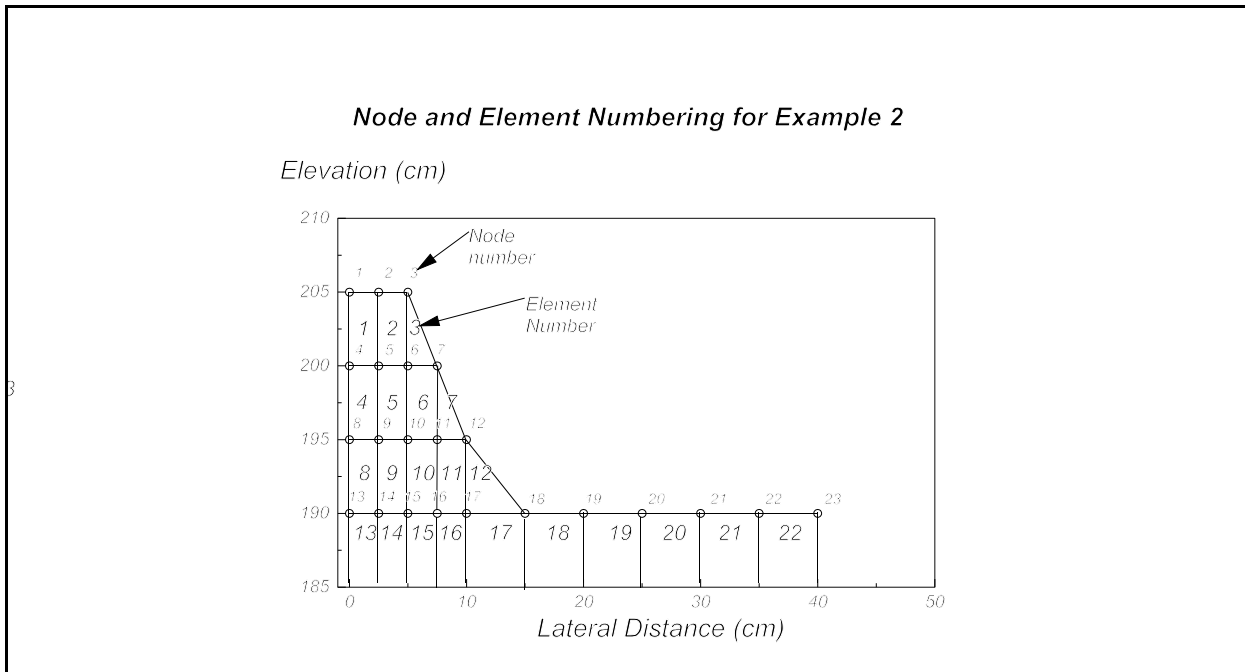


**Figure 14.6** Node and element numbering for ridges in Example 14.2

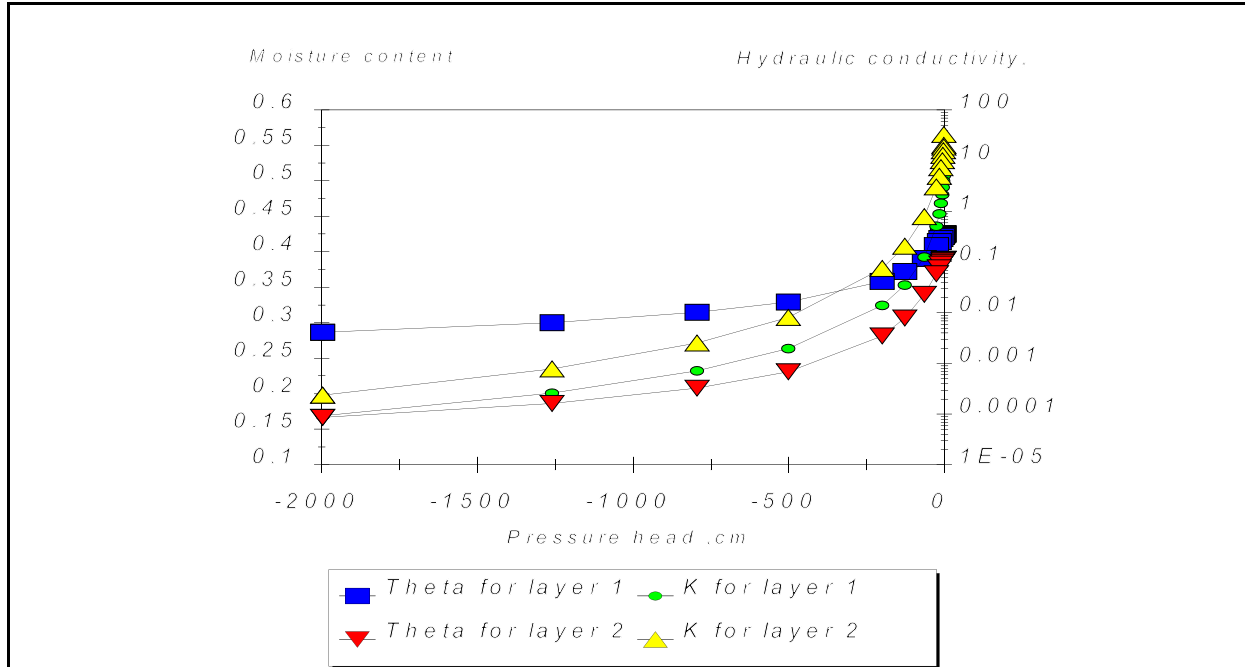


**Figure 14.7** Hydraulic functions for the layered soil used in Example 14.2. The surface soil texture is sandy loam, the subsurface texture is loam.

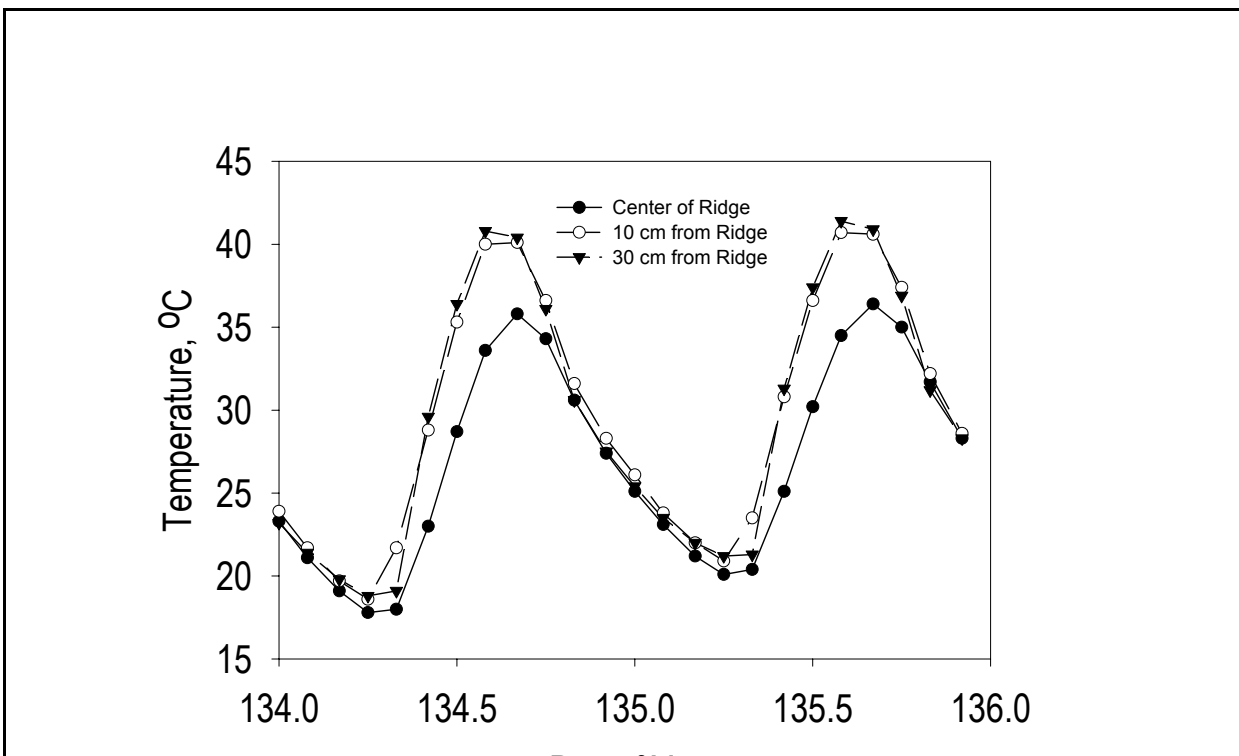


**Figure 14.9** Hourly temperature distribution of surface soil in ridge and interridge zones during days of year 134 and 135, before canopy closure.

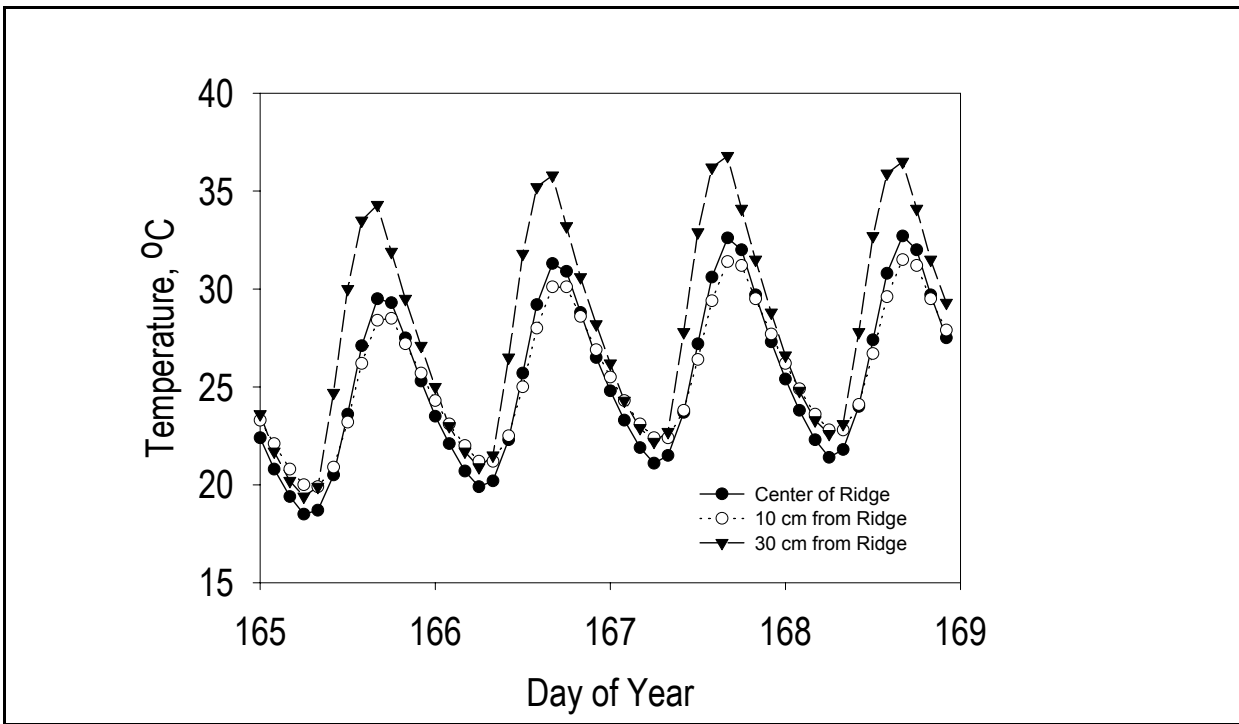


**Figure 14.8** Hourly temperature distribution of surface soil in the ridge and interridge zones during days of year 165 through 169, after canopy closure.

near the morning of day 135. This results in the soil cooling to ambient temperature because the sun is no longer heating the soil at this node. Note that this example is given to illustrate the effects of shade on evaporation of water from soil, and on soil temperature. Only a very simple plant model was used.

After day 145 there was no more precipitation. The soil is again allowed to dry by transpiration but plant shade covers all of the interridge zone. As shown in Fig. 14.9 it can be seen that the surface soil in the ridge zone becomes warmer than the soil in the interridge zone and has a wider range of temperature fluctuation. This occurs because the ridge is drier than the interridge zone due to greater root mass and more water uptake. Because the soil on the ridge is drier than the soil in the interridge zone, the heat capacity and thermal conductivity are lower. The soil in the interridge zone can conduct more heat to and from the subsoil and retain more heat, hence it remains cooler during the day and warmer at night.

#### **14.3 Example 14.3: Leaching of the saline soil column**

The leaching of dissolved substances in soils involves complex chemical interactions among soil phases. This example demonstrates the influence of gypsum on the concentrations of several selected ions in the soil solution during leaching. Water movement, solute movement and chemical interactions are simulated. Here we consider one-dimensional movement of water and solutes. 2DSOIL still requires two columns of nodes to have one element per depth increment, however. The grid shown in Fig. 14.10 has spacing that is dense at the top of the column and gradually increases downwards. We expect steep gradients of water potential and solute concentrations only in the upper part of the column. Since the horizontal spacing does not matter for one-dimensional simulations, a 1-cm width was chosen. The soil in the column is homogeneous. Cation exchange properties of the soil are illustrated in Fig. 14.11 for solutions of  $\text{CaCl}_2\text{-NaCl-H}_2\text{O}$  and  $\text{CaCl}_2\text{-MgCl}_2\text{-H}_2\text{O}$ . The equilibrium contents of exchangeable Na depend not only on the Na fraction in solution but also on total concentration of the ions in solution. The

smaller the total concentration, the smaller is the exchangeable sodium fraction provided the fraction of total sodium in the solution is the same. The equilibrium contents of magnesium depend only on the magnesium fraction in the solution. The selectivity coefficient of Ca-Mg exchange at 100 meq/L is close to 1 and the corresponding line in Fig. 14.11 is close to the 1:1 line.

The initial gypsum and calcite contents were both 0.05 g per g of soil, and the exchangeable cation contents were 0.07, 0.05, and 0.02 eq per kg of soil for  $\text{Ca}^{2+}$ ,  $\text{Mg}^{2+}$ , and  $\text{Na}^+$ , respectively. The solution was saturated with respect to gypsum and calcite at 0.005 atm partial  $\text{CO}_2$  pressure and the partial pressure of  $\text{CO}_2$  was held constant in the column.. The sum of cations in the initial soil solution concentration was about 70 meq  $\text{L}^{-1}$  and the concentrations of cations were 27.4, 20.4, and 22.5 meq  $\text{L}^{-1}$  for  $\text{Ca}^{2+}$ ,  $\text{Mg}^{2+}$ , and  $\text{Na}^+$  respectively. The main anion was sulphate, there were 58.2 meq  $\text{L}^{-1}$  of  $\text{SO}_4^{2-}$  against 10 meq  $\text{L}^{-1}$  of  $\text{Cl}^-$ . The water applied for leaching had a very low content of soluble salts: 0.01 meq  $\text{L}^{-1}$  of  $\text{Ca}^{2+}$ ,  $\text{Mg}^{2+}$ ,  $\text{Na}^+$ , and  $\text{Cl}^-$ , 0.02 meq  $\text{L}^{-1}$  of  $\text{SO}_4^{2-}$  and a ponding depth of 2 cm was maintained during the whole run of 40 days simulated time. The initial soil matric potential was -150 cm, and the saturated hydraulic conductivity was  $1 \text{ cm day}^{-1}$ .

Results of the simulations are summarized in Fig. 14.12 for the top 20-cm layer where noticeable changes occurred during the simulated time. The chloride ion had the simplest behavior as it gradually leached. The main mechanisms for chloride transport included convective transport by moving water and hydrodynamic dispersion due to variations in velocities among different regions of the pore space. The concentration profiles of magnesium and sodium were influenced not only by solute transport mechanisms but also by cation

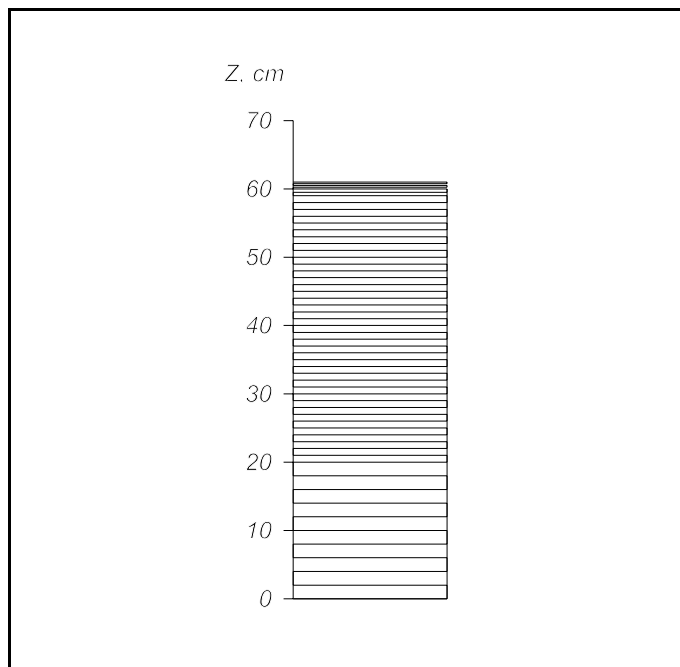


**Figure 14.10** Finite element grid for one-dimensional simulations of Example 3.

exchange. The concentration of magnesium decreased with time at all depths but the magnesium concentration did not decrease as fast as did the chloride ion's concentration because the solution had a constant source of magnesium in the soil. As gypsum continuously dissolved, calcium ions were exchanged with magnesium. The sodium concentration decreased with time much faster than did magnesium, partly because the Ca-Na cation exchange depended on solute concentration. The graphs in Fig. 14.12 suggest that the leaching of sodium was accelerated by the decrease of total concentration of soluble salts in solution. A small but sharp decrease in sodium and magnesium

concentrations during the first day of leaching can be explained by dilution.

The infiltration front moved 9 cm by 0.5 day and then to the 16 cm depth after 1 day of simulated time. The decrease in concentration attributed to dilution took place at a depth less than that of the infiltration front.

The sulphate ion concentration was influenced by the dissolution-precipitation of gypsum and solute transport. The sulfate concentration stayed relatively high as long as some gypsum was present in the solid phase. However, the sulfate concentration also gradually decreased with time in the upper part of the column in the presence of gypsum due to the decrease of the total concentration of soluble salts in solution. When the calcium concentration was nearly constant, the sulphate concentration increased as well as the total concentration of soluble salts. At day 40 the gypsum was apparently leached from the upper 2 cm layer and the sulphate ion concentration was decreasing primarily due to convective-dispersive transport without chemical interactions.

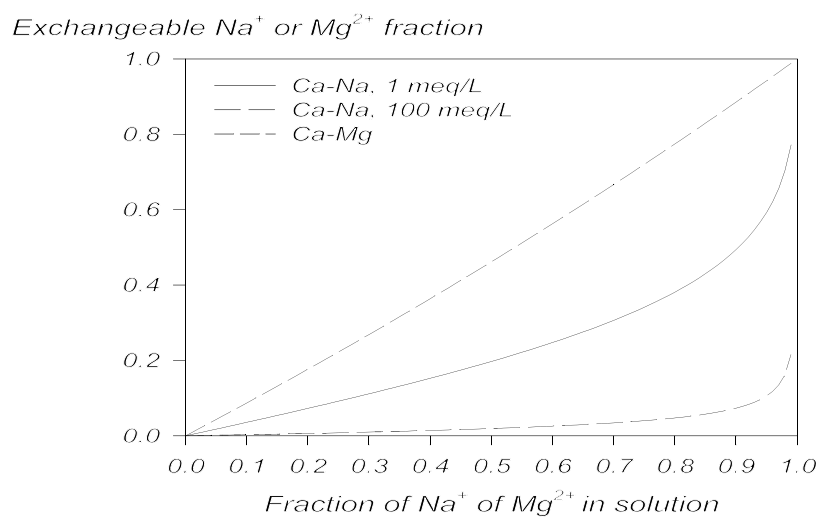


**Figure 14.11** Equilibrium contents of cations in the solution and in soil exchangeable complex after binary cation exchange Ca-Mg and Ca-Na from solutions of calcium, magnesium and sodium chlorides.

The calcium ions demonstrated the most complex behavior as their concentration was dependent on the solubility of gypsum and calcite, cation exchange, and solute transport phenomena. Relatively high levels of calcium were maintained as long as gypsum was present in the solid phase. During the last 30 days, calcium concentration slightly increased with time as a result of the decrease of magnesium sulphate and sodium sulphate in solution. The latter are known to inhibit the solubility of gypsum. After the depletion of gypsum, the calcium concentration began to decrease under the influence of convective-dispersive solute transport. We can expect the calcium concentration to stabilize at the level that corresponds to the solubility of calcite. Because the solubility of calcite is low the calcium concentration had not stabilized during the simulation time.

This simulation illustrates the complex process interactions that can occur in the vicinity of granules of sparingly soluble fertilizers in soil. The importance of soil chemical interactions and solute transport for fertilizer efficiency can be initially examined by means of modeling. In many cases 2DSOIL can be used after addition of an appropriate chemical module.

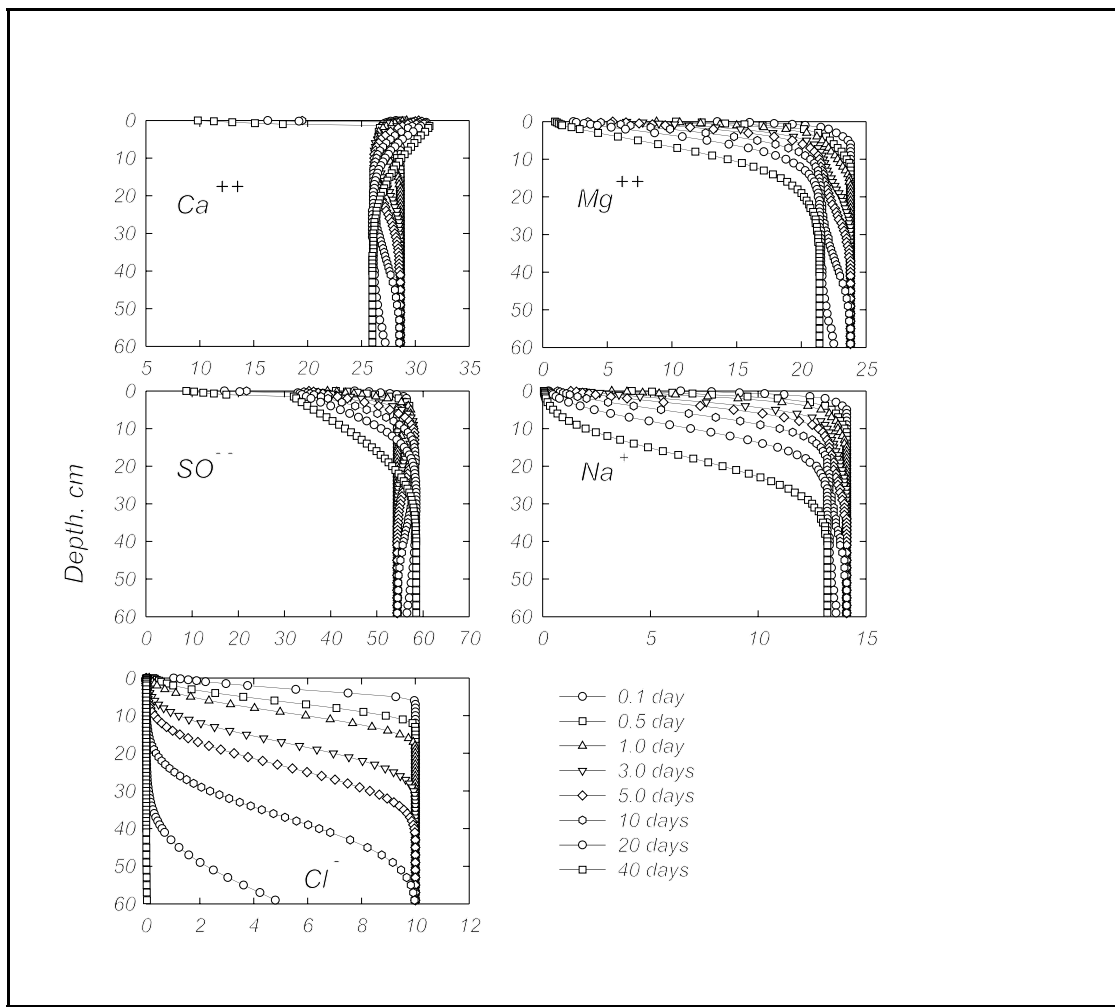


**Figure 14.12** Simulated distributions of ions in the soil solution of the soil column at different stages of leaching

#### **14.4 Example 14.4: Nitrogen dynamics in the soil and plant uptake of nitrogen**

The purpose of this example is to illustrate the addition and use of the soil nitrogen module **SoilNitrogen**. A new module, **SoluteUptake**, has also been introduced. In this example we present two scenarios, fertilizer banded on the ridge and fertilizer applied evenly all along the soil surface. The other modules used are **Watuptake01**, **Shootimitator01**, **Setsurf02**, **HeatMover**, **SoluteMover**, and **Mngm**. There are two fertilizer applications, one at planting and the other 30 days after planting. For the banded application, fertilizer is initially applied to the top of the ridge. The top dressing is applied at the side of the ridge and buried. In the case of the even application, the top dressed nitrogen is also applied to all the surface nodes. The same amount of fertilizer is applied in both cases. Here, the nodal concentrations of N have been adjusted for the initial fertilization in the initialization file ‘*Nodal\_S.dat*’. A management module has been added to simulate fertilization with additional nitrogen 30 days after germination. This module is described in greater detail in section 15. The grid used in this example has the shape of a ridge-furrow system and is similar to the grid used in Example 14.2. The weather data is shown in Figure 14.13 and the soil hydraulic properties are in Fig 14.7. The initial amount of nitrate-N for the profile in both cases is  $169 \text{ kg N ha}^{-1}$ . The soil organic matter content is  $1.6 \text{ kg kg}^{-1}$  soil. It is assumed that 60% of the organic matter is carbon and the ratio of N to C is 1:10.

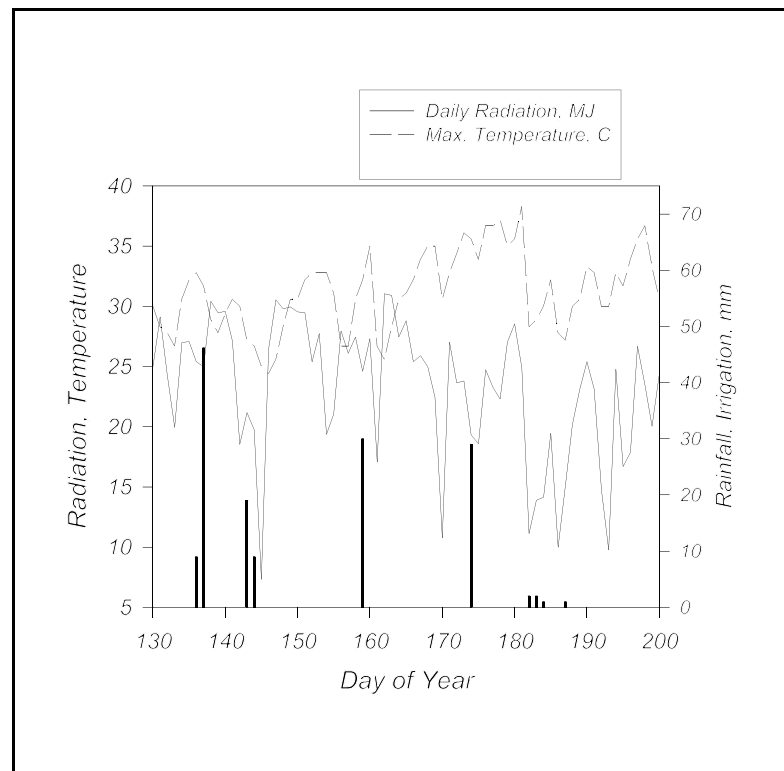


**Figure 14.13** Weather data for example 14.4

Nitrogen is added at the rate of  $150 \text{ kg ha}^{-1}$  for the first fertilization and  $100 \text{ kg ha}^{-1}$  for the second fertilization. Nitrogen uptake is proportional to the water uptake and the nitrogen concentration in the element from which the water is extracted. The shoot imitator described in Section 10 was used to simulate above-ground plant growth.

Cumulative nitrogen uptake and  $\text{NO}_3\text{-N}$  content in the soil as a function of time for both treatments are in Figure 14.14. Total nitrogen uptake for the banded treatment was greater than for the uniform nitrogen application ( $153 \text{ kg ha}^{-1}$  vs  $99 \text{ kg ha}^{-1}$ ). As a result, the  $\text{NO}_3\text{-N}$  content of the soil with the uniform N application was greater at the end of the season. Cumulative water uptake for the plant with the banded fertilizer application was also higher (Fig 14.14), this also contributed to the larger N uptake. The plant receiving the banded application also grew taller

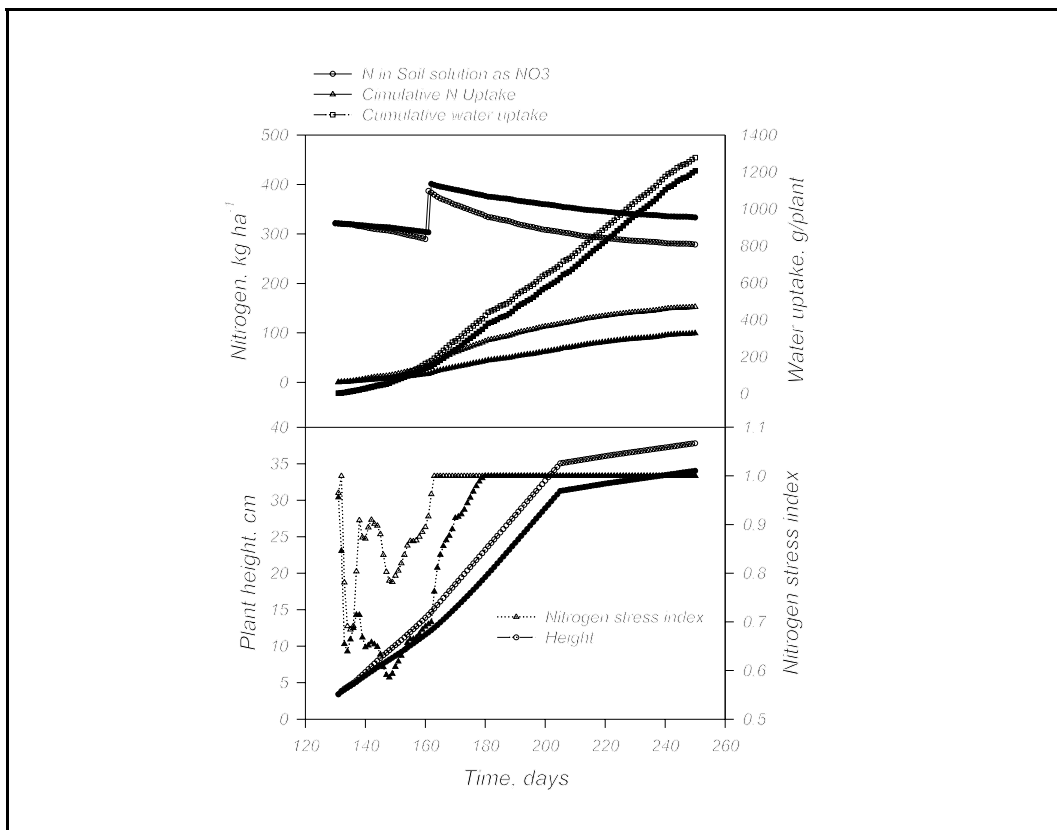


**Figure 14.14** Plant uptake of water and nitrogen, nitrogen as  $\text{NO}_3$  in the soil, nitrogen stress and plant height for Example 14.4 for two methods of nitrogen application, banded and uniformly applied. The open symbols represent data for the banded application and the closed symbols uniform application.

because there was less nitrogen stress (Fig 14.14). This also contributed to the greater uptake of water and hence nitrogen in the banded treatment. The nitrogen stress early in the season is probably unrealistic and is due to the lack of N reserve in seed which usually carries a plant through its early growth stages. The distribution of  $\text{NO}_3^-$  in the soil for both treatments was similar (Fig 14.15). The nitrate, however, was more dispersed in the right side of the profile in the banded treatment. This probably reflects distribution of nitrate under the influence of root activity alone. The zone of high nitrate concentration at the right of the profile is more distinct in the uniform application which reflects the addition of nitrogen at the surface.

The amount of nitrogen remaining in the soil profile at the end of the growing season was higher for the uniform application than for the banded application. This may result in greater leaching losses of N over the winter season from the profile to which the nitrogen was applied uniformly. The banded nitrogen was used more efficiently because it was placed close to where there was the largest density of roots.

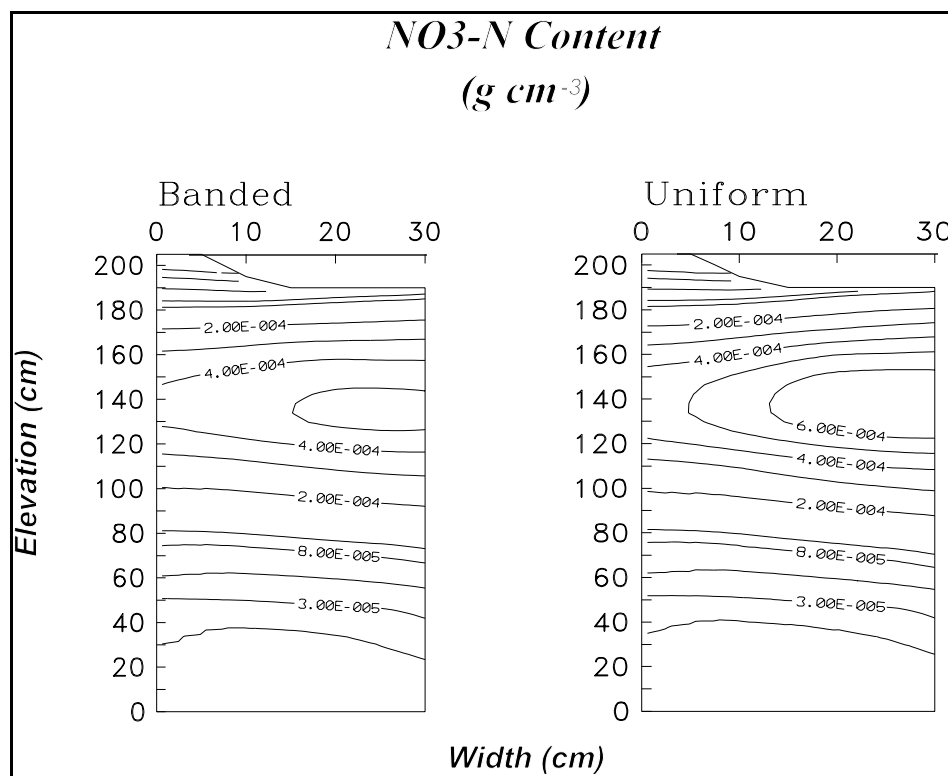


**Figure 14.15** Nitrate distributions after last day of simulations for Example 14.4.



# Chapter 15: Addition or Replacement of Soil Process Modules.

**Dennis Timlin and Yakov Pachepsky**

The rules listed below will guide the user to add or replace a process module in 2DSOIL. Illustrations of the application of these rules are also given in this section.

## **15.1 Rules for introducing a new module**

The modules of 2DSOIL interact by sharing public variables that may be used or updated by any other process module. The list of public variables is given in Table 15.1 and are collected in the file '**public.ins**'. This is an 'INCLUDE' file that contains declarations and COMMON statement definitions for all the public variables. A reference to this file name must be at the beginning of the source code for every process module. The user must also be careful not to create any private variables that share the same name as a public variable. The placement of a module relative to other modules is also important because the sequence reflects the method by which transport processes and intrasoil interactions are decoupled during a time step. Transport calculations precede any calculations of intrasoil interactions because transport calculations require time steps and use values of sources and sinks from the previous, or 'old', time level. Intrasoil and surface interactions may use soil state variable values both from the current, or 'new' time step and/or from the previous or 'old' time step. Among transport modules the **WaterMover** must be called first because it produces information, such as water velocities, that other transport modules require.

Rules for introducing a new module are listed below.

1. A new module can use soil state variables that are public and are listed in Table 15.1. Other soil state variables not needed by other modules must only be present in the list of private variables for the new module.
2. There are two special cases for handling variables, these are:

- a. Variables that are used by several modules but not modified by any modules and not calculated using specific parameters. They can be either

- i. GLOBAL, and input or initialized by a particular module or
  - ii. LOCAL, and read by each module that uses that variable.

For example, bulk density is used by more than one module, e.g., the chemistry and the root growth modules. If none of the process modules change bulk density, then each module reads bulk density from its own data files. Therefore, a new module will use this variable as private if this module does not change bulk density.

- b. Variables that are used by several modules and modified during calculations or calculated using parameters. The following apply for this case:

- i. The variables are GLOBAL.
  - ii. The variables should be modified or initialized by only one module though, in practice, this may not always be practical.
  - iii. The variable or the parameters used to calculate it must be read in by the module that does the modifications.
  - iv. This module that reads a variable or its parameters must be called to initialize the variable before other modules that use the variable are called.
  - v. The variable will be stored in a COMMON block in a section with its own name.

An example is bulk density. Bulk density can be changed by tillage but is also used in root growth or chemistry routines. Because the tillage module changes bulk density, this module should read it in and be called before the root growth or chemistry modules.

- 3. A replacement module must update all public variables that were updated by the module being replaced. For example, if a new water mover that simulates steady state water movement and a stationary velocity field is introduced, this water mover must still produce actual values of boundary fluxes. Table 15.2 shows which variables are updated by each module.

4. Calculation of sinks or modification of soil state variables must be done for the whole grid, if the region of changes is not specified. For example, if a soil denitrification module is introduced, it must update nitrate concentrations in all grid nodes. However, if the module simulates a nitrogen fertilizer application to the soil surface, then nitrate concentrations must be updated only in the designated nodes.
5. If a new module has special time step requirements, it must update certain variables in the '*time\_public*' common field (see Table 15.1). If a new module simulates transport processes, it must update the corresponding *DtMx* value at the beginning of simulation and after every time it updates the soil state variables. If a new module has its own time step or it will act only at prescribed times, then it must update the corresponding *tNext* value at the beginning of the simulation, and after every time it is called and updates soil state variables.
6. It is advisable to use Fig. 1.3. as a template for a new module.
7. If a new module uses or introduces plant parameters, it is the responsibility of the user to add plant variables to the '**puplant.ins**' file to be linked with plant and root modules.

Three simple examples that illustrate the addition of a module are given here. These new modules are: 1) a management module to add fertilizer, 2) a root respiration module, and 3) a solute uptake module.

## **15.1 Overview of the examples**

### **15.1.1 Example 15.1: A management module for chemical application**

This example is a simple management module, called **Mngm**, that simulates surface chemical application with instantaneous dissolution at a given time within the growing season. At time *tAppl* the mass of the chemical in (g/L) near the soil surface in nodes *nAppl(1)*, *nAppl(2)*, ..., *nAppl(NumAp)* is set equal to *cAppl*. The FORTRAN code of the module is shown in Fig. 15.1.

```

*
*||||||||||||||||||||||||||||||||||||||||||*
Line # * Chemical application module - example 1 from section 15.1 *
*||||||||||||||||||||||||||||||||||||||*
1   Subroutine Mngm()
2   Include 'public.ins'
3   Common /Mngmnt/tAppl, cAppl, NumAp, nAppl(NumBPD), ModNum
4   If (lInput.eq.1) then
5       Open(40,file='Mngm.dat')
6       Read(40,*,ERR=20) tAppl, cAppl, NumAp
7       Read(40,*,ERR=20) (nAppl(I),I=1,NumAp)
8       NumMod=NumMod+1
9       ModNum=NumMod
10      ModNum=ModNum
10      Close(40)
11      tNext(ModNum)=tAppl
12      Endif
13      If(Abs(Time-tNext(ModNum).lt.0.001*Step) then
14          Do I=1,NumAp
15              Conc(nAppl(I),3)=cAppl/ThNew(nAppl(I))
16          Enddo
17          tNext(ModNum)=1.E+32
18      Endif
19      Return
20      Stop 'Mngm data error'
21      End

```

**Figure 15.1** Listing of FORTRAN code for a chemical application module.

- ▶ Line 1 names the module. The module must be invoked in the main program. Since the module must make it's calculations after the end of a time step **Mngm** must be called after all soil process subroutines.
- ▶ Line 2 makes all public information available to this module.
- ▶ Line 3 defines the common field *Mngmnt* as a storage of private information and lists the private variables: *tAppl* -application time, *cAppl* -applied concentration, *NumAp* - total number of nodes to which fertilizer is applied; and *nAppl* -the number of application nodes.
- ▶ Lines 4 - 11 describe actions of the module during the initialization stage at the beginning of the simulation run. Private time-independent information is read from the external unit 40, which is then closed because this unit number may be used by other modules. Any errors during file read statements will lead to termination of the run, as shown in line 18. The module is given a sequential number, *ModNum*, as an identifier and the variable that

hold the number of module,  $ModNum$ , is updated. Because one of the time steps must end exactly at  $tAppl$ ,  $tNext(ModNum)$  is set to  $tAppl$ .

- ▶ Lines 13 - 18 describe the actions of the module during the simulation run. If simulated time value  $Time$  coincides with the application time ( $tAppl$ ), then the concentration of the first solute is altered in given nodes. Because the module will not be invoked again,  $tNext(ModNum)$  is given an unreachable value.

The use of this module is illustrated in Section 15.4.1

### 15.1.2 Example 15.2: Simulation of root respiration

Root respiration is a source of  $\text{CO}_2$  in soil. This module, called **GasUptake**, will modify the concentration of gas # 1 in the soil atmosphere. The rate of  $\text{CO}_2$  production is assumed to be proportional to the increase in root mass in the soil:

$$G_g = \alpha_g \frac{d\rho_R}{dt} \quad (15.1)$$

where  $G_g$  is the rate of  $\text{CO}_2$  supply due to root respiration,  $\text{g cm}^{-3} \text{ day}^{-1}$ ;  $\rho_R$  is root mass density;  $\text{g cm}^{-3}$ ;  $t$  is time, day; and  $\alpha_g$  is respiration rate constant,  $\text{day}^{-1}$ . Derivation of the model equation and values of  $\alpha_g$  may be found in the work of Penning de Fries (1975). For a finite difference approximation of equation 15.1 using discrete time steps we replace the derivative in the right side by the difference:

$$G_g = \alpha_g \frac{m_R^{new} - m_R^{old}}{A\Delta t} \quad (15.2)$$

Here  $m_R^{new}$  is root mass in the soil cell at the new time level,  $m_R^{old}$  is root mass in the soil cell at the old time level,  $A$  is area of the cell, and  $\Delta t$  is time step.

The FORTRAN code of the module is shown in Fig. 15.2.

- ▶ Line 1 names the module which must be invoked in the main program. **GasUptake** is called after all soil transport process modules because **GasUptake** has a time step, and so must work during every time step.

```

*|||||||||||||||||||||||||||||||||
Line # * Root respiration module - example 2 from section 15.1      *
*|||||||||||||||||||||||||||||
1   Subroutine GasUptake()
2   Include 'public.ins'
3   Common /GasCom/ alphaR, RTWTOLD(NumElD),ModNum
4   If (lInput.eq.1) then
5       Open(40,file='GasUpt.dat')
6       Read(40,*,ERR=20) alphaR
7       Close(40)
8       Do I=1,NumEl
9           RTWTOLD(I)=RTWT(I)
10      Enddo
11      NumMod=NumMod+1
12      ModNum=NumMod
13      tNext(ModNum)=1.0E+32
14      Endif
15      Do I=1,NumEl
16          gSink(i,I)=alphaR*(RTWT(I)-RTWTOLD(I))/Area(I)/Step
17          RTWTOLD(I)=RTWT(I)
18      Enddo
19      Return
20      Stop 'GasUpt data error'
21      End

```

**Figure 15.2** Listing of FORTRAN code for a root respiration module

- ▶ Line 2 makes all public information available to this module.
- ▶ Line 3 defines the common field *GasCom* as storage of private information and presents the list of private variables: *alphag* and *RTWTOLD*. The latter variable represents root mass in soil cells at the previous or 'old' time level. This value is needed because *RTWT* has a new value each time *GasUptake* is called and the old value is not available in the public data block. Because the *GasUptake* module needs the 'old' values of *RTWT*, it stores it as its own private information.
- ▶ Lines 4 - 13 describe actions of the module in the beginning of the simulation run. Private time-independent information is read and the external unit 40 is closed. The module is given a sequential number, *ModNum*, as an identifier and the variable that hold the number of module, *ModNum*, is updated. This module will not specify limitations on the time steps, and therefore *tNext(ModNum)* is set to an unreachable value of 1.E+32.

- ▶ Lines 15 - 18 describe the actions of the module during a simulation run. Because the module is executed at every time step, there is no check of coincidence between simulated time, *Time*, and some specific time as in the previous example. In all nodes, *gSink* receives a new value. The 'new' RTWT will be the 'old' one at the next time step and the necessary assignment is made.

The use of this module is illustrated in Section 15.3.2

## **15.2 Solute uptake module**

This module calculates passive solute uptake by roots as they take up water. The total solute uptake is calculated from the concentration of the solute in the water taken up by the roots and the amount of water. This module was used in example 4 of Chapter 14, the example using nitrogen.

```

*****      Solute Uptake subroutine from Example 14-4*****
1      subroutine SoluteUptake()
2      include 'public.ins'
3      IncLude 'Puplant.ins'
4      Include 'Puweath.ins'
5      real bi(3),ci(3)
6      Common /SUP/ TotWSink,TotSSink
7      If(lInput.eq.1) then
8          TotWSink=0.
9          TotSSINK=0.
10     Endif
11     SincrSink=0.
12     WincrSink=0.
13 C calculate sum of N in all forms in soil using triangluar elements
14     Do n=1,NumEl
15         CSink(n,1)=0.
16         NUS=4
17         if(KX(n,3).eq.KX(n,4)) NUS=3
18 *      Loop on subelements
19         AE=0.0
20         do k=1,NUS-2
21             i=KX(n,1)
22             j=KX(n,k+1)
23             l=KX(n,k+2)
24             Ci(1)=x(l)-x(j)
25             Ci(2)=x(i)-x(l)
26             Ci(3)=x(j)-x(i)
27             Bi(1)=y(j)-y(l)
28             Bi(2)=y(l)-y(i)
29             Bi(3)=y(i)-y(j)
30             AE=AE+(Ci(3)*Bi(2)-Ci(2)*Bi(3))/2.
31             Csink(n,1)=CSink(n,1)+(Conc(i,1) +
32             &           Conc(j,1)+Conc(l,1))/3.
33             Enddo
34             Csink(n,1)=CSink(n,1)*Sink(n)
35             SincrSink=SIncrSink+cSink(n,1)*step*I4./62.*AE
36             Enddo
37         enddo
38         TotWSink=TotWSink+WIncrSink
39         TotSSINK=TotSSINK+SIncrSink
40         return
41     end

```

**Figure 15.3** Listing of FORTRAN code for the solute uptake module

Table 15.1. Public soil state variables used for the exchange of information among modules.

Variable	Description	Reference chapter
	Parameters	
NumNPD	Maximum number of nodal points	3
NumElD	Maximum number of elements (soil cells)	3
NumBPD	Maximum number of boundary points	3, 5
NSeepD	Maximum number of seepage surfaces	3, 6
NumSPD	Maximum number of nodal points on the seepage surfaces	3, 6
NumSD	Maximum number of solutes	7
NumGD	Maximum number of gases	9
NMatD	Maximum number of different soil layers or horizons	3
NumObjD	Maximum number of soil process modules	2
MBandD	Maximum allowed difference between numbers of corner nodes for any two elements having at least one common node	6, 7, 8, 9
common /object_public/		
NumObj	Number of modules describing soil processes	2
CObj	Switch to show if the module is included in the present simulation run	2
KAT	Switch to show if axisymmetrical or planar movement is to be simulated	2, 6, 7, 8
NumSol	Actual number of solutes	7
NumG	Actual number of gases	9
common /grid_public/		
NumNP	Actual total number of nodal points	3
NumEl	Actual total number of elements (soil cells)	3
IJ	Maximum number of nodes along the transverse grid lines	3
MBand	Actual maximum difference between numbers of corner nodes for any two elements having at least one common node	3
x	Transverse coordinates of nodal points	3
y	Vertical coordinates of nodal points	3
KX	Numbers of corner nodes for every element	3
Area	Areas of elements (soil cells)	3, 6

Variable	Description	Reference chapter
common /nodal_public/		
hNew	Nodal pressure heads at the end of current time step	6
ThNew	Nodal moisture contents at the end of current time step	6
Vx	Nodal transverse water velocities at the end of current time step	6
Vz	Same as above for vertical water velocities	6
Q	Nodal water fluxes at the end of current time step	6
Conc	Nodal concentrations of solutes in soil solution at the end of current time step	7,11
Tmpr	Nodal temperature values at the end of current time step	8
g	Nodal gas contents in soil air at the end of current time step	9
MatNumN	Number of soil layer or horizon in which node occur	3
Con	Nodal soil hydraulic conductivity	6
Tcon	Nodal soil thermal conductivity	8
common /elem_public/		
Sink	Water extraction rates for elements	6,10
cSink	Solute extraction rates for elements	7
gSink	Gas extraction rates for elements	9
MatNumE	Number of soil layer or horizon in which element occurs	3
RTWT	Root mass in the elements (soil cells)	10
common /bound_public/		
NumBP	Actual total number of boundary points	3,4,5
NSurf	Total number of nodes on the soil-atmosphere surface	5
NVarBW	Total number of boundary nodes where time-dependent water fluxes or pressure heads are prescribed	3,4,6
NVarBS	Total number of boundary nodes where time-dependent solute concentrations are prescribed	3,7
NVarBT	Total number of boundary nodes where time-dependent temperatures are prescribed	3,8
NVarBG	Total number of boundary nodes where time-dependent gas contents are prescribed	3,9
NSeep	Actual total number of seepage faces	3
NSP	Total number of nodes at every seepage face	3

Variable	Description	Reference chapter
NP	Nodal numbers of boundary points at seepage faces	3
KXB	List of boundary node numbers	3
Width	Width of strips associated with boundary nodes	3
CodeW	Codes of boundary condition for water movement	3, 4
CodeS	Same as above for the solute movement	3, 4
CodeT	Same as above for the heat movement	3, 4
CodeG	Same as above for the gas movement	3, 4
VarBW	Boundary pressure heads or water fluxes	3, 4, 5
VarBS	Boundary concentrations or fluxes of solutes	3, 4, 5
VarBT	Boundary temperatures or heat flux components	3, 4, 5
VarBG	Boundary gas contents or gas flux components	3, 4, 5
EO	Potential transpiration rate from the unit of crop area	5, 10
Tpot	Potential transpiration from the unit soil area	5, 10
common /time_public/		
lInput	Switch to show if initial data have to be read	2
tNext	Obligatory time step end times	2
Tinit	Time of the beginning of calculations	2
Time	Current value of the time step end time	2
Step	Current time step	2
tAtm	Time of the next soil-atmosphere boundary update	5
Iter	Maximum number of iterations in soil transport modules	2
dtMin	Minimum reasonable time step	2
DtMx	Maximum next time steps allowed by soil transport process modules	2, 6, 7, 8, 9
tTDB	Time of the next update of the time-dependent boundary conditions	4
Tfin	Time of the end of calculations	2

Table 15.02. Alteration (\*) of public variables by modules of 2DSOIL

Table 15.02. Alteration (\*) of public variables by modules of 2DSOIL

Table 15.02. Alteration (\*) of public variables by modules of 2DSOIL

Variable	obj_time	grid bnd	synchron	set srf1	set srf2	set TDB	wat mov	sol mov	heat mov	gas mov	wat upt1	wat upt2	macro chem
NumSol	-	-	-	-	-	-	-	*	-	-	-	-	-
NVarBG	-	*	-	-	-	-	-	-	-	-	-	-	-
NVarBS	-	*	-	-	-	-	-	-	-	-	-	-	-
NVarBT	-	*	-	-	-	-	-	-	-	-	-	-	-
NVarBW	-	*	-	-	-	-	-	-	-	-	-	-	-
Q	-	-	-	-	-	-	*	-	-	-	-	-	-
RTWT	-	-	-	-	-	-	-	-	-	-	*	-	-
Sink	-	-	-	-	-	-	-	-	-	-	*	*	-
Step	-	-	*	-	-	-	*	-	-	-	-	-	-
tAtm	-	-	-	*	*	-	-	-	-	-	-	-	-
TCon	-	-	-	-	-	-	-	-	*	-	-	-	-
tFin	*	-	-	-	-	-	-	-	-	-	-	-	-
ThNew	-	-	-	-	-	-	*	-	-	-	-	-	-
Time	-	-	*	-	-	-	*	-	-	-	-	-	-
tInit	*	-	-	-	-	-	-	-	-	-	-	-	-
Tmpr	-	-	-	-	-	-	-	-	*	-	-	-	-
tNext	-	-	-	-	-	-	-	-	-	-	*	*	-
Tpot	-	-	-	*	*	-	-	-	-	-	-	-	-
tTDB	-	-	-	-	-	*	-	-	-	-	-	-	-
VarBG	-	-	-	*	*	*	-	-	-	-	-	-	-
VarBS	-	-	-	*	*	*	-	-	-	-	-	-	-
VarBT	-	-	-	*	*	*	-	-	-	-	-	-	-
VarBW	-	-	-	*	*	*	-	-	-	-	-	-	-
Vx	-	-	-	-	-	-	*	-	-	-	-	-	-
Vz	-	-	-	-	-	-	*	-	-	-	-	-	-
Width	-	*	-	-	-	-	-	-	-	-	-	-	-
x	-	*	-	-	-	-	-	-	-	-	-	-	-
y	-	*	-	-	-	-	-	-	-	-	-	-	-

### 15.3 The examples: Specific applications and simulation results

### 15.3.1 Example 15.1. A chemical application module: influence of the root system on chemical transport

This example demonstrates the addition of a new module to carry out a management practice, in this case application of a chemical. The example is a simulation of solute movement in row and interrow zones of a row crop. The roots of a crop planted in rows will dry the soil under the rows more rapidly than between the rows by nature of the uneven root distribution. Because the soil is more wet between the rows than in the row zone, the wetting front during infiltration will penetrate deeper in the interrow zone than in the row zone. As a result, there will also be higher solute fluxes in the interrow zone than in the row zone. The modules used for this simulation are **Mngm**, the management module that applies the chemical at a specified time as described in Section 15.1, **WaterMover**, **SoluteMover**, **RootWaterUptake01**, and **SetSurf01**.

The following are the specific steps taken to incorporate the management module **Mngm** into 2DSOIL.

Changes in program loading. A line to invoke **Mngm** is inserted into the main program (2dmain.For), then the file 'Mngm.for' (Fig. 15.1) is compiled and linked with the other modules.

#### Changes in data files.

(1) A new file 'Mngm.dat' that provides input data for Mngm ('Mngm.for') is created.

#### Description of the physical

system and parameters. Figure 15.3 is a graphical representation of the finite element grid. A simple rectangular grid with a flat surface boundary was used. Nodes and elements are numbered downward in the z direction with distance between nodes increasing with depth and with lateral distance. The soil consisted of one layer and the soil texture was a loam. The soil hydraulic

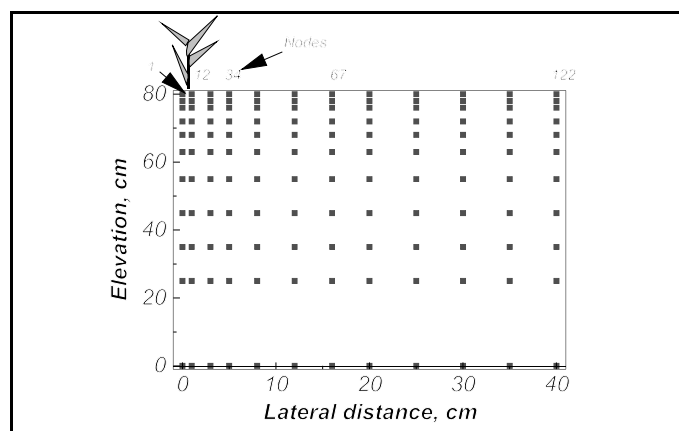


**Figure 15.4** Finite element grid for Example 15.2, nodes and elements are numbered in vertical direction

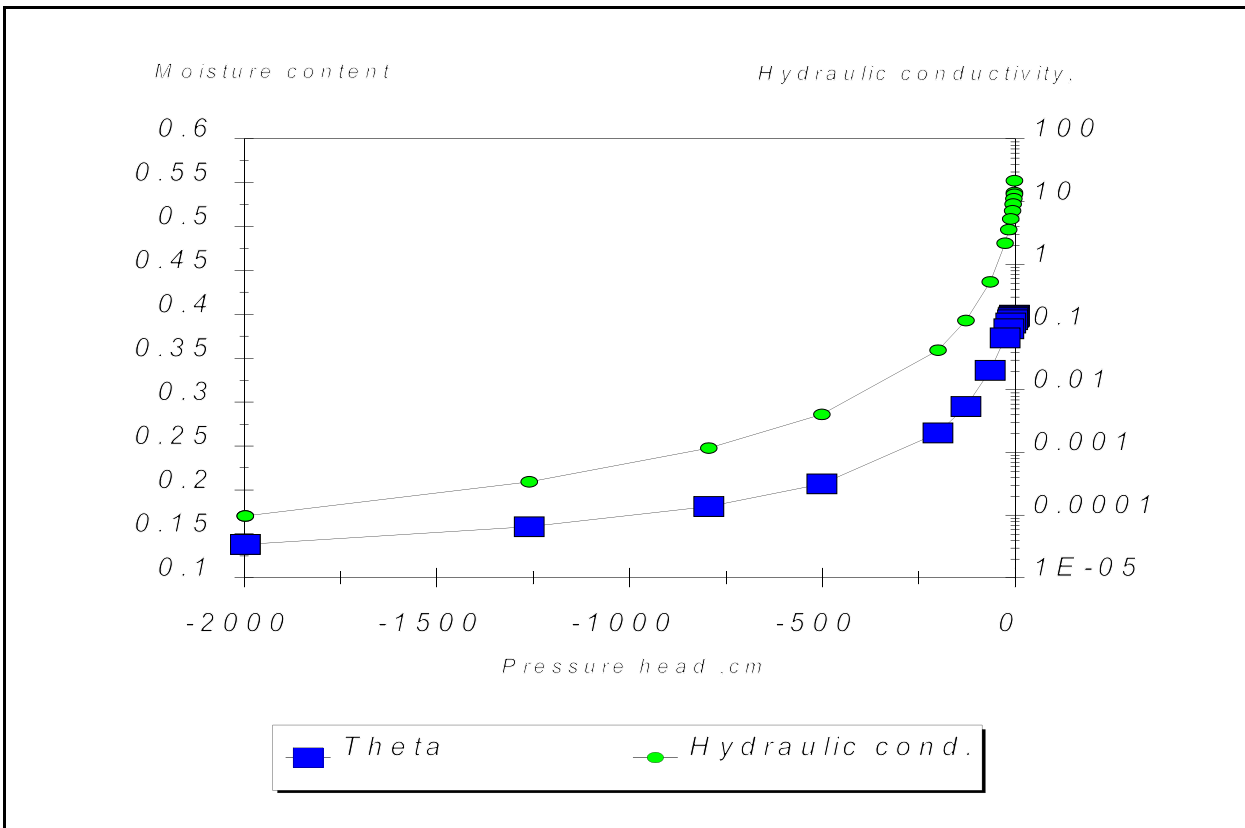


**Figure 15.5** Soil hydraulic functions for Example 15.1

functions are in Fig. 15.4. The atmospheric boundary data, precipitation and evapotranspiration, were input directly from **SetSurf.Dat**. Heat and gas movement were not simulated. The initial chemical concentration was zero throughout the profile, and there were no chemical gradients across the left or right boundaries. The bottom boundary was impermeable to both chemical and water. The plant was placed at the left end of the grid at  $x=0$  cm, and 5 cm deep (Fig 15.3). Soybean root parameters were used. Simulated time began at day 1 and ran a total of 57 days.

The chemical was a non-reactive tracer similar in properties to bromide. Chemical was applied at day 44 at a rate of  $300 \mu\text{g cm}^{-2}$ . During the preceding 44 days, only 11 cm of rain-fall was applied and evapotranspiration was 29 cm. This simulates a moderately dry period. Immediately after chemical application 3 cm of water was applied. The details of the surface boundary data can be found in the file 'SetSurf.Dat'.

Results of simulations. The water content and root distribution before chemical application and water distribution after rainfall are presented in Fig. 15.5. The root distribution is concentrated in the soil under the plant. It can be seen that values of water content are lowest under the plant where the root distribution is high. Water content increases with depth and horizontal distance from the plant. After rainfall, the water contents are still highest in the interrow zone (Fig. 15.5). The chemical concentration directly below the plant row (at  $x=1$ ) and under the interrow position ( $x=35$ ) at day 56 are plotted in Fig. 15.6. There is more chemical in the soil under the row position than the interrow position. Furthermore, the chemical concentrations near the surface are still rather high in spite of 2 rain-fall events after chemical application. Evaporation and transpiration act to move the water with chemical toward the soil surface and toward the plant. This results in concentration of chemical in the soil under the plant and depletion of chemical in the interrow zone.

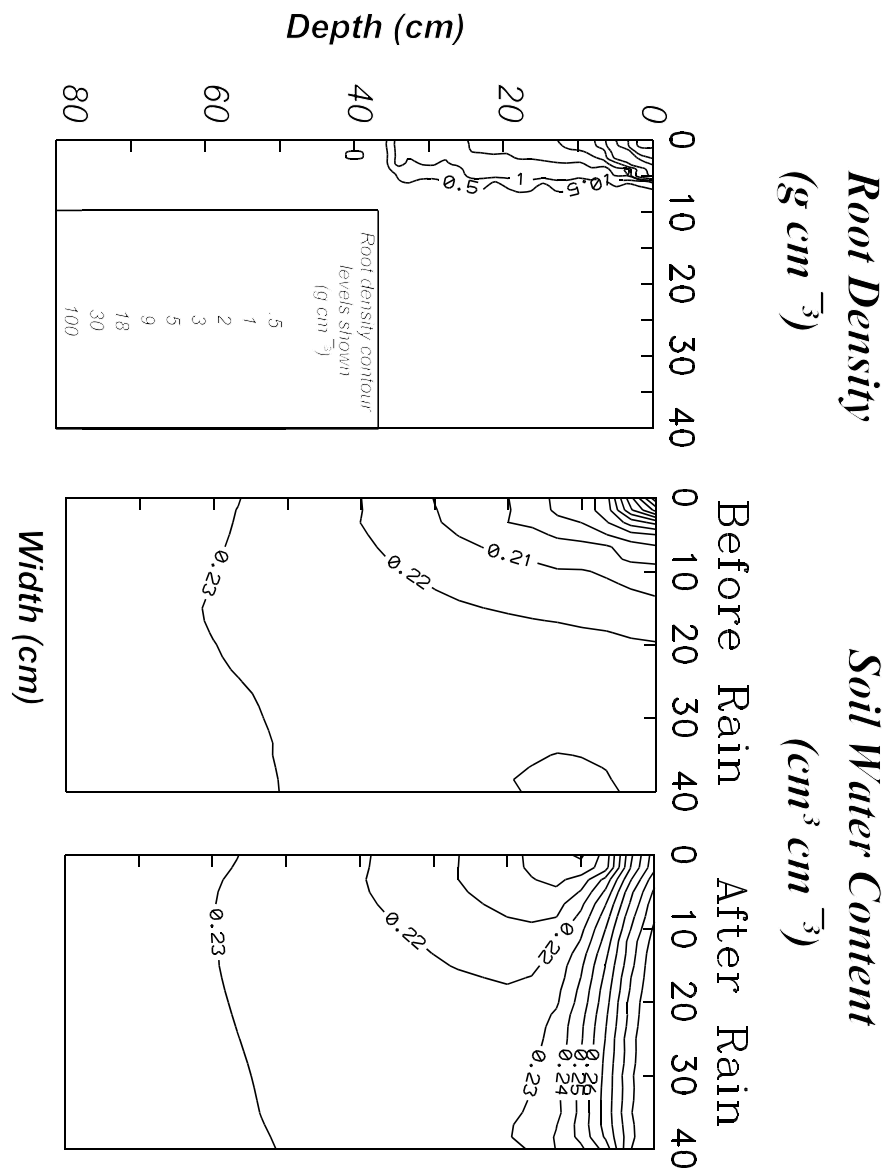


**Figure 15.6** Root density and water content at day 44 before chemical application and rainfall, and water content after chemical application and rainfall, day 44.8.

It has been suggested that placement of chemicals in areas not conducive to leaching would be a possible management practice to reduce leaching of chemicals out of the root zone. This model with a comprehensive plant simulator can be used to evaluate the relative merits of such management practices.

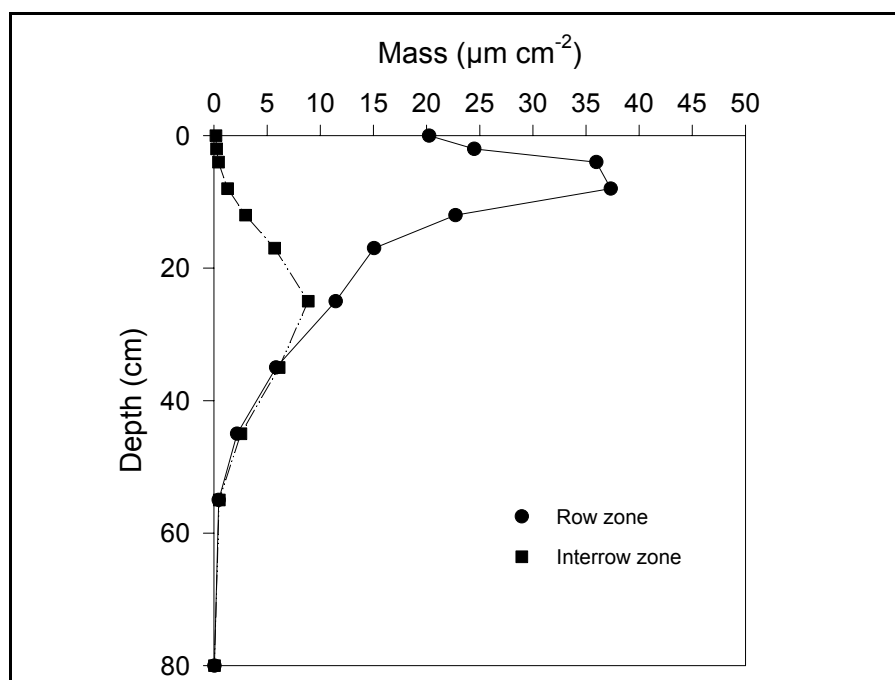


**Figure 15.7** Chemical concentration vs soil depth in the row zone ( $x=1 \text{ cm}$ ) and in the interrow zone ( $x=35 \text{ cm}$ )

An interesting extension to this simulation would be to consider the fluxes of water as precipitation to be nonhomogeneous along the surface.

### 15.3.2 Example 15.2: Adding a module of root respiration: a two-dimensional pattern of CO<sub>2</sub> content in soil induced by root respiration

In this section we take the example in Section 14.1 and add the **GasUptake** module described in Section 15.1.

Changes in program loading. A line is added to the main file '**2DSOIL.FOR**' to call **GasUptake** and the file '**GasUpt.for**' is compiled and linked to other modules.

#### Changes in data files.

- (1) Data file '**Grid\_bnd.dat**' is modified: codes of gas movement boundaries are included.
- (2) Data file '**Weather.Dat**' is modified to include soil-atmosphere gas exchange parameters: parameters *PG* and *GAIR* are added in line 11 according to Table 5.5.
- (3) Data file '**GasUpt.dat**' is added.

All these changes can be traced by comparing files in directories EXE13.1R and EXE15.2 on the distribution diskette.

Results of gas movement simulations. Gas content distributions are shown in Fig. 15.6 for 30 and 60 days after emergence. There is little difference in transversal distributions of gas contents. Diffusion coefficients are very high, and diffusion has enough time to redistribute the

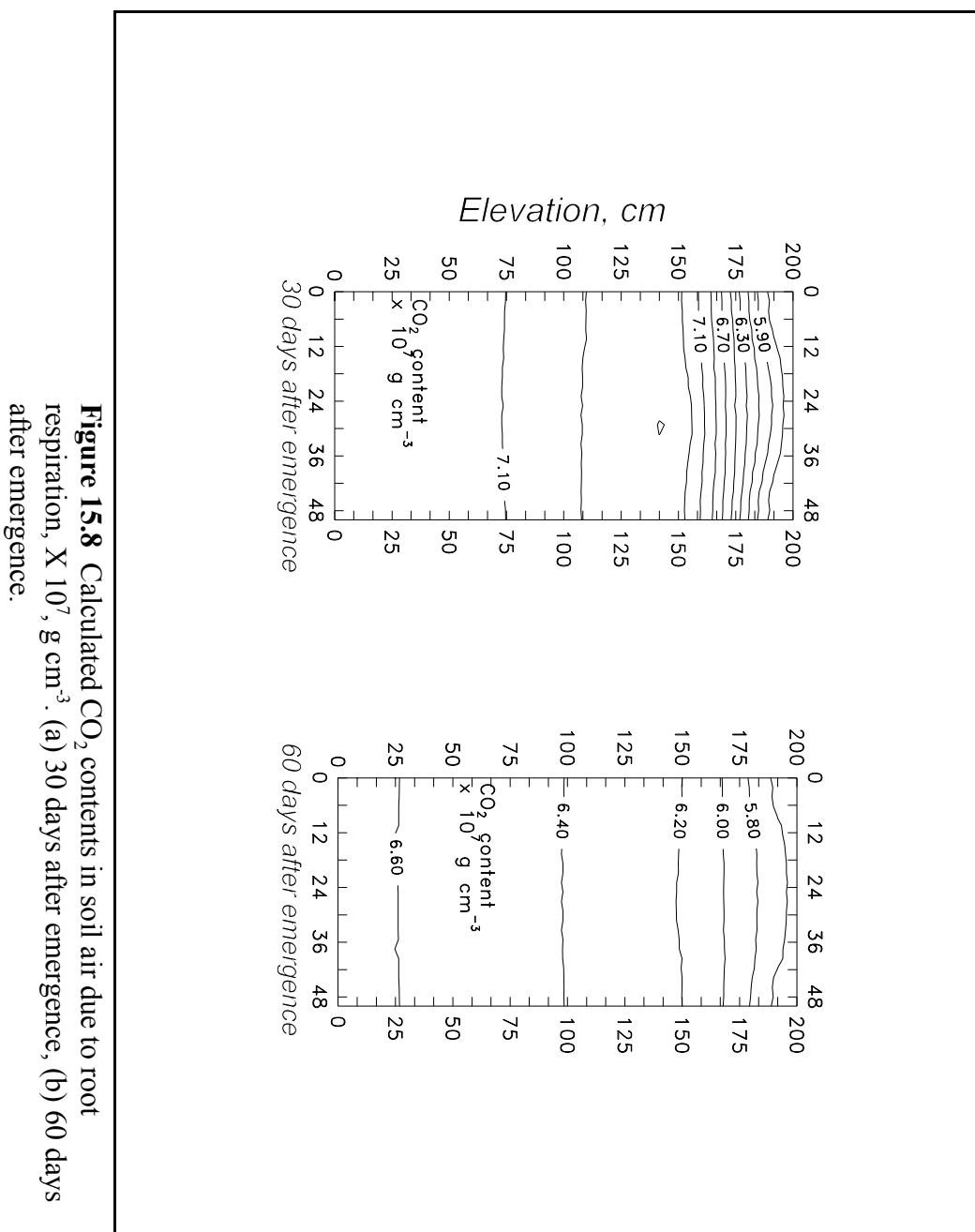


**Figure 15.8** Calculated  $\text{CO}_2$  contents in soil air due to root respiration,  $X 10^7, \text{g cm}^{-3}$ . (a) 30 days after emergence, (b) 60 days after emergence.

CO<sub>2</sub> produced by roots in spite of the common perception of diffusion as a slow process. At early stages of the simulation, gas contents tend to be higher in the row zone than in interrow position. This may be due to the high intensity of early root growth simulated by the shoot imitator. Diffusion moves gas downwards and simultaneously sends it to the atmosphere. As a result, the maximum concentration of CO<sub>2</sub> is found at approximately 80 cm depth. At later stages of the simulation the roots produce less CO<sub>2</sub> and gas exchange between the soil and atmosphere is able to remove almost all excess gas from the soil. CO<sub>2</sub> transport even occurs from deep horizons of the soil.

In general, the calculated gas contents are very low and do not exceed gas contents in the atmosphere by more than 25 %. In a field soil one can readily obtain gas content values that are 10-30 times larger than contents in the atmosphere. This suggests microbial activity must be taken into account for realistic predictions of CO<sub>2</sub> dynamics in soil. One should also consider the more complex tortuosity patterns in field soil as opposed to repacked soils.

# Chapter 16: Modules and Variables of 2DSOIL

Dennis Timlin and Yakov Pachepsky

The modules of 2DSOIL have been designed to be as independent as possible, and only variables (global public variables) needed by two or more modules are shared. The global public variables are stored in a FORTRAN COMMON block that is inserted into each process module via the file ‘**public.ins**’. The division of information into public and private components is one of the important advantages of modular programming and makes the modules of 2DSOIL completely autonomous. There are no subroutines that are shared or otherwise called by more than one module even though two or more modules may use similar algorithms. This has been done to allow a user to substitute their own modules with a minimum of changes to their module. Because most variables are private (i.e., not in common statements shared among modules), there is less chance for conflicts among variable names. The disadvantage is that this structure may result in duplication of code and similar variable names in two or more modules, and longer code.

## **16.1 Structure of the code.**

2DSOIL consists of a main program and a number of subroutines. The subroutines are distributed among a number of source files. A list of source files in the code and routines called is shown in Table 16.1. Although there are a large number of subroutines available, any particular application of 2DSOIL will, generally, only require a subset of these subroutines. If a user wishes to build an application that simulates only water flow, for example, modules for chemistry, solute transport, heat flow, etc. are not necessary. A complete description for building an application was given in chapter 15.

- ▶ Subroutine **Initialize** zeroes all public variables.
- ▶ Subroutine **Get\_Grid\_and\_Boundary** reads data on grid and boundary parameters and calculates areas of elements.

- ▶ Subroutine **Synchronizer** reads the time stepping parameters including the start and stop times, and finds the next time step. It uses data on the next input and output times, information on iteration convergence, and values of time steps produced by the soil transport process modules.
- ▶ Subroutine **SetSurface** produces potential fluxes of water, solutes, heat, and gases at the soil-atmosphere boundary. The **SetSurface** in 'SetSurf01.for' source file reads boundary values from the data file. The **SetSurface** in the 'SetSurf02.for' source file calculates boundary values from daily meteorological data sets.
- ▶ Subroutine **Fill** sends boundary data sets to the prescribed node. Subroutine **SetTDB** sets potential boundary fluxes and/or boundary values of state variables for soil transport processes.
- ▶ Subroutine **WaterMover** simulates water movement in soil. Subroutine **Veloc** calculates water fluxes.
- ▶ Subroutine **SetMat** produces parameters of water transport. Source file 'SetMat01.for' contains subroutines for closed-form approximation of soil hydraulic properties using the formula of van Genuchten (1980). The functions **FK**, **FC**, **FQ**, **FH** calculate unsaturated hydraulic conductivity, specific water capacity, moisture content, and hydraulic head, respectively. Source file 'SetMat02.for' contains subroutines for piece-wise polynomial approximation of soil hydraulic functions.
- ▶ Subroutine **HydSub** approximates moisture release curves and hydraulic conductivity curves for soil layers by piece-wise smooth polynomials. For a given suction value and soil layer **HydSub** calculates moisture content, specific water capacity, and hydraulic conductivity. Subroutine **prep** calculates coefficients of cubic polynomials from data on measured pairs of moisture content-soil suction and hydraulic conductivity-soil suction.
- ▶ Subroutine **SLNQ** solves a system of linear equations. Subroutine **qeq** solves a cubic equation for moisture contents. Functions **Curt** and **Akwrt** calculate cubic and square roots of complex variables, respectively.

- ▶ Subroutine **SoilNitrogen** calculates nitrogen transformations in soil. Subroutine **SetAbio** calculates the correction factors for the various rate constants as a function of soil temperature and soil water content.
- ▶ Subroutine **SoluteUptake** calculates active uptake of a solute, e.g., nitrogen (solute number 1) with water.
- ▶ Subroutine **SoluteMover** calculates redistribution of solute concentrations during water movement. Subroutine **Disper** gives values of solute transport parameters, and subroutine **WeFact** calculates weighting factors for upstream weighting of velocities. Function **Tau** gives tortuosity factor values.
- ▶ Subroutine **HeatMover** calculates soil temperature changes due to heat movement. Subroutine **Thermal** gives heat transport parameters.
- ▶ Subroutine **GasMover** calculates gas contents in soil air. Subroutine **DiffCoef** gives values of gas diffusion coefficients and air-filled porosity.
- ▶ Subroutine **RootWaterUptake** simulates root water uptake and root growth. The **RootWaterUptake** module in the source file '*WatUpt01.for*' calculates the functional balance between shoot and root which will satisfy transpiration demand as long as carbon is available for root growth. Subroutine **SORT** orders soil cells in descending order with respect to favorability for root growth. The **RootWaterUptake** module in the source file '*WatUpt02.for*' uses a static root distribution and calculates root water uptake as a function of soil moisture potential and transpiration demand.
- ▶ Subroutine **ShootImitator** produces shoot variables that are used by the **RootWaterUptake** subroutine. The **ShootImitator** in the source file '*Shootim1.for*' calculates carbon assimilation as a function of radiation and gives values of carbon available for roots to grow and estimates the shadowing of soil by plants. This module does not consider nitrogen stress. It must be used with the **RootWaterUptake** from the source file '*WatUpt01.for*'. The subroutine **ShootImitator** in the source file '*ShootIm2.for*' is similar to the one in '*Shootim1.for*' but uses nitrogen stress. It must be used with the same subroutines mentioned above as well as the **SoluteMover**, **SoluteUptake**, **SoilNitrogen**, and **HeatMover**. The **ShootImitator** in the source file

'ShootIm3.for' only estimates shadowing of soil by plants, and it must be used with the **RootWaterUptake** in the source file 'WatUpt02.for'.

- ▶ Subroutine **MacrChem** calculates equilibrium distributions of ions between soil phases. Subroutine **Actic** prepares auxiliary variables for calculation of solution composition and ion pair contents. Subroutine **Backs** solves a system of linear equations. **Block Data** contains constant parameters of the chemical equilibrium model. Subroutines **HEQ3** and **HEQ4** solve cubic and biquadratic equations for the hydrogen concentration, respectively. Subroutine **Inisl** calculates initial estimates for the distribution of given total amounts of ions between soil phases. Subroutine **Ion** calculates contents of species in the solution. Subroutine **Libra** calculates chemical equilibrium for one node. Subroutine **Nonlin** solves a system of nonlinear equations using a modified Newton's method. Subroutine **Res** calculates residuals of nonlinear equations. Subroutine **Resolv** prepares and controls the process of solution of the nonlinear system of equations describing equilibrium in the soil chemical system. Function **Rwndr** generates random numbers. Subroutine **WSMPLX** solves a system of nonlinear equations using a weighted simplex method. Subroutine **Xform** updates, if necessary, the weight coefficients for amounts of non-associated ions.
- ▶ Subroutine **Output** prints arrays of grid variables to disk files at prescribed simulated times. Subroutines **ArrElemOut** and **ArrNodOut** print variables associated with grid elements and with grid nodes, respectively.
- ▶ Subroutine **ErrMes** prints error messages to the screen and to disk file.

Table 16.2. Subroutines in 2DSOIL code

Source file	Modules	Submodules included and/or called
2dmain.for	Initialize Get_Objects_and_Timeset Get_Grid_and_Boundary Synchronizer SetSurface SetTDB SoluteMover WaterMover HeatMover GasMover RootWaterUptake SoilNDen SoluteUptake ShootImitator Management Output ScreenOutput MacroChem	
errmes.for	ErrMes	
gasmov.for	GasMover	DiffCoeff
grid_bnd.for	Get_Grid_and_Boundary	
heatmov.for	HeatMover	Thermal
init.for	Initialize	
macrchem.for	MacroChem	Libra, RESOL, Xform, ION, SORPT, HEQ3, HEQ4, NONLIN, Backs, Wsmplx, RWRND
output.for	Output	ArrElemOut , ArrNodOut
setmat01.for	SetMat	FK, FC, FQ, FH
setmat02.for	SetMat	HYDSUB, qeq, curt, Akwrt, prep, SLNQ
setsur01.for	SetSurface	Fill
setsur02.for	SetSurface	
settbd.for	SetTDB	
shootim1.for	ShootImitator	
shootim2.for	ShootImitator	
shootim3.for	ShootImitator	
soilnden.for	SoilNitrogen	SetAbio

Table 16.2. Subroutines in 2DSOIL code

Source file	Modules	Submodules included and/or called
solmov.for	SoluteMover	Disper, WeFact, Tau
solutp.for	SoluteUptake	
syncron.for	Synchronizer	
watmov.for	WaterMover	Veloc, SetMat
watupt01.for	RootWaterUptake	SORT
watupt02.for	RootWaterUptake	

## 16.2 Notes on compiling 2DSOIL with different arrangements of subroutines.

This setup of 2DSOIL is constructed so that the structure and content of 2DMAIN.FOR will stay the same regardless or which components are compiled. All the calls to the main 2DSOIL subroutines are retained in 2DMAIN.FOR. If a component (subroutine) such as **HeatMover** is not used in a particular variation of 2DSOIL, the call to **HeatMover** still remains in the 2DMAIN.FOR file. A call to a dummy routine is placed in an additional FORTRAN file and the **HeatMover** code (**heatmov.for**) is not linked with the rest of the code. For instance, each example contains a FORTRAN file with the example's name i.e., Ex14-3.FOR. This file contains calls to all the subroutines listed in 2DSOIL.FOR but not used in an application. The file Ex14-4.FOR will look like this:

```
C These are dummy subroutines to replace any modules
C not used by a particular model application
c use this module for example 14-3

Subroutine GasMover()
return
end

Subroutine GasUptake()
return
end

Subroutine SoilNitrogen()
return
end
```

```
Subroutine SoluteUptake()
return
end

Subroutine ScreenOutput()
return
end

Subroutine Mngm()
return
end

Subroutine ShootImitator
return
end

Subroutine RootWaterUptake
return
end

Subroutine SetSurface
return
end

Subroutine HeatMover
return
end
```

Calls to subroutines that contain components that are not used in a particular application of 2DSOIL are done in one file. These files are given as Ex14-1.FOR etc. When dummy calls to unused components are used like this, the 2DMAIN.FOR file does not have to be modified for a particular variation of 2DSOIL. The file with the dummy calls e.g., Ex14-3.FOR, is compiled and linked with all the other FORTRAN files. The distribution disk contains a FORTRAN file for each example that provides stubs for subroutines of components that are not used. Table 16.2 lists the files compiled and linked for each of the examples. A make file ‘\*.mk’ and a link file ‘\*.lnk’ for each example are available in the distribution disk. These files are applicable to the Salford Fortran compiler. If you use another compiler the syntax will probably change.

Table 16.2 list of files to be linked for each example.

Example 1	Example 2	Example 3	Example 4	Example 5
2dmain	2dmain	2dmain	2dmain	2dmain
errmes	errmes	errmes	errmes	errmes
Ex14-1	Ex14-2	Ex14-3	Ex14-4	Ex14-5
grid_bnd	grid_bnd	grid_bnd	grid_bnd	grid_bnd
init	heatmov	init	init	heatmov
output	init	macrchem	mngmb	init
setmat01	output	output	output	mngmb
setsur02	setmat01	setmat01	setmat01	n_massbl
settbd	setsur02	settbd	setsur01	output
shootim3	settbd	solmov	settbd	setmat01
synchron	shootim2	synchron	shootim2	setsur02
watmov	synchron	watmov	solmov	settbd
watupt01	watmov		synchron	shootim1
	watupt01		watmov	soilnden
			watupt01	solmov
				solutp
				synchron
				watmov
				watupt01

### 16.3 Variables of 2DSOIL.03.

All important variables are listed in the Table 16.3. There is also a complete reference of variables, available in a separate file, '*RefVar.lst*', which shows where a variable is used and altered in a module. The beginning of this reference is in Table 16.4 for illustrative purposes.

Table 16.3. List of significant variables of 2DSOIL

---

A(MBAND,NumNPD)	Coefficient matrix of the global system of equations of the finite element method.
ADRL(NumEl)	Actual change in root length in soil cell for past period, cm.
ADWR(NumEl)	Actual rate of increase in root dry weight in soil cell, g hr-1.
ALPM	Potential relative old root growth rate, day-1
ALPY	Same as above for the young roots
AMMON_N	Ammonia Nitrogen kg ha-1
AS	See listing of the SLNQ subroutine.
AS1	See listing of the SLNQ subroutine.
ATEMP	Factor for changing temperature units.
ATRANS	Atmospheric transmission coefficient.
AVAIL	Ammonium available for immobilization
AVP	Actual water vapor pressure for day (assumed constant), kPa.
AWR(NumEl)	Actual increase in root weight in soil cells for past period, g.
AWUP(NumEl)	Rate of water extraction from soil cells by roots, g hr-1.
Ac(NumNP)	Nodal values of the coefficient at time derivative term
Acc	See listing of the WSMPLX routine.
Aleng	Length of the triangular element side
Alfa	Parameter in the soil water retention function (see section 6.3). Activity coefficient of univalent nonassociated ions after previous iteration.
B(NumNPD)	Coefficient vector.
BB	See listing of the SLNQ subroutine.
BCH	New value of soil carbon g cm-3 soil
BCL	new value of carbon content in the litter g cm-3 soil
BCM	new value of carbon content in the organic fertilizer g cm-3 soil
BEERS	Beer's law correction for light passing through the canopy.
BIR	Factor for changing rainfall intensity units.
BNH	New value of nitrogen in the organic matter g cm-3 soil
BNH4	New value of ammonium-N in the soil g cm-3 soil
BNL	New value of nitrogen in the litter g cm-3 soil
BNM	New value of nitrogen in the manure g cm-3 soil
BNNH4	New value of ammonium-N in the soil g cm-3 soil
BNO3	New value of nitrate-N in the soil g cm-3 soil
BSOLAR	Factor for changing solar radiation units.
BTEMP	Factor for changing temperature units.
BTPL	Lowest value of leaf turgor pressure reached so far today, bar.
BWIND	Factor for changing wind units.
BlkDn	Current nodal value of the soil bulk density
BulkDn(NumNP)	Array of nodal values of the soil bulk density, g cm-3.
CEC	Canopy extinction coefficient. Also: Soil cation exchange capacity, eq per L of the soil solution.
CLDFAC	Cloud cover factor for this latitude.

Table 16.3. List of significant variables of 2DSOIL

---

CLIMAT	Array of climatic variables for the next day.
CLOUD	Proportion of sky covered with cloud (1 = full cover).
CM	Current value of carbon in the manure g cm-3
CO3	Concentration of non-assosiated bicarbonate ions, mol L-1.
COND(NumEl)	Unsaturated hydraulic conductivity averaged over elements, cm day-1.
CONVR	Amount of carbon needed to make unit root dry weight, g g-1.
COVER	Proportion of soil covered by crop.
CPREC	Concentrations of solutes in the rain/irrigation water, g cm-3.
CS	Michaelis-Menton constant of denitrification g cm-3 soil
CXT(NumEl)	Oxygen concentrations in soil air (volume fraction of air).
Ca	Concentration of nonassociated calcium ions, mol L-1
CaCO3	Concentration of the CaCO30 ion pairs, mol L-1
CaHCO3	Same as above for the CaHCO3+ ion pairs.
CaOH	Concentration of the CaOH+ ion pairs, mol L-1.
CaSO4	Concentration of the CaSO40 ion pairs, mol L-1.
Cal	Nodal value of the calcite content. g per g of dry soil.
Calcite	Calcite content in mol of solid salt per L of the solution.
CalciteNod	Solid calcite content, g per g dry soil
Cap(NumNP)	Nodal values of the soil water hydraulic capacity, cm-1.
CapE	Soil water hydraulic capacity of the element, cm-1.
CapTab(NTab,NMat)	Tabulated values of the soil water hydraulic capacity, cm-1
ChName	Constant strings in the names of output files
Cl	Concentration of nonassociated chloride ions, mol L-1.
CodeG	Codes of boundary condition for the gas movement
CodeS	Same as above for the solute movement
CodeT	Same as above for the heat movement
CodeW	Same as above fot the water movement
Coef	See listing of the NONLIN subroutine.
Con(NumNP)	Nodal values of the hydraulic conductivity, cm day-1.
ConAxx(NumEl)	Nodal values of the 'xx' component of the anisotropy tensor.
ConAxz(NumEl)	Same as above for the 'xz' component
ConAzz(NumEl)	Same as above for the 'zz' component
ConE	Same as above
ConSat(NMat)	hydraulic conductivities of soil layers, cm day-1.
ConTab(NTab,NMat)	Tabulated soil hydraulic conductivity, cm day-1.
Conc(NumNP, NumS)	Nodal values of the concentrations, g cm-3.
ConcCa	Nodal value of calcium ions concentration in g L-1.
ConcCl	Same as above for chloride ions.
ConcMg	Same as above for magnesium ions.
ConcNa	Same as above for sodium ions.
ConcSO4	Same as above for sulphate ions.

---

Table 16.3. List of significant variables of 2DSOIL

ConcUnitCa	Factor to convert Ca <sup>2+</sup> concentration units to mol L <sup>-1</sup> .
ConcUnitCl	Same as above for the Cl <sup>-</sup> concentration.
ConcUnitMg	Same as above for the Mg <sup>2+</sup> concentration.
ConcUnitNa	Same as above for the Na <sup>+</sup> concentration.
ConcUnitSO4	Same as above for the SO <sub>4</sub> <sup>2-</sup> concentration.
CourMaX	Maximum allowed Curant number.
Courant	Maximum local Courant number.
Cwat	Heat capacity of water, J g <sup>-1</sup>
DAWN	Time of dawn, hr.
DAYLNG	Daylength, hr.
DDIF	Amount by which daylength exceeds an even number of hours, hr.
DEC	Solar declination, radians (first calculated in degrees).
DEGRAD	Degree to radian conversion factor ( /180).
DEL(24)	Hourly slopes of saturation vapor pressure curve at air temperature, kPa oC <sup>-1</sup> .
DENIT(i)	amount of N denitrified in node I g cm <sup>-3</sup>
DENITR	cumulative amount of N denitrified in profile kg ha <sup>-1</sup>
DIFFIN	Proportion of diffuse radiation intercepted by "solid" rows.
DIFINT(20)	Proportion of sky obscured by "solid" rows from a given point at soil level.
DIFWAT(24)	Hourly proportions of total radiation that is diffuse.
DIRINT(24)	Hourly proportions of direct radiation intercepted by rows of plants assuming they are opaque cylinders.
DPSI02	Change in leaf water potential corresponding to a change of 2 bar in leaf turgor pressure, bar.
DRL(NumEI)	Potential changes in root length in elements for past period, cm
DS(NumNP)	Vector {D} in the global equation for water flow, cm <sup>2</sup> day <sup>-1</sup> or cm <sup>3</sup> day <sup>-1</sup> (see Eq. (6.7)); also used for the diagonal of the coefficient matrix [Q] in the global matrix equation for solute, heat and gas transport, cm <sup>2</sup> or cm <sup>3</sup> (see Eq. (7.9)).
DTHH	highest volumetric water content for which the N process is optimal
DTHL	lowest volumetric water content for which the process is optimal
DTOT	Total nitrogen during a time step g cm <sup>-3</sup>
DUSK	Time of dusk, hr.
Dair(NumG)	Diffusion coefficients of gases in free air, cm <sup>2</sup> day <sup>-1</sup> .
DerMax	See listing of the NONLIN subroutine
Diff(NumNP)	Nodal values of gas diffusion coefficients, cm <sup>2</sup> day <sup>-1</sup> .
Dispxx(NumNP)	Nodal values of the 'xx' component of the solute dispersion tensor, cm <sup>2</sup> day <sup>-1</sup> .
Dispxz(NumNP)	Same as above for the 'xz' component.
Dispzz(NumNP)	Same as above for the 'zz' component.
Dlng(NMat,NumSol)	Longitudinal dispersivity of solutes, cm.
Dmol(NumSol)	Ionic or molecular diffusion coefficients of solutes in free water, cm <sup>2</sup> day <sup>-1</sup> .
Dpom	Factor in the correction terms for eliminating of the numerical dispersion, day <sup>-1</sup> .
DtRain	Duration of rain, day.

Table 16.3. List of significant variables of 2DSOIL

Dtrn(NMat, NumSol)	Transversal dispersivities of solutes, cm.
E(3,3)	Element contributions to the global matrix A for water flow, cm-2
ED	Relative effect of moisture on denitrification
ELCAI	Effective leaf area per unit ground area covered by crop canopy allowing for the fact that light at a low angle traverses more leaf layers to the soil.
ENOUGH	if .true. then there is enough mineral N for immobilization
EO	Potential transpiration (=leaf water evaporation) rate for a canopy, cm3 per cm of row per day
EOMult	Multipliyer depending on the plant position (=1 if the plant is not on the border of the soil slab, =0 if it is on the border).
EOR	Potential transpiration rate per half cm of row (=EORSCF at night) (g hr-1).
EORSCF	EOR*SCF=potential transpiration rate from leaves per half cm of row as limited by stomatal closure, g day-1.
EPO	Potential transpiration rate from the crop, g m-2 hr-1.
ERAIN	Factor for changing units of the amount of rainfall.
ESO	Potential evaporation rate from soil surface, g m-2 hr-1.
ET	(in soilNden) Correction factor for temperature
EW	Correction factor for water for immobilization and mineralization of N
Ec	Gas diffusion coefficient in an element, cm2 day-1.
Ec1	The 'xx' component of the dispersion, diffusion or thermal conductivity averaged over an element, cm2 day-1.
Ec3	Same as above for the 'zz' component.
Eps5	Tolerable residual of the cubic equation for the hydrogen concentration
EpsD	Tolerable relative error for ion mass balance.
Epsilon	Absolute change in the nodal pressure head between two successive iterations, cm
ExCa	Nodal content of the exchageable calcium in g g-1.
ExMg	Nodal content of the exchageable magnesium in g g-1
ExNa	Same as above for the sodium.
ExchCa(NumNP)	Array of exchageable calcium nodal contents, g g-1.
ExchMg	Same as above for the magnesium.
ExchNa	Same as above for the sodium.
ExchUnitCa	Factor for changing of exchangeable Ca <sup>2+</sup> content units
ExchUnitMg	Same as above for the exchangeable Mg <sup>2+</sup> content.
ExchUnitNa	Same as above for the exchangeable Na <sup>+</sup> content.
Explic	Logical variable indicating whether an explicit or implicit scheme was used for solving the water flow equation.
F(NumNP)	Diagonal of the coefficient matrix [F] in the global matrix equation for water flow, cm2 or cm3.
FA	Fraction of the mineral N available for immobilization

Table 16.3. List of significant variables of 2DSOIL

---

FCO3	ame as above for carbonate ions.
FCSH	Coefficient of convective heat transfer for bare soil, J cm-2 d-1 oC-1)
FH	Humification fraction, the fraction of carbon that is available to become organic matter
FHCO3	Concentration of bicarbonate ions in the solution, mol L-1
FOH	Same as above for hydroxil ions.
FSO4	Concentration of sulphate ions in the solution, mol L-1
Fc(NumNP)	Components of the vector {f} in the solute, heat and gas transport equations (see Eq. (7.9)), g cm2 day-1.
FcE	Nodal components of the Fc averaged over an element, g cm2 day-1.
Fca	Concentration of the calcium ions in the solution, mol L-1.
Fcl	Concentration of the chloride ions in the solution, mol L-1.
Fmg	Same as above for magnesium ions.
Fna	Same as above for sodium ions.
FracClay(NMat)	Mass fraction of clay, %
FracOM(NMat)	Mass fraction of organic matter, %
FracSind(NMatN)	Mass fraction of sand+silt, %
IDAWN	Number of calculation period during which dawn occurs.
IDN	Number of calculation period prior to IDUSK.
IDUSK	Number of calculation period during which dusk occurs.
IFUR	Switch that indicates presence or absence of the furrow irrigation.
IHPERD	IPERD/2.
IJ	Maximum number of nodes on any transverse line.
IPERD	Number of calculation periods in the photoperiod. The arrays are currently set up for a maximum of IPERD=24.
IRAV	Average rain intensity, cm day-1.
IS1	Switch to show presence of calcite in solid phase.
IS2	Same as above for gypsum
IS3	Same as above for magnesite.
ISCH	Code of usage for the HYDSUB subroutine (see listing).
ISOL	Code that shows whether solute cocentraions in rainfall are to be read
ITIME	Number of the current hour counting from midnight.
IUP	Number of hours following IDAWN.
Isc	Current code of the present solid salts set: $Isc = 4*Is3+2*Is2+Is1$ .
ItCrit	Logical variable indicating whether or not convergence was achieved.
Iter	Number of iterations.
Itmax	See listing of NONLIN.
Ittry	Number of trials to improve initial estimates for NLE solver.
Ivar	.true., if the variable is included in the system of nonlinear equations.
JDAY	Day of year.
JDFRST	Day of year on which model run starts.

Table 16.3. List of significant variables of 2DSOIL

---

JDLAST	Day of year on which model run stops.
KAT	Code to show if axisymmetrical or planar movement is to be simulated.
KD	denitrification rate adjusted for temperature and soil moisture, day-1
KD0	Potential denitrification rate, day-1
KH	mineralization rate constant adjusted for temperature and soil moisture, day-1
KH0	Potential mineralization rate constant, day-1
KL	The rate constant for the decomposition of plant residues, day-1
KM	The rate constant for decomposition of organic fertilizer corrected for soil water content and temperature, day-1
KM0	the potential rate constant for decomposition of organic fertilizers, day-1
KN	the nitrification rate corrected for water and temperature, day-1
KN0	the potential nitrification rate day-1
KX(NumEl,4)	Global nodal numbers of element corner nodes.
KXB(NumBP)	Global nodal numbers of sequentially numbered boundary nodes .
Ks	Saturated hydraulic conductivity, cm <sup>2</sup> day-1.
LAMDAC	Albedo of crop.
LAMDAS	Albedo of soil.
LAREAT	Total leaf area per plant, cm <sup>2</sup> .
LATUDE	Latitude, degrees.
LCAI	Leaf area per unit ground area covered by crop canopy.
LINE	String to accomodated data prior to printing.
LITTER_N	Total amount of N in the litter, kg ha <sup>-1</sup>
LOCATE	See listing of the SORT subroutine.
Length	Width of soil surface associated with transpiration, cm or cm <sup>2</sup> .
Level	Number of the assembling of A and B matrices during time step.
List	Array of numbers of variables which are included in the system of nonlinear equations
ListE(NumEl)	List of elements that form the reduced flow region for the second and subsequent iterations in water movement calculations.
ListNE(NumNP)	Number of subelements adjacent to a particular node.
MANURE_N	Total amount of N in manure, kg ha <sup>-1</sup>
MARRAY	See listing of the SORT subroutine.
MDAY	Day of year for line of weather data file just read.
MECHR	Soil mechanical resistance to root growth, bar.
MIN_N	Total amount of in in the form of nitrate, kg ha <sup>-1</sup>
MLAY	Maximum number of soil layers.
MREL	Maximum number of measured water retention values.
MSW1	Switch to indicate if daily wet bulb temperatures are available (=1 if they are).
MSW2	Switch to indicate if daily wind is available (=1 if it is).
MSW3	Switch to indicate if daily rain intensities are available (=1 if yes)

Table 16.3. List of significant variables of 2DSOIL

---

MSW4	Switch to indicate if daily solute concentrations in the rain water are available (=1 if yes)
MSW5	Switch to indicate if flooding irrigation will be applied (=1 if yes).
Magnesite	Magnesite content in mol of solid salt per L of the solution.
MatNumE(NumEl)	Numbers of soil layers or horizons where the elemnts are.
MatNumN(NumNP)	Numbers of soil layers or horizons where the nodes are.
MaxIt	Maximum number of iterations allowed during any time step or during one NLE solver call.
Mband	Bandwidth (half-bandwidth) of the symmetric (asymmetric) matrix A.
MbandA	Bandwidth of Matrix A for the second and subsequent iterations of water movement calculations (reduced flow region).
MbandD	Maximum permitted bandwidth of matrix A - maximum allowed difference between numbers of corner nodes for any two elements having at least one common node.
Mg	Concentration of nonassociated magnesium ions, mol L-1.
MgCO3	Concentration of MgCO <sub>3</sub> ion pairs, mol L-1.
MgHCO3	Concentration of MgHCO <sub>3</sub> <sup>+</sup> ion pairs, mol L-1.
MgOH	Concentration of MgOH <sup>+</sup> ion pairs, mol L-1.
MgSO4	Concentration of MgSO <sub>4</sub> ion pairs, mol L-1.
ModNum	ID number of module
NARRAY	See listing of the SORT subroutine.
NCD	Number of climatic variables available for each day.
NH(i)	Nitrogen in humus g cm <sup>-3</sup>
NL(i)	Nitrogen in Litter g cm <sup>-3</sup>
NM(i)	Nitrogen in organic fertilizer, g cm <sup>-3</sup>
NN	Number of nodes in the reduced flow region for the second and subsequent iterations.
NNH4(i)	Nitrogen in the form of ammonium, g cm <sup>-3</sup>
NNO3_SOL	Nitrate in solution, g cm <sup>-3</sup>
NP(NSeep,NumSP)	Sequential numbers of nodes on the seepage faces
NQ	ratio of mineral nitrate to the mineral ammonium characteristic for a particular soil
NRATIO	Nitrogen supply/demand ratio for vegetative parts.
NSP(NSeep)	Numbers of nodes on seepage faces.
NUS	Number of corner nodes of a particular element
Na	Concentration of nonassociated sodium ions, mol L-1.
NaCO3	Concentration of NaCO <sub>3</sub> <sup>-</sup> ion pairs, mol L-1.
NaCl	Concentration of NaClO ion pairs, mol L-1.
NaHCO3	Concentration of NaHCO <sub>3</sub> ion pairs, mol L-1.
NaSO4	Concentration of NaSO <sub>4</sub> <sup>-</sup> ion pairs, mol L-1.

Table 16.3. List of significant variables of 2DSOIL

---

Nch	Number of stream or external unit
Ncode	Code indicating the way of data supply for surface nodes.
Ncorn	Number of corner nodes of a particular element.
Nlevel	Number of time levels at which the matrix A and vector B are assembled for solute, heat and gas transport.
Nmat	Number of soil layers (soil materials).
NmatD	Maximum number of soil layers (soil materials).
NodNum(NumLinNod,N	Global numbers of nodes for which the information is to be printed.
umPoint())	
Npar	Number of parameters specified for each soil layer (soil material)
Nseep	Number of seepage faces expected to develop.
Nsurf	Number of nodes at the soil-atmosphere boundary.
NtabD	Number of entries in the internally generated tables of the hydraulic properties.
NumBP	Actual total number of boundary nodes.
NumBPD	Maximum allowed number of boundary nodes.
NumCell(NumLinCell)	Total numbers of values to be printed in printout lines.
NumEl	Actual number of elements (quadrilaterals and/or triangles).
NumEID	Maximum number of elements in finite element mesh.
NumF	Total number of nodes where the flooding irrigation is applied.
NumFP(NumF)	Global numbers of nodes where the flooding irrigation is applied.
NumGD	Maximum allowed number of gases.
NumLinCell	Total number of horizontal layers of elements
NumLinNod	Total number of transverse grid lines.
NumMod	Total number of modules
NumNP	Actual number of nodal points.
NumNPD	Maximum allowed number of nodes in finite element mesh.
NumPoint(NumLinNod)	Numbers of values to be printed in printout lines.
NumPrint	Number of specified print times.
NumSD	Maximum allowed number of solutes.
NumSEI	Number of subelements (triangles).
NumSol	Actual number of solutes for which the transport is to be simulated.
NumSurfDat	Actual number of values in one line of soil-atmosphere surface data.
NumSurfDatD	Maximum allowed number of values in one line of soil-atmosphere surface data.
NvarBG	Total number of boundary nodes where time-dependent gas contents of fluxes are prescribed.
NvarBS	Total number of boundary nodes where time-dependent solute concentrations are prescribed.
NvarBT	Total number of boundary nodes where time-dependent temperatures or heat fluxes are prescribed

---

Table 16.3. List of significant variables of 2DSOIL

NvarBW	Total number of boundary nodes where time-dependent water fluxes or pressure heads are prescribed.
OH	Concentration of nonassociated hydroxil ions.
ORG_N	Total amount of N in the form of organic matter, kg ha <sup>-1</sup>
OSMFAC	Factor describing ability of plant to osmoregulate when water stressed (= change in osmotic potential/change in water potential).
OSMREG	Switch to indicate that osmoregulation should occur (positive value decreases leaf osmotic potential).
P0	Value of pressure head h0 below which roots start to extract water from the soil, cm.
P1	rate of carbon release from organic matter g cm <sup>-3</sup> day <sup>-1</sup>
P12	rate of carbon transfer from organic fertilizer to organic matter g cm <sup>-3</sup> day <sup>-1</sup>
P13	rate of carbon release from organic fertilizers, g cm <sup>-3</sup> day <sup>-1</sup>
P1415	potential rate for carbon transfer to the organic fertilizer and litter pools, g cm <sup>-3</sup> day <sup>-1</sup>
P2	rate of carbon transfer from plant residues to humus, g cm <sup>-3</sup> day <sup>-1</sup>
P2H	Value of the limiting pressure head h2,high below which the roots cannot extract water at the maximum rate (assuming a potential transpiration rate of Ec,high), cm.
P2L	Value of the limiting pressure head h2,low above which the roots can extract water only at the minimum rate (assuming a potential transpiration rate of Ec,low), cm.
P3	rate of carbon release from plant residues, g cm <sup>-3</sup> day <sup>-1</sup>
P45	flux of carbon to the litter and organic fertilizer pools, g cm <sup>-3</sup> day <sup>-1</sup>
PARTRT	The proportion of VEGSRC partitioned to the root.
PCO2Nod(NumNP)	Array of nodal carbon dioxide pressure values, atm.
PCRL	Rate at which carbon would be supplied to growing roots in a soil slab if all potential shoot growth had been satisfied, g day <sup>-1</sup> .
PCRQ	Rate at which carbon would be supplied to growing roots in a soil slab if all translocated carbon went to the roots, g day <sup>-1</sup> .
PCRS	Actual rate at which carbon is supplied to roots in a soil slab, g day <sup>-1</sup> .
PCRTS	Sum of potential rates of carbon use by roots in selected soil cells in a soil slab, g day <sup>-1</sup> .
PDRL	Potential rate of change in root length in soil cell under consideration if carbon is not limiting, cm day <sup>-1</sup> .
PDWR(NumEl)	Potential rate of increase of root dry weight in soil cell, g day <sup>-1</sup> .
PERIOD	Length of calculation period under consideration, day.
PG	Kinetic rate constant of the gas exchange between the soil and the atmosphere at the surface, day <sup>-1</sup> .

Table 16.3. List of significant variables of 2DSOIL

---

PH	Surface heat flux change per degree of soil surface temperature (bT) for the boundary surface around a node (J d-1 oC-1)
PILD	Leaf osmotic potential at dawn, bar.
PIOSM	Leaf osmotic potential at dawn adjusted for osmoregulation caused by water stress, bar.
POPROW	Plant population per meter of row.
POPSLB	Plant population per soil slab.
POTLOST	potential amount of N lost through immobilization
PPDRL(NumEl)	Value of PDRL for soil cells at previous calculation time.
PPSIL	Value of PSIL_ at previous calculation time.
PPSILT	Leaf water potential which just prevented all shoot growth during the last calculation period, bar.
PRESENT	total amount of solution N at the current node
PROFILE_N	total amount of N in the profile, kg ha-1
PSILD	Leaf water potential at dawn, bar.
PSILT	Leaf water potential which just prevents all shoot growth at time under consideration, bar.
PSILZ	Leaf water potential at zero turgor, bar
PSIL_	Leaf water potential, bar.
PSIM	Average soil moisture potential over cells with active roots, bar.
PSIRD(NumEl)	Water potential in soil cells at dawn, bar.
PSIS(NumEl)	Water potential of soil cells, bar.
PSISM	Soil water potential averaged over cells from which water is extracted when potential shoot growth is satisfied (weighted for the amount of water extracted), bar.
PSIST	Soil water potential averaged over cells from which water is extracted when all carbon translocated goes to the roots (weighted for the amount of water extracted), bar.
PTPL	TPL at previous calculation time, bar.
Par(10,NMat)	Parameters which describe the hydraulic properties of soil.
Pivot	See listing of the NONLIN subroutine.
Plevel	Number of the next print time.
Poptm(NMat)	Values of the pressure head, cm, below which roots start to extract water at the maximum possible rate.
Q(NumNP)	Nodal values of the recharge/discharge rate, cm2 day-1 for planar flow and cm3 day-1 for axisymmetrical flow.
Q1	Mineralization of N from stable organic matter, g cm-3 day-1
Q12	amount of N immobilized during decomposition of organic fertilizer, g cm-3 day-1

---

Table 16.3. List of significant variables of 2DSOIL

---

Q13	The rate of N release from organic fertilizer, g cm-3 day-1
Q14	The rate of immobilization of NH4-N in organic fertilizers, g cm-3 day-1
Q1415ACT	the actual rate of immobilization of NO3-N and NH4-N in organic fertilizers, g cm-3 day-1
Q1415POT	the potential rate of immobilization of NO3-N and NH4-N in organic fertilizers, g cm-3 day-1
Q15	the immobilization of NO3-N in organic fertilizer, g cm-3 day-1
Q2	rate of immobilization of N from plant residues in the humus pool, g cm-3 day-1
Q3	the rate of N release from litter, g cm-3 day-1
Q4	the immobilization of solution NH4-N into the litter pool, g cm-3 day-1
Q45ACT	the actual sum of fluxes Q4 and Q5, g cm-3 day-1
Q45POT	The potential sum of fluxes Q4 and Q5, g cm-3 day-1
Q5	The immobilization of solution NO3-N in litter, g cm-3 day-1
Q6	nitrification of NH4-N to NO3-N, g cm-3 day-1
Q7	N lost through denitrification g cm-3 day-1
QF	Current amount of water infiltrated into soil during flooding irrigation event, cm.
QT	factor change in rate with a 10 degree change in temperature
Qa	Moisture content a (see Section 6.3)
Qg	Constant component of the surface gas flux for the given time step, g cm-2 day-1.
Qh	Heat flux component that does not depend on surface temperature, J d-1
Qk	Moisture content k (see Section 6.3)
Qm	Moisture content m (see Section 6.3)
Qn	Actual latent heat of evaporation for for the boundary surface around a node (J d-1)
Qr	Moisture content r (see Section 6.3)
Qs	Moisture content s (see Section 6.3)
R0	C/N ratio of the decomposer biomass and humification products
RADINT(24)	Fractions of solar radiation intercepted hourly by the crop.
RADVEC	Radius vector of the earth.
RAIN	Rainfall, mm day-1.
RGCF(NumEl)	Proportional reductions of root growth from all physical causes in soil cells.
RGCF1	Proportional reduction of root growth caused by mechanical soil resistance and soil water potential.
RGCF2	Proportional reduction of root growth caused by soil temperature.
RGCF3	Proportional reduction of root growth caused by soil oxygen.
RI	Daily solar radiation integral, J m-2.
RINT(24)	Rain intensity hourly, cm day-2.
RL	C/N ratio of plant residues
RM	C/N ratio of organic fertilizer

Table 16.3. List of significant variables of 2DSOIL

---

RNC	Net radiation on the crop assuming complete cover, W m-2.
RNLU	Net upward long wave radiation, W m-2.
RNS	Net radiation on the soil surface assuming bare soil, W m-2
ROOTFR(NumEl)	Root water uptake activity distribution.
ROUGH	A crop surface roughness parameter.
ROWANG	Row orientation measured eastward from north, degrees.
ROWINC(20)	Distance between a row and the midpoint of an increment of rowspacing, cm.
ROWSP	Row spacing, cm.
RRRM	Radial resistance of old roots per cm of root, bar day g-1.
RRRY	Radial resistance of young roots per cm of root, bar day g-1.
RTMINW	Minimum dry weight of root that must be present in a cell before it can grow into adjacent cells, g.
RTWL	Average root dry weight per unit length, g cm-1.
RTWT(NumEl)	Dry weight of root in soil cells, g.
RUTDEN(NumEl)	Root density in soil cells, cm cm-3.
RVR(NumEl)	Root vascular resistance between base of stem and soil cells, bar day g-1.
RVRL	Root vascular resistance per cm of root, bar day g-1.
Radd	Correction in solute movement equations to accomodate solute content in rain water.
SARANG(24)	Angle between row orientation and solar azimuth hourly, radians
SCF	Stomatal closure factor for reducing H <sub>2</sub> O and CO <sub>2</sub> flux.
SDERP(9)	Empirical regression coefficients for calculating solar declination.
SED(3)	Contents of gypsum, calcite and magnesite in array, mol of solid salt L-1
SGT	Proportion of time for which shoot grows: limited by shoot turgor.
SGTLI	Proportion of shoot growing time lost irretrievably because of low turgor.
SGTLT	Proportion of shoot growing time lost temporarily while turgor is decreasing. It is regained when turgor increases.
SHADE	Width of the shaded strip on the soil surface.
SHADOW(24)	Hourly width of shadow cast by crop row measured at rightangles to the row, cm.
SINALT(24)	Sine of solar altitude hourly.
SINAZI(24)	Sine of solar azimuth hourly
SO4	Concentration of non-assosiated sulphate ion in the solution, mol L-1
SOLALT(24)	Solar altitude hourly, radians.
SOLAIZI(24)	Solar azimuth hourly, radians.
SR(NumEl)	Soil resistance to water flow to roots in soil cells, bar day g-1.
SVPW	Water saturation vapor pressure at the wet bulb temperature, kPa.
Sc(NumNP)	Area around a node where the node-associated sink term is valid
Sca	Exchangeable calcium content, eq L-1.
SelCoefCaNa	Array of nodal selectivity coefficients of cation exchange Ca - Na for the Gaines-Thomas isoterm equation, (mol L-1)-1/2.

Table 16.3. List of significant variables of 2DSOIL

SelCoefMgNa	Same as above for the Mg-Na exchange.
Sink(NumEl)	Values of water extraction rates for elements, day-1.
SinkE	Water extraction rate for an element, day-1.
Smg	Exchangeable magnesium content, eq L-1.
Sna	Exchangeable sodium content, eq L-1.
Step	Time step value, day.
Str	Ionic strength of the solution, mol L-1.
TAIR(I)	Air temperature hourly, oC.
TB	base temperature at which ET=1, oC
TCAIR	Thermal conductivity of dry air, mcal cm-2 s-1 oC-1
TCH2O	Thermal conductivity of water, mcal cm-2 s-1 oC-1
TCSAT	Thermal conductivity of air with water vapor, mcal cm-2 s-1 oC-1
TCSxx(NumNP)	'x' component of thermal conductivity of the soil, J cm-2 d-1 oC-1
TCSzz(NumNP)	'z' component of thermal conductivity of the soil, J cm-2 d-1 oC-1
TCVAP	Thermal conductivity of water vapor, mcal cm-2 s-1 oC-1
TDRY	Dry bulb temperature, oC.
TDUSK	Air temperature at sunset, oC.
TDUSKY	Air temperature at sunset yesterday, oC.
TEND	Proportion of total daily solar radiation received in the period during which dawn or dusk occurs.
TESAZI	Solar azimuth (SOLAZI) calculated for the current hour angle (HRANG) decremented by 0.01. It is used to test if azimuth is decreasing, in which case azimuth is being calculated incorrectly because it is less than $\pi/2$ , radians.
TETC(NMat,MCON)	Measured soil hydraulic conductivity values, cm day-1.
TETR(NMat,MREL)	Measured soil moisture contents at water retention curve.
THD	threshold water content at which no denitrification occurs
THH	intermediate value for calculating the correction factors for nitrogen transformations
THL	intermediate value for calculating the correction factors for nitrogen transformations
THW	Wilting point water content cm <sup>3</sup> /cm <sup>3</sup>
TH_D	exponent used to calculate dependence of ED on theta.
TH_M	exponent used to calculate dependence of Etheta on water content
TMAX	Maximum air temperature during the day, oC.
TMAXHR	Time of maximum air temperature measured from dawn, hr.
TMIN	Minimum air temperature during the day, oC.
TMINT	Minimum air temperature during the next day, oC.
TOTNIT	total amount of nitrogen during current time step in current node, g cm-3
TOTNITO	total amount of nitrogen during past time step in current node, g cm-3
TPI	$2 * \pi = 6.2832185$ .

Table 16.3. List of significant variables of 2DSOIL

---

TPL	Leaf turgor pressure, bar.
TPLD	Leaf turgor pressure at dawn, bar.
TPLT	Leaf turgor pressure which just prevents all shoot growth at time under consideration, bar.
TPRD(NumEl)	Root turgor pressures at dawn minus the threshold turgor for growth, bar.
TS(NumEl)	Temperature of soil in elements, oC.
TSO4	Total amount of SO42- ions in all soil phases, mol L-1 of soil solution.
TWET	Wet bulb temperature, oC.
Tca	Total amount of calcium in all soil phases, mol L-1 of soil solution.
Tcl	Same as above for the chloride ion.
Tfin	Time of the end of simulations, day.
ThAMin(NMat)	Minimum values of air-filled porosity
ThANew(NumNP)	Nodal air-filled porosity value at the new time level.
ThAOld(NumNP)	Same as above for the old time level.
ThATr(NMat)	Threshold values of air-filled porosity.
ThNew(NumNP)	Nodal values of the water content at the new time level.
ThOld(NumNP)	Nodal values of the water content at the old time level.
ThTot(NMat)	Porosity of soil materials.
TheTab(NTab,NMat)	Internal table of the soil water content.
Theta(NumNP)	Intermediate values of soil moisture content.
ThetaA(NumNP)	Nodal values of air-filled porosity.
Thta(NumNP)	Nodal soil water contents.
Ti	Interpolated soil moisture content.
Time	Common time value of all modules.
Tinit	Time of the beginning of calculations, day.
Tmg	Total amount of magnesium in all soil phases, mol L-1 of soil solution
Tmpr(NumNP)	Nodal soil temperature values, oC.
Tna	Total amount of sodium in all soil phases, mol L-1 of soil solution.
TolAbs	Absolute pressure head tolerance limit, cm.
TolRel	Relative pressure head tolerance limit.
Total(5)	Array of total amounts of conservative ions in the chemical system: Total(1), Total(2), Total(3), Total(4), Total(5) correspond to Ca2+, Mg2+, Na+, SO42-, Cl-, respectively.
Totl	Same as above.
Tpot	Potential transpiration from the unit area, cm day-1.
Trel	Time from emergency, day.
VALUE(N)	See listing of the subroutine SORT.
VEGSRC	Rate of carbon supply to the vegetative parts of the shoot and root, g plant-1day-1.
VH2OC(NumEl)	Volumetric water contents of soil cells, cm3 cm-3.
VMAX	Maximum value of VEGSRC.

Table 16.3. List of significant variables of 2DSOIL

VPD(24)	Water vapor pressure deficit hourly, kPa.
VSind(NMatN)	Volumetric fraction of sand and silt (%)
Vabs	Absolute value of the nodal Darcy fluid flux density, cm day-1.
VarB	Time-dependent pressure head or water flux in a particular surface node
VarB1	Surface temperature or surface gas content at the time-dependent boundary.
VarB2	Kinetic rate of the heat exchange or gas exchange between the soil slab and outer space at the time dependent boundary.
VarB3	Soil-independent component of the heat exchange or gas exchange between the soil slab and outer space at the time dependent boundary.
VarBG(NumBP,3)	Current boundary values for gas transport (VarB1, VarB2, VarB3).
VarBS(NumBP,NumS)	Current boundary concentrations of solutes
VarBT(NumBP,3)	Current boundary values for heat transport (VarB1, VarB2, VarB3).
VarBW(NumBP,3)	Current boundary values for water transport.
Vclay(NmatN)	Volumetric fraction of clay (%)
VorgM(NMatN)	Volumetric fraction of organic matter (%)
Vx(NumNP)	Nodal values of the x-component of the Darcian velocity vector, cm day-1.
VxE	The x-component of the Darcian velocity vector for an element, cm day-1.
VxH(NumNP)	Same as Vx at new time level.
VxOld(NumNP)	Same as Vx at new time level.
Vxx	The 'x' component of the Darcian velocity vector, cm day-1.
Vz(NumNPD)	Nodal values of the z-component of the Darcian velocity vector, cm day-1.
VzE	The z-component of the Darcian velocity vector for an element, cm day-1.
VzH(NumNP)	Same as Vz at new time level.
VzOld(NumNP)	Same as Vz at new time level.
Vzz	The 'z' component of the Darcian velocity vector, cm day-1.
W	Nodal value of volumetric soil moisture content.
WACT	Actual radiation incident at earth's surface at noon, W m-2.
WATATM	Radiation incident at the top of the atmosphere at noon, W m-2.
WATPL	Total radiation intercepted by the crop canopy expressed as equivalent radiation from one direction, W m-2.
WATPOT	Potential radiation incident at earth's surface at noon, W m-2.
WATRAT	Proportion of radiation that can penetrate the cloud cover (=WACT/WATPOT).
WATTS(24)	Actual radiation incident at earth's surface hourly, W m-2.
WIND	Windspeed at 2 metres, km hr-1.
WINDA	Average windspeed for the territory under consideration
WINDL	Effective windspeed as augmented by convection currents, km hr-1.
WUP0S	Rate of water uptake from a soil slab when leaf turgor pressure equals to zero bar, g day-1.

Table 16.3. List of significant variables of 2DSOIL

WUP2S	Rate of water uptake from a soil slab when leaf turgor pressure equals to 2 bar, g day-1.
WUPDS	Rate of water uptake from a soil slab if leaf water potential has not risen above the threshold which just prevented all shoot expansion in the last period, g day-1.
WUPGS	Rate of water uptake from a soil slab for various values of leaf water potential.
	Used to select a value of leaf water potential iteratively, g day-1.
WUPM(NumEl)	Rate of water uptake from soil cells by roots more than 0.2 days old, when leaf water potential is at the threshold, i.e., prevents shoot growth, g day-1.
WUPMS	Sum of WUPM(NumEl) and WUPN(NumEl) over all soil cells in a soil slab, g day-1.
WUPN(NumEl)	Rate of water uptake from soil cells by young roots when leaf water potential is at the threshold, i.e., prevents shoot growth, g day-1.
WUPRS	Rate of water uptake from a soil slab by new roots grown after shoot growth potential has been satisfied, g day-1.
WUPSI	Sum of (soil water potential) * (rate of water extraction) over cells in a soil slab from which water is extracted, bar.g day-1.
WUPT(NumEl)	Rate of water uptake from soil cells when leaf water potential is at the threshold, i.e., prevents shoot growth, g day-1.
WUPTS	Rate of water uptake from a soil slab by new roots grown when all translocated carbon goes to the roots, g day-1.
WW	Same as W.
Wa	Weighing factor for the upper adjacent cell to find the proportion of new roots proliferating to this cell from given one.
Wb	Same as Wa for the lower adjacent cell.
WeTab(3,2*NumEl)	Weighing factors associated with the sides of subelements.
WeightCell	Weight of a given soil cell in the distribution of its root mass increment between the given cell and its neighbors.
WeightLeft	
WeightLower	Same as above for the lower adjacent cell
WeightRight	
WeightUpper	Same as above for the upper adjacent cell
Width(NumBP)	Width of the boundary strip associated with boundary nodes, cm, for planar flow; area of this strip, cm2, for the axisymmetrical flow.
WidthE	Array of maximum horizontal sizes of soil cells.
Wi	Same as Wa for the 'Left' adjacent cell. The 'Left' adjacent cell is in the same horizontal layer of cells as a given one, and is closer to stem base than given cell.

Table 16.3. List of significant variables of 2DSOIL

Wr	Same as Wa for the 'Right' adjacent cell. The 'Right' adjacent cell is in the same horizontal layer of cells as a given one, and is further from stem base than given cell.
Wx	Upstream weighing factor for the tranverse direction.
Wz	Same as above for the vertical direction.
XAIR	Weighting factor ( ) for thermal conductivity of air
XCLAY	Weighting factor ( ) for thermal conductivity of clay
XGAIR	Relative proportion of water in pores
XION	Array of concentrations of non-associated ions in the solution.
XLAT	Latitude, radians.
XMUCK	Weighting factor ( ) for thermal conductivity of organic matter
XSIND	Weighting factor ( ) for thermal conductivity of sand and silt
XTEMP	Constant controlling the rate at which air temperature falls after dusk, oC. Temperature falls more slowly as XTEMP increases.
YRL(NumEl)	Length of young root in soil cells, cm.
aCO3	Same as above for the carbonate ions.
aCa	Activity of calcium ions in the solution.
aCl	Activity of chloride ions in the solution.
aHCO3	Same as above for the bicarbonate ions
aMg	Activity of magnesium ions in the solution.
aNa	Activity of sodium ions in the solution.
aOH	Same as above fot the hydroxyl ions.
aSO4	Activity of sulphate ions in the solution.
aa1	Coefficient in the zero degree term in the cubic polynomial.
aa2	Same as above in the first degree term.
aa3	Same as above in the second degree term.
aa4	Same as above in the third degree term.
alf	Weight of values at old time level in temporal discretization.
alpha	parameter for equation to obtain carbon fixed by light (mg CO <sub>2</sub> /umole photons)
alphar	Scale factor for gas uptake
bTort	Tortuosity change per unit of air-filled porosity (See Section 9).
cBnd	Boundary solute concentration for solute transport, g per cm <sup>-3</sup>
cSink(NumEl)	Solute extraction rates, g cm <sup>-3</sup> day <sup>-1</sup> .
carbon_t	Total carbon used by the above ground plant ,g per plant
dMul1	Dimensionless number by which time step is multiplied if the number of iterations is greater than or equal to 7
dMul2	Dimensionless number by which time step is multiplied if the number of iterations is less than or equal to 3
dlh	Spacing (logarithmic scale) between consecutive pressure heads in the internally generated tables of the hydraulic properties.

Table 16.3. List of significant variables of 2DSOIL

---

dt	Time step, day.
dtMax	Maximum permitted time step, day.
dtMin	Minimum permitted time step, day.
dtMx(4)	Maximim time steps allowed by transport modules, day.
dtOld	Previous time step, day.
eorscs	Cumulative value of EORSCF
eps(6)	Set of tolerable errors
epsA	Tolerable relative error of activity coefficients.
epsN	Tolerable residual for nonlinear solver NONLIN.
epsP	Tolerable error of activity products.
epsi	Weight of values at new time level in temporal discretization.
err	Switch to show if there is an error in input data.
gair	Concentration of gas in the air (ppm)
gamma	Psychrometric constant (kPa /C)
hSat(NMat)	Air entry values for soil layers, cm.
hTab(NTab)	Internal table of the pressure heads, cm
hTab1	Lower limit [L] of the pressure head interval for which tables of hydraulic properties are generated, cm
hTabN	Upper limit of the pressure head interval for which tables of hydraulic properties are generated, cm.
hTemp(NumNP)	Nodal values of the pressure head, cm, at the previous iteration.
hcrita	Critical Pressure head at the soil surface for evaporation
hcrits	Critical pressure head at the soil surface for infiltration
iCheck	Switch that shows if at least one node at the seepage face has became saturated
iFavRoot(NumEl)	Array of element (cell) numbers from the best to the worst conditions for root activity.
iForm	Code of the printout format
iLeft	Number of the element neighboring to given one from its left side; it is equal to the number ob the given element for elements at the left boundary of the soil slab.
iLower	Number of the element neighboring to given one from its bottom side; it is equal to the number ob the given element for elements at the bottom boundary of the soil slab.
iRight	Number of the element neighboring to given one from its right side; it is equal to the number ob the given element for elements at the right boundary of the soil slab.

---

Table 16.3. List of significant variables of 2DSOIL

iUpper	Number of the element neighboring to given one from its upper side; it is equal to the number ob the given element for elements at the upper boundary of the soil slab.
ir0	Seed for the random generator.
jjj	Current number of solute or gas.
IConst	Logical variable indicating whether or not there is a constant number of nodes at any transverse line.
lInput	Shows a stage of calculations: = 1, if only initial and time independent data are read;= 0, if time step is to be done.
lUpW	Logical variable indicating if upstream weighing or the standard Galerkin formulation is to be used.
light_i	Light intensity
movers(n)	Array of transport process subroutines
msw6	Switch to indicate if relative humidity is available
nbpC(MLAY)	Number of points in the interpolation table for the hydraulic conductivity.
nbpR(MLAY)	Number of points in the interpolation table for the water retention.
ndef	Nitrogen stress factor
nfrac	cumulative fraction of N in plant tissue
nitrogen_t	Total nitrogen uptake by the plant, g per plant
nshoot	Switch to indicate above ground plant growth (1 if plant growth is simulated)
p_vegsrc	Actual rate of carbon fixation (g/plant /day)
p_vmax	Maximum rate of carbon fixation (g/plant/day)
parint(12)	Fraction of light intercepted by crop at time i
pcarbon_t	Potential carbon production, g per plant
popare	Plant population per unit area (m2)
propar	Proportion of photo synthet active light on outside of crop canopy
psh	Switch to indicate of node is covered, 1 if yes
r2H	Critical potential transpiration rate Ec,high, cm.
r2L	Critical potential transpiration rate Ec,low, cm.
rel_humid	value of relative humidity
sincrsink	Cumulative solute uptake, g
svpa	Water saturation vapor pressure at the wet bulb temprerature (kPa)
t	Time at current time level, day.
tBnd	Temperature at the boundary node when temperature at the boundary node is given, oC
tFix	Next time resulting from time discretizations rules No.2 and No.3, day
tKod	Boundary code for heat set in HeatMover.1=Dirichlet boundary condition 3=Cauchy
tNext	Array of time values at which a modules require to choose a new time step value - obligatory time step end times.

Table 16.3. List of significant variables of 2DSOIL

---

tOld	Time at the previous time level, day.	
tPrint	Array of times when output must be done, day.	
tRigid	Minimum of tNext values.	
tTDB(4)	Times to alter time-dependent boundary conditions for transport modules.	
tatm	Time of the next alteration of soil-atmosphere boundary values.	
tau	Tortuosity factor.	
tau	Parameter in equation to obtain carbon fixed from light (m/s)	
thR(NMat)	Residual water contents.	
thSat(NMat)	Saturated water contents.	
total_carbon	Total Carbon fixed by plant (g/plant)	
total_eor	Total water uptake by plants in a strip 1 cm wide and the width of a row	
total_pcgs	Total Carbon used to grow roots g/half soil slab)	
totssink	Cumulative chemical uptake by plant roots (g/d)	
totwsink	Cumulative water uptake by roots (g/half soil slab 1 cm wide)	
tsink	Heat sink	
ucarbon		0
ucarbon_t		0
wincrsink	Total water uptake during a time step (cm <sup>3</sup> / 1 cm wide half slab)	
x(NumNP)	'x' coordinates of the nodal points, cm.	
xBSTEM	'x' coordinate of the plant stem base, cm.	
xMean	Horizontal distance between of the element center of gravity and plant stem base, cm.	
xMul	Modifying factor to transform equations of planar flow to equations of axisymmetric flow, cm.	
xgc	Horizontal coordinate of the center of gravity of an element.	
y(NumNP)	'y' or 'z' coordinates, cm, of the nodal points.	
yBSTEM	Vertical coordinate of the plant stem base, cm.	
yMean	Vertical distance between of the element center of gravity and plant stem base, cm.	
ygc	Vertical coordinate of the center of gravity of an element.	
zsize	See listing of the WSMPLX subroutine.	

Table 16.4. Example of the 'RefVar.lst' file content

Variable	Module	Subroutine	Alteration
A	solmov.for	SoluteMover	X
	solmov.for	WeFact	X
	watmov.for	WaterMover	X
	watmov.for	Veloc	X
	gasmov.for	GasMover	X
	setmat01.for	FK	
	setmat01.for	FC	
	setmat01.for	FQ	
	setmat01.for	FH	
	setmat02.for	peq	X
	setmat02.for	prep	X
aa	solmov.for	WeFact	X
aa1	setmat02.for	peq	
aa2	setmat02.for	peq	
aa3	setmat02.for	peq	
aa4	setmat02.for	peq	
Ac	solmov.for	SoluteMover	X
	gasmov.for	GasMover	X



**LIST OF REFERENCES**

Acock, B., and A. Trent. 1991. The soybean simulator, GLYCIM: Documentation for the modular version 91. Agric. Exp. Stn., Univ. of Idaho, Moscow, ID.

Acock, B, M.C. Acock, V.R. Reddy and D.N. Baker. 1985. The simulation with GLYCIM of soybean crops grown in the field and at various CO<sub>2</sub> concentrations in open-top chambers during 1982. Responses of vegetation to carbon dioxide no. 011 U.S. Dept. of Energy and USDA.

Ahuja, L. R., D. G. Decoursey, B. B. Barnes, and K. W. Rojas. 1991. Characteristics and importance of preferential macropore transport studied with the ARS root zone water quality models. In Proc. Nat. Symp. Preferential Flow, Chicago, IL. 16-17 Dec., 1991. ASAE Publ. 9:32-42.

Alessi, S., L. Prunty, and W.M. Schuh. 1992. Infiltration simulations among five hydraulic property models. Soil Sci. Soc. Am. J. 56:657-682.

Allmaras, R. R., and W. W. Nelson. 1971. Corn root configuration as influenced by some row-interrow variants of tillage and straw mulch management. Soil Sci. Soc. Am. J. 35:974-980.

American Institute of Physics Handbook. 1972. 3rd ed. Vol. 1. McGraw-Hill, New York, p. 2-250.

Baker, D. G. 1975. Solar radiation reception, probabilities, and areal distribution in the north-central region. Univ. of Minnesota Agric. Exp. Stn. Tech. Bull. 300.

Bear, J. 1972. Dynamics of fluid in porous media. Elsevier, New York.

Benjamin, J. G., M. R. Ghaffarzadeh, and R. M. Cruse. 1990. Coupled water and heat movement in ridged soil. *Soil Sci. Soc. Am. J.* 54:963-969.

Bergström, L., H. Johnson, and G. Torstensson. 1991. Simulation of soil nitrogen dynamics using the SOILN model. 181-188. *In: Nitrogen turnover in the soil-crop system.* Groot, J.J.R., P. de Willigen and E.L.J. Verberne - Eds. Cluver Academic Publishers, 1991

Beven, K.J., Henderson, D.E., and A.A. Reeves. 1993. Dispersion parameters for undisturbed partially saturated soil. *J. Hydrol.* 143(1/2):19-26

Blake, G. R., and J. B. Page. 1948. Direct measurement of gaseous diffusion in soils. *Soil Sci. Soc. Am. Proc.* 13:37-41.

Blum, B.I., 1992. Software Engineering : A Holistic View Oxford University Press, New York.

Bolt, G. H. (ed.) 1982. Soil chemistry. B. Physico-chemical models. Elsevier, New York.

Bowers, S. A., and R. D. Hanks. 1965. Reflection of radiant energy from soils. *Soil Sci.* 100:130-138.

Boyer, J. S. 1970. Differing sensitivity of photosynthesis to low leaf water potentials in corn and soybean. *Plant Physiol.* 46:236-239.

Boyer, J. S. 1971. Resistances to water transport in soybean, bean and sunflower. *Crop Sci.* 11:403-407.

Brouwer, R. 1965. Water movement across the root. In C. E. Fogg (ed.) *The state and movement of water in living organisms.* Cambridge Univ. Press, Cambridge.

- Bruckler, L., B. C. Ball, and P. Renault. 1989. Laboratory estimation of gas diffusion coefficient and effective porosity in soils. *Soil Sci.* 147:1-10.
- Budyko, M. I. 1974. Climate and life. D. H. Miller (ed. and trans.) Academic Press, New York.
- Bunce, J. A. 1978. Effects of shoot environment on apparent root resistance to water flow in whole soybean and cotton plants. *J. Exp. Bot.* 29:595-601.
- Call, F. 1957. Soil Fumigation. 5. Diffusion of ethylene dibromide through soils. *J. Sci. Food Agric.* 8:143-150.
- Cowan, I. 1965. Transport of water in soil-plant-atmosphere system. *J. Appl. Ecol.* 2:221-239.
- Currie, J. A. 1984. Gas diffusion through soil crumbs: The effect of compaction and wetting. *J. Soil Sci.* 35:1-10.
- Dalton, F. N., and W. R. Gardner. 1978. Temperature dependence of water uptake by plant roots. *Agron. J.* 70:404-406.
- de Willingen, P. 1991. Comparison of fourteen simulation models. p. 141-150. In: *Nitrogen turnover in the soil-crop system* /de Groot, J.J.R, P. de Willingen, and E.L.J.Verberne - eds./. Kluwer Academic Publishers, Dordrecht/Boston/London.
- DeVries, D. A. 1966. Thermal properties of soils. p. 210-235. In Van Wijk (ed.) *Physics of the plant environment*. North Holland Pub., Amsterdam.
- Eavis, B. W., H. M. Taylor, and M. G. Huck. 1971. Radicle elongation of pea seedlings as affected by oxygen concentration and gradients between shoot and root. *Agron. J.* 63:770-772.

Einbu, J. 1989. A program Architecture for Improved Maintainability in Software Engineering. Ellis Horwood, New York.

Feddes, R. A., P. J. Kowalik, and H. Zaradny. 1978. Simulation of field water use and crop yield. Simulation Monographs. Wageningen, PUDOC, The Netherlands.

Flerchinger, G. N., and K. E. Saxton. 1989. Simultaneous heat and water model of a freezing snow-residue-soil system. 1. Theory and development. Trans. ASAE 32:565-571.

Fritschen, L. J. 1967. Net and solar radiation over irrigated field crops. Agric. Meteorol. 4:55-62.

Gardner, W. R. 1960. Dynamic aspects of water availability to plants. Soil Sci. 89:63-73.

Gates, D. M. 1968. Transpiration and leaf temperature. Ann. Rev. Plant Physiol. 19:211-238.

Grable, A. R., and E. G. Siemer. 1968. Effects of bulk density, aggregate size, and soil water suction on oxygen diffusion, redox potentials, and elongation of corn roots. Soil Sci. Soc. Am. Proc. 32:180-186.

Gradwell, M. W. 1961. Laboratory study of the diffusion of oxygen through pasture topsoils. New Zealand J. Sci. 4:250-270.

Greacen, E. L., and J. S. Oh. 1972. Physics of root growth. Nat. New Biol. 235:24-25.

Hailey, J. L., E. A. Hiler, W. R. Jordan, and C. H. M. van Bavel. 1973. Resistance to water flow in *Vigna sinensis* L. at high rates of transpiration. Crop Sci. 13:264-266.

Hoogenboom, G., and M. G. Huck. 1986. ROOTSIMU V4.0. A dynamic simulation of root growth, water uptake, and biomass partitioning in a soil-plant-atmosphere continuum. Update

and documentation. Agronomy and Soils Departmental Series No. 109. Auburn Univ., Auburn, AL.

Huang, K., B.P. Mohanty, and M.Th. Van Genuchten. 1996. A new convergence criterion for the modified picard iteration method to solve the variably-saturated flow equation. *Water Resour. Res.* (In press)

Istok, J. 1989. Groundwater modeling by the finite element method. Water Resources Research Monograph 13. American Geophysical Union, Washington, DC.

Jabro, J.D., J.M.Jemison,Jr., L.L.Lengnick, R.H.Fox, and D.D.Fritton. 1993. Field validation and comparison of LEACHM and NCSWAP models for predicting nitrate leaching. *Transactions of ASAE*. 36: 1651-1657.

Johnsson, H., L. Bergström, P.E.Jansson, and K. Paustian. 1987.

Simulated nitrogen dynamics and losses in a layered agricultural soil. *Agriculture, Ecosystems, and Environment*, 18:333-356.

Jones, C. A., and J. R. Kiniry (eds.). 1986. CERES-MAIZE. A simulation model of maize growth and development. Texas A&M Univ. Press, College Station, TX.

Kimball, B. A. 1965. Soil atmosphere composition as related to microbial activity and diffusion coefficient. M.S. Thesis. Iowa State Univ., Ames, Iowa (unpublished).

Kirk, B.R. 1990. Designing systems with objects, processes, and modules. pp 387-404. In P. Hall (ed.) SE90: Proceedings of Software Engineering 90, Brighton, July 1990. Cambridge Univ. Press.

Kirk and P. Nye. 1991. A model of ammonia volatilization from applied urea. VI. The effects of transient-state water evaporation. *J. Soil Science*. 42:115-125.

Linacre, E. T. 1968. Estimation of net radiation flux. *Agric. Meteorol.* 5:49-63.

Lindsay, W. L. 1979. Chemical equilibria in soils. Wiley, New York.

List, R. J. (ed.). 1966. Smithsonian meteorological tables. 6th ed. Smithsonian Institute, Washington, DC.

Logsdon, S. D., R. R. Allmaras, J. B. Wu, J. B. Swan, and G. M. Randall. 1990. Macroporosity and its relation to saturated hydraulic conductivity under different tillage practices. *Soil Sci. Soc. Am. J.* 54:1096-1101.

Luckner, L., M. van Genuchten, and D. Nielsen. 1989. A consistent set of parametric models for the two-phase flow of immiscible fluids in the subsurface. *Water Resour. Res.* 25:2187-2193.

Miller, D. H. 1981. Energy at the surface of the earth. Academic Press, New York.

Millington, R. J., and J. P. Quirk. 1960. Transport in porous media. *Trans. 7th Int. Con. Soil Sci.* 1:97-106.

Mualem, Y. 1976. A new model for predicting the hydraulic conductivity of unsaturated porous media. *Water Resour. Res.* 12:513-522.

Neuman, S. P. 1972. Finite element computer programs for flow in saturated-unsaturated porous media. Second Annual Report, Project A10-SWC-77. Hydraulic Engineering Laboratory, Technion, Haifa, Israel.

Nye, P.H., and P. B. Tinker. 1977. Solute movement in the soil-root system. Univ. of California Press, Los Angeles.

Pachepsky, Ya., and N. Zborishchuk. 1984. Mathematical models of water movement in heavy clay soils. pp. 101-113. In J. Bouma and P. A. C. Raats (eds.) Proceedings of the ISSS symposium on water and solute movement in heavy clay soils. International Institute for Land Reclamation and Improvement, Wageningen, The Netherlands.

Pachepsky, Ya. 1990. Mathematical models of physical chemistry in soil science. Moscow, Nauka. (In Russian.)

Pachepsky, Ya. 1992. Mathematical models of processes in soils under reclamation. Moscow, Moscow State University. (In Russian.)

Pachepsky, Ya., and D. Timlin. 1993. Interpolation of soil hydraulic properties by piecewise polynomials. *Soil Sci. Soc. Am. J.* (in press).

Penman, H. L. 1940. Gas and vapor movement in soil. 1. The diffusion of vapors through porous solids. *J. Agric. Sci.* 30:437-463.

Penman, H. L. 1963. Vegetation and hydrology. C.A.B. Tech. Comm. 53. Commonwealth Agricultural Bureau, Harpenden, Hertfordshire, U.K.

Platonova, T.K., and Ya. Pachepsky. 1988. Simulation of mass-exchange processes in soil under leaching. *Pochvovedenie* 5:70-81.

Ritchie, J.T. 1964. Soil aeration characterization using gas chromatography. Ph.D. Thesis, Iowa State Univ., Ames, IA. Univ. Microfilm no. 65-03807.

Ritchie, J. T. 1971. Model for prediction of evaporation from a row crop with incomplete cover. *Water Resour. Res.* 8:1204-1213.

Robertson, G. W., and D. A. Russelo. 1968. Astrometeorological estimator. Agric. Meteorol. Tech. Bull. 14. Plant Res. Inst., C.E.F., Ottawa, Canada.

Russel, S. 1977. Plant root systems. McGraw-Hill, London.

Shaffer, M. J., A. D. Halvorson, and F. J. Pierce. Nitrate leaching and economic analysis package (NLEAP): Model description and application. pp. 285-322. In R. F. Folett, D. R. Keeney, and R. M. Cruse (eds.) Managing nitrogen for groundwater quality and farm profitability. Soil Sci. Soc. of Am., Madison, WI.

Shcherbakov, R. A., Ya. A. Pachepsky, and M. S. Kuznetsov. 1981. Migration of ions and chemical compounds in soils: Water movement. ECOMODEL software series, No. 7, USSR Academy of Science, Pushchino. (In Russian.)

Simunek, J., T. Vogel, and M. van Genuchten. 1992. The SWMS\_2D code for simulating water flow and solute transport in two-dimensional variably saturated media. Version 1.1. Res. Rep. 126. United States Salinity Laboratory, Riverside, CA.

Smithsonian Meteorological Tables. 1963. 6<sup>th</sup> edition. R.J. List (ed.). Smithsonian Institution, Washington, DC.

Stoker, R., and P. E. Weatherly. 1971. The influence of the root system on the relationship between the rate of transpiration and depression of leaf water potential. New Phytol. 70:547-554.

Taylor, H. M., and B. Klepper. 1975. Water uptake by the cotton root systems: An examination of assumptions in the single root model. Soil Sci. Soc. Am. J. 40:57-67.

Taylor, S. A. 1949. Oxygen diffusion in porous media as a measure of soil aeration. Soil Sci. Soc. Am. Proc. 14:55-61.

ten Berge, H.F.M., D.M. Jansen, K. Rappoldt, and W. Stol. 1992. The soil water balance model SAWAH: description and users guide. Simulation Reports CABO-TT nr. 22. DLO-Centre for Agrobiological Research (CABO-DLO) and Dept of Theoretical Production Ecology (TPE), Wageningen, The Netherlands.

Thomas, D. 1989. What's in an object? Byte 14:231-240.

Thompson, T. E., and G. W. Fick. 1980. Modeling the effects of excess water on alfalfa growth. Cornell Univ., Ithaca, NY.

Tillotson, P., and D. Fontaine. 1991. GRASP: Geographically-based Risk Analysis System for Pesticides. 1. Methodology. Environ. Toxicol. and Chem. 14:713-721.

Timlin, D. J., R. B. Bryant, V. Snyder, and R. J. Wagenet. 1989. Modeling corn grain yield in relation to soil erosion using a water budget approach. Soil Sci. Soc. Am. J. 50:718-723.

Timlin, D. J., G. G. Heathman, and L. R. Ahuja. 1992. Solute leaching in row vs interrow zones. Soil Sci. Soc. Am. J. 56:384-392.

Troeh, F. R., J. D. Jabro, and D. Kirkham. 1982. Gaseous diffusion equations for porous materials. Geoderma 27:239-253.

Van Genuchten, M. T. 1980. A closed-form equation for predicting the hydraulic conductivity of unsaturated soils. Soil Sci. Soc. Am. J. 44:892-898.

Vogel, T. 1987. SWMII - Numerical model of two-dimensional flow in a variably saturated porous medium. Res. Rep. 87. Dept. of Hydraulics and Catchment Hydrology. Agricultural Univ., Wageningen, The Netherlands.

Vogel, T., and M. Císlerová. 1988. On the reliability of unsaturated hydraulic conductivity calculated from the moisture retention curve. *Transport in Porous Media* 3:1-15.

Wagenet, R. J., and J. L. Hudson. 1987. LEACHM: Leaching Estimation and Chemistry Model. Center for Environmental Research, Cornell Univ., Ithaca, NY.

Weiss, A. 1977. Algorithms for the calculation of moist air properties on a hand calculator. *Trans. ASAE* 20:1133-1136.

Wesseling, J. 1962. Some solutions of steady-state diffusion of carbon dioxide through soils. *Neth. J. Agric. Sci.* 10:109-117.

Wesseling, J. E., and T. Brandyk. 1985. Introduction of the occurrence of high groundwater level and surface water storage in computer program SWATRE. Nota 1636. Institute for Land and Water Management Research, Wageningen, The Netherlands.

Wesseling, J., and W. R. van Wijk. 1957. Land drainage in relation to soil and crops. 1. Soil physical conditions in relation to drain depth. pp. 461-504. In J. D. Luthin (ed.) *Drainage of Agricultural Land*. Am. Soc. Agron., Madison, WI.

Wirfs-Brock, R., B. Wilkerson, and L. Weiner. 1990. *Designing Object Oriented Software*. Prentice Hall Publ. Co., Englewood Cliffs, NJ.

White, P.R., 1937. Seasonal fluctuations in growth rates of exised tomato root tips. *Plant Physiol.* 12:183-190.

Witt, B.I., F.T. Baker, and E.W. Meritt. 1994. *Software architecture and design. Principles. Models, and Methods*. Van Nostrand Reinhold. NY.

Yeh, G.T., and V.S. Tripathi. 1991. A model for simulating transport of reactive multispecies components: Model development and demonstration. Water Resour. Res. 27:3075-3094.